Acquisition of azole resistant *Aspergillus fumigatus* in individuals with chronic respiratory diseases.

Amélie Poppy Brackin

Imperial College London

Department of Infectious Disease

A thesis submitted for the degree of Doctor of Philosophy

October 2024

Declaration of Originality

I declare that this thesis is the result of my own work. All sources of information, whether from published or unpublished material, have been acknowledged appropriately and cited throughout.

Copyright declaration

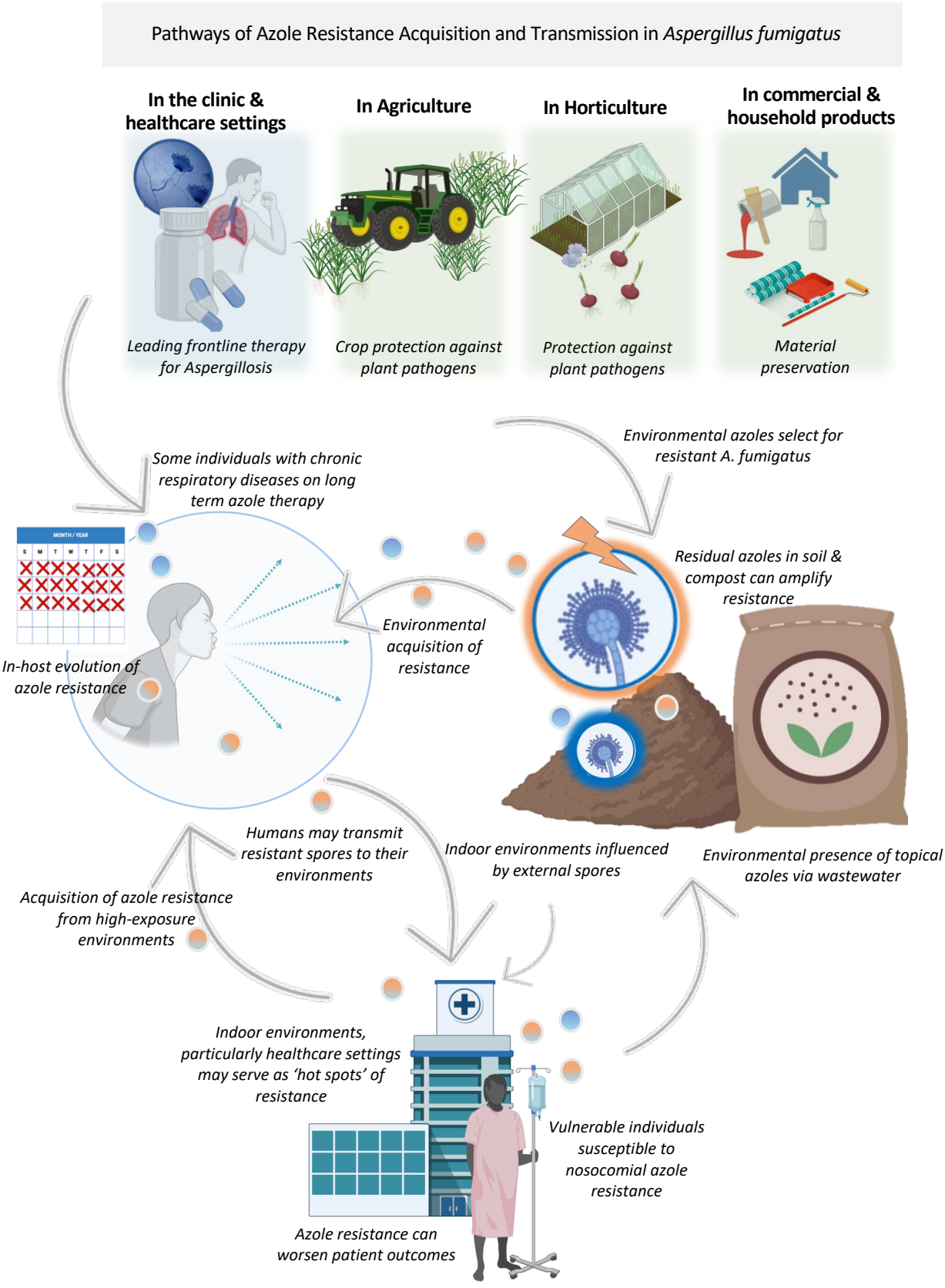
The copyright of this thesis rests with the author. Unless otherwise indicated, its contents are licensed under a Creative Commons Attribution-NonCommercial 4.0 International Licence (CCBY-NC).

Under this licence, you may copy and redistribute the material in any medium or format. You may also create and distribute modified versions of the work. This is on the condition that: you credit the author and do not use it, or any derivative works, for a commercial purpose.

When reusing or sharing this work, ensure you make the licence terms clear to others by naming the licence and linking to the licence text. Where a work has been adapted, you should indicate that the work has been changed and describe those changes. Please seek permission from the copyright holder for uses of this work that are not included in this licence or permitted under UK Copyright Law.

Abstract

Azole resistance in *Aspergillus fumigatus* presents a significant challenge to effective treatment in chronic respiratory diseases, where prolonged azole antifungal therapy is routinely employed. Individuals with chronic respiratory diseases are disproportionately impacted by the emergence of drug resistance, thought to be driven by strong selective pressures associated with environmental fungicide use and oral azole therapy. The mechanisms driving antifungal resistance acquisition and evolution in individuals with chronic respiratory diseases remain poorly described. This thesis investigates the prevalence, genetic diversity, and transmission dynamics of azole resistant *A. fumigatus* across clinical and environmental settings in the UK, with a focus on the TR_{34}/L98H resistance mechanism. Utilising whole-genome sequencing (WGS) and high-throughput phenotyping, 912 isolates were characterised to elucidate the genetic basis of resistance and adaptation. Analysis of 210 virulence-associated genes revealed increased frequencies of nonsynonymous SNPs in TR_{34}/L98H isolates, indicating genetic diversification that may support adaptation under antifungal pressures. Phenotypic profiling under 384 growth conditions highlighted metabolic adaptations in TR_{34}/L98H isolates, including shifts in carbon and nitrogen utilisation, osmotic stress tolerance, and reduced reliance on d-trehalose during germination, potentially contributing to persistence in clinical settings. Prospective longitudinal surveillance of 55 individuals with chronic respiratory diseases identified a 25% prevalence of azole resistance, predominantly among those with chronic pulmonary aspergillosis and cystic fibrosis. WGS of clinical and environmental isolates revealed the dominance of TR_{34}/L98H and emerging TR_{46}/Y121F/T289A resistance mechanisms. Integration of environmental and clinical WGS data from hospital settings revealed genetic similarities between isolates, suggesting bidirectional transmission pathways. Additionally, home environments were surveyed through a citizen science approach, identifying resistant isolates in 60% of homes, with soil as a key reservoir. These findings emphasise the role of environmental reservoirs in the persistence and transmission of azole-resistant *A. fumigatus*, underscoring the need for advanced surveillance strategies.



Schematic summary of thesis: Overview of azole resistance acquisition in *Aspergillus fumigatus* and its impact in clinical and environmental contexts.

Acknowledgements

I wish to acknowledge my supervisors whose guidance and expertise have been essential in shaping this work. I hope that my contributions bring value to your ongoing research. Firstly, I would like to extend my sincerest thanks to Professor Darius Armstrong-James, thank you for your remarkable patience and for finding the perfect balance between being a mentor and letting me explore my own research path. To Dr. Anand Shah, I feel incredibly fortunate to have had such an approachable and personable supervisor from whom I have learnt so much. You have provided unwavering support and encouragement throughout, thank you for making even the toughest days more bearable. My deepest gratitude goes to Professor Matthew Fisher, who welcomed me into his lab over five years ago and saw potential in me to pursue a PhD, despite my very limited knowledge of mycology. His belief in me has instilled a lasting sense of confidence, and I will always be truly grateful for the opportunity. I owe a heartfelt thanks to all the participants and healthcare professionals whose contributions to the sampling and monitoring efforts were invaluable to this research. I would also like to express my appreciation to the Imperial College teams in the DAJ and Fisher labs for a creating relaxed and enjoyable working environment. A special thanks to Rodrigo for his invaluable technical support and to Jo for her computational advice, both of which greatly enhanced the quality of this thesis. Thank you both for your continued support and for regularly checking in. To my wonderful Essex girlfriends, especially Claire Healey—the Patsy to my Eddie—you are an absolutely fabulous friend. A big thanks to my Uncle Lloyd, who never failed to remind me that there are always jobs at Aldi if all else fails. To my older siblings, Konrad and Tamesin, my go-to forever team and the ones I've always looked up to, thank you for your support. I owe all my achievements to my wonderful parents, Ron and Denise, whose kindness and unwavering encouragement have been a constant inspiration and the driving force behind my education. I hope I have made you proud.

Finally, I want to dedicate this work to Thomas, my lifelong adventure partner, the kindest, most patient person I know and without whom I could not accomplish so much in life. No words can express my gratitude, thank you for being by my side every step of the way.

Abbreviations

ABC: ATP-binding cassette

ABPA: Allergic broncho-pulmonary aspergillosis

AFLP: Amplified fragment length polymorphism

AIDS: Acquired Immunodeficiency Syndrome

AMR: Antimicrobial resistance

AR*Af*: Azole resistant *Aspergillus fumigatus*

ARDS: Acute respiratory distress syndrome

ART: Antiretroviral therapy

AUC: Area under the curve

BAL: Broncho-alveolar lavage

bp: Base pair

BR: Broad range

BSC: Biological safety cabinet

BWA: Burrows-Wheeler Aligner

C: Centigrade celsius

CAAs: Carboxylic acid amides

CAPA: COVID-19-associated pulmonary aspergillosis

CF: Cystic fibrosis

CFTR: CF transmembrane conductance regulator

CFUs: Colony Forming Units

CNS: Central Nervous System:

COPD: Chronic obstructive pulmonary disease

CPA: Chronic pulmonary aspergillosis

CrAg: Cryptococcal antigen

CT: Computed Tomography

DALY: Disability-adjusted life year

DAPC: Discriminate analysis of principle components

DNA: Deoxyribonucleic acid

DHODH: Dihydroorotate dehydrogenase

ds: Double stranded

EB: Elution Buffer

ECA: Erythritol chloramphenicol agar

EDCs: Electrostatic Dust Collectors

EAPCRI: European *Aspergillus* PCR Initiative

EPA: Environmental Protection Agency

EUCAST: European Committee on Antimicrobial Susceptibility Testing

ELISA: Enzyme-linked immunosorbent assays

FPPL: Fungal priority pathogens list

FRAC: Fungicide Resistance Action Committee

FREAL: Fungal Resistance Evolution and Acquisition in chronic Lung disease

g: Gram

GATK: Genome analysis toolkit

gDNA: genomic DNA

GTR: General Time Reversible

HEPA: High-efficiency particulate air

HIV: Human immunodeficiency virus

HPC: High Performance Computer

HRA: Health Regulator Authority

IA: Invasive aspergillosis

ID: Identification

ICU: Intensive Care Unit

ITS: Internal transcribed spacer

L: Litre

LPCB: Lactophenol-cotton blue

µL: Microlitre

m: Meter

mL: Millilitre

mg: Milligram

MARDy: mycology antifungal resistance database

MFS: Major facilitator superfamily

MIC: Minimum inhibitory concentration

MLST: Multi-locus sequence typing

MMR: Mismatch repair

MPA: Mould Preservation Agar

MRC: Medical Research Council

MTR: Multi-triazole resistance

NCBI: National Centre for Biotechnology Information

nsSNPs: Nonsynonymous Single Nucleotide Polymorphism

PAMPs: Pathogen-associated molecular patterns

PAHs: Polycyclic aromatic hydrocarbons

PRRs: Pattern recognition receptors

PBS: Phosphate buffered saline

PC: Principal Components

PCA: Principal component analysis

PCR: Polymerase Chain Reaction

PLS-DA: Partial least squares - discriminant analysis

PTB: Pulmonary tuberculosis

QC: Quality Control

QOIs: Quinone outside inhibitors

RedCap: Research Electronic data capture

RAxML-NG: Randomized Axelerated Maximum Likelihood Next- generation

RBH: Royal Brompton Hospital

RBHT: Royal Brompton and Harefield NHS Foundation Trust

RFLP: Restriction fragment length polymorphism

rRNA: Ribosomal ribonucleic acid

Rpm: Rotations per minute

SAFS: Severe Asthma with Fungal Sensitization

SCARE: Surveillance Collaboration on *Aspergillus* Resistance in Europe

SDA: Sabouraud dextrose Agar

SDB: Sabouraud dextrose Broth

SNP: Single Nucleotide Polymorphism

STR: Short Tandem Repeats

STR*Af*: Short tandem repeats of *Aspergillus fumigatus*

TR: Tandem repeat

TRiFIC: Targeting Immunotherapy for Fungal Infections in Cystic Fibrosis

UV: Ultra violet

VCF: Variant call format

VIP: Variable influence on the projection

WHO: World Health organisation

WGS: Whole Genome Sequencing

Table of Contents

Chapter 1 Introduction ***1***

1.1 Human associated mycoses **1**

1.2 Respiratory mycoses **5**

1.2.1 *Exophiala dermatitidis* 6

1.2.2 *Scedosporidium spp.* 7

1.2.3 Mucormycosis 7

1.2.4 Fusaria 8

1.2.5 *Cryptococcus gattii/neoformans* species complexes 9

1.3 *Aspergillus fumigatus* **11**

1.3.1 Interaction with host immune response 11

1.3.2 Aspergillosis 13

1.3.3 Environmental reservoirs of *A. fumigatus* 16

1.3.4 Life cycle and adaptation strategies 17

1.4 Azole resistant *A. fumigatus* **20**

1.4.1 Clinically acquired azole resistance 20

1.4.2 Environmentally acquired azole resistance 23

1.4.3 Patient-to-environment transmission pathways 25

1.4.4 Epidemiology of azole resistance 26

1.5 Current Diagnostics **27**

1.5.1 Culture based techniques 27

1.5.2 Molecular diagnostics 29

1.5.3 Typing schemes 30

1.5.4 Next Generation Sequencing 31

1.6 Concluding remarks **34**

1.7 Thesis Overview **35**

1.8 Thesis Aims **37**

1.9 Funding **38**

Chapter 2 General Materials and Methods ***39***

2.1 Ethical Approval **39**

2.2 Participant selection and inclusion criteria for prospective surveillance **39**

2.3 Fungal Isolates **39**

2.4 Fungal culture and isolation **40**

2.4.1 Handling of *A. fumigatus* and other fungi 40

2.4.2 Culture Media 40

2.4.3 Fungal isolation from primary cultures 41

2.4.4 Confirmation of mixed colonies 42

2.4.5 Storage of fungal isolates 43

2.5 *A. fumigatus* identification and conidial harvest **43**

2.5.1 Macroscopic and microscopic characteristics 43

2.5.2 β-tubulin amplification, PCR and Sanger sequencing 43

2.5.3 Conidial harvesting for downstream analysis 44

2.8 Azole susceptibility screening **44**

2.8.1 Azole susceptibility testing using VIPCheck™ plates 44

2.8.2 Tebuconazole susceptibility testing 45

2.9 Genomic DNA (gDNA) extraction for WGS **46**

2.9.1 Isolate selection for next generation sequencing 46

2.9.2 Genomic DNA extraction 47

2.9.3 Extraction of gDNA from low sporulating and poor growth isolates 48

2.9.4 gDNA quantification and quality control 48

2.10 Next Generation Sequencing & Bioinformatic Analysis **49**

2.10.1 Illumina short read sequencing 49

2.10.2 UK Retrospective Genomic Library 50
2.10.3 Sequence alignment and variant calling 50
2.10.4 Mapping Statistics 51
2.10.5 Discovery of cyp51a alleles 51
2.10.6 Multisequence alignments 51
2.12 Phylogenetic Analysis 52
2.13 Calculating pairwise unique SNPs 52
2.14 Multivariate analysis of genomic data 53
2.15 Statistical analysis 53
Chapter 3 Genotypic and phenotypic characterisation of A. fumigatus: Insights into the TR_{34}/L98H resistance mechanism 55
3.1 Abstract 55
3.2 Introduction 55
3.3 Methods 57
3.3.1 UK *A. fumigatus* WGS dataset 57
3.3.2 Discovery of nsSNPs in the coding region of virulence related genes 57
3.3.3 Antifungal susceptibility screening 58
3.3.4 Phylogenomic analysis 58
3.3.5 Phenotypic characterisation using the high throughput Omnilog® Phenotype Microarray (PM) system 58
3.4 Results 61
3.4.1 WGS of 912 *A. fumigatus* isolates from the UK 61
3.4.2 Multi-triazole resistance association with *cyp51a* genotypes 62
3.4.3 Phylogenetic diversity 66
3.4.4 Distribution of nsSNPs in the coding regions of virulence related genes 68
3.4.5 Phenotypic characterisation using the high-throughput OmniLog™ platform 70

3.4 Discussion **82**

Chapter 4 Epidemiology of azole resistant A. fumigatus in a respiratory disease cohort ***89***

4.1 Abstract **89**

4.2 Introduction **89**

4.3 Methods **92**

4.3.1 Impact of COVID-19 on Prospective Clinical Surveillance 92

4.3.2 Remote sputum sample collection 92

4.3.3 Sputum sample processing 92

4.3.4 Isolation of *A. fumigatus* colonies 93

4.3.5 Antifungal susceptibility screening 93

4.3.6 Retrospective clinical isolate collection 93

4.3.7 DNA extraction and quantification 94

4.3.8 Next Generation Sequencing & Bioinformatic analysis 94

4.3.9 Incorporation of 118 RBH retrospective genomes 94

4.3.10 Phylogenomic analysis 95

4.3.11 Calculating pairwise SNPs 95

4.3.12 Multivariate analysis of genomic data 95

4.3.13 Genetic diversity 95

4.3.14 Statistical analysis 95

4.4 Results **96**

4.4.1 Patient participation and sputum sample collection 96

4.4.2 Azole resistance detected in 146/321 of prospective clinical isolates. 96

4.4.3 Azole resistance detected in 25% of the RBH respiratory disease cohort 98

4.4.4 Association of azole resistance with clinical diagnosis and demographics 98

4.4.5 WGS of 182 longitudinal *A. fumigatus* isolates 100

4.4.6 Genotypic characterisation of clinical *A. fumigatus* isolates 100

4.4.7 Genetic diversity of *A. fumigatus* isolates from the prospective chronic respiratory disease cohort. 102

4.4.8 Phylogenomic and population structure analysis of *A. fumigatus* in chronic respiratory disease cohorts 104

4.5 Discussion 107

Chapter 5 Environmental reservoirs of azole-resistant A. fumigatus detected in a Hospital setting 114

5.1 Abstract 114

5.2 Introduction 115

5.3 Methods 118

5.3.1 Impact of COVID-19 on environmental surveillance 118

5.3.2 Hospital sampling locations 118

5.3.3 Hospital Air Surveillance 120

5.3.4 Hospital Soil Surveillance 121

5.3.5 Spatiotemporal distribution of *A. fumigatus* CFUs 121

5.3.6 Isolation of *A. fumigatus* colonies 121

5.3.7 Antifungal susceptibility testing 121

5.3.8 gDNA extraction and quantification 122

5.3.9 Next Generation sequencing & Bioinformatic Analysis 122

5.3.10 Investigating a potential vector of azole resistance 122

5.3.11 Incorporation of clinical WGS from RBH respiratory disease cohort and the UK dataset 122

5.3.12 Phylogenomic analysis 123

5.3.14 Calculating unique pairwise SNPs 123

5.3.15 Multivariate analysis of genomic data 123

5.3.16 Statistical Analysis 123

5.4 Results 124

5.4.1 Sample Collection 124
5.4.2 Spatial distribution of CFUs 125
5.4.3 Temporal distribution of colony forming units 127
5.4.4 Pan-azole resistance detected within the hospital environment. 129
5.4.5 WGS of 102 *A. fumigatus* isolates from the hospital environment 129
5.4.6 Genotypic characterisation confirmed presence of *cyp51a* alleles 129
5.4.7 Genetic diversity and population structure of *A. fumigatus* in the hospital environment. 130
5.4.9 Epidemiological links between clinical and environmental isolates 135
5.5 Discussion 140
Chapter 6 Characterising azole resistant A. fumigatus in home environments of chronic respiratory disease cohorts. 145
6.1 Abstract 145
6.2 Introduction 145
6.3 Methods 148
6.3.1 Participant selection for home surveillance 148
6.3.2 Fine scale home surveillance: Case 34 148
6.3.3 Remote environmental surveillance 148
6.3.4 Sample Collection 149
6.3.5 Fungal cultivation 150
6.3.6 Sample Processing 150
6.3.7 Spatiotemporal distribution of *A. fumigatus* CFUs 152
6.3.8 Isolation of *A. fumigatus* colonies 152
6.3.9 Antifungal susceptibility testing 152
6.3.10 gDNA extraction and quantification 152
6.3.11 Next Generation sequencing & Bioinformatic Analysis 152
6.3.12 Phylogenomic analysis 153
6.3.13 Calculating pairwise SNPs 153

6.3.14 Incorporation of RBH clinical WGS 153
6.3.15 Multivariate analysis of genomic data 153
6.3.16 Statistical Analysis 153
6.5 Results 154
6.5.1 Patient participation and sample collection 154
6.5.2 Spatial distribution of CFUs 154
6.5.3 Azole resistance detected in 6/10 homes 155
6.5.4 Comparison of azole resistance in environmental *A. fumigatus* isolates from participants homes and the hospital 156
6.5.5 WGS of 101 *A. fumigatus* isolates from home environments 157
6.5.6 Genotypic Characterisation 157
6.5.7 Genetic diversity and population structure of *A. fumigatus* across home environments 158
6.5.8 No epidemiological links between home and clinical isolates 162
6.6 Discussion 163
Chapter 7 Concluding Remarks 166
Appendices 239

List of Figures

Figure 1.1. **Global triazole, diazole and benzimidazole use (tonnes) from 1990 to 2022**.....3

Figure 1.2. **Illustration of common azole resistance mechanisms that occur within *cyp51a* promoter and coding regions (adapted from Zhang et al., 2017)** 23

Figure 2.1. **Isolation of *A. fumigatus* and other moulds**.....41

Figure 2.2. **Isolation of yeasts.**.....41

Figure 2.3. **Susceptibility profiles of *A. fumigatus* to tebuconazole.** 45

Figure 3.1. **Geographical distribution of UK *A. fumigatus* isolates.** 60

Figure 3.2. **Distribution of *cyp51a* alleles in the UK dataset.**.....61

Figure 3.3. **Heatmap showing the percentage of azole resistant *A. fumigatus* isolates per genotype**.....62

Figure 3.4. **Phylogenetic analysis of UK *A. fumigatus* clinical and environmental isolates**.....64

Figure 3.5. **Distribution of nsSNPs in the coding regions of virulence related genes.** 66

Figure 3.6. **Heatmap of *A. fumigatus* metabolic activity across carbon sources.** 68

Figure 3.7. **Heatmap of *A. fumigatus* metabolic activity across nitrogen sources**.....69

Figure 3.8. **Heatmap of *A.fumigatus* metabolic activity under osmotic stress conditions** 70

Figure 3.9. **Heatmap of *A. fumigatus* metabolic activity under pH stress conditions** 71

Figure 3.10. **PCA of carbon utilisation kinetics** 73

Figure 3.11. **PLSA-DA of nitrogen utilisation kinetics** 74

Figure 3.12. **PLS-DA of osmolyte response kinetics**.....77

Figure 3.13. **PCA of pH response kinetics** 78

Figure 4.1. **Geographical distribution and clinical diagnosis of individuals participating in prospective clinical surveillance**. 94

Figure 4.2. **Azole resistance prevalence across the prospective chronic respiratory disease cohort.**.....95

Figure 4.3. **Effect of clinical diagnosis, gender and age on predicted probability of resistance**.96

Figure 4.4. **Distribution of *cyp51a* polymorphisms detected during prospective surveillance of individuals diagnosed with chronic respiratory diseases.** 98

Figure 4.5. **Genetic diversity of *A. fumigatus* isolates from the prospective chronic respiratory disease cohort.** 100

Figure 4.6. **Phylogenetic tree illustrating the evolutionary relationships of *A. fumigatus* isolates from individuals diagnosed chronic respiratory diseases.** 102

Figure 4.7. **DAPC of 300 *A. fumigatus* WGS from individuals with ABPA, CF, non-CF and CPA** 103

Figure 4.8. **Nucleotide diversity (π) of 300 *A. fumigatus* WGS from individuals with ABPA, CF, and CPA.** 103

Figure 5.1. **Hospital sampling locations.** 116

Figure 5.2. **Hospital air surveillance method.** 117

Figure 5.3. **Spatial distribution of *A. fumigatus* in the air at the Royal Brompton Hospital.** 123

Figure 5.4. **Spatial distribution of *A. fumigatus* in soils at the Royal Brompton Hospital.** 124

Figure 5.5. **Temporal distribution of *A. fumigatus* in air and soil samples at the Royal Brompton Hospital** 125

Figure 5.6. **Distribution of pairwise unique SNPs among *A. fumigatus* isolates collected from the hospital environment.** 128

Figure 5.7. **Phylogenetic tree illustrating the evolutionary relationships of environmental *A. fumigatus* isolates from the Royal Brompton Hospital.** 130

Figure 5.8. **DAPC based on SNP variants from hospital environmental samples.** 131

Figure 5.9. **Phylogenetic tree illustrating the evolutionary relationships of environmental *A. fumigatus* isolates from the Royal Brompton Hospital and clinical isolates from the RBH respiratory disease cohort.** 133

Figure 5.10. **Phylogenetic analysis and genotypic characterisation of UK *A. fumigatus* clinical and environmental isolates.** 134

Figure 5.11. **Distribution of *A. fumigatus* pairwise SNPs and genomic clustering** 136

Figure 6.1. **Average CFU counts from samples collected in participant homes** 151

Figure 6.2. **Average CFU counts across participating home environments** 151

Figure 6.3. **Comparison of azole resistance prevalence of hospital and home environments** 153

Figure 6.4. **Population diversity of *A. fumigatus* from the home environments of individuals with chronic respiratory diseases**.....156

Figure 6.5. **Phylogenetic tree illustrating the evolutionary relationships of environmental *A. fumigatus* isolates from home environments.**.....157

Figure 6.6 **Phylogenetic tree showing evolutionary relationships between *A. fumigatus* isolates from participant homes and corresponding clinical samples**.....158

List of tables

Table 1.1. Summary of Aspergillosis diseases (adapted from Latgé & Chamilos, 2020) 15

Table 2.1. Summary of Qubit™ working solution 49

Table 2.2. Summary of library preparation protocols and specific sequencers employed for each sequencing panel (2021-2023) during this PhD.....50

Table 3.1. List of isolates phenotypically characterised using the OmniLog® platform 59

Table 3.2. Univariate analysis of carbon substrates showing significant differences ($p < 0.05$) in utilisation between TR_{34}/L98H and *cyp51a* wildtype isolates of *A. fumigatus*. Statistical tests used include t-tests and Mann-Whitney tests.....75

Table 3.3. Univariate analysis of nitrogen substrates showing significant differences ($p < 0.05$) in utilisation between TR_{34}/L98H and *cyp51a* wildtype isolates of *A. fumigatus*. Statistical tests used include t-tests and Mann-Whitney tests.....78

Table 3.4. Univariate analysis of osmolyte stress tolerance showing significant differences ($p < 0.05$) between TR_{34}/L98H and *cyp51a* wildtype isolates of *A. fumigatus*. Statistical tests used include t-tests and Mann-Whitney tests 79

Table 3.5. Univariate analysis of pH stress tolerance showing significant differences ($p < 0.05$) between TR_{34}/L98H and wildtype *cyp51a* genotypes of *A. fumigatus*. Statistical tests used include t-tests and Mann-Whitney tests 81

Table 5.1. Summary of sampling effort for hospital surveillance, including the number of air and samples collected.....124

Table 5.2. Summary of genetically similar isolate pairs in the hospital environment sharing <6% of the observed genetic diversity.....131

Table 6.1. Summary of genetically similar isolate pairs from home environments sharing <3% of the observed genetic diversity. 160

Chapter 1 Introduction

1.1 Human associated mycoses

Fungi are intrinsic ecosystem engineers, and arguably one of the most important organisms on the planet. Their ecological success has resulted in a diversity of over 2.2 million species, with approximately 120,000 species currently described (1). Over 600 of these species have been characterised as opportunistic pathogens capable of thriving in hostile environments and evading human defence mechanisms (2,3). In nature, fungi are confronted by a multitude of biotic and abiotic stressors, including other competing microorganisms, nutrient starvation, pH imbalances and fluctuating thermal landscapes. In response, fungi have adapted elaborate mechanisms which enable a penetrative and absorptive mode of life. The production of extracellular digestive enzymes degrades complex organic matter such as cellulose and hemicellulose into simple sugars for cell growth and assimilation, otherwise known as 'osmotrophy' (4,5). Fungal osmotrophy is fundamentally influenced by the availability of environmental nutrients, which dictates how fungi occupy and adapt to their ecological niches. Consequently, these nutrient acquisition systems are inherently shaped by natural selection (5). Heterogenous nutrient availability in the external environment influences the transcriptional regulation of fungal nutrition genes, known as catabolic repression (6–8). Carbon catabolic repression is driven by glucose availability, the primary source for the carbon regulatory system, while ammonia and glutamine availability dictate the nitrogen regulatory system (9,10). In nutrient limited conditions, transcription of alternative uptake systems and catabolic enzymes are employed. In concert, fungi deploy secondary metabolites, either excreted directly into the environment or as volatiles, which contribute to resource acquisition, protection, competition and inter and intraspecific interactions (11). Toxic metabolites, known as mycotoxins, can contaminate human and livestock food and indoor environments, resulting in illness and economic losses (12). The most important genera of mycotoxigenic fungi include *Aspergillus, Alternarua, Claviceps, Fusarium*, *Penicillium* and *Stachybotrys* (12).

The remarkable adaptability of fungi has undoubtedly contributed to the global burden of fungal infections, which is predicted to affect between 8-49 million individuals annually, resulting in 1.5 - 4.6 million deaths, surpassing the mortality rates of both malaria and HIV/AIDS combined (13,14). As medical treatments and immunotherapies advance, the population of at-risk individuals increases, rendering them susceptible to the most critically important fungal pathogens. Despite this substantial burden, accurate assessments of the global burden of fungal pathogens are often limited by underfunded surveillance, limited diagnostics, and inadequate reporting systems (13,15). Notably, fungal research receives less than 1.5% of the total infectious disease research funding globally (16), highlighting a severe imbalance in funding allocation. Moreover, fewer than 10 countries have implemented national surveillance programs for fungal infections, and fewer than 20 maintain fungal reference diagnostic laboratories (17). Without significant interventions, projections indicate that the burden of fungal diseases could increase 3-fold by 2040 (14). Anthropogenic activities and climate change are likely to further impact fungal disease epidemiology and promote the establishment of fungal pathogens. With global temperatures predicted to rise by 1.5°F-5°C by 2050, research suggests that thermophilic pathogenic fungi could expand their geographic reach, leading to elevated rates of infection (18–21). Furthermore, the escalation of extreme weather events, such as floods and hurricanes, may contribute to the dispersal of fungal spores over vast distances (18,22). Anthropogenic activities such as urbanisation and deforestation, which leads to the loss of 10 million hectares of forest annually (23), further promotes the spread of pathogens into previously isolated areas (22,24).

Of all reported fungal deaths, approximately 90% are attributed to five genera *Cryptococcus, Candida, Histoplasma, Pneumocystis* and *Aspergillus* (25). Remarkably, up to 80% of these fatalities could be mitigated through improved access to advanced fungal diagnostics and effective antifungal therapies (15). However, the therapeutic efficacy of the limited antifungal drug classes is increasingly compromised by the emergence of drug-resistant fungal pathogens, driven in part by the extensive and often unregulated use of antifungal agents across multiple sectors (26–31). The stagnant pipeline for new antifungal agents is largely a consequence of the significant genetic homology between fungal

and human eukaryotic cells, which complicates the development of selective drug targets (32,33). Additionally, the lack of dedicated research initiatives and inadequate resource allocation has limited advances in antifungal drug discovery (34). Consequently, over the past two decades, few antifungal drugs have been approved, with the most recent class being the echinocandins, introduced in the early 2000s. In clinical settings, global consumption of antifungal agents has steadily increased, with an

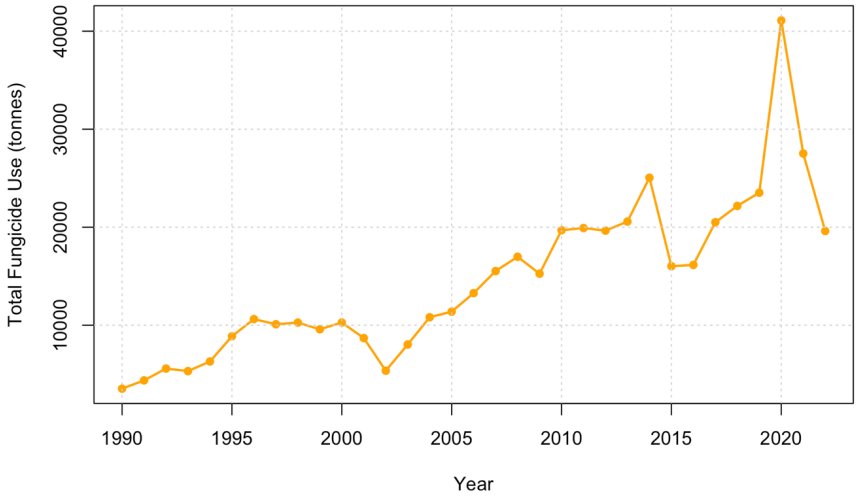


Figure 1.1. **Global triazole, diazole and benzimidazole usage (tonnes) from 1990 to 2022**. Annual trends in agricultural use of azole, diazole and benzimidazole fungicides based on FAOSTAT data from countries with available reports (FAOSTAT, 2024) (36).

estimated annual growth rate of 6.2% over the last decade (35). In agriculture, fungicides are the second most sold class of pesticides worldwide, accounting for 23% of total pesticide sales in 2020 (36). Since 1990, the global distribution of triazoles, diazoles, and benzimidazoles has reached over 40,000 tonnes, with an average annual increase of ~502 tonnes (Figure 1.1) (36). Pesticide sales demonstrate considerable variation across continents, with South America accounting for the highest proportion at 29%, followed by Asia (25%), North America (22%), and Europe (18%) (36,37). These variations are attributed to economic development, population density, regulatory frameworks, land use, and climate (37,38). Environmental applications, such as antifouling paints and wood preservation further expose fungal populations to antifungal agents, broadening the scope of resistance development (39). To combat the rising threat of antifungal resistance, a multi-sector "One Health" approach is crucial, recognising the interconnected nature of human, animal, and environmental health (34).

On October 25th, 2022, The World Health Organisation (WHO) identified emerging fungal pathogens as a major global health threat, emphasising the urgent need for enhanced diagnostics, robust surveillance, and accelerated development of novel antifungal treatments to combat the increasing prevalence of drug-resistant strains (40). The WHO's fungal priority pathogens list (FPPL) was modelled after the bacterial priority pathogens list, which successfully mobilised a global response to combat antibacterial resistance (41). Similarly, the FPPL aims to address the growing threat of antifungal resistance by enhancing global surveillance, promoting the development of affordable and accessible diagnostic tools, and significantly increasing financial support for research and development. The FPPL list includes 19 fungal pathogens, categorised on the severity of the risks they pose to human health, particularly to immunocompromised individuals. The pathogens are prioritised on several key factors, including their associated rates of mortality, prevalence of drug resistance, diagnostic and therapeutic limitations, and the overall global burden. Pathogens of the highest clinical concern include *Candida auris*, *Cryptococcus neoformans*, and *Aspergillus fumigatus*, identified for their substantial mortality rates, particularly among immunocompromised individuals, such as those undergoing solid organ or hematopoietic stem cell transplantation, as well as individuals with HIV/AIDS (16,42). These pathogens are also ranked due to their widespread resistance to current antifungal treatments, making infections exceptionally difficult to manage. The COVID-19 pandemic further highlighted the prevalence of fungal co-infections, particularly among hospitalised patients with severe cases and those on mechanical ventilation (43–45). Patients were notably susceptible to fungal co-infections, with *Candidiasis*, *Mucorales* and *Aspergillosis* being the most prevalent (45–48), emphasising the need for effective fungal infection management in the context of viral pandemics. The ordering of pathogens in the FPPL reflects a strategic focus on those that pose the most urgent threats to global health, particularly in vulnerable populations where infections can be rapidly fatal if not properly addressed.

1.2 Respiratory mycoses

Although fungal pathogens have the capacity to invade multiple organs, the primary route of infection is *via* the respiratory tract (13). Typically, in healthy individuals, conidia are quickly removed by mucociliary action, and those that are missed encounter neutrophils and alveolar macrophages, preventing attachment to the lung and subsequent infection (49). In susceptible individuals, such as those undergoing long-term corticosteroid or immunosuppressive therapy, suffering from hematologic malignancies, or facing prolonged critical care, exposure to environmental fungal spores is associated with severe health outcomes. Depending on the immune status of the host, outcomes can range from progressive respiratory decline and increased hospitalisation rates to mortality in the most severe cases (13). The threat is particularly acute for those with underlying respiratory conditions like asthma, chronic obstructive pulmonary disease (COPD), or cystic fibrosis (CF), where inhalation of fungal spores can precipitate exacerbations, complicate clinical management, and significantly worsen prognosis. Additionally, chronic respiratory diseases are often marked by persistent colonisation with fungal pathogens, necessitating long-term antifungal therapy to manage symptoms. However, sustained exposure to antifungal agents, can drive the development of drug resistance within these fungal populations. Consequently, many respiratory mycoses exhibit resistance to standard antifungal treatments, complicating management and underscoring the need for a deeper understanding of transmission pathways, and mechanisms of resistance.

This thesis centres on *A. fumigatus*, the most prevalent respiratory fungal pathogen, responsible for approximately 50% of the global burden of fungal diseases (14), and presenting significant challenges due to the rising threat of antifungal resistance. While *A. fumigatus* remains the primary focus, this introductory chapter also examines other notable respiratory fungi, including *Exophiala*, *Scedosporidium*, *Mucorales*, *Fusarium*, and *Cryptococcus*. Although these pathogens are less common, a comprehensive understanding of respiratory mycoses, particularly regarding antifungal resistance, surveillance strategies, and implications for patient management, is essential for managing fungal epidemics.

1.2.1 *Exophiala dermatitidis*

Exophiala dermatitidis is a melanised, yeast-like fungus exhibiting a broad environmental distribution. Typically found in soil and plant debris, *E. dermatitidis* also thrives in highly humid environments such as kitchens and dishwashers, where it colonises rubber seals through biofilm formation (50). Human infections caused by *Exophiala* species are relatively rare; however, reports of *E. dermatitidis* as a pathogen in both immunocompetent and immunocompromised individuals have notably increased (51–55). Infections by *E. dermatitidis* are categorised into three primary groups: superficial; cutaneous and subcutaneous; and systemic or visceral. Superficial infections are often associated with surgical procedures or trauma, whereas non-superficial infections are predominantly observed in patients with predisposing illness (56). Notably, individuals with CF exhibit a high prevalence of *E. dermatitidis*, which frequently colonises the respiratory tract and are considered pathogenic (57,58). The identification of *Exophiala* species is commonly achieved through the isolation of strains on Sabouraud dextrose agar (SDA) or erythritol chloramphenicol agar (ECA), followed by sequencing of fungal-specific internal transcribed spacer (ITS) regions, particularly ITS1 and ITS2 (59). Despite limited data on antifungal susceptibility, *Exophiala* infections are generally sensitive to azoles such as voriconazole, itraconazole, and posaconazole, but show reduced susceptibility to echinocandins and fluconazole (59,60). The *Exophiala* species complex is extensive, and considerable research has employed genomic analysis to investigate both environmental and clinical isolates. A notable study in 2021 analysed the genomes and transcriptomes of *E. dermatitidis* isolates, revealing that some strains can modify their transcriptomes to manage moderate stress before reverting to their original state, facilitating their survival and pathogenicity in human hosts (61). Complementary research utilising long-read sequencing and transcriptomics on *E. spinifera* highlighted similar adaptive strategies, suggesting that *Exophiala spp.* possess intrinsic mechanisms to adjust to different habitats and infect susceptible patient populations (62).

1.2.2 *Scedosporidium spp.*

The genus *Scedosporidium* encompasses several clinically relevant fungal species, including *Scedosporium apiospermum*, *Scedosporium boydii*, *Scedosporium aurantiacum*, *Scedosporium dehoogii*, and *Scedosporium minutisporum* (63,64). Patients with CF are particularly prone to chronic airway colonisation by *Scedosporium* species (65). However, the reported prevalence of *Scedosporium* in CF populations varies widely, largely due to the challenges in detecting and accurately diagnosing these infections (66). Prevalence estimates in CF patients range from 3.3% to 25.3% (67–70), a disparity that is partly due to the difficulties associated with isolating *Scedosporium* from clinical samples, as it is often outcompeted by other, more rapidly growing fungi (70). However, the utilisation of selective media, such as SceSel+, and nucleic acid sequencing techniques have markedly improved the detection rates of these culture-sensitive species (70,71). A major clinical challenge presented by *Scedosporium* species is their extensive resistance to a wide range of antifungal agents. These species commonly exhibit resistance to polyenes, such as amphotericin B and nystatin, and azoles, including fluconazole, itraconazole, and isavuconazole, while also demonstrating reduced susceptibility to echinocandins like caspofungin and anidulafungin (72–77). Furthermore, the heterogeneity in antifungal susceptibility among different *Scedosporium* species complicates treatment strategies, making the establishment of standardised therapeutic protocols more challenging (78,79). Consequently, accurate species identification and antifungal susceptibility testing are crucial to guiding effective treatment strategies and improving patient outcomes (77).

1.2.3 Mucormycosis

Mucormycosis is a rare, aggressive infection caused by filamentous fungi of the order Mucorales, predominantly reported in Asia, with morbidity and mortality rates ranging from 6.6% to over 30% (80,81). The most frequent causal agents of mucormycosis include *Rhizopus spp., Lichtheimia spp., Apophysomyces spp., Rhizomucor spp., Mucor spp.* and *Cunninghamella spp.* (82,83) and are commonly detected in patients with prolonged neutropenia, diabetes mellitus and recipients of solid organ or haematopoietic stem cell transplants (84–86). Despite its severity, the low prevalence of

mucormycosis results in a scarcity of comprehensive data on diagnosis, treatment, and epidemiology (81). Most available data come from case reports or small case series (83), which may not adequately capture the full spectrum of the disease or its outcomes. However, the emergence of mucormycosis in patients with COVID-19, particularly those in the Indian subcontinent (87) underscore the dynamic nature of its epidemiology and the need for ongoing vigilance and epidemiological surveillance. Standardising diagnostic criteria for mucormycosis is difficult due to its varied clinical presentations affecting sites such as the sinuses, brain, lungs, or skin, where overlapping symptoms can often result in misdiagnosis or delayed diagnosis (83). Traditional diagnostic methods for mucormycosis are often constrained by low culture sensitivity or require invasive histopathological examination, which may not always be practical or possible (86). Although traditionally considered a community-acquired infection, there has been a growing recognition of nosocomial cases. Several reports have documented instances of mucormycosis linked to contaminated medical supplies, such as wooden tongue depressors (88,89) and bandages (90). In a U.S nosocomial outbreak reported by Duffy *et al*., (91) *Rhizopus* species, a common cause of mucormycosis, was isolated from 42% of samples taken from contaminated linens, underscoring the importance of rigorous infection control practices, including regular monitoring of hospital hygiene standards and sterilisation procedures.

1.2.4 Fusaria

The genus *Fusarium* encompasses numerous plant pathogens renowned for their diverse infection mechanisms, such as vascular wilt by *F. oxysporum* (92), head blight in cereals by *F. graminearum* (93), root and stem rot by *F. solani* (94), and ear rot with mycotoxin production by *F. verticillioides* (95), all of which present substantial threats to global agricultural productivity (96,97). Certain *Fusarium* species have also emerged as opportunistic pathogens in humans, particularly affecting immunocompromised individuals, causing respiratory conditions such as allergic and chronic non-invasive sinusitis (98,99). In severe cases, disseminated *Fusarium* infections can spread to multiple organs, with mortality rates ranging from 50% to 80% (100–103). Current estimates indicate the global burden of *Fusarium* infections is approximately 1-1.2 million cases each year (13). The lungs are often affected, where pneumonia is a frequent complication in neutropenic patients with

systemic fusariosis, displaying clinical signs and outcomes similar to aspergillosis (104,105). Treating fusariosis, especially from *Fusarium solani*, is difficult due to the pathogen's intrinsic resistance to many antifungals, including echinocandins and azoles (106,107). This is further complicated by acquired resistance, such as the overexpression of efflux pumps and CYP51 genes linked to agricultural fungicide resistance, which can also affect medical antifungals, complicating treatment plans (108,109). Despite these challenges, polyene antifungal agents like natamycin have shown activity against *Fusarium* species and are frequently employed in combination therapies, such as with voriconazole, to treat Fusarium-associated fungal keratitis (106,110). The environmental prevalence of *Fusarium* in healthcare settings emphasises the risk of nosocomial infections. Surveillance studies have consistently recovered *Fusarium* species from hospital water systems, and molecular investigations have traced the transmission of conidia through airborne dispersal during activities such as showering, directly linking environmental isolates to patient infections (111).

1.2.5 *Cryptococcus gattii/neoformans* species complexes

Pulmonary cryptococcosis is an infection caused by the encapsulated yeasts *Cryptococcus neoformans* and *Cryptococcus gattii*. *C. neoformans* is primarily associated with environments contaminated by bird droppings (112), while *C. gattii* is found more frequently in soil, air, and water, as well as on various tree species, especially eucalyptus (113–115). Infection begins when airborne basidiospores are inhaled into the respiratory tract, potentially establishing pulmonary infection depending on the host's immune status and the virulence of the strain (116). Simultaneous or sequential inhalation of different strains of *C. neoformans* can lead to mixed infections, resulting in multiple yeast genotypes coexisting within the host (117). The pathogenicity of *C. neoformans* and *C. gattii* varies with the host's immune competence: *C. gattii* more frequently affects immunocompetent individuals, while *C. neoformans* is a major cause of cryptococcal meningitis, particularly in immunocompromised patients such as those with HIV/AIDS (118,119). Globally, *C. neoformans* is approximately nine times more commonly isolated than *C. gattii* (120,121). In the lower airways, pulmonary macrophages typically phagocytose and eliminate fungal cells. However, in immunocompromised individuals, these fungi can evade immune clearance, persist, and proliferate,

leading to pulmonary infection. This infection can progress to acute respiratory distress syndrome (ARDS) and potentially disseminate to other sites, including the central nervous system (CNS), causing cryptococcal meningitis (120,122–124).

Diagnosing pulmonary cryptococcosis is radiologically challenging due to its nonspecific presentation, often resembling infections such as tuberculosis, pneumonia, or malignancies (124). Consequently, accurate diagnosis relies on traditional laboratory methods involving the identification of encapsulated *Cryptococcus* yeasts or culturing the organism from respiratory specimens (125). During hematogenous dissemination, identification can be achieved through cryptococcal antigen (CrAg) testing and fungal blood cultures, which detect the presence of the pathogen in the bloodstream (125). Recent advancements, particularly the introduction of lateral flow assays for CrAg detection, have greatly enhanced diagnostic accuracy and speed, enabling earlier diagnosis and intervention across various clinical settings. Analysis of bio-banked samples from a Ugandan cohort demonstrated that blood CrAg was detectable a median of 22 days before the onset of symptoms of cryptococcal meningitis, highlighting the potential for early identification and pre-emptive treatment in high-risk populations (126).

Over the past decade, the global incidence of HIV-associated cryptococcal meningitis has declined, yet it still accounts for about 19% of AIDS-related deaths (127,128). This decline is primarily attributed to improved access to antiretroviral therapy (ART), which has reduced the overall burden of HIV, as well as the expansion of CrAg screening programs and the use of pre-emptive antifungal therapy in patients who test positive for the antigen (120). These strategies have collectively contributed to earlier detection and treatment, thereby reducing the progression to severe disease and associated mortality. The global epidemiology of non-HIV cryptococcal meningitis is unclear, but incidence is rising in high-income countries due to more immunosuppressive therapy and aging populations with multiple comorbidities (129).

1.3 *Aspergillus fumigatus*

A. fumigatus, is a ubiquitous environmental saprobe and opportunistic fungal pathogen, primarily found in soil and decaying vegetation. It plays a fundamental ecological role in decomposition and nutrient recycling, facilitated by the secretion of hydrolytic enzymes that degrade complex organic matter into simpler compounds (130–132). The extensive production and efficient dispersal of aerosolised conidia allow *A. fumigatus* to achieve a broad geographical distribution, facilitating its colonisation of diverse environments and adaptation to distinct ecological niches (133,134). *A. fumigatus* demonstrates exceptional resilience to biotic and abiotic stresses, enabling it to thrive in extreme environments. It has been isolated from Antarctic penguin nests, indicating its ability to withstand sub-zero temperatures and desiccation (135), while also persisting in arid desert soils, enduring significant heat fluctuations (136). Most interestingly, it has been found decomposing carbon-based radioactive debris from within the Chernobyl nuclear reactor site (137), and on board the International Space Station, surviving microgravity, limited nutrient availability and heightened radiation levels (138). Among the 300 known species of aspergilli described (139), approximately 50 are recognised as human pathogens, with *A. fumigatus* being the most clinically relevant (140,141). The primary route of infection occurs via the inhalation of aerosolised conidia, with humans estimated to inhale up to 1,000 spores daily (132). At 2–3 μm in size, some conidia can reach the distal airways, potentially triggering a spectrum of respiratory diseases. For susceptible individuals, repeated inhalation of these spores poses a significant health risk, potentially leading to a range of respiratory symptoms, from mild allergic reactions to severe fungal infections (13).

1.3.1 Interaction with host immune response

Upon inhalation, *A. fumigatus* conidia can penetrate deep into the pulmonary alveoli. At this initial stage, the negatively charged carbohydrates on their surface facilitate adhesion to host proteins such as fibronectin and laminin, marking the critical first step in establishing an infection (142,143). The cell wall of *A. fumigatus* is central to its pathogenicity, serving as both a protective barrier and a means for immune evasion (144,145). The outermost layer of the cell wall, primarily composed of

hydrophobin proteins, form a hydrophobic coating that effectively masks the underlying cell wall components from immune detection (146). *RodA*, is the most important and well-characterized of these hydrophobins (147), concealing pathogen-associated molecular patterns (PAMPs) from pattern recognition receptors (PRRs) that would otherwise trigger an immune response (148). In healthy individuals, inhaled conidia are typically removed by mucociliary clearance, a vital first line defence of the respiratory tract. This mechanism relies on the coordinated action of pulmonary cilia and mucus, which trap and transport conidia out of the respiratory tract (149–151). However, mucociliary dysfunction is common in respiratory diseases. In individuals with impaired mucosal defences, such as those with bronchiectasis or preexisting lung cavities, conidia may germinate into hyphae, provoking an inflammatory response. Individuals with CF, a genetic disorder linked to a defective CF transmembrane conductance regulator (CFTR) gene, are particularly susceptible to *A. fumigatus* colonisation which can lead to decreased lung functioning (152,153). In CF, reduced chloride secretion leads to increased sodium and water absorption, resulting in dehydrated, poorly cleared mucus. Consequently, it is estimated that 30-80% of CF patients persistently test positive for *A. fumigatus* in their sputum samples (154–156) and over 90% of CF-related mortality is due to pulmonary infections (157).

As conidia mature, the proteinaceous hydrophobic layer is lost, exposing the inner cell wall (147). The cell wall contains several polysaccharides, including b-glucan, chitin, mannan and galactomannan, which bind to PRRs triggering a signalling cascade, activating recruitment of additional phagocytes (158–160). During infection, fugal β-glucan accumulation correlates with inflammatory responses such as neutrophil recruitment (161), while galactomannan is released as a principal exoantigen during tissue invasion (143). Chitin, another critical polysaccharide in the fungal cell wall, is essential for maintaining cell wall structure and has been a target for antifungals (162). Following germination, the hyphae of *A. fumigatus* invade alveolar endothelial cells and extend into pulmonary arterioles (163), causing endothelial cell damage, inflammation, activation of the coagulation cascade, and intravascular coagulation (164). These events lead to tissue hypoperfusion, necrosis, and an environment conducive to fungal survival and proliferation (165). *A. fumigatus* produces several

metabolites that further contribute to its virulence. Gliotoxin, one of the most toxic and well characterised fungal metabolites, induces apoptosis in macrophages (166). Helvolic acid, found in higher concentrations, inhibits the oxidative burst of macrophages (167), and ruptures epithelial cells (168), while fumagillin, a potent inhibitor of angiogenesis, affects endothelial cell proliferation and ciliary function of the respiratory epithelium, further compromising the host's ability to clear the fungus (169).

1.3.2 Aspergillosis

Aspergillosis encompasses a range of respiratory diseases caused by Aspergillus species, broadly classified as invasive, saprophytic, or allergic (170) (Table 1.1.). Allergic aspergillosis includes allergic bronchopulmonary aspergillosis (ABPA) and severe asthma with fungal sensitisation. ABPA results from hypersensitivity to Aspergillus allergens due to impaired immune clearance, enabling fungal hyphae formation. It is often associated with individuals diagnosed with reduced lung functioning such as those with asthma, CF and bronchiectasis (171,172). Asthma affects over 357 million individuals worldwide, with an estimated 2.5% diagnosed with ABPA (173–175). In India however, ABPA is more common, with prevalence estimated at 5% (175–177). Estimates of ABPA among individuals with CF show considerable variation, ranging from 3%-25%, influenced by multiple factors including geographic variation, differences in diagnostic criteria, and disparities in the populations studied, such as age groups (178). However, However, pooled data indicates that the prevalence of ABPA in individuals with CF is approximately 8.9% (178). In individuals with structural lung diseases, such as those with a history of tuberculosis, COPD, or sarcoidosis, *Aspergillus* infections can result in chronic pulmonary aspergillosis (CPA), a condition characterised by the gradual degradation of lung tissue and often associated with the formation of aspergillomas that develop in pre-existing lung cavities (179). CPA progressively impairs respiratory function, significantly diminishing patient quality of life and increasing the risk of further complications. It's a condition that, together with candidemia/invasive candidiasis, accounts for around 39%–45% of the total death and DALY burden from fungal diseases (14). Treatment is relatively expensive in most countries and typically requires daily antifungal medication for 6 to 12 months (14), which increases the risk for

resistance development, especially in cases where adherence to long-term therapy is inconsistent or interrupted. Diagnosis of CPA relies primarily on chronic symptoms lasting more than three months in generally immunocompetent individuals, combined with radiological findings of lung cavities that may or may not contain an aspergilloma (180). However, the clinical presentation and radiological features of CPA often overlap with those of the underlying pulmonary conditions, such as tuberculosis or COPD, complicating accurate diagnosis (181,182). CPA is estimated to affect over 3 million people worldwide, with a reported mortality rate of at least 15% within the first six months following diagnosis (13). Pulmonary tuberculosis (PTB) is a significant risk factor, with approximately 1.2 million cases attributed to previously treated PTB, contributing to a greater disease burden in areas where PTB is prevalent (182,183). Invasive aspergillosis (IA) stands among the most life-threatening fungal diseases, primarily affecting severely immunocompromised individuals and associated with exceptionally high morbidity with mortality rates of up to 85% (13,175,184,185). While prevalence can vary significantly between geographical regions and patient populations globally, it is estimated that over 2 million people develop IA annually (175). Populations at greatest risk for developing IA include those with underlying haematological malignancies, cancers, and HIV/AIDS, as well as recipients of solid organ transplants and critically ill patients, particularly those in intensive care units (186). Current estimates suggest that approximately 63,000 patients develop IA within ICUs annually, highlighting the critical need for effective prevention and management strategies (14). Similarly, patients with advanced liver cirrhosis and those undergoing prolonged corticosteroid therapy are also considered at elevated risk for IA (186,187). The COVID-19 pandemic has further expanded the at at-risk groups for IA, with emerging reports of COVID-19-associated pulmonary aspergillosis (CAPA) (48). Additionally, individuals with chronic respiratory diseases such as CF, ABPA and CPA are especially vulnerable to chronic microbial colonisation, substantially increasing their risk of developing IA.

Table.1.1. Summary of Aspergillosis diseases (adapted from Latgé & Chamilos, 2020 (556))

Aspergillosis disease		Pathogenesis	Symptoms	Predisposing factors	Treatments
Hypersensitivity	ABPA	Hypersensitivity to *Aspergillus* allergens due to impaired immune clearance, allowing fungal hyphae formation.	Wheezing, low-grade chronic fevers and cough, sputum containing brown mucus and plugs, chest pain, sputum.	Asthma, CF, bronchiectasis, genetic predisposition environmental exposure to spores (170).	Oral and inhaled corticosteroids to modulate the immune response. Triazoles: itraconazole voriconazole, posaconazole, and isavuconazole to reduce fungal burden (188,189).
	Severe Asthma with fungal sensitivity (SAFS)	Asthma: Inflammatory disorder of the airways characterised by airflow limitation and airway hyperresponsiveness (190). SAFS: Steroid-resistant asthma with fungal sensitisation to fungal allergens in the absence of ABPA.	Chest tightness, cough and wheeze.	Allergic rhinitis or chronic sinusitis, poor asthma control. Indoor environmental exposure (188).	Antifungal azoles can be useful in the treatment of SAFS (189).
Structural Diseases	Aspergilloma & CPA	Aspergilloma: Saprophytic colonisation of the fungus in a preexisting pulmonary cavity consists of both dead and living mycelial elements, inflammatory cells, fibrin, mucus, and components of degenerating blood and epithelia. CPA: Persistent fungal colonisation or infection, leading to chronic inflammation, lung tissue damage, and fibrosis. Defects in mucociliary clearance associated with structural lung disease and deregulated inflammatory responses.	Persistent (>3 months) symptoms of chronic inflammation, chronic productive cough and weight loss, fatigue, mild hemoptysis.	Aspergilloma: Pre-existing cavities due to TB, COPD, Sarcoidosis, Bronchiectasis CPA: most commonly due to pulmonary tuberculosis (TB). Also, emphysema, and COPD, or other chronic structural lung abnormalities.	Aspergilloma: Surgical removal – often associated with significant complications. CPA requires prolonged use of antifungal agents Itraconazole and voriconazole are regarded as the treatment of choice (179,190,191)
Immunodeficiency	IA	Germination of spores & invasion into lung tissue, respiratory epithelium and blood vessels (angioinvasion). Tissue necrosis and potential dissemination to other organs	Fever, chest pain, hemoptysis, shortness of breath	HIV/AIDS, solid-organ transplant recipients. Critically ill patients admitted to the ICU with severe influenza (192) or other viral infections Hematological malignancies, or inflammatory diseases	Voriconazole preferred drug for first-line therapy (193). Posaconazole, regarded as an alternative therapeutic option (141)

1.3.3 Environmental reservoirs of *A. fumigatus*

Seasonal variations in *A. fumigatus* spore concentrations are well-documented, often correlating with the availability of organic substrates, such as decaying leaves, which provide a rich source of nutrients that promote fungal proliferation (194). Reported annual airborne concentrations of *A. fumigatus* typically range from 0.3 to 13 colony-forming units (CFUs) per cubic meter (m^3) (195,196), though episodic spikes up to 400 CFUs/m^3 have also been observed (195). As a thermotolerant fungus, *A. fumigatus* thrives in warm, organic-rich environments such as self-heating compost heaps, where spore densities can reach 10^6 to 10^7 CFU per gram of dry weight (197). Industrial composting processes, especially those involving agitation, can release large quantities of spores into the air, with concentrations ranging from 10^4 to 10^7 CFUs/m^3 (195,198). Epidemiological evidence suggests a correlation between occupational exposure to high concentrations of airborne spores and the development of aspergillosis. Workers in industries handling compost, landfill materials, or sewage sludge are frequently exposed to elevated levels of *A. fumigatus* spores, which can lead to diseases such as ABPA and hypersensitivity pneumonitis (199–201). Cases include a garbage collector developing ABPA likely due to continuous exposure to household waste (202) and 7% of workers in an Indian sugar mill diagnosed with ABPA, where *A. fumigatus* comprised 44-55% of environmental fungal counts (203). Similar cases have been documented among workers in soybean processing factories in Japan, where exposure to *Aspergillus oryzae*, a related species used in fermentation, posed a substantial risk (204). However, these studies often lack longitudinal data and control groups, limiting the ability to definitively attribute ABPA to occupational exposure alone. In the home environment, dust is a significant reservoir for *A. fumigatus* spores, which can accumulate in areas such as loft spaces, basements, and other infrequently cleaned locations. Certain food products, including tea, biscuits, fruits, and spices, have also been identified as vectors for *A. fumigatus* conidia (205,206). Both tobacco and marijuana smoking have been shown to release substantial quantities of fungal spores into the air (207). Routine activities, such as gardening and household cleaning can aerosolise *A. fumigatus* spores, thus elevating the risk of inhalation and subsequent infection.

Given the inevitable exposure to *A. fumigatus* conidia, hospitals must adopt rigorous monitoring and control strategies to safeguard immunocompromised patients. Regular environmental surveillance, including air sampling, is key to evaluating the effectiveness of infection control measures and to identify areas requiring further intervention. Air surveillance during hospital construction and renovation often revels elevated levels of *Aspergillus* spore concentrations, significantly increasing the risk of exposure for immunocompromised individuals (208–211). High-efficiency particulate air (HEPA) filtration systems are recommended for their proven ability to lower airborne spore levels and reduce the incidence of IA (212–214). However, dust containing spores can accumulate within air ducts and other infrequently cleaned areas, leading to the release of spores when disturbed (215,216). Viable *Aspergillus* conidia are frequently isolated from various hospital environments, including carpets, walls, sinks, trolleys, blankets and beds and medical devices (217). Additionally, contaminated medical supplies such as intravenous catheters, arm boards, and bedding can act as potential reservoirs for *Aspergillus* spores, contributing to nosocomial transmission (218). *A. fumigatus* spores present in water systems can become aerosolised during routine activities like patient showering, introducing another significant route of exposure to hospital occupants (219). The relative impact and importance of environmental sources is unknown and most likely varies for each patient, depending on their amount of exposure and severity of immunosuppression. Although *A. fumigatus* accounts for only about 0.3% of airborne spores in hospitals, it is responsible for roughly 90% of systemic *Aspergillus* infections (220), likely due to its unique virulence factors (221).

1.3.4 Life cycle and adaptation strategies

1.3.4.1 Asexual lifecycle

In *A. fumigatus*, asexual reproduction begins with the formation and dispersal of asexual spores called conidia. These conidia, formed at the tips of specialised hyphae known as conidiophores, are released into the environment where they can remain dormant, enduring harsh conditions until they encounter nutrient rich conditions favourable for growth. When a haploid spore germinates, the conidium swells producing a germ tube that elongates by apical extension, a process driven by the continuous addition of new cell wall components at the growing tip. The germ tubes continue to grow and branch outward,

creating a dense network of hyphae that expands through repeated mitotic divisions to form mycelium, the main vegetative structure of the fungus. The mycelium extends its hyphal tips through the surrounding substrate, secreting enzymes that break down complex organic material, enabling the fungus to absorb nutrients. As the mycelium matures, some hyphal cells differentiate into aerial hyphae, which develop a foot cell at the base and a conidiophore at the apex. At the tip of the conidiophore, a vesicle forms, providing a base for conidia formation. The vesicle surface produces phialides, which are conidiogenous cells arranged in a radiating pattern. These cells undergo multiple rounds of mitotic division to generate chains of conidia. The conidia are produced in a sequential manner, ensuring a continuous supply of spores for dispersal and colonisation. Asexual reproduction is central to the ecological success and pathogenicity of *A. fumigatus*. A single colony can generate up to 10^9 asexual spores within a week, enabling rapid and widespread dispersal across diverse environments, from soil and decaying organic matter to the airways of a susceptible host (222). These conidia are generally clonal, preserving advantageous genetic combinations that have been well-adapted to their environment. Although asexual, this high reproductive output allows for rare genetic mutations that may confer an adaptive advantage under selective pressures, enhancing the survival of the fungus in hostile or rapidly changing conditions (222). In the multicellular mycelium, recessive mutations are usually masked by dominant alleles, but in single-celled conidia, mutations are expressed immediately, allowing beneficial traits to be rapidly selected (223). Beyond asexual reproduction, *A. fumigatus* employs other reproductive modes, including parasexual recombination and sexual cycles, which generate further genetic diversity. These alternative reproductive strategies enhance the pathogen's adaptability, ensuring its continued survival and ecological dominance.

1.3.4.2 Sexual lifecycle

The sexual lifecycle of *A. fumigatus* remained largely unresolved until 2009, when researchers successfully initiated a heterothallic sexual cycle in vitro (224). It was discovered that under nutrient limited conditions, *A. fumigatus* can undergo sexual reproduction, resulting in the formation of cleistothecia, resilient fruiting bodies capable of withstanding extreme environments (225). Sexual reproduction involves considerable metabolic costs, including energy investment in the production of

fruiting bodies and the challenge of locating a genetically compatible mating partner. However, sexual recombination facilitates the exchange of genetic material, producing genetically diverse progeny better equipped for survival and adaption to fluctuating environmental conditions (226). This genetic mixing mitigates clonal interference, preventing deleterious mutations hitchhiking to fixation with the population (227). The process of sexual reproduction relies on the presence of two compatible mating types, determined by genes at a single 'MAT' locus, 'MAT1-1' and 'MAT1-2,' which contains either a *MAT1-1* or *MAT1-2* "idiomorph" highly divergent in sequence (228,229). Although morphologically identical, the two mating types produce distinct peptide pheromones that promote recognition and attraction between compatible partners. Upon encountering an opposite mating type, the hyphae undergo plasmogamy, leading to the formation of diploid zygotes, which subsequently undergo meiosis to generate haploid ascospores (230). These ascospores contribute to genetic diversity and can be dispersed to new environments, enhancing the species' ability to adapt. *A. fumigatus* requires highly specific conditions for sexual reproduction, a temperature of 30 °C on oatmeal agar in complete darkness for a period of 3 to 6 months (224). The natural habitat for the formation of ascospores remains unidentified, yet some hypothesise that composting plant material may provide the ideal environment (231). It seems improbable that the sexual cycle occurs within the human body, as opposing mating types are required to initiate a sexual cycle, as well as highly specific environmental and nutritional conditions (232).

1.3.4.3 Parasexual cycle

The parasexual cycle, first described in *Aspergillus nidulans* in the 1950s (233) and later identified in *A. fumigatus* over a decade later (234), represents a distinct mechanism of genetic recombination, separate from the sexual cycle. The parasexual cycle begins with the fusion of two compatible hyphae, leading to the formation of a heterokaryon that contains two or more genetically distinct nuclei within a shared cytoplasm. Here, the nuclei can undergo karyogamy, resulting in a heterozygous diploid nucleus. Subsequently, the diploid nucleus can undergo mitotic recombination, generating diverse genotypes through chromosomal rearrangement (235). While the parasexual cycle can enhance genetic diversity, it is often limited by heterokaryon incompatibility, which prevents the fusion of

genetically distinct hyphae (223,236). Despite this, it remains a key process for generating diversity, assisting *A. fumigatus* in adapting to challenging environments like the human lung. In clinical settings, the parasexual cycle is frequently observed among patients with severe lung diseases, highlighting its role in the adaptability and pathogenicity of *A. fumigatus* (235). In CF, *A. fumigatus* often colonises the epithelial mucus, forming biofilms that shield it from a range of stressors, including competing microorganisms, antifungal drugs, and host immune responses (237,238). To investigate whether parasexual recombination serves as a mechanism for generating genetic diversity in chronic biofilms, a study screened 799 isolates for diploid formation, a hallmark of parasex (235). The results demonstrated that diploids were present in isolates from CF patients, while none were identified in acute infection or environmental samples.

1.4 Azole resistant *A. fumigatus*

1.4.1 Clinically acquired azole resistance

Until the 1990s, intravenous amphotericin B, was the cornerstone of aspergillosis treatment due to its potent and rapid fungicidal activity. Despite decades of extensive clinical use, the polyene amphotericin B maintains efficacy against a broad spectrum of fungi, including *A. fumigatus*, with minimal emergence of resistance reported (239,240). However, the clinical use of amphotericin B is significantly limited by its toxicity profile, particularly nephrotoxicity, which has been documented in over 50% of patients in certain cohorts (241–244). The introduction of itraconazole in the early 1990s marked a significant advance in antifungal therapy, offering an oral alternative with a substantially reduced toxicity profile compared to amphotericin B (245,246). Itraconazole quickly became a preferred option for many clinicians due to its broader spectrum of activity, improved tolerability, and ease of administration. However, by the late 1990s, the emergence of clinical resistance to itraconazole (247) revealed the adaptive capacity of *Aspergillus* species, instigating efforts to enhance the monitoring of antifungal resistance.

Newer antifungal agents, such as second-generation azoles (voriconazole, posaconazole, and isavuconazole), and echinocandins, expanded the therapeutic arsenal, providing safer and more

effective therapies. Triazoles, are considered the first-line treatment for aspergillosis due to their broad-spectrum antifungal activity, low toxicity, and oral availability, which improve patient convenience and reduce treatment costs (248–251). Their primary mode of action involves inhibiting the lanosterol 14-α-demethylase enzyme, encoded by *cyp51a*. Resistance to azole compounds primarily arises due to the selective pressure they exert across various environments, which favour the survival and proliferation of resistant strains (252–254). In *A. fumigatus*, azole resistance is often driven by nonsynonymous mutations in *cyp51A*. These mutations induce conformational changes in the enzymes structure, reducing the binding affinity of azoles and thereby diminishing their antifungal efficacy (251,255,256). Additionally, triazoles can exhibit fungistatic activity against *Aspergillus* species, primarily inhibiting fungal growth without achieving complete eradication, thereby allowing the potential for resistance development (240). For example, one study demonstrated that voriconazole exhibited fungistatic activity against 94% of *A. fumigatus* clinical isolates, indicating that the fungus could survive and potentially adapt in an azole rich environment (240). The clinical management of azole-resistant infections is further complicated by the frequent cross-resistance observed among *A. fumigatus* isolates. For instance, in France, voriconazole resistance was detected in 4.9% of patients and itraconazole resistance in 14.3%, with 95% of voriconazole-resistant isolates also exhibiting cross-resistance to itraconazole (257). Cross-resistance significantly limits treatment options, necessitating the use of alternative therapeutic strategies. Alternative therapies include amphotericin B, though often restricted due to significant toxicity, and the echinocandins. Echinocandins are generally well tolerated but have limited efficacy against *Aspergillus* species due to their fungistatic properties. Consequently, they are often used in combination with other antifungals to enhance therapeutic outcomes, which can complicate treatment regimens and increase the risk of drug interactions and adverse effect (258,259).

In host evolution of azole resistance presents a substantial clinical challenge, particularly in patients with chronic respiratory diseases where persistent fungal infections are prevalent. Initial isolates often display an azole susceptible phenotype, but resistance can emerge with prolonged antifungal exposure (260). This adaptive evolution, frequently seen in chronic infections, underscores the challenges in managing these cases. Pulmonary cavities associated with CPA and aspergillomas

provide microenvironments conducive to fungal growth and asexual sporulation, increasing spontaneous genetic mutations under azole therapy pressure (222,260–263). A study of 154 patients, mostly with CPA, demonstrated a strong correlation between prolonged itraconazole treatment (exceeding 115 days) and resistance development, with all resistant isolates stemming from such cases (264). Aspergillomas, which form dense biofilm-like structures within lung cavities, may contain conidiophores, which play a crucial role for the development of resistant mutations (264). In CPA, the emergence of azole resistance has been shown to contribute to therapeutic failure where azole-resistant strains render standard azole therapy ineffective (261). A similar pattern of in-host evolution is observed in CF patients. The combination of persistent infection and variable, often subtherapeutic azole dosing significantly increases the risk of resistance, with an estimated ~20% probability of developing azole resistance within two years of continuous exposure (265). However, the precise mechanisms by which resistance develops in these patients is unclear. A recent study found that parasexual recombination in *A. fumigatus* biofilms, especially in CF patients, contributes to genetic diversity (235). Among 799 isolates screened, 11 diploid strains were identified, primarily from CF patients, indicating parasexual recombination. The formation of diploids was linked to elevated mutation rates and the production of diverse haploid offspring, including strains resistant to voriconazole (235).

Some patients are infected with *A. fumigatus* strains harbouring pre-adapted antifungal resistance mechanisms, despite never receiving antifungal therapy, indicating an environmental route of transmission and further complicating the management of aspergillosis (266). The rise of environmentally acquired azole-resistant *A. fumigatus* poses a severe challenge in treating aspergillosis, particularly in immunocompromised patients, where the rapid onset of IA often requires early and aggressive treatment. Histology of IA tissue shows *A. fumigatus* grows through hyphal elongation, limiting genetic variation and significantly reducing the risk of developing resistance during treatment (263). Consequently, immunocompromised individuals are particularly vulnerable to environmentally acquired azole resistance (267,268). Azole-resistant infections in IA carry a devastating 21% increase in overall mortality compared to azole-sensitive infections, underscoring

the urgent need to address environmental reservoirs of resistance to improve patient survival outcomes (269–271).

1.4.2 Environmentally acquired azole resistance

The pervasive use of environmental azoles has played a substantial role in the emergence of azole-resistant *A. fumigatus* within clinical settings. The molecular similarity between agricultural azoles, such as propiconazole and tebuconazole, and those used in medical treatments indicates that agricultural practices facilitate the selection and dissemination of azole resistance beyond clinical settings (272), emphasising the need for coordinated antifungal stewardship to mitigate the impact on clinical outcomes (34).

Since their introduction in the 1970s, agricultural azoles have played a central role in controlling fungal diseases across agriculture and horticulture, providing protection for a diverse range of crops, including cereals, rice, oilseed rape, sugar beet, banana, citrus, and soybeans, as well as being applied in amenity grass, wood preservation, and as plant growth regulators (273). Azole antifungals are the most widely used class of fungicides in agriculture, surpassing others such as benzimidazoles, dicarboximides, quinone outside inhibitors (QOIs), and carboxylic acid amides (CAAs), due to their cost-effectiveness, high efficiency, broad-spectrum activity, and environmental persistence (109,274). Beyond agriculture, azoles are also widely used in industrial applications, as biocides in paints, coatings, wallpaper paste, clothing, and wood preservatives, creating a widespread environmental presence of these compounds resulting in subsequent exposure and resistance development (275). Over 25 different azole compounds have been developed for diverse environmental uses, representing 20-25% of the global fungicide market (273), with azole fungicides prothioconazole, epoxiconazole and tebuconazole being some of the most used fungicide in the United Kingdom (UK) (39). The widespread use of azoles across multiple sectors has led to significant contamination in soils, wastewater, and sewage sludge (276).

Soil and air represent key reservoirs for the evolution and dissemination of azole-resistant *Aspergillus fumigatus*. In compost heaps, triazole-resistant isolates were detected in 91% of triazole-exposed compost samples, compared to just 2% in non-exposed compost (231), highlighting the role of environmental azole fungicide exposure in driving resistance. A UK-wide surveillance study identified azole resistance in ~ 4% of air samples and 14% of soil samples (277). Genomic analysis showed no significant genetic divergence between resistant strains in the environment and those infecting patients, highting that at least 40% of azole-resistant *A. fumigatus* infections in humans are likely derived from environmental sources (277).

Environmentally derived azole-resistant phenotypes commonly emerge from specific mutations in *cyp51a*, including point mutations that result in amino acid substitutions, and structural variants such as the insertion of tandem repeats (TR) in the promoter region, which result in gene overexpression and reduced drug binding affinity (278). Genotypes, such as TR_{34}/L98H and TR_{46}/Y121F/T289A (Figure 1.2), have become predominant contributors to resistance in both clinical and environmental settings.

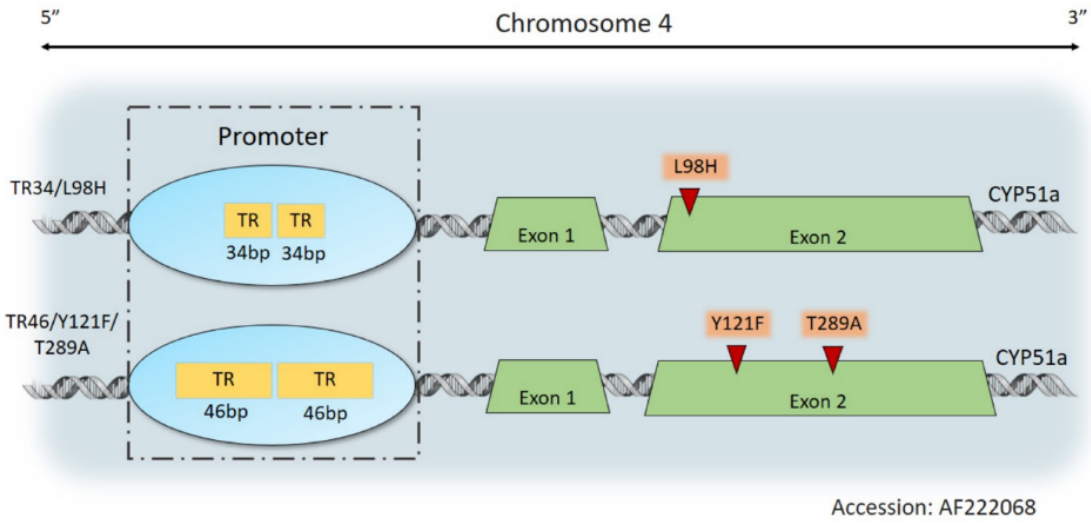


Figure 1.2. **Illustration of common azole-resistance mutations that occur within the cyp51A gene within the promoter and coding regions (adapted from Zhang et al., 2017)** (231).

The emergence and widespread distribution of these resistant genotypes raise significant concerns, particularly as they often appear on clonally related backgrounds, suggesting a complex interplay between *de novo* mutation events and clonal expansion driven by environmental and anthropogenic pressures (279). The TR_{34}/L98H genotype, first detected in the Netherlands in 1998, has since achieved global prevalence, particularly across Europe, with increasing reports from other continents (280,281). Epidemiological surveillance conducted by University Medical Centres (UMCs) in the Netherlands has increasingly highlighted the importance of environmental reservoirs as a significant source of azole-resistant aspergillosis. Strikingly, up to 80-90% of clinical isolates exhibiting azole resistance harbour resistance mechanisms typically associated with environmental strains, such as the TR_{34}/L98H and TR_{46}/Y121F/T289A alleles (282). Supporting this notion, Snelders *et al*., (254) demonstrated that azole-resistant *A. fumigatus* strains from the environment could transmit to human hosts, identifying the TR_{34}/L98H resistance allele in both clinical samples and environmental sources, such as hospital flower beds, commercial seeds, leaves, and compost. The high degree of genetic homology between clinical and environmental isolates provides compelling evidence for the existence of an environmental transmission pathway. Several case reports further illustrate this link. A French farmer developed IA with the TR_{34}/L98H mutation after working in fungicide-treated fields where TR_{34}/L98H resistant strains were found (283). Similarly, a woodworker developed sinonasal aspergillosis from a strain with the TR_{34}/L98H mutation; subsequent environmental sampling at sawmills confirmed the presence of TR_{34}/L98H resistant strains (284). In Spain, four cases of IA were diagnosed within a four-month period, three of which involved azole-resistant strains carrying TR_{34}/L98H (285). Another Spanish case revealed isogenic TR_{34}/L98H and G448S azole-resistant strains in both a patient and the hospital environment, underscoring hospitals as potential sources of resistant infections (286). Such findings highlight the growing dominance of azole-resistant TR_{34}/L98H *A. fumigatus* strains in clinical environments (287).

1.4.3 Patient-to-environment transmission pathways

Some evidence supports a patient-to-environment transmission pathway. In a 2018 nosocomial surveillance study, continuous airborne fungal monitoring with electrostatic dust-fall collectors

(EDCs) identified a patient's airway as the primary source of airborne *A. fumigatus* contamination, following unsuccessful environmental surveillance efforts to detect the organism within the hospital environment (288). This has been further supported by research which identified isogenic short tandem repeats of *A. fumigatus* (STR*Af*) genotypes in cough samples from two CF patients, indicating potential contamination of the environment through bioaerosols (289). Earlier case reports have described patient-to-patient transmission, with patients in ICUs infected with isogenic strains of *A. fumigatus* (290). The isogenic nature of multiple strains across different sources suggests that both direct acquisition from the environment and dissemination via patient-generated bioaerosols are plausible.

1.4.4 Epidemiology of azole resistance

Mortality rates in severe cases of azole-resistant *A. fumigatus* infections range from 50% to 100%, underscoring the growing impact of antifungal resistance (34,261,269–271,291–294). However, accurately estimating resistance rates is complicated by significant global variability, influenced by factors such as azole drug type, patient demographics, screening methods, and clinical settings (295). A two-year (January 2009 to January 2011) prospective multi-centre study by the Surveillance Collaboration on Aspergillus Resistance in Europe (SCARE) network, which included 3,788 isolates from 1,450 patients across 22 centres in 19 countries, found an overall azole-resistant *A. fumigatus* prevalence of 3.2%, with the TR_{34}/L98H mutation being the most common resistance mechanism (48.8%) (296). Another international surveillance study, the SENTRY Antimicrobial Surveillance Program, analysed 1,263 *A. fumigatus* isolates from 2010 to 2017 and identified resistance rates ranging from 0.6–1.3% for itraconazole, 0.9–6.3% for posaconazole, and 0.4–1.1% for voriconazole (297). In Europe, azole resistant *A. fumigatus* has been extensively documented in both clinical and environmental isolates, with widely variable resistance rates, from 0.6% to 28% (298), with a consistent upward trend observed over recent decades (299–301). In the Netherlands, a single medical centre reported an overall azole resistance frequency of 4.2% over 23 years (1994-2016) (297). Resistance rates at this centre varied markedly over time, ranging from 0.79% between 1996 and 2001 to 7.17% between 2007 and 2011 (297). More recent national surveillance data from the

Netherlands indicated a further increase in resistance among patients, with rates nearly doubling from 7.6% to 14.7% over a six-year period (2013-2018) (302). Resistance rates vary significantly between institutions and among different patient populations within the same country, however, a similar pattern of rising azole resistance in *A. fumigatus* has been observed in the United Kingdom, with increasing resistance rates reported across multiple centres. Surveillance data from the National Mycology Reference Laboratory showed a marked increase in the proportion of *A. fumigatus* isolates resistant to itraconazole, rising from 1.4% in 2012 to 8.5% in 2016 (303), while earlier findings by Bueid *et al*., (292) documented a rise from 14% in 2008 to 20% in 2009. Studies across Europe have documented higher rates of azole resistant *A. fumigatus* among CF patients, with reported prevalence ranging from 3.5% to 8.2% depending on the country (304–306). Even more concerning, some centres have reported resistance rates as high as 9.1% in Germany and up to 20% in CF patients who had prior exposure to azole antifungals in France (305,307). These increasing resistance trends are a serious threat to the effectiveness of current antifungal therapies, particularly as treatment options become more limited. The growing prevalence of azole resistance emphasises the need for robust surveillance systems to monitor and control the spread of resistance. Coordinated efforts are crucial to developing new treatments, improving diagnostic methods, and implementing rigorous infection control practices to prevent further escalation of this public health threat (308).

1.5 Current Diagnostics

1.5.1 Culture based techniques

A significant challenge in managing fungal infections is the limited accessibility to rapid and sensitive diagnostic tools. While culture techniques are often considered the 'gold standard' diagnostic method, they are inherently time-consuming which can result in delayed treatment and possible disease progression (309). Serum antigen assays offer a sensitive non-molecular diagnostic approach, which can complement culture techniques for detecting fungal infections (309). Notable examples include assays for the biomarker β-D-glucan, a key component of the fungal cell wall (310), and assays for galactomannan, a polysaccharide released during the growth of *Aspergillus spp*. (311). However, β-D-

glucan can be found in the sera of patients infected by *Aspergillus spp*., *Fusarium* spp., and *Pneumocystis* spp., and therefore although sensitive these assays are not species specific (309). Enzyme-linked immunosorbent assays (ELISA) targeting fungal-specific IgG have been developed for faster detection of fungal infections from patient samples (312,313). Although ELISA provides quicker results compared to culture methods, antibody detection methods often suffer from low specificity and cross-reactivity with closely related fungal species. Moreover, severely immunosuppressed individuals, who are highly susceptible to fungal respiratory diseases, may exhibit reduced sensitivity to these assays due to a weakened humoral response (314). Furthermore, such tests give no information about azole sensitivity of the infecting species.

Labor-intensive (and often costly) protocols such as Minimum inhibitory concentration (MIC) testing, can prohibit adequate sample collection, undermining reproducibility and statistical power, consequently the relationship between *in vitro* azole susceptibility in fungal cultures and clinical outcomes can be unclear, thus complicating disease management further (315). An agar-based screening method VIP Check™ (Beneden-Leeuwen, The Netherlands) provides a practical alternative by detecting resistance with high sensitivity and specificity (316). Multiple colonies are sub-cultured on a four-well plate with a growth control and itraconazole, voriconazole and posaconazole added to the agar. This approach detects resistance in the isolates in a simplified, cost effect way. Alternatively, isolates can also be screened with the Etest method. This screening can best be done with itraconazole, although some resistance mechanisms can be missed. Culture-negative samples complicate the diagnosis of fungal infections, especially in cases like aspergillosis, where traditional methods frequently fail to detect the pathogen. Conventional cultures from bronchoalveolar lavage (BAL) fluid and other respiratory samples yield negative results in up to 90% of patients with aspergillosis (317). This high rate of negative cultures makes it challenging to confirm the presence of the fungus and determine its resistance profile. Such delays in accurate diagnosis can lead to inappropriate treatment and poorer clinical outcomes. As reports of fungal infections continues to rise globally, the urgency for rapid and specific diagnostics employing molecular-based detection techniques has increased. This

necessity has driven the advancement of molecular diagnostics for identifying fungal pathogens and resistance in patients who are culture negative.

1.5.2 Molecular diagnostics

Polymerase Chain Reaction (PCR) is a widely employed molecular tool for species level identification through the amplification of specific DNA regions. Common PCR targets include highly conserved regions such as the 18S rRNA gene, 28S rRNA gene and ITS, chosen for their specificity and reliability in identifying fungal DNA (318,319). The ITS regions of the rRNA gene cluster, for example, are highly variable between species and are commonly used for this purpose. Additionally, other genetic markers such as the β-tubulin and calmodulin gene can also be used for species-level differentiation. When combined with Sanger sequencing, PCR enables precise identification of resistance mutations, providing a powerful tool for clinical diagnostics. One of the primary benefits of PCR over traditional fungal culture methods is its ability to rapidly screen for both the presence of *A. fumigatus* DNA and specific resistance mutations in a much shorter timeframe. This rapid turnaround is essential for timely clinical decision-making, particularly when dealing with severe, life-threatening infections where delays in treatment can lead to poor outcomes.

Multiplex PCR assays further enhance the utility of this method by allowing the simultaneous detection of multiple clinically relevant species and associated resistance mechanisms within a single assay (320–322). For instance, the MycoGENIE real-time PCR kit detects the 28S rRNA gene of *A. fumigatus* and the TR_{34} and L98H mutations associated with azole resistance in *cyp51a* (323). Similarly, other commercial assays, such as the PathoNostics AsperGenius assay (PathoNostics, Maastricht, Netherlands) and the Fungiplex® Aspergillus Azole-R in vitro diagnostics (IVD) PCR (Bruker Daltonik GmbH, Bremen, Germany), are designed to detect azole-resistant strains of *A. fumigatus* (324–326). However, the use of diagnostic PCR in clinical practice remains selective due to the lack of comprehensive validation of commercial assays and the variability in methodologies reported in the literature (327). In response to these challenges, the European *Aspergillus* PCR initiative (EAPCRI) was established to standardise *Aspergillus* PCR methods and validate these

methods through clinical trials (328). Despite the advantages of PCR, its suboptimal sensitivity for detecting azole resistance directly from sputum samples often necessitates confirmation using traditional culture methods, which still remain the 'gold standard' (329).

1.5.3 Typing schemes

Typing schemes such as multi-locus sequence typing (MLST), short tandem repeat (STR) analysis, restriction fragment length polymorphism (RFLP), and amplified fragment length polymorphism (AFLP) assays are widely utilised due to their rapidity, reproducibility, cost-efficiency, and ease in assessing population genetics across numerous isolates (330,331). Microsatellite markers, in particular, offer superior reproducibility, lower costs, and high discriminatory power (332,333).

Investigations using various typing schemes to study the genetic diversity and population structure of *A. fumigatus* have provided valuable insights into the pathogen's adaptive mechanisms and the development of antifungal drug resistance, contributing to our understanding of its epidemiology and resistance evolution. A 2005 study by Pringle *et al*., (133) identified two globally distributed genetic clusters of *A. fumigatus*, with no correlation between genotype and geographic origin. However, a 2009 study using AFLP on 55 isolates from four countries found some evidence of differentiation by geographic and ecological origins (334). However, AFLP results often suffer from limited reproducibility, complicating inter-laboratory comparisons and interpretation (335). Klassen *et al*., (336) conducted a genotypic analysis of 225 *A. fumigatus* isolates from the Netherlands, including 25 exhibiting the multi triazole-resistant (MTR) phenotype, utilising 20 molecular markers. This study aimed to investigate the genetic structure and reproductive strategies of *A. fumigatus* in response to the rising triazole resistance in the region. Genotyping revealed five genetically distinct populations, of which four were predominantly clonal or asexual, while one demonstrated evidence of sexual reproduction. Notably, all MTR isolates were confined to a single asexual population, highlighting the pivotal role of reproductive mechanisms in the evolution and dissemination of triazole resistance in *A. fumigatus.* In 2017, Ashu and colleagues (335) conducted a comprehensive study on the global genetic diversity of *A. fumigatus* by analysing 2,026 isolates collected from 13 countries spanning four

continents, utilising nine polymorphic microsatellite markers. The study identified eight distinct clusters, seven with broad geographic distribution, suggesting deep evolutionary divergence. The authors hypothesised that contemporary factors, such as extensive gene flow and heightened selective pressures, particularly driven by the widespread use of azole antifungals, are actively influencing the pathogen's current evolutionary dynamics. A more recent study analysed the genetic relatedness of 4,089 *A. fumigatus* isolates, by genotyping across nine microsatellite loci (337). Hierarchical clustering revealed two distinct clusters within the species, indicating substantial genetic diversity and providing important insights into its epidemiological patterns and evolutionary dynamics. Notably, the azole resistant genotypes TR_{34}/L98H and TR_{46}/Y121F/T289A exhibited uneven distributions across the clusters, with reduced genetic diversity compared to wildtype isolates. Clonal isolates of these resistant genotypes were detected in multiple regions worldwide, highlighting the global spread of resistance. This international clonal dissemination emphasised the urgent need for coordinated global surveillance and control strategies to combat the rise of resistant strains. Furthermore, the discovery of identical azole resistant clones in both clinical and environmental samples across diverse geographic regions highlighted the significant public health threat posed by the global emergence of azole resistance.

1.5.4 Next Generation Sequencing

Next-generation sequencing technologies have revolutionised the field of mycology by positioning whole genome sequencing (WGS) as an indispensable tool for comprehensive genetic analysis. WGS provides a complete genomic landscape at costs increasingly competitive with traditional methods such as MLST (338). Consequently, WGS is rapidly emerging as the preferred method for molecular epidemiological studies, offering superior resolution and a cost-effective approach to data acquisition (282). Beyond genotyping, WGS facilitates high-resolution single nucleotide polymorphism (SNP) analysis to uncover evolutionary changes, genetic diversity, and gene flow, which are vital for understanding fungal adaptation and the emergence of new resistance mechanisms (282,339–341). In the context of clinical mycology, WGS has demonstrated its utility in the study a of fungal pathogens. For example, genomic research on *Scedosporium* species has provided new insights into the

mechanisms of antifungal resistance and pathogenicity. The publication of draft genomes for *Scedosporium apiospermum* in 2014 (342), *Scedosporium boydii* in 2017 (343), and most recently, *Scedosporium dehoogii* in 2021 (344) have been instrumental in identifying genetic determinants related to cell wall integrity, protease activity, and stress response, which are critical for both environmental survival and human infection (345).

Genomic research has significantly advanced our understanding of cryptococcosis, particularly in distinguishing relapse from reinfection in HIV/AIDS patients. WGS of serial *Cryptococcus neoformans* isolates, as demonstrated by Rhodes *et al*., (346) revealed that recurrent infections are often due to relapses of the original strain, evidenced by clonal relationships and low genetic diversity between isolates. Furthermore, the study identified a hypermutator phenotype associated with nonsense mutations in the *msh2* gene, impairing DNA mismatch repair and facilitating rapid adaptation to antifungal drugs (346). These findings are supported by research on *Cryptococcus deuterogattii*, where a hypermutator state promotes within-host adaptation (347), suggesting similar adaptive potential in *C. neoformans.* Stone *et al*. (348) utilised WGS to demonstrate that aneuploidy in *C. neoformans* contributes to heteroresistance against fluconazole monotherapy, underscoring the necessity for combination drug therapies in clinical practice. Moreover, genomic epidemiology has also proven valuable in outbreak investigations, such as the 2018 outbreak of *C. neoformans* in a Glaswegian hospital, where WGS revealed that the infections were not due to direct transmission of clonal isolates but rather independent acquisitions (349).

Similarly, WGS has emerged as a powerful tool in resolving hospital outbreaks caused by *Mucorales* species. In 2019, an outbreak of mucormycosis occurred among heart and lung transplant recipients over a six-month period (350), WGS demonstrated that the isolates were genetically diverse, suggesting that the patients were unlikely to have acquired the infection from a common source. A larger outbreak, this time of *M. circinelloides* f. *circinelloides* within a burns unit used WGS to resolve what appeared to be genotypically divergent isolates according to ITS sequencing (351). WGS analysis

provided additional insight into the nature of the outbreak, revealing that the patients were again not infected from a clonal strain, but from a pool of diverse strains in the environment (351).

WGS has provided invaluable insights into population and evolutionary dynamics *A. fumigatus,* which underpin its success as a human pathogen. In 2015, WGS of 24 clinical and environmental *A. fumigatus* isolates from India, the Netherlands, and the United Kingdom revealed a broadly panmictic population structure (341). However, isolates from India carrying the TR_{34}/L98H allele were found to be highly related despite their geographical separation, indicating a recent selective sweep of a highly fit genotype associated with this allele (352). More recent work on 218 *A. fumigatus* isolates from the UK identified two genetic clusters and demonstrated that resistant environmental isolates can infect patients, suggesting a polygenic basis for resistance, with selective sweeps in known resistance genes and other unidentified regions. These findings underscore the urgent need to understand the factors driving fungal drug resistance (353).

A longitudinal study of 13 *A. fumigatus* isolates, collected over two years from a single patient receiving azole and echinocandin combination therapy, identified 248 non-synonymous single nucleotide polymorphisms (nsSNPs) reflecting dynamic evolutionary changes within the host environment (354). While some of these single nucleotide polymorphisms (SNPs) in *cyp51a* appeared to result from azole-induced selective pressure, many of the resistance profiles observed could not be fully explained by these mutations alone. This finding suggests that additional, non-*cyp51a* SNPs may contribute to azole tolerance through novel, yet-to-be-identified mechanisms (354). Complementary WGS studies have highlighted the role of alternative genetic mechanisms in resistance. For example, mutations in the *hapE* and *hmg1* genes have been shown to contribute to pan-triazole resistance, indicating the importance of exploring *cyp51a*-independent pathways for developing effective treatment strategies (355). Furthermore, research into the DNA mismatch repair (MMR) system has uncovered a potential link between MMR gene variations and resistance acquisition. A study found that a mutation (G240A) in the *msh6* gene was common among strains exhibiting azole resistance (356). Deletion of the *msh6* gene increased the mutation frequency for resistance to certain fungicides,

suggesting that defects in MMR pathways may enhance the ability of *A. fumigatus* to acquire resistance to multiple drug classes (356).

WGS has revealed significant within host genetic diversity of *A. fumigatus* infections, showing that multiple isolates from a single patient can exhibit genetic variation, highlighting the need for comprehensive sampling strategies to accurately identify linked exposures and transmission routes (357). Beyond individual cases, WGS has proven invaluable for resolving complex *A. fumigatus* outbreak scenarios. In early 2024, a WGS-based investigation of a fungal outbreak in an intensive care unit (ICU) linked to construction work found no genetic similarity among the *A. fumigatus* isolates from patients and the environment (358), highlighting the utility of WGS in clarifying fungal outbreaks and origins. Overall, these studies illustrate the power of WGS to uncover the genetic and evolutionary mechanisms underpinning *A. fumigatus* resistance and pathogenicity, offering new opportunities for targeted interventions and improved clinical management. As resistance continues to emerge through diverse and complex pathways, a deeper understanding of the genetic factors driving these changes is essential for developing effective therapeutic strategies and mitigating the impact of fungal infections on human health.

1.6 Concluding remarks

Human fungal pathogens represent a significant and growing threat to global health, with rising rates of infection and antifungal resistance complicating treatment strategies. As a primary respiratory pathogen, *A. fumigatus* exemplifies the adaptive potential of fungi, thriving in diverse environments and developing resistance to widely used antifungal agents. The spread of antifungal resistance, driven by the extensive use of azole compounds in the environment and health care settings, has led to the emergence of azole resistant strains, notably TR_{34}/L98H and TR_{46}/Y121F/T289A genotypes, which pose critical challenges to patient management. These strains not only demonstrate significant drug resistance but may also possess other fitness advantages that enhance their transmission and persistence across both clinical and environmental settings. Understanding the environmental reservoirs of azole resistance is crucial for identifying transmission hotspots and developing effective

control measures to safeguard vulnerable cohorts. Next-generation sequencing combined with advanced bioinformatics provides unparalleled resolution for analysing the spatiotemporal dynamics and evolution of azole resistance. It enables comprehensive identification of genome-wide mutations and non-drug target resistance mechanisms, offering deep insights into the underlying processes driving resistance. By revealing the genetic diversity within fungal populations and tracing outbreaks, WGS supports more targeted approaches to treatment and epidemiological control. Furthermore, next-generation sequencing data facilitates easy sharing and integration with public health databases, enhancing collaborative efforts to track and control azole resistance on a global scale.

1.7 Thesis Overview

This thesis aimed to determine the prevalence of azole-resistant *A. fumigatus* in individuals with chronic respiratory diseases and their environments, while characterising the genotypic profiles associated with resistance. The overarching objectives were:

1) Conduct longitudinal surveillance of patients diagnosed with chronic respiratory diseases to investigate potential environmental and *de novo* acquisition of azole resistant *A. fumigatus.*
2) Conduct surveillance within the participants home and hospital environments to identify 'hot spots' of azole resistance and patient exposures
3) Utilise high-resolution WGS to explore genetic clusters, spatial population structure, routes of transmission and diversification of azole resistant mutations over time.
4) Explore patient and environmental genotype – phenotype associations to identify determinants that influence resistance and adaptation

Chapter 1 introduces the core themes and objectives of this PhD, while **Chapter 2** outlines the general methodologies employed throughout the research.

Chapter 3 introduces the UK *A. fumigatus* population. The initial UK dataset published in 2019 included 218 clinical and environmental WGS samples, providing a comprehensive view of the genetic landscape (353). Subsequent nationwide environmental sampling contributed 297 WGS samples to

this dataset and revealed that TR_{34}/L98H (59%) and TR_{46}/Y121F/T289A (6%) were the most prevalent resistance-associated polymorphisms within aerosolised *A. fumigatus* (359). Incorporating 407 whole genome sequenced isolates collected during targeted clinical and environmental surveillance throughout this PhD expanded the UK *A. fumigatus* dataset to a total of 912 genomes. The predominance of TR_{34}/L98H in the UK prompted a focused genotypic and phenotypic analysis to investigate adaptive mechanisms underpinning the persistence and ecological success of the TR_{34}/L98H resistance mechanism in the UK.

Chapter 4 establishes the foundation for targeted surveillance strategies which aimed to investigate the acquisition and diversification of antifungal resistance in individuals with chronic respiratory disease. This chapter builds upon previous findings of environmental and clinical azole-resistant *A. fumigatus* isolates sharing clonal backgrounds, highlighting environmental acquisition as a key contributor (353). Notably, a high prevalence of azole resistance (~13%) has been reported among individuals with chronic respiratory diseases (301), suggesting increased vulnerability to acquiring resistant strains. Longitudinal clinical surveillance examined the role of environmental fungicide exposure and/or oral azole therapy in resistance development, offering key insights into how environmental and clinical factors contribute to antifungal resistance in chronic respiratory conditions.

In **Chapter 5**, targeted environmental surveillance was conducted within a hospital setting to identify potential 'hotspots' of azole resistance in a high-exposure environment. Detailed sampling across multiple hospital sites was carried out to assess the prevalence and incidence of azole resistant *A. fumigatus* and to characterise genotypes associated with resistance. Isolates collected from the hospital environment underwent WGS and were integrated with the clinical WGS dataset from Chapter 4 to investigate potential environmental acquisition and transmission pathways. Comparator isolates from the broader UK WGS dataset were incorporated to enhance the statistical power of the analysis and refine the final conclusions.

Chapter 6 extends the analysis to include participant home environments, providing further exploration of potential environmental routes of azole resistance acquisition and transmission. A citizen science approach facilitated the sampling of participant homes, addressing logistical constraints associated with home surveillance. This home-based surveillance enabled a comparative analysis of the azole resistance burden between home and hospital environments, offering insights into potential associations with resistance. Findings are discussed and concluded in **Chapter 7**.

1.8 Thesis Aims

Hypothesis 1: The azole resistant TR_{34}/L98H genotype of *A. fumigatus* exhibits distinct genotypic and phenotypic variations which may influence functional potential and overall fitness.

Aims:

1) Characterise *cyp51a* genotypes in a UK panel of 912 *A. fumigatus* isolates.
2) Investigate the frequency of nsSNPs in 210 virulence genes between TR_{34}/L98H and wildtype *A. fumigatus* genotypes to explore the impact on functional potential
3) Phenotypic profiling of TR_{34}/L98H and wildtype isolates in 384 growth conditions using the high-throughput OmniLog® phenotypic microarray system.

Hypothesis 2: The occurrence of azole resistant genotypes in patients with chronic respiratory disease is associated with environmental exposures and / or oral azole therapy.

Aims:

1) Determine the prevalence of azole resistance among individuals diagnosed with chronic respiratory diseases through prospective remote surveillance.
2) Genotypic characterisation of *A. fumigatus* isolates collected during prospective surveillance using high-resolution WGS.
3) Integration of retrospective and prospective WGS data, resulting in 300 clinical genomes from chronic respiratory disease cohorts,
4) Explore phylodynamic relationships and within-host diversification of azole resistance in *A. fumigatus*.

Hypothesis 3: Hospital environments serve as reservoirs for azole resistant *A. fumigatus*, facilitating environmental exposures that contribute to patient acquisition of resistant strains.

Aims:

1) Conduct comprehensive environmental surveillance of a central London hospital to assess the prevalence and incidence of azole resistance within a high exposure environment.
2) Genotypic characterisation of *A. fumigatus* isolates collected during environmental surveillance using WGS.
3) Explore possible transmission pathways by integrating WGS data from clinical and hospital environmental isolates collected through prospective surveillance.

Hypothesis 4: Azole-resistant *A. fumigatus* is prevalent in the home environments of individuals with chronic respiratory diseases, and citizen science approaches enable effective surveillance of resistance.

Aims:

1) Use citizen science to assess the prevalence of azole resistant *A. fumigatus* in the home environments of individuals with chronic respiratory diseases.
2) Genotypic characterisation of *A. fumigatus* isolates collected from the home environments using WGS.
3) Integrate WGS *A. fumigatus* isolates collected from participants home environment with corresponding clinically derived WGS isolates to determine possible epidemiological links.

1.9 Funding

This PhD was funded through:

Wellcome Trust 219551/Z/19/Z: Understanding and mitigating the impact of emerging antifungal resistance. **NERC NE/X00547X/1**: Understanding the eco-evolutionary drivers of emerging antifungal resistance. **MRC MR/R015600/1**: MRC Centre for Global Infectious Disease Analysis.

Chapter 2 General Materials and Methods

2.1 Ethical Approval

Prospective clinical and environmental isolates were collected through the MRC (Medical Research Council) FREAL (Fungal Resistance Evolution and Acquisition in chronic Lung disease) study, approved by the Research Ethics Committee (REC ref:19/LO/1663), Health Regulator Authority (HRA) and the participating NHS Trust.

2.2 Participant selection and inclusion criteria for prospective surveillance

Participants aged 16 years and above with verified diagnoses of chronic pulmonary disease (CF, non-CF bronchiectasis, CPA, COPD, other chronic lung conditions) were actively recruited to participate in the MRC funded FREAL study within the domains of the Royal Brompton and Harefield NHS Foundation Trust (RBHT). Prior to enrolment, informed consent was obtained from each individual and detailed clinical data was collected including patient demographics, medical history, details of current and/or previous medication and respiratory health information. Sputum samples were collected during the initial screening visit and obtained monthly via remote sampling. All clinical and laboratory data were recorded in the online RedCap® (Research Electronic data capture) data collection platform hosted at Imperial College London, UK (360,361).

2.3 Fungal Isolates

Clinical and environmental *A. fumigatus* isolates were prospectively collected from patients diagnosed with chronic respiratory diseases and their environments as part of the MRC FREAL study between 2020 and 2023. Additionally, retrospective clinical isolates were acquired through the CF Trust TrIFIC (Targeting Immunotherapy for Fungal Infections in Cystic Fibrosis) Study (REC ref: 20/L0/0110) led by Professor Darius Armstrong-James, and subsequently included into the *A. fumigatus* isolate collections. Isolates were integrated into an existing collection of 515 UK *A. fumigatus* isolates,

collected during previous surveillance studies, dating from 2009 to 2023 (277,353,359). *A. fumigatus* isolates were collected, processed, and analysed using protocols outlined in the following sections, unless stated otherwise.

2.4 Fungal culture and isolation

2.4.1 Handling of *A. fumigatus* and other fungi

Sample processing and culture work was conducted in a Class II laminar-flow biosafety cabinet (BSC) in a Category II laboratory. To minimise risk of cross-contamination, the BSC was disinfected using 10% Chemegene HLD4 disinfectant (Medimark International) prior and after each use. Additionally, as standard practice, the BSC was UV sterilised for 20 minutes daily. To monitor for potential cross-contamination, an open control agar plate was placed in the safety cabinet during culture and conidia harvesting work. Culture plates were either sealed with parafilm or placed inside ziplock bags and stored in plastic containers during incubation, transportation, and 4°C storage to further mitigate cross contamination. Prior to autoclaving and disposal, culture plates were securely sealed with sellotape to prevent the release of aerosolised conidia.

2.4.2 Culture Media

All fungal isolates were cultured under aseptic conditions on either SDA (Oxoid Ltd, UK) or Sabouraud dextrose Broth (SDB) (Oxoid Ltd, UK), unless stated otherwise. Fungal conidia were cultivated in either 90mm petri dishes or T25 cm^2 Nunc flasks. For liquid cultures, isolates were incubated in 50 ml Falcon tubes containing SDB in a shaking incubator (150-250 rpm) for 2-5 days. Culturing temperatures were maintained at either 37°C or specifically at 45°C for the targeted cultivation of *A. fumigatus*, unless otherwise specified. Due to the thermophilic nature of *A. fumigatus*, growth at 45°C excludes fungal species and most cryptic species of the *A. fumigatus* complex. All culture media were sterilised by autoclaving at 121°C for 15 minutes and poured in Class II biological safety cabinets under sterile conditions.

2.4.2.1 Sabouraud Dextrose Agar

SDA, supplemented with antibiotics to prevent bacterial contamination, served as the primary medium for yeast and mould cultivation throughout this PhD. This medium is used as standard practice in the hospital Microbiology Diagnostics Laboratory and was used to maintain consistency in fungal cultivation across the laboratory settings.

2.4.2.2 Sabouraud dextrose broth (SDB)

SDB was used to revive retrospective and historical *A. fumigatus* isolates. Liquid medium enhances nutrient absorption and gas exchange, creating optimal growth conditions. This can be beneficial for culturing *A. fumigatus,* particularly when isolates exhibit intrinsically slow growth rates. SDB is also routinely employed as a standard medium for enhancing fungal cultivation in the hospital Microbiology Diagnostics Laboratory.

2.4.3 Fungal isolation from primary cultures

A. fumigatus colonies were sub-cultured from primary cultures on to SDA in 90 mm plates at 45°C for 2-5 days. Non-*A. fumigatus* moulds were cultured under the same conditions but at 37°C. The three-spot method was employed for all moulds to ensure purity (Figure 2.1); a sterile toothpick was used to collect fresh conidia from the outer edge of a single colony and transferred to an SDA plate. Each colony was visually inspected for uniform morphology, if the morphology was consistent across the three colonies, it was considered a pure culture and stored at 4°C until processing for downstream analysis or cryopreservation at -80°C. For yeasts, colonies chosen for subculturing were visually inspected for purity and typical yeast morphology, characterised by a smooth, convex appearance. A sterile 10 µl inoculating loop was used to lift the yeast cells to be transferred onto a fresh SDA plate using the quadrant streaking method to ensure the isolation of single colonies (Figure 2.2). Plates were incubated at 37°C for up to 4 weeks and growth was monitored daily.

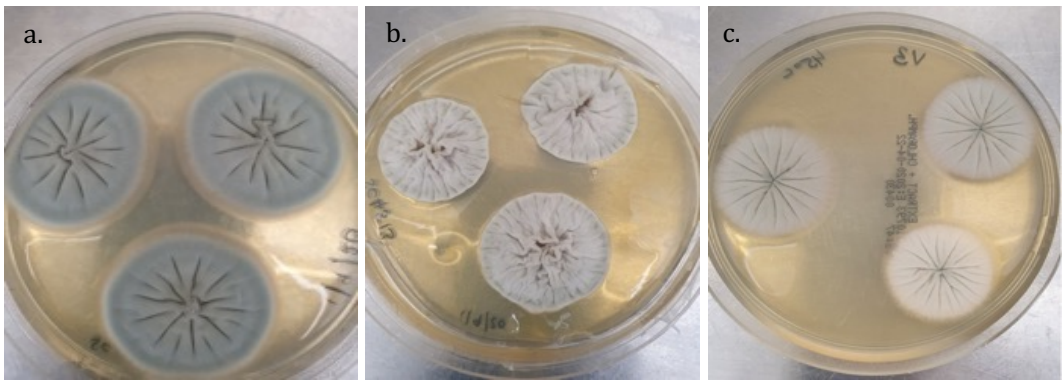


Figure 2.1. **Isolation of *A. fumigatus* and other moulds**. Sporulating moulds were isolated using the three-spot method and assessed for purity through visual inspection. Isolates were identified as *A. fumigatus* based on their characteristic morphological features when cultured at 45°C (a). Isolates grown at 45°C that did not display typical *A. fumigatus* morphology were confirmed through PCR sequencing to ascertain their genetic identity (b-c).

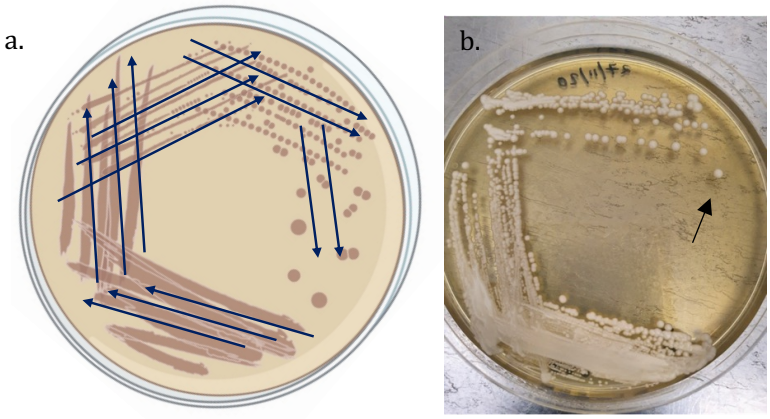


Figure 2.2**. Isolation of yeasts.** Illustrative representation of sequential steps involved in the quadrant streaking method with direction of inoculation: Initial streaking in the first quadrant, followed by streaks into subsequent quadrants to ensure isolation of single colonies (a). Plates were incubated at 37◦C and isolated colonies, as shown in (b) were stored at -80◦C for future downstream analysis.

2.4.4 Confirmation of mixed colonies

Isolates displaying morphological traits typical of *A. fumigatus* yet showing growth anomalies in the three-spot culture technique were further examined to identify mixed colonies. Conidial suspensions were first passed through sterile glass wool to remove hyphal fragments before adjusting to an equivalent turbidity of 0.5 McFarland. Serial dilutions were plated to facilitate the growth of individual

colonies. Colonies were examined macroscopically to determine purity. Isolates consisting of mixed colonies were excluded from further analysis.

2.4.5 Storage of fungal isolates

Isolated colonies showing optimal growth without contamination were stored for long term preservation and future downstream analysis. No more than 3 passages from the original culture plate were performed prior to cryopreservation. Fungal isolates were cryopreserved in duplicate in 30% (v/v) glycerol stock at -80°C. When necessary, short term conidial suspensions were preserved in mould preservation agar (MPA) (MPA; 0.2% agar and 0.05% Tween®-80 in sterile diH_20 and stored at 4°C to limit genetic and phenotypic instability which may occur from the repeated freeze-thaw of primary cryopreserved stocks.

2.5 *A. fumigatus* identification and conidial harvest

2.5.1 Macroscopic and microscopic characteristics

Initial identification of *A. fumigatus* isolates was based on their growth at 45°C and macroscopic and morphological characteristics when grown on SDA (Figure 2.1a). For further confirmation, an adhesive tape technique was used for microscopic identification of *A. fumigatus* culture. The adhesive side of tape was gently pressed onto the colony to collect the fungal spores and placed onto slides prepared with lactophenol-cotton blue (LPCB) as mounting and staining fluid. Microscopic characteristics were examined at 400x magnification.

2.5.2 β-tubulin amplification, PCR and Sanger sequencing

Species identification was performed using PCR amplification of the b-tubulin gene for isolates with atypical morphological characteristics of *A. fumigatus* when cultured at 45°C (Figure 2.1b-c). Total gDNA was extracted from conidia harvested on SDA for 3-5 days at 45°C as per sections 2.9.2 - 3, with quantification performed using a NanoDrop™ (ThermoFisher Scientific, UK) spectrophotometer as per section 2.9.4.1 prior to PCR. The b-tubulin gene was amplified using specific primers; 5'-

GACCGTATGATGGCGACCTT-3' and the reverse primer 5'- AGCTGACCAGGGAAACGAAG-3' in 50 µl reaction mixtures composed of FIREPol® Master Mix (10 µl), forward primer (10 µl), reverse primer (10 µl), nuclease-free water (18 µl), and 2 µl of DNA. PCR conditions included an initial denaturation at 94°C for 3 minutes, followed by 30 cycles of 94°C for 15 seconds, 55°C for 30 seconds, and 68°C for 3 minutes, with a final hold at 4°C. PCR products were visualized via agarose gel electrophoresis, purified with a Zymo Research Genomic DNA Clean and Concentrator Kit as per the manufacturers protocol (362) and sequenced using Azenta Life Sciences Sanger sequencing (363). Sequences were analysed using the National Centre for Biotechnology Information (NCBI) BLAST database, with 97-100% sequence similarity required for species identification.

2.5.3 Conidial harvesting for downstream analysis

A. fumigatus isolates were cultured on T25 cm^2 flasks at 45°C until sporulation, either from cryopreserved glycerol stocks using a 10 ml sterile inoculating loop or from primary subcultures using a sterile swab to collect fresh conidia. Conidial suspensions were prepared by washing the surface of colony with 10 ml of sterile phosphate buffered saline (PBS) containing 0.05% Tween®-80. Conidia were disrupted and washed by gently hand shaking the T25 cm^2 flask. Conidia suspensions were left for at least 5 minutes to allow aerosolised conidia to settle prior to opening the flask to collect conidia suspension aliquots.

2.8 Azole susceptibility screening

2.8.1 Azole susceptibility testing using VIPCheck™ plates

Azole susceptibility was assessed using the commercially available 4-well VIPCheck™ plates (Mediaproducts BV, Netherlands) containing agar supplemented with itraconazole (4 mg/L), voriconazole (2 mg/L), posaconazole (0.5 mg/L) and an azole-free positive control well (316). Isolates were initially cultured on SDA at 45°C for 3-5 days, followed by washing with 0.05% Tween®-80. Conidial suspensions were adjusted to a turbidity equivalent to 0.5 McFarland and inoculated into each well at of volume of 25 ml. Plates were incubated at 37°C for 2-3 days and visually inspected on

day 3. Isolates demonstrating no growth in the azole-supplemented wells were categorised as 'susceptible', while isolates that exhibited growth equal or slightly less than the control well were categorised as 'resistant'. For large-scale azole susceptibility screening, conidial suspensions from up to 10 colonies were pooled and tested on a single plate. If growth occurred in any of the wells containing azoles, the pooled isolates were subsequently re-tested individually to accurately determine resistant profiles.

2.8.2 Tebuconazole susceptibility testing

The agricultural azole, tebuconazole was used to determine the efficacy of using an agricultural azole as a cost-effective approach for screening clinical azole resistance as previously described (364). Briefly, 25 µl aliquots of conidial harvest suspensions (adjusted to 0.5 McFarland) were inoculated on tebuconazole incorporated agar at 3 concentrations (6 mg/L, 8 mg/L and 16 mg/L) and an azole free control well (0 mg/L) (Figure 2.3). The 4-well plates were incubated for 3-5 days at 37°C. Growth on each well was visually determined and assessed for azole resistance. Isolates demonstrating no growth in the azole-supplemented wells were categorised as 'susceptible', while isolates that exhibited growth equal or slightly less than the control well were categorised as 'resistant'. For high-throughput susceptibility screening, conidial suspensions from no more than 10 colonies were pooled and assessed on a single plate. If growth was observed in any of the azole-supplemented wells, the pooled isolates were individually tested.

2.9 Genomic DNA (gDNA) extraction for WGS

2.9.1 Isolate selection for next generation sequencing

Isolates exhibiting phenotypic resistance to at least one triazole class antifungal were selected for WGS. For comparative genomic analysis, azole susceptible strains were also selected. This selection was mirrored across both clinical (within-patient) and environmental (same origin) sources. The AF293 reference strain (365) was included as a control for sequencing, alignment, and variant detection.

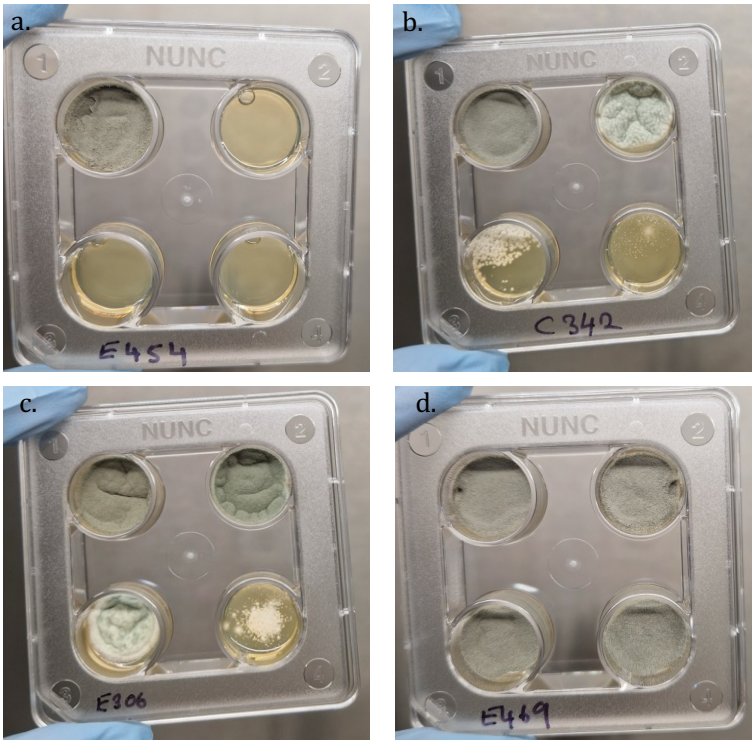


Figure 2.3. **Susceptibility profiles of *A. fumigatus* to tebuconazole.** Images (a-d) display four isolates of *A. fumigatus* grown on SDA with varying concentrations of tebuconazole. Control wells (1) contain no tebuconazole, while wells 2, 3, and 4 contain tebuconazole at concentrations of 6 mg/L, 8 mg/L, and 16 mg/L, respectively. Isolate E454 exhibited growth only in the control well, indicating tebuconazole susceptibility (a). In contrast, isolates C342 (b), E306 (c), and E469 (d) demonstrated varying degrees of resistance, with observable growth even at higher concentrations of 6 mg/L, 8 mg/L, and 16 mg/L, respectively.

2.9.2 Genomic DNA extraction

2.9.2.1 Culture and preparation of conidial harvests

Isolates were cultured in T25 cm^2 culture flasks containing SDA at 37°C for 3-5 days to encourage sporulation. Preparation of conidial harvests prior to extraction were performed in a Class II laminar-flow BSC as described in sections 2.4.1 – 2.4.2. Conidia were washed by centrifuge at 5000 rpm for 10 minutes.

2.9.2.2 gDNA extraction

Genomic DNA was extracted using MasterPure Yeast Cell Lysis Solution (Epicentre Biotechnologies, Cambridge, United Kingdom). A bead-beating step was included using 1.0 mm diameter zirconia beads (Thistle Scientific, Glasgow, U.K) in a FastPrep®-24 system (MP Biomedicals, Solon, OH) under specific homogenisation conditions (6.0m/s for 40 seconds with two cycles and a cooling period of 5 minutes between cycles). The homogenised solution was centrifuged at 14,000 rpm for 2 minutes to pellet the debris and the supernatant removed and incubated with 1 µl RNase Cocktail™ Enzyme Mix (Thermo Fisher Scientific) at 65°C for 15 minutes. Samples were left to cool on ice for 15 minutes prior to adding 20 µl Proteinase K for protein and nuclease digestion. Samples were vortex mixed with Qiagen AL lysis wash buffer (Qiagen, Venlo, Netherlands) and incubated at 56°C for 10 minutes to further remove contaminants and residual cellular components that may affect downstream DNA purification.

2.9.2.3 gDNA purification

DNA was precipitated with 98-100% ethanol, washed on Qiagen spin columns using AW1 and AW2 wash buffers (Qiagen, Venlo, Netherlands) and eluted in 40 µl Elution Buffer (EB). Samples were stored at -20˚C.

2.9.3 Extraction of gDNA from low sporulating and poor growth isolates

2.9.3.1 Culture and colony preparation

Isolates were cultured on 90 mm plates containing SDA for 3-7 days or in liquid SDB, as detailed in sections 2.4.1 – 2.4.2. Colony fragments or hyphal masses were removed using a sterile scalpel and placed into a 2 ml Eppendorf tube. The samples were vortexed to detach residual agar, then centrifuged at 14,000 rpm for 2 minutes in PBS to pellet debris. The supernatant was discarded, and the pellet was washed repeatedly in fresh PBS until completely free of agar.

2.9.3.2 gDNA extraction

DNA was extracted using the MasterPure Yeast DNA Purification kit (Epicentre Biotechnologies, Cambridge, United Kingdom), incorporating a bead beating step as described in section 2.9.2.2. Post homogenisation, the solution was centrifuged at 14,000 rpm for 2 minutes to pellet the debris. The supernatant was then treated with MasterPure protein precipitation reagent and centrifuged again to pellet any residual debris, ensuring purity of the DNA sample.

2.9.3.3 gDNA precipitation and purification

gDNA was precipitated from the supernatant using 100% Isopropanol, followed by centrifugation at 14,000 rpm to pellet the DNA. The pellet was washed with 70% ethanol and allowed to air dry to ensure complete evaporation of residual ethanol. Samples were resuspended in 40 ml EB buffer and stored at -20^{o}C.

2.9.4 gDNA quantification and quality control

2.9.4.1 gDNA quantification NanoDrop™ Spectrophotometer

Concentration and absorbance ratios were measured using a NanoDrop™ (ThermoFisher Scientific, UK) spectrophotometer. A 2 µL blank control with EB buffer was measured to establish the baseline control. Subsequently, 2 µL of each gDNA sample was loaded onto the pedestal for spectral analysis.

Absorbance ratios at 260/280 and 260/230 were recorded to assess DNA purity with concentrations recorded as ng/μL. Samples that did not meet the specified absorbance criteria (A260/A280 ratio: 1.8-2.0 and A260/A230 ratio: >2.0) for genome sequencing were further processed using the Zymo DNA Clean & Concentrator™ (Zymo Research) to achieve ultra-pure gDNA.

2.9.4.2 gDNA quantification using Qubit™ assay

Purified gDNA was quantified using a Qubit™ 2.0 fluorometer with a Qubit™ dsDNA BR (broad range) assay kit (ThermoFisher Scientific, UK). The Qubit™ working solution was prepared by diluting Qubit™ dsDNA BR Reagent 1:200 in Qubit™ dsDNA BR Buffer. Standards and samples were adjusted to a final volume of 200 μL, as specified in Table 2.1. Samples were vortexed and incubated at room temperature for 2 minutes prior to fluorescence measurement in thin-walled Qubit™ assay tubes using the Qubit™ 2.0 fluorometer.

Table 2.1. Summary of Qubit™ working solution

Volume of	Standard	Test sample
Working solution	190 μl	198 μl
Standard	10 μl	-
gDNA sample	-	2 μl
Total volume	200 μl	200 μl

2.10 Next Generation Sequencing & Bioinformatic Analysis

2.10.1 Illumina short read sequencing

Genomic DNA was processed for library construction and sequencing at the Earlham Institute, Liverpool across 6 sequencing runs, between 2021-2023 (Table 2.2). Libraries were prepared using the LITE and LITTE 2.0 library prep. protocols. Whole genome libraries were sequenced utilising the Illumina NovaSeq sequencing platforms producing 150 base pair (bp) paired end reads. WGS with a read depth of < 30 x coverage were omitted from subsequent analyses to ensure data quality and

reliability. All bioinformatic analysis were performed on the Imperial College London High Performance Computer (HPC) utilising the BASH command line. Alignment and sequence analysis was performed following the genome analysis toolkit (GATK) version 4.0 best practices (366).

Table 2.2 Summary of library preparation protocols and specific sequencers employed for each sequencing panel (2021-2023) during this PhD.

Panel Number (Year Sequenced)	Library Prep Protocol	Sequencer
1 (2021)	LITE	Illumina NovaSeq 6000 SP v1.5 Lane (150PE)
2 (2021)	LITE	Illumina NovaSeq 6000 SP v1.5 Lane (150PE)
3 (2022)	LITE	Illumina NovaSeq 6000 SP v1.5 Lane (150PE)
4 (2022)	LITE	Illumina NovaSeq 6000 SP v1.5 Lane (150PE)
5 (2023)	LITE 2.0	Illumina NovaSeq X Plus 10B lane (300 cycles)
6 (2023)	LITE 2.0	Illumina NovaSeq X Plus 10B lane (300 cycles)

2.10.2 UK Retrospective Genomic Library

All *A. fumigatus* WGS data processed throughout this PhD were consolidated with an existing UK *A. fumigatus* WGS collection. The existing raw fastq files were accessed and managed through the Imperial College London HPC. Sequence alignments and quality controls and variant discovery were performed as per the following sections.

2.10.3 Sequence alignment and variant calling

Raw paired end reads were quality checked using FastQC (Babraham Institute, version 0.10.1). Reads were aligned to the *A. fumigatus* AF293 reference genome (365) using the 'MEM' algorithm of Burrows-Wheeler Aligner (BWA) software package (version 0.7.15) (367). The resulting SAM files were converted to the binary BAM format and sorted by coordinates using SAMtools (version 1.3.1). The 'AddOrReplaceReadGroups' command provided in the Picard Tool (version 2.6.0) was used to modify the BAM file to include read group information for downstream analysis and interpretation of

the sequencing data. To mitigate false-positive variant calls from technical artifacts, duplicate reads were identified and marked using Picard 'MarkDuplicates' and excluded from subsequent analyses. Variant calling was performed with GATK (version 4.0) HaplotypeCaller, with a ploidy setting of 1 and excluded repetitive regions using the '-XL' parameter. Reads were aligned to the AF293 reference genome (365) and variants were filtered by applying a minimum confidence threshold of 30 and a minimum base quality of 20 to ensure a high confidence threshold). Base Quality Score Recalibration was applied to correct systematic errors. High confidence SNPs were retained using GATK 'VariantFiltration' with filter expressions "QD < 2.0 || FS > 60.0 || MQ < 40.0 || MQRankSum < -12.5 || ReadPosRankSum < -8.0 || SOR > 4.0". SNPs that did not meet these criteria were labelled as 'LowConf' and removed.

2.10.4 Mapping Statistics

Alignment quality was evaluated using SAMtools flagstat (368), which quantified the total number of reads aligned to the reference genome, the proportion of properly paired reads, and the prevalence of singleton reads. These metrics verify accurate read pairing and correct mapping, essential for ensuring the integrity of downstream variant analysis.

2.10.5 Discovery of cyp51a alleles

Tandem repeat (TR) sequences (TR_{34}, TR_{46}, TR_{53}, TR_{120}) were identified in raw FASTA files using the 'grep' command while nsSNPs were annotated using VCFannotator (Broad Institute). Polymorphisms were cross-referenced with the MARDy database (369) to identify known resistance-conferring variants.

2.10.6 Multisequence alignments

For population genomics analysis, the vcf-merge tool was used to consolidate multiple VCF files into a single VCF file. The -R option was employed to retain all variant records, such as position, reference and alternative alleles by setting missing genotypes to '0'. This step enabled the conversion of the

merged VCF into FASTA format, given that FASTA format requires uniform sequence lengths for proper alignment and comparison of homologous positions.

2.12 Phylogenetic Analysis

Phylogenetic trees were inferred using the Randomized Axelerated Maximum Likelihood Next-generation (RAxML-NG) tool (370). RAxML-NG was used for its ability to support checkpointing restarts for analyses exceeding 72 hrs on the Imperial College HPC. Due to high computational demand, an initial analysis was performed on a subset of 100 genomes to identify the most likely tree topology. Four runs, incorporating starting trees based on 10, 25, 40, and 50 parsimony-based and randomly generated trees, were implemented to assess the impact of starting tree variability on the accuracy of the final maximum likelihood tree topology. The optimal topology was indicated by peak log-likelihood values at 40 starting trees. The General Time Reversible (GTR) model with a gamma distribution was selected to account for rate heterogeneity across sites. Bootstrap analyses were performed to enhance the statistical reliability of the inferred phylogenetic relationships with additional post-hoc convergence testing via the --bsconverge command. Bootstrap replicates were concatenated until convergence had been achieved. Phylogenetic trees were visualised in R version 4.3.1 utilising the ggTree (371) and ggTreeExtra (372) packages and made available as interactive Microreact projects. (Appendix 2). Genomes included in the phylogenomic analysis were sequenced across multiple runs and different sequencing platforms. Quality control metrics, including total reads, percentage of reads mapped, and percentage of paired reads, were mapped to the phylogeny to confirm that the observed genetic diversity was not an artifact of sequencing technology.

2.13 Calculating pairwise unique SNPs

Pairwise unique SNPs were calculated between VCF files using a customised Python script (Appendix 1). Variant data was extracted using the “parse_vcf” function, which captures chromosome, position, reference allele, and alternative alleles. File names were extracted for identification using the “extract_vcf_name” function. All possible pairs of VCF files were then compared using the “compare_vcf” function to determine unique SNPs in each pair. The results, including file names and

the count of unique SNPs, were written to a CSV file. The results were visualized as histograms in R to illustrate the genetic variation across samples. Isolates pairs sharing less than 3% of the total SNP diversity were subset to identify clonal groups.

2.14 Multivariate analysis of genomic data

Multivariate analyses were conducted in R version 4.3.1 using the adegenet package (version 2.1.10) following established protocols (373–376). Multisequence alignments in FASTA format (section 2.10.7) were converted into a genind object, applying a polymorphism threshold of 0.01 to account for low frequency variants. Population groupings were assigned to the genind object from a supplementary file. Missing data were imputed using mean allele frequencies via the NA.method='mean' function. Discriminate analysis of principle components (DAPC) based on SNP variants extracted from VCF files was conducted to assess genetic differentiation among isolates. To determine the appropriate number of principal components (PCs) for DAPC, cross-validation was performed using the 'xvalDapc' function. The cross-validation process involved 90% of the data for training and 10% for validation, with a minimum of 100 replicates, depending on the dataset's computational demands. The optimal number of PCs was chosen based on the lowest mean squared error (MSE). DAPC results were visualised as scatter plots, with population groups represented on the data points, and an inset plot showing the cumulative variance explained by the principal components. Reference genomes were included as controls.

2.15 Statistical analysis

Data analysis was conducted using R version 4.3.1. Statistical significance was set at $p < 0.05$. Normality assumptions were assessed with Shapiro-Wilk tests. For data that deviated from normality, nonparametric tests were applied. The Kruskal-Wallis test was used to detect significant differences between groups, and when significant, Dunn's post-hoc test facilitated pairwise comparisons. Categorical data were analysed using chi-squared tests to examine associations between variables. Fisher's exact test was applied when expected counts were below 5.

Acknowledgements: I would like to acknowledge Dr. Johanna L. Rhodes (Imperial College London/Radboudumc, Nijmegen) for providing sequence alignment pipelines and bioinformatic support throughout this PhD.

Chapter 3 Genotypic and phenotypic characterisation of *A. fumigatus*: Insights into the TR_{34}/L98H resistance mechanism

3.1 Abstract

The increasing frequency of azole resistance in *A. fumigatus* presents a significant challenge to effective antifungal therapy, necessitating a deeper understanding of the genetic and phenotypic mechanisms that underpin fitness and pathogenicity in resistant strains. This study examines the genetic and phenotypic diversity of 912 *A. fumigatus* isolates from the United Kingdom, with a particular focus on the TR_{34}/L98H resistance mechanism. WGS and high-throughput phenotyping were used to assess the distribution of nsSNPs in 210 virulence-associated genes and evaluate metabolic profiles under diverse conditions. TR_{34}/L98H isolates exhibited increased nsSNP frequencies in genes linked to toxin biosynthesis, secondary metabolism, and immune evasion, indicating genetic diversification that may support adaptive responses to environmental stressors and antifungal agents. Phenotypic characterisation highlighted overlapping metabolic profiles between TR_{34}/L98H and wildtype strains, though differences in carbon and nitrogen utilisation, osmolyte tolerance, and pH response were observed. These findings reveal a multifaceted adaptive strategy in TR_{34}/L98H isolates, where genetic and metabolic flexibility contributes to their persistence and resistance. These findings highlight the complex evolutionary dynamics of *A. fumigatus* resistance mechanisms, emphasising the need for further investigation into the genetic and metabolic factors that sustain the persistence of resistant strains.

3.2 Introduction

The *A. fumigatus* population in the United Kingdom represents a critical area of study due to the high prevalence of azole resistance in the environment and the clinic. The widespread distribution of the canonical azole-resistant genotype TR_{34}/L98H suggests that genotypes bearing this allele have successfully adapted to both human-associated and environmental niches. This is likely due to their enhanced resistance to near-ubiquitous azoles in the environment, coupled with a broad fitness

advantage, including adaptations to environmental factors such as temperature, hypoxia, and nutrient availability, which collectively influence both virulence and drug susceptibility (377–379). These adaptations underscore the importance of investigating the biological mechanisms driving resistance and virulence in *A. fumigatus*, especially given its extensive gene flow across diverse environments (282).

Various biological functions and gene classes are implicated in the pathogenicity of *A. fumigatus* (380,381). As an environmental saprophyte*, A. fumigatus* typically acquires nutrients from soil and compost. However, during infection, it demonstrates the ability to rewire its nutrient acquisition pathways, an adaptive mechanism that enhances both survival and virulence (382,383). By simultaneously testing hundreds of conditions, high-throughput phenotyping tools, such as the Omnilog® Phenotype Microarray system, complement genomic data by enabling the analysis of microbial adaptability under diverse conditions. These tools enable the comprehensive analysis of microbial growth and metabolic activity, offering insight into how microbial species like *A. fumigatus* respond to different stresses, nutrients, and environmental factors.

In clinical settings, microbial pathogens must rapidly adapt to dynamic host conditions, overcoming immune defences and fluctuating nutrient availability to survive (384). Studies have highlighted several aspects of *A. fumigatus* virulence, including differences in colony and spore colour phenotypes (385), adaptation to low-oxygen microenvironments (379), and the ability to modify gene expression to survive under immunosuppressive conditions in the host (386). A recent pan-genome study, based on 300 globally sampled genomes, expanded our understanding of the genetic diversity of *A. fumigatus,* identifying both core and accessory genes that distinguish clinical and environmental isolates (387). Importantly, accessory genes implicated in virulence and antifungal resistance were enriched in clinical isolates, highlighting the adaptive potential of *A. fumigatus* in human hosts. Complementing these findings, this study utilises a targeted approach by analysing the distribution of nsSNPs in 210 virulence-associated genes. By comparing nsSNP frequencies between wildtype and

azole resistant TR_{34}/L98H isolates, this work provides further insight into how genetic variation may contribute to the adaptive success of resistant strains.

This chapter presents an in-depth analysis of 912 clinical and environmental *A. fumigatus* isolates from across the UK, utilising WGS and high-throughput phenotypic data. Through the application of univariate and multivariate statistical methods, the study identifies significant differences in genotypic and metabolic profiles between azole-resistant TR_{34}/L98H genotypes and azole-susceptible wildtypes. These findings offer insights into the genetic adaptations that drive resistance, informing the development of targeted strategies to manage and limit the spread of resistant strains.

3.3 Methods

3.3.1 UK *A. fumigatus* WGS dataset

A dataset of 912 WGS of *A. fumigatus* isolates from the UK was compiled from prospective (section 2.1) and retrospective (section 2.10.2) surveillance studies. Raw FASTQ files were processed and managed using the Imperial College London HPC. The sequence data underwent quality control, alignment, and variant discovery as outlined in sections 2.10.3 – 2.10.6.

3.3.2 Discovery of nsSNPs in the coding region of virulence related genes

nsSNPs within the coding regions of 210 *A. fumigatus* virulence-related genes were identified and annotated using VCFannotator and a custom Bash script (Appendix 1). These genes categorised into six functional groups - immune response, cell wall biosynthesis, nutrient acquisition, signal transduction, toxin biosynthesis, and secondary metabolism (Appendix 3)- constitute the organism's pathogenic arsenal (388). nsSNP counts were normalised to gene length for comparison of mutation frequencies across genes. The Wilcoxon Rank Sum test was applied to compare mutation frequencies between TR_{34}/L98H and *cyp51a* wildtype genotypes, with $p < 0.001$ considered significant. All analyses were performed using R version 4.3.1.

3.3.3 Antifungal susceptibility screening

Prospective isolates were screened for susceptibility to three clinical azoles and agricultural azoles, as outlined in sections 2.8. For retrospectively collected isolates, antifungal susceptibility testing was completed during the original sampling project, with profiles provided in an Excel sheet. Retrospective isolates missing complete profiles were additionally tested for clinical azoles and tebuconazole to enhance the UK dataset. Susceptibility testing for voriconazole, itraconazole, and posaconazole was performed in RPMI-1640 medium to ensure standardised conditions. MICs were determined according to EUCAST breakpoints: >2 mg/L for itraconazole and voriconazole, and > 0.25 mg/L for posaconazole (389). UK isolates were screened for tebuconazole susceptibility as per section 2.8.2.

3.3.4 Phylogenomic analysis

Phylogenetic trees were inferred from 912 WGS using RAxML-NG (370) as described in section 2.12. Bootstrap replicates (n = 150) were concatenated with the inferred trees. Phylogenetic trees were visualised in R 4.3.1 using the ggTree (371) and ggTreeExtra (372) packages and uploaded as an interactive Microreact project (Appendix 2).

3.3.5 Phenotypic characterisation using the high throughput Omnilog® Phenotype Microarray (PM) system

3.3.5.1 Experimental Design

To assess the impact of azole resistance on *A. fumigatus* growth, 23 genotyped isolates (Table 3.1) were phenotypically characterised using the high-throughput Omnilog® platform (Biolog, Hayward, CA, USA). Growth parameters of clinical and environmental azole resistant TR_{34}/L98H and azole susceptible *cyp51a* wildtype isolates were analysed across 384 culture conditions, including pH, osmolytes, carbon and nitrogen sources. Each isolate was cultured in triplicate to reduce phenotypic

variability, and five biological replicates per genotype and source were used to account for genome-wide and technical variability.

Table 3.1. List of isolates phenotypically characterised using the OmniLog® platform

Isolate ID	*cyp51a allele*	Source	AMR
E371	wildtype	Environmental	Susceptible
E344	wildtype	Environmental	Susceptible
FN012	wildtype	Environmental	Susceptible
E379	wildtype	Environmental	Susceptible
E313	wildtype	Environmental	Susceptible
FP064	wildtype	Clinical	Susceptible
C392	wildtype	Clinical	Susceptible
C386	wildtype	Clinical	Susceptible
C422	wildtype	Clinical	Susceptible
C398	wildtype	Clinical	Susceptible
E242	TR_{34}/L98H	Environmental	Resistant
FN022	TR_{34}/L98H	Environmental	Resistant
E486	TR_{34}/L98H	Environmental	Resistant
E316	TR_{34}/L98H	Environmental	Resistant
E247	TR_{34}/L98H	Environmental	Resistant
FP116	TR_{34}/L98H	Clinical	Resistant
C318	TR_{34}/L98H	Clinical	Resistant
C358	TR_{34}/L98H	Clinical	Resistant
FP135	TR_{34}/L98H	Clinical	Resistant
C321	TR_{34}/L98H	Clinical	Resistant
C338	wildtype	Clinical	Susceptible
C387	wildtype	Clinical	Susceptible
AF293	wildtype	Reference	Susceptible

3.3.5.2 Additive Preparation

Additive stock solutions were prepared by dissolving each additive in diH_20 to achieve the recommended concentration for the phenotypic assays (Appendix 4). Stock solutions were filter sterilised and stored at 4°C until further use.

3.3.5.3 *A. fumigatus* conidia harvest and PM culture

Conidia were cultivated in T25 cm^2 Nunc flasks at 37°C for up to 3 days or until sporulation. Harvested conidia were suspended in sterile Biolog FF inoculating fluid (Biolog Inc, Hayward, US) and adjusted to 75% transmission using a Biolog turbidimeter (Biolog Inc, Hayward, US). Cell suspensions were added to PM fluids and inoculated into four substrate plates: PM1 (Carbon sources), PM3B (Nitrogen Sources), PM9 (Osmolytes) & PM10 (pH). Plates were incubated in the Omnilog® platform at 37°C, with optical density recorded every 15 minutes for 120 hours.

3.3.5.4 Data organisation and metadata integration

Data visualization and analysis were performed using OmniLog software (Biolog Data Analysis v1.7) and the R package 'OPM' (On-Plate Microbiology) (390). Raw kinetic data were exported as CSV files from OmniLog® and imported into R as S4 objects for downstream analysis. Groups were manually defined in R, stored as metadata, and combined with the S4 objects for comparative analysis.

3.3.5.5 Curve parameter calculation and data visualisation.

The opm_mcp function was utilized to perform simultaneous multiple comparisons of group means. Descriptive curve parameters from the kinetic raw data were calculated using the do_aggr function. The area under the curve (AUC) parameters were estimated to provide insights into the growth kinetics. Heat maps were generated using the pheatmap package (391) in R for visual comparisons of the estimated curve parameters.

3.3.5.6 Univariate analysis

To identify substrates distinguishing TR_{34}/L98H from wildtype *A. fumigatus* isolates, mean AUC values were analysed. The Shapiro-Wilk test assessed data normality, followed by a t-test for normally distributed data or a Mann-Whitney test for non-normal data. Substrates with $p < 0.05$ were considered significantly different.

3.3.5.7 Multivariate Analysis

Multivariate analysis was employed to capture the combined effects of multiple features, improving discrimination between the TR_{34}/L98H and wildtype groups. Analysis was performed using the online platform MetaboAnalyst version 5.0 (392). The mean AUC data were uploaded as a CSV file and normalised using Pareto scaling to correct for systematic biases while preserving natural variance and minimising outliers. Partial least squares discriminant analysis (PLS-DA) was performed to distinguish between the TR_{34}/L98H, and wildtypes based on metabolomic profiles. Cross-validation using the 10-fold method assessed the robustness of PLS-DA model. Model performance was interpreted by examining the Q2 value, which reflects the model's predictive ability. A permutation test was conducted to evaluate the significance of the PLS-DA model. The class labels (TR_{34}/L98H and wildtype isolates) were randomly permuted 2,000 times to generate a null distribution of R2 and Q2 values. The original values were then compared to this distribution, with significance determined if they exceeded 95% of the permuted values (p-value < 0.05), validating the model's robustness. The Variable Importance in the Projection (VIP) score measures each variable's contribution to group separation, with higher values indicating greater discriminatory power. Metabolites with VIP values above 1.0 were considered significant for differentiating between groups. A Principal Component Analysis (PCA) was employed as an alternative to PLS-DA when cross-validation results indicated poor model performance, or the permutation test showed a non-significant p-value (p > 0.05).

3.4 Results

3.4.1 WGS of 912 *A. fumigatus* isolates from the UK

Of the 912 sequenced isolates collected across the UK, 452 (49.9%) were clinical and 450 (51.1%) were of environmental origin (Figure 3.1a). Of the 810 isolates screened for azole susceptibility, 386 (47.7%) demonstrated resistance to at least one azole. The geographical distribution of isolates exhibiting azole resistance is shown in Figure 3.1b. Resistance to specific azoles was observed in 37.1% (272/734) of isolates for itraconazole (> 2 mg/L), 26.8% (214/799) for voriconazole (> 2 mg/L), 33% (240/726) for posaconazole (> 0.5 mg/L), and 36.3% (206/567) for tebuconazole (> 6

mg/L). MTR was found in 18.5% (*n* = 150) of clinical and 11.1% (*n* = 90) of environmental isolates. Fifty isolates showed resistance without *cyp51a* polymorphisms, with 70% (*n* = 35) clinical and 30% environmental origin (*n* = 15). The distribution of *cyp51a* polymorphisms in the UK *A. fumigatus* WGS dataset is shown in Figure 3.2. Alignments of the sequenced genomes are summarised in Appendix 5**.**

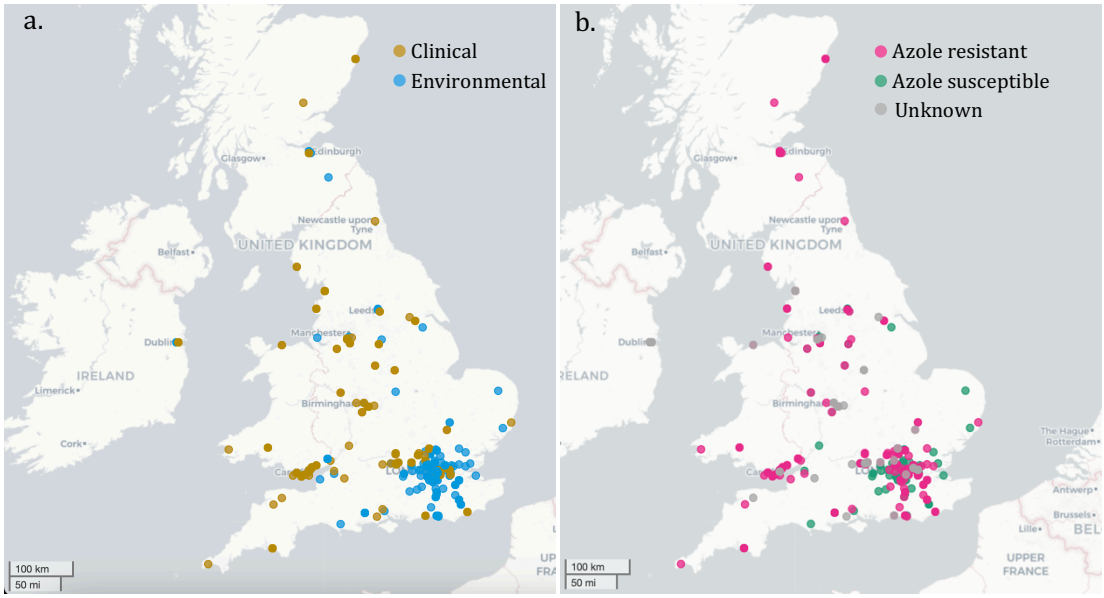


Figure 3.1. **Geographical distribution of UK *A. fumigatus* isolates.** Left panel showing *A. fumigatus* isolates of clinical (orange points) and environmental (blue points) origin (a). Right panel showing distribution of *A. fumigatus* exhibiting resistance (pink points) to at least one clinical azole (itraconazole (4 mg/L), voriconazole (2mg/L) & posaconazole (0.5mg/L)). Isolates with azole susceptible (green points) and unknown resistance (grey points) profiles are also shown (b).

3.4.2 Multi-triazole resistance association with *cyp51a* genotypes

Azole susceptibility profiles, categorized by *cyp51A* alleles, showed significant variation across itraconazole, voriconazole, posaconazole, and tebuconazole (Figure 3.3). Tebuconazole effectively detected the majority of clinical resistance mechanisms, except in G54 polymorphisms, highlighting its potential as a cost-effective screening tool. At least 83% (25/30) of G54 polymorphisms were resistant to itraconazole but displayed lower resistance to posaconazole (0–18%) (0-5/30) and remained susceptible to tebuconazole. M220I, M129T, and Q351K polymorphisms exhibited resistance to all clinical azoles. Isolates containing TR_{34} demonstrated varying resistant rates to all azoles. Among TR_{34}/L98H isolates, 86% (147/171) exhibited resistance to both itraconazole and tebuconazole. Notably, up to 100% of those with additional mutations alongside TR_{34}/L98H demonstrated MTR. Of the 18 TR_{46}/Y121F/T289A isolates, 100% were resistant to tebuconazole, 85%

(15/18) were resistant to voriconazole and 88% (16/18) to posaconazole. One TR_{120} isolate was susceptible to clinical azoles but resistant to tebuconazole, while TR_{120} combined with point mutations exhibited variable resistance. Among the *cyp51a* wildtype isolates, 11% (47/428) were resistant to tebuconazole, 7% (30/428) to itraconazole, 4% (17/428) to voriconazole, and 5% (21/428) to posaconazole. Polymorphisms such as M172V, A9T, D262Y, G434S, P109T, and I242V were universally susceptible to all clinical azoles.

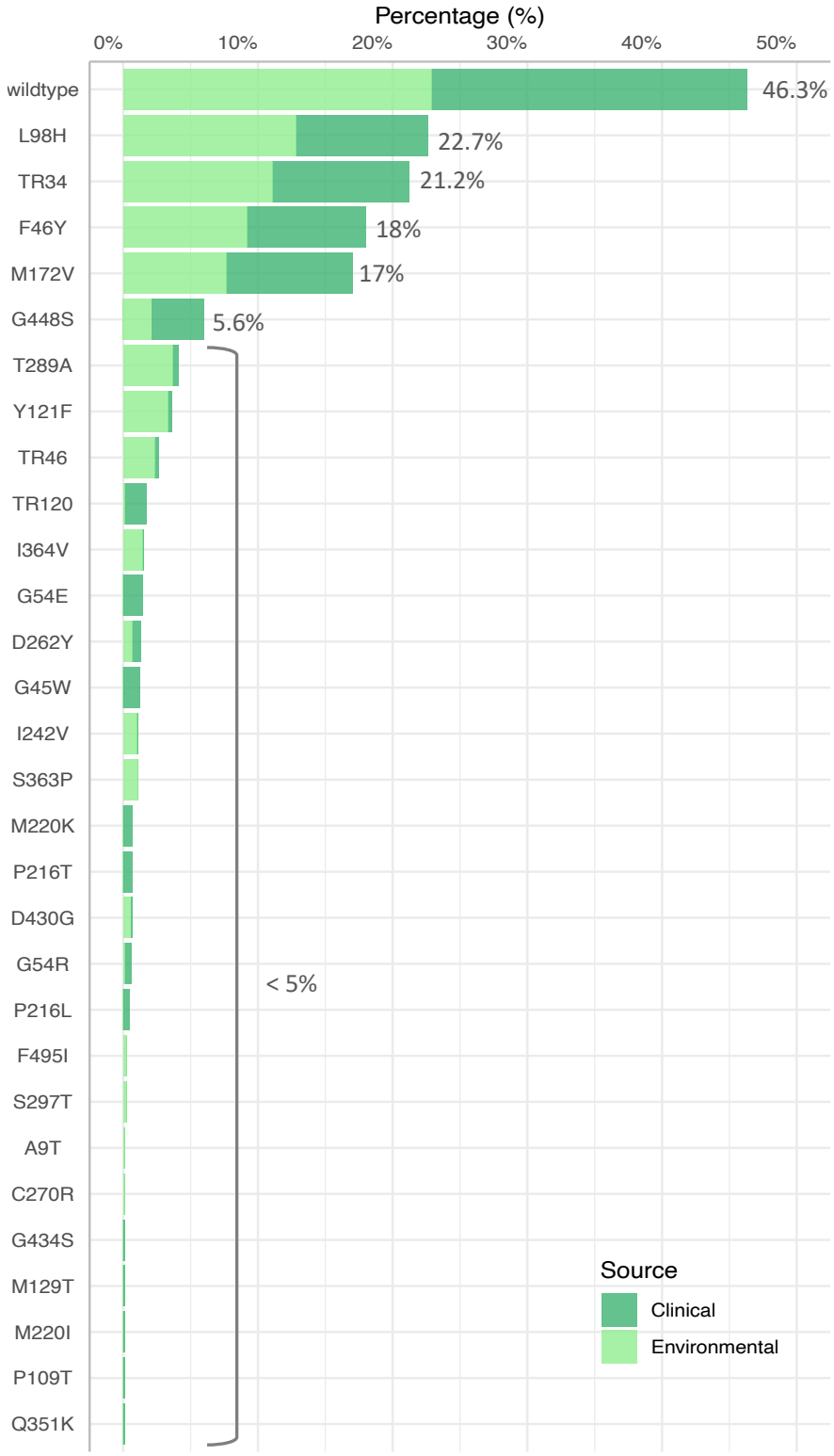


Figure 3.2. **Distribution of *cyp51a* alleles in the UK dataset**. Bars indicate the frequency of each allele from clinical (dark green) and environmental (light green) sources, with labels for those above 5% and grouped category for those below 5%.

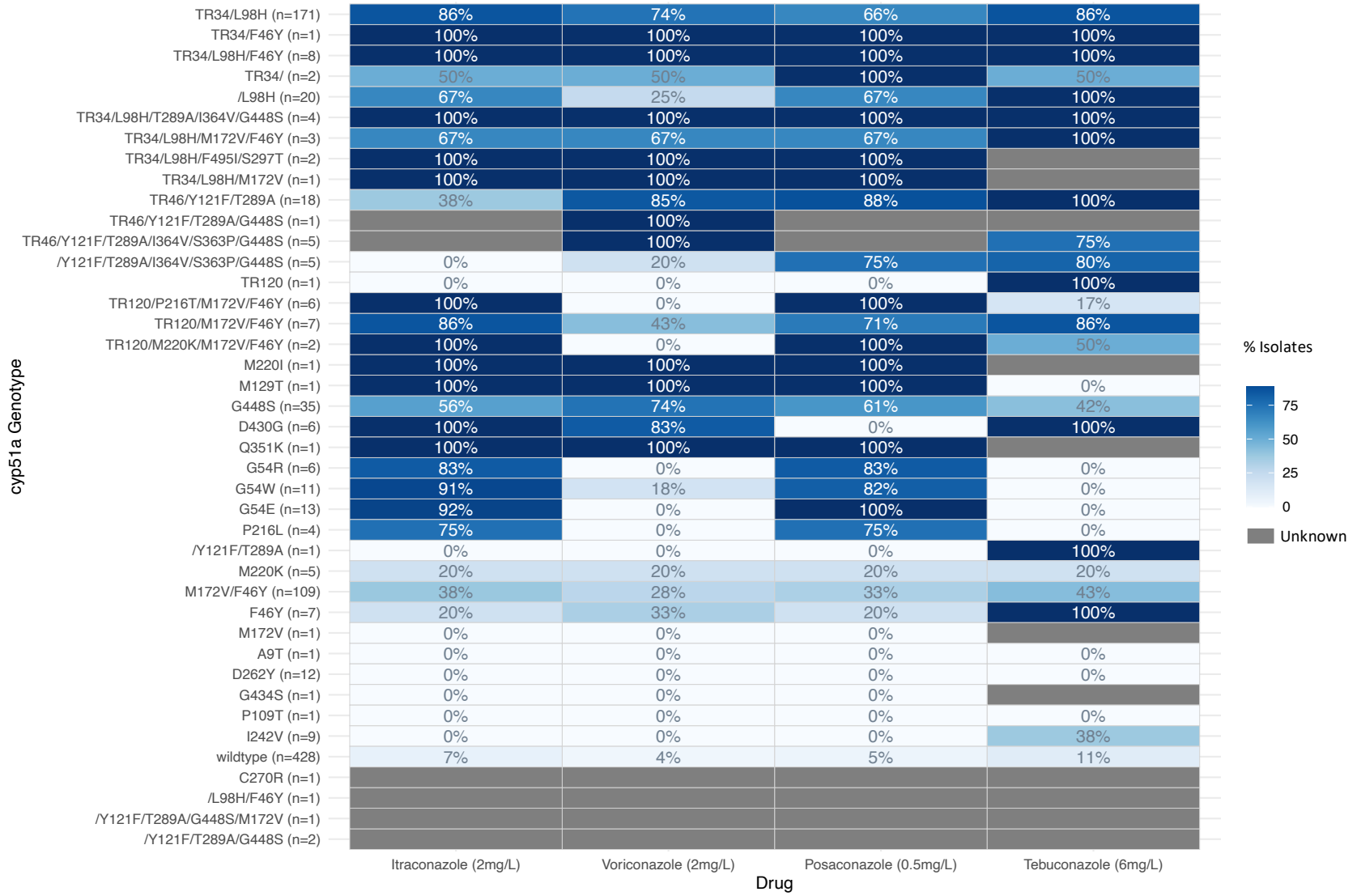


Figure 3.3 **Heatmap showing the percentage of azole resistant *A. fumigatus* isolates per genotype.** Rows represent genotypes with the number of genotypes (n) in parentheses. The cells indicate the percentage of isolates resistant to itraconazole (2 mg/L), voriconazole (2 mg/L), posaconazole (0.5 mg/L), and tebuconazole (6 mg/L), with dark blue indicating 100% resistance and lighter shades indicating lower percentages. Grey cells represent missing data

3.4.3 Phylogenetic diversity

The phylogenetic analysis revealed four distinct clusters (C1–C4), with nodes showing median bootstrap support of 78% (Appendix 5). Across the phylogeny, clinical and environmental isolates displayed a heterogeneous distribution, reflecting the diverse origins of these strains (Figure 3.4). Cluster 1 (C1) predominantly comprised azole susceptible wildtype isolates but also included clinically derived resistant isolates harbouring point mutations such as G448S and G54. Azole resistant *cyp*51a wildtypes were also interspersed throughout C1. Cluster 2 (C2) showed a mix of azole susceptible and resistant isolates including those with TR_{120}/M172V/F46Y and TR_{120}/P216T/M172V/F46Y but predominantly M172V/F46Y. Cluster 3 (C3) branched from C2 and included a highly clonal subcluster of TR_{34}/L98H genotypes sourced from both clinical and environmental origins. Finally, Cluster 4 was dominated by resistant isolates harbouring TR_{34}/L98H and TR_{46}/Y121F/T289A mutations, alongside some susceptible wildtype strains. This phylogenetic structure highlights the concentration of azole-resistant isolates in C3 and C4.



Figure 3.4. **Phylogenetic analysis of UK *A. fumigatus* clinical and environmental isolates.** Outer rings indicate the antifungal susceptibility profiles, and the inner ring denotes cyp51a alleles. Clinical isolates are shown in blue and UK environmental isolates in yellow. Notable clusters are labelled C1-C4.

3.4.4 Distribution of nsSNPs in the coding regions of virulence related genes

To explore the virulence potential of the TR_{34}/L98H resistance mechanism, genome sequences of TR_{34}/L98H (*n* = 171) and *cyp51a* wildtype isolates (*n* = 428) were examined for the presence of nsSNPs in the coding regions of 210 virulence related genes distributed across six functional categories. Figures 3.5a–3.5f present the mean nsSNP frequencies observed between TR_{34}/L98H and *cyp51a* wildtypes within each functional group. Significant differences in mutation frequencies were detected between the two groups across all categories, with certain genes showing conservation. The most pronounced differences were observed in genes involved in the biosynthesis of toxins and secondary metabolites, where 28 out of 49 genes (57.1%) exhibited significant variation ($p < 0.001$), particularly in *easK*, *CYP5081B1*, and *CYP5081A* (Figure 3.5a). In nutrient uptake genes, 13 of 41 genes (31.7%) displayed significant differences ($p < 0.001$), predominantly in *dppIV*, *pkaC2*, and *ctsD* (Figure 3.5b). Among genes related to immune response evasion, 10 of 34 genes (29.4%) showed significant differences ($p < 0.001$), notably *rodA* (Figure 3.5c). Similarly, 7 of 23 genes (30.4%) involved in signalling and regulation exhibited significant variation ($p < 0.001$), most prominently *fos.1* and *gpD* (Figure 3.5d). In the cell wall biosynthesis group, 9 of 37 genes (24.3%) demonstrated significant variation ($p < 0.001$), with a marked variation in *och1* (Figure 3.5e). For allergens, 4 of 26 genes (15%) exhibited significant variation ($p < 0.001$), particularly *csn*, *aspHS*, *mreA*, *exg12*, and *aspf8* (Figure 3.5f).

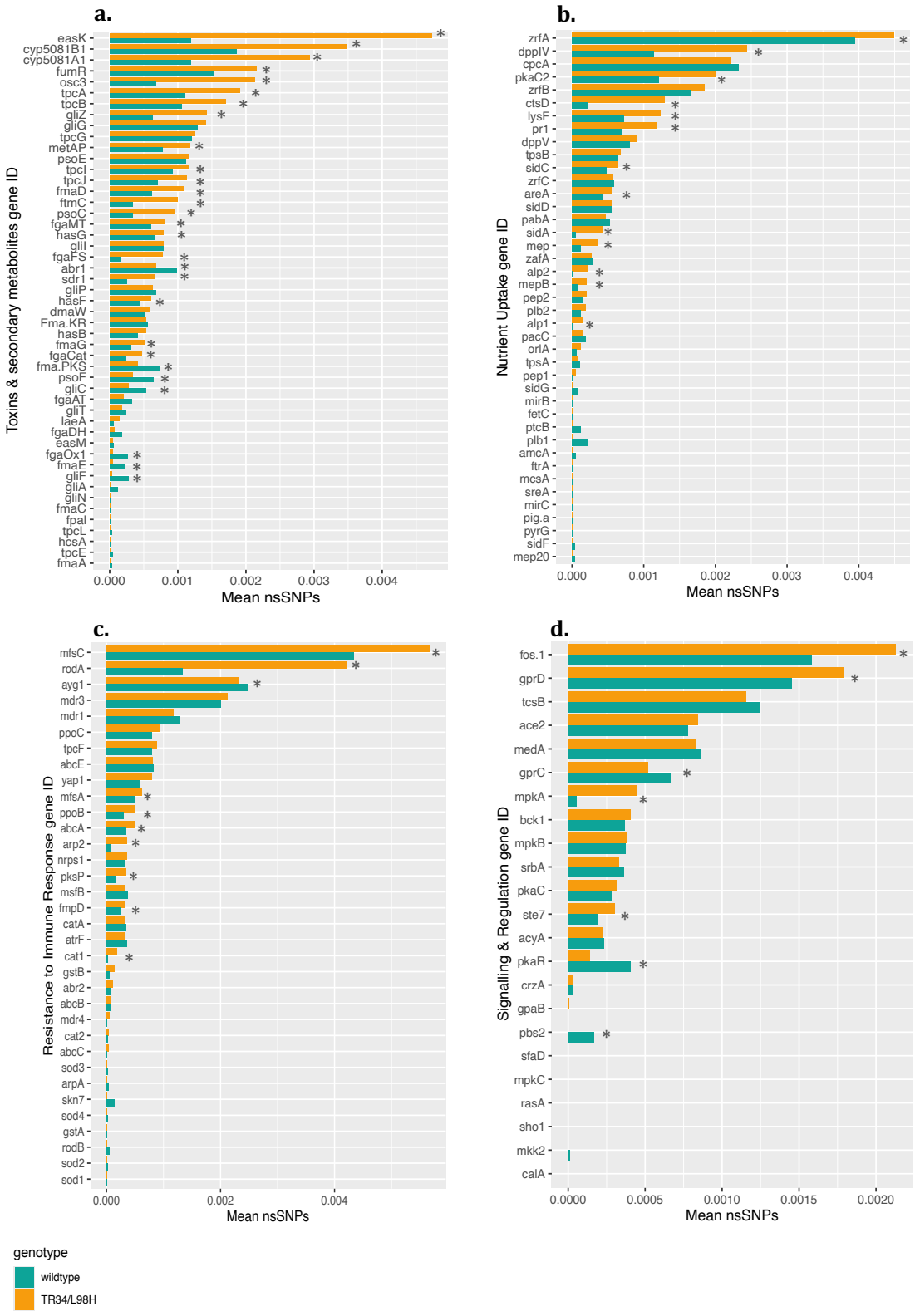


Figure 3.5. **Distribution of nsSNPs in the coding regions of virulence related genes.** The bars represent the mean number of nsSNPs (normalised by gene length) for TR_{34}/L98H (orange) and *cyp51a* wildtypes (teal) in genes associated with toxins and secondary metabolites (a), nutrient uptake (b), resistance to immune response (c) and signalling and regulation (d).

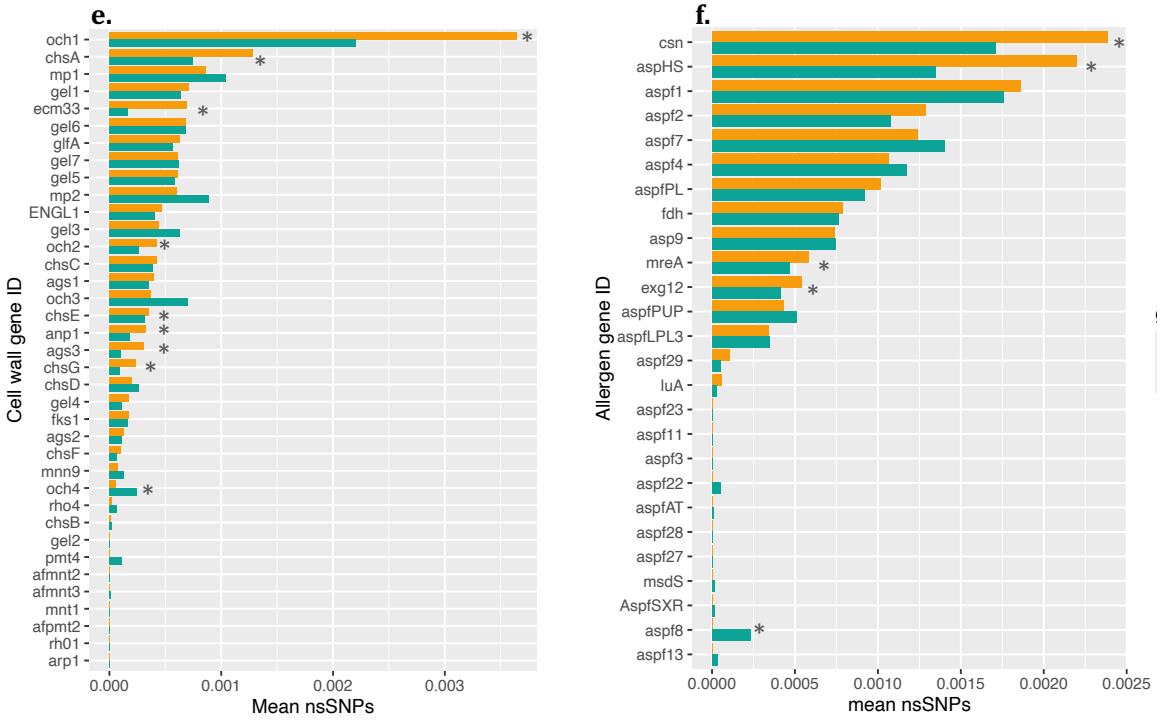


Figure 3.5 continued. **Distribution of nsSNPs in the coding regions of virulence related genes.** The bars represent the mean number of nsSNPs (normalised by gene length) for TR_{34}/L98H (orange) and cyp51a wildtypes (teal) in genes associated with cell wall biosynthesis (e) and allergens (f).

3.4.5 Phenotypic characterisation using the high-throughput OmniLog™ platform

Metabolic profiles of *A. fumigatus* strains were analysed across 384 substrates, including carbon (PM01, Figure 3.6) and nitrogen (PM03, Figure 3.7) utilisation, and tolerance to osmolytes (PM09, Figure 3.8) and pH conditions (PM10, Figure 3.9). Heatmaps of AUC values indicated that nitrogen sources were the most utilised substrates, indicating strong nitrogen assimilation capabilities in both TR_{34}/L98H and wildtype strains. Additionally, all strains demonstrated broad tolerance to a wide range of pH levels and osmolytes, suggesting metabolic flexibility and environmental resilience.

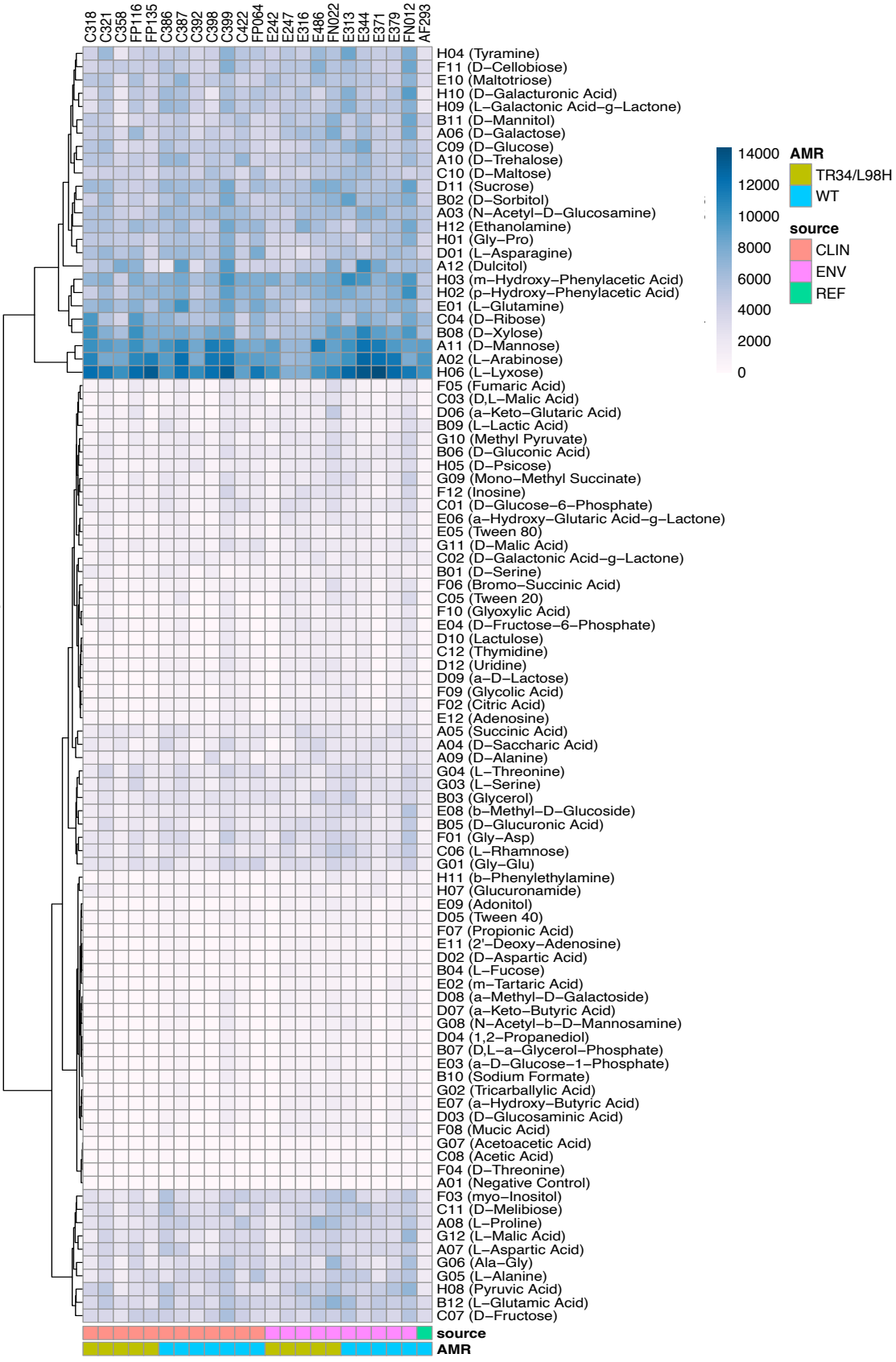


Figure 3.6 **Heatmap of *A. fumigatus* metabolic activity across carbon sources.** Each cell represents the metabolic activity (measured as AUC) of TR_{34}/L98H, *cyp51a* wildtypes and AF293 (REF) isolates across 96 carbon sources, with darker blue indicating higher activity. Columns represent different isolates, grouped by AMR genotype and clinical (CLIN) and environmental (ENV) sources. Rows correspond to individual carbon sources.

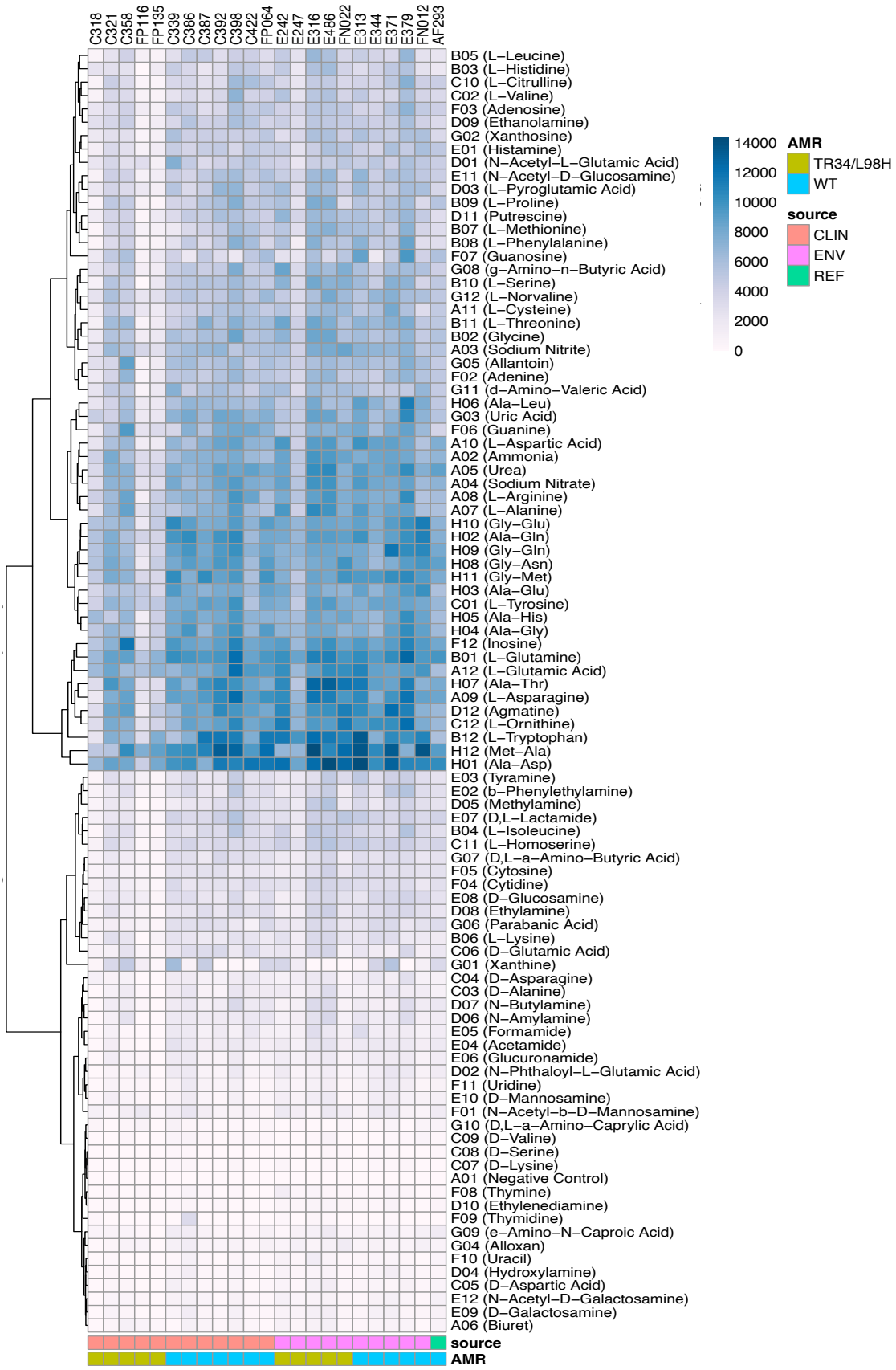


Figure 3.7. **Heatmap of *A. fumigatus* metabolic activity across nitrogen sources.** Each cell represents the metabolic activity (measured as AUC) of TR_{34}/L98H, *cyp51a* wildtypes and AF293 (REF) isolates across 96 nitrogen sources, with darker blue indicating higher activity. Columns represent different isolates, grouped by AMR genotype and clinical (CLIN) and environmental (ENV) sources. Rows correspond to individual nitrogen sources.

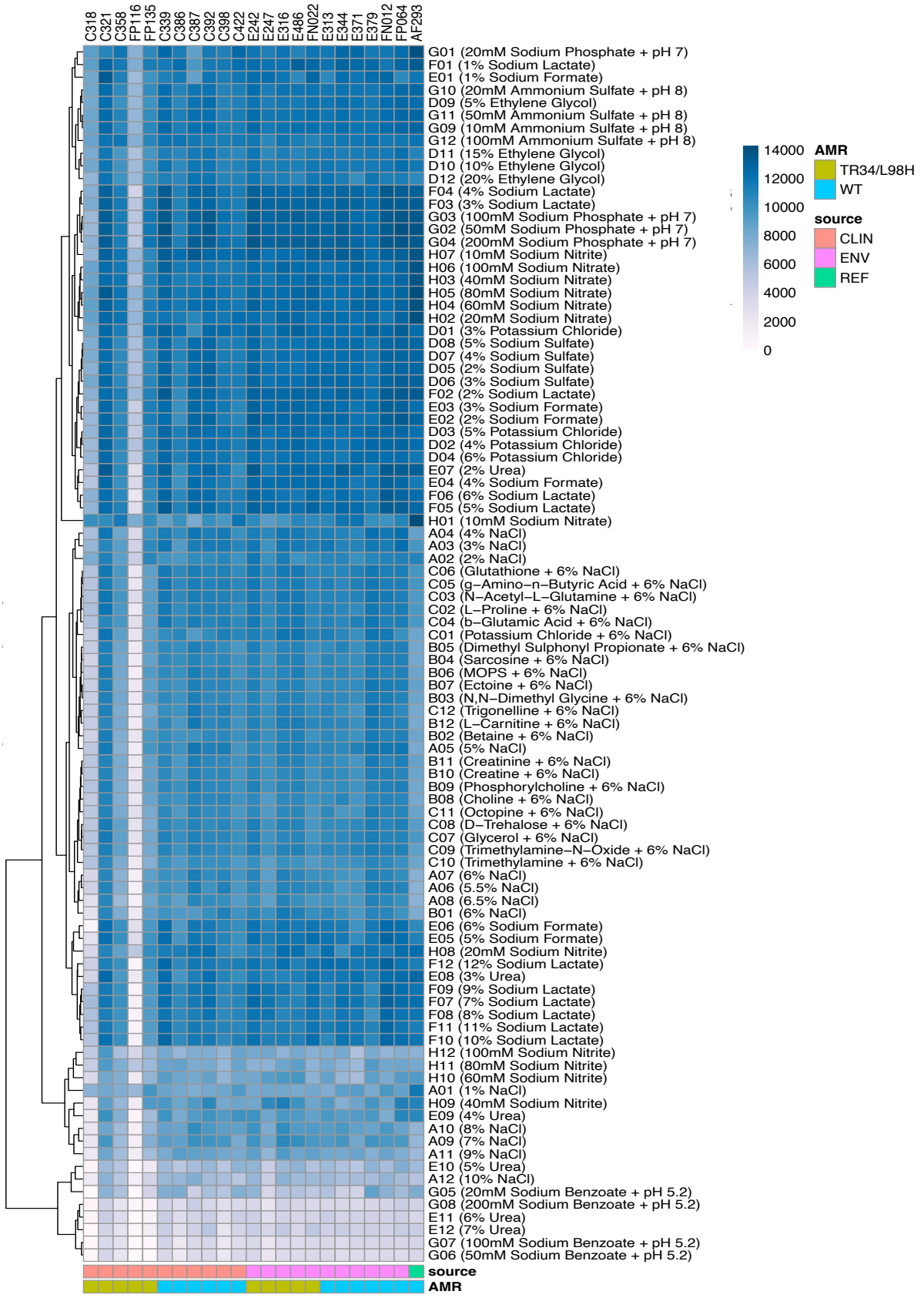


Figure 3.8. **Heatmap of *A. fumigatus* metabolic activity under osmotic stress conditions.** Each cell represents the metabolic activity (measured as AUC) of TR_{34}/L98H, *cyp51a* wildtypes and AF293 (REF) isolates under 96 osmotic stress conditions, with darker blue indicating higher activity. Columns represent different isolates, grouped by AMR genotype and clinical (CLIN) and environmental (ENV) sources. Rows correspond to individual osmolytes.

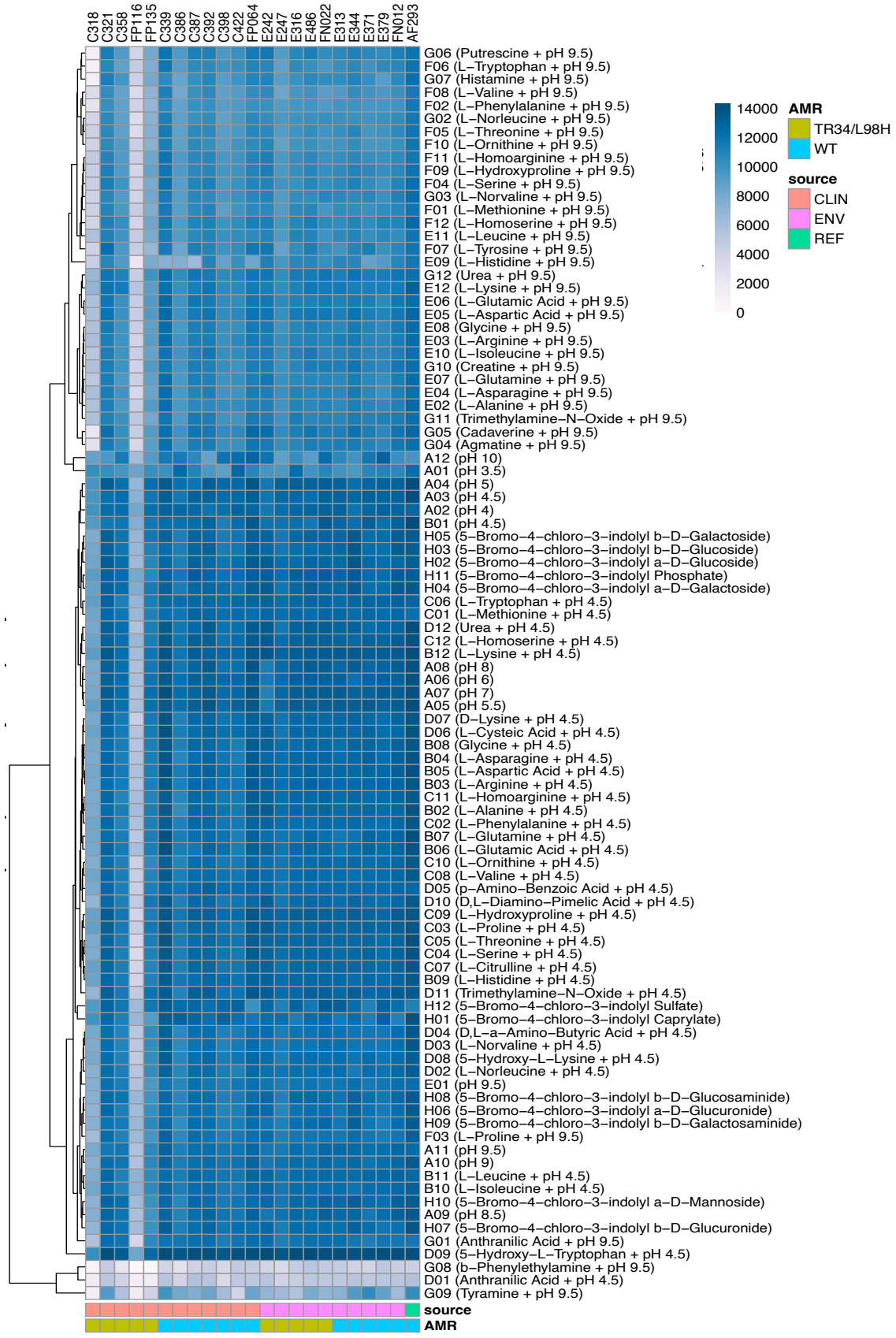


Figure 3.9. **Heatmap of *A. fumigatus* metabolic activity under pH stress conditions** Each cell represents the metabolic activity (measured as AUC) of TR_{34}/L98H, *cyp51a* wildtypes and AF293 (REF) isolates under 96 pH stress conditions, with darker blue indicating higher activity. Columns represent different isolates, grouped by AMR genotype and clinical (CLIN) and environmental (ENV) sources. Rows correspond to individual pH conditions.

3.4.5.1. Carbon utilisation (PM01)

Univariate analysis identified 6 metabolites with significant differences ($p < 0.05$) in carbon utilisation between TR_{34}/L98H and *cyp51A* wildtypes (Table 3.2), including N-Acetyl-D-Glucosamine (Well A03), Glycine-L-Proline (Well H01), D-Trehalose (well A10), D-Maltose (well C10), L-Asparagine (well D01), and L-Arabinose (well A02). Although PLS-DA was initially used to differentiate metabolic profiles, cross-validation revealed poor model performance, (permutation $n = 2000$, $p > 0.05$), prompting the use of PCA instead (Figure 3.10). The resulting overlap of the 95% confidence ellipses for TR_{34}/L98H and wildtype strains in PCA suggests substantial metabolic similarity between the groups. Despite some differences in carbon substrate utilisation, multivariate analysis did not distinctly separate the two groups.

Table 3.2. Univariate analysis of carbon substrates showing significant differences ($p < 0.05$) in utilisation between TR_{34}/L98H and *cyp51a* wildtype *A. fumigatus* isolates. Statistical tests used include t-tests and Mann-Whitney tests.

Wells	test	t-statistic	p-value
A03 (N-Acetyl-D-Glucosamine)	t-test	-2.7	0.014
C10 (D-Maltose)	t-test	-2.3	0.029
H01 (Gly-Pro)	Mann-Whitney	30	0.030
D01 (L-Asparagine)	t-test	-2.2	0.041
A10 (D-Trehalose)	t-test	-2.1	0.049
A02 (L-Arabinose)	t-test	-2.0	0.051

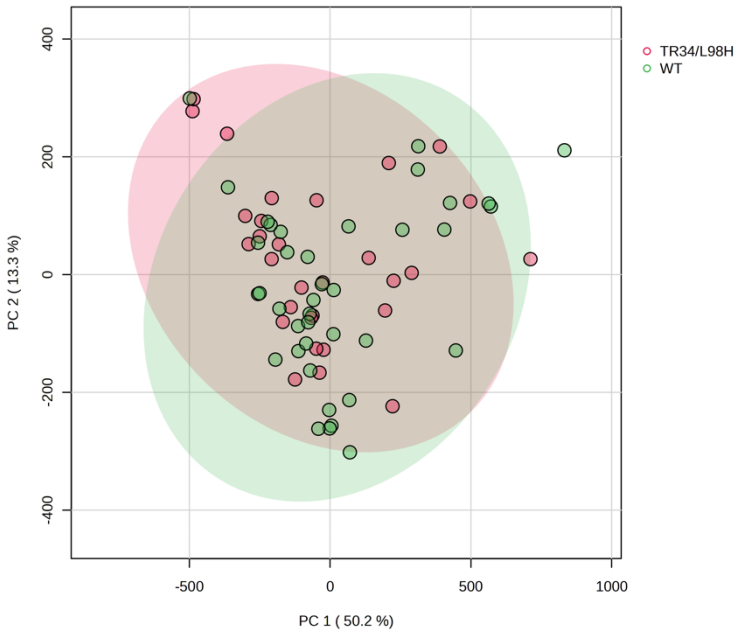


Figure 3.10. **PCA of carbon utilisation kinetics**. Distribution of TR_{34}/L98H (pink circles) and WT (wildtype, green circles) isolates along the first two principal components (PC1 and PC2). Each point represents an individual isolate, with ellipses indicating the 95% confidence intervals for each group.

3.4.5.2 Nitrogen utilisation (PM03B)

Univariate analysis identified 21 metabolites with significant differences ($p < 0.05$) in nitrogen utilisation between TR_{34}/L98H and wildtype isolates (Table 3.3), with Gly-Gln (well H09) and Ala-Glu (well H03) showing particularly strong variations ($p < 0.005$). Cross-validation determined that 5 components were optimal for PLS-DA, balancing model complexity and predictive accuracy and a permutation test ($n = 2000$, $p < 0.05$) confirmed good predictive ability. While confidence ellipses overlapped, indicating some shared metabolic traits, the separation along Component 1 revealed notable differences driven by the TR_{34}/L98H mutation (Figure 3.11a). VIP scores highlighted L-Glutamine (well B01), L-Alanine (well A07), and Ammonia (well A02) as key differentiators in the metabolic profiles of these strains (Figure 3.11b).

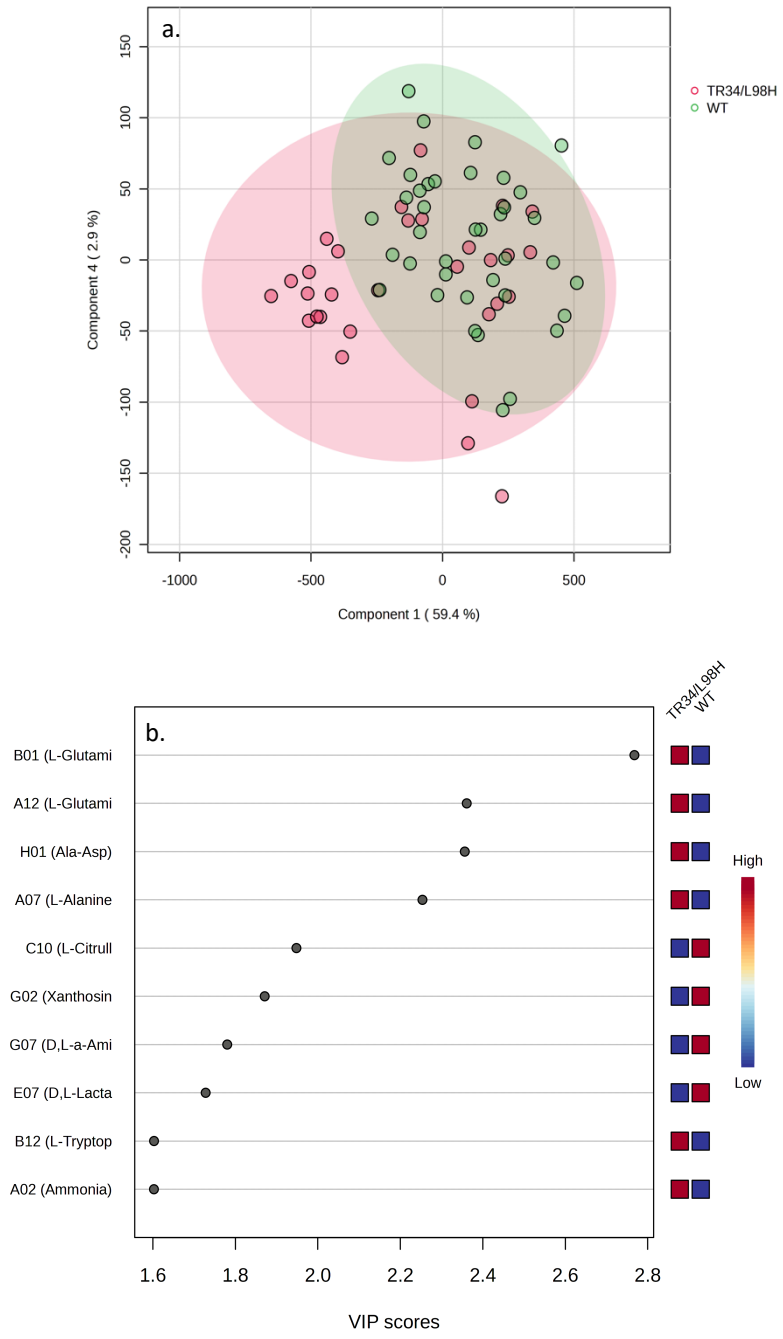


Figure 3.11. **PLSA-DA of nitrogen utilisation kinetics.** Distribution of TR_{34}/L98H (pink circles) and WT (wildtype, green circles) samples along the first two principal components (PC1 and PC2) (a). Each point represents an individual isolate, with ellipses indicating the 95% confidence intervals for each group. VIP scores plot showing the most significant differentiation of TR_{34}/L98H and *cyp51a* wildtypes based on the PLS-DA analysis with higher scores representing greater importance (b). The utilisation levels for TR_{34}/L98H and WT isolates are shown with colour gradients from blue (low utilisation) to red (high utilisation).

Table 3.3. Univariate analysis of nitrogen substrates showing significant differences ($p < 0.05$) in utilisation between TR_{34}/L98H and *cyp51a* wildtype *A. fumigatus* isolates. Statistical tests used include t-tests and Mann-Whitney tests.

Wells	test	t statistic	p-value
H09 (Gly-Gln)	t-test	-3.4	0.004
H03 (Ala-Glu)	t-test	-3.3	0.004
H04 (Ala-Gly)	t-test	-3.1	0.006
H06 (Ala-Leu)	Mann-Whitney	22	0.006
H11 (Gly-Met)	t-test	-3.19	0.006
D01 (N-Acetyl-L-Glutamic Acid)	Mann-Whitney	23	0.008
H10 (Gly-Glu)	t-test	-3.06	0.008
G07 (D,L-a-Amino-Butyric Acid)	t-test	-3.21	0.008
H02 (Ala-Gln)	t-test	-2.30	0.009
G02 (Xanthosine)	t-test	-2.8	0.02
G03 (Uric Acid)	t-test	-2.7	0.02
C10 (L-Citrulline)	t-test	-2.6	0.02
E08 (D-Glucosamine)	t-test	-2.6	0.02
E02 (b-Phenylethylamine)	t-test	-2.5	0.02
G06 (Parabanic Acid)	t-test	-2.6	0.02
E07 (D,L-Lactamide)	t-test	-2.5	0.03
H05 (Ala-His)	t-test	-2.4	0.03
F05 (Cytosine)	t-test	-2.5	0.03
E01 (Histamine)	t-test	-2.4	0.03
D02 (N-Phthaloyl-L-Glutamic Acid)	t-test	-2.2	0.04
C01 (L-Tyrosine)	t-test	-2.2	0.04

3.4.5.3 Osmolytes tolerance (PM09)

The univariate analysis of osmolyte tolerance revealed significant differences in 8 metabolites between the tested groups (Table 3.4). Tolerance to 10 mM Sodium Nitrite (well H07) showed a strong

difference ($p < 0.05$) according to the Mann-Whitney test. Other osmolytes, including 4% Sodium Sulfate (well D07), 6% Urea (well E11), and 20 mM Sodium Benzoate at pH 5.2 (well G05), also demonstrated significant differences with p-values ranging from 0.03 to 0.04. Cross-validation for PLS-DA analysis determined that 5 components were optimal, supported by a permutation test (n = 2000, $p < 0.05$) The overlap in 95% confidence ellipses for both groups suggest significant metabolic similarity between the groups, with some heterogeneity within the TR_{34}/L98H strains (Figure 3.12a). The VIP scores (Figure 3.12b) highlight the most influential osmolytes in distinguishing the metabolic profiles of TR_{34}/L98H and wildtype isolates, with Urea (well E09) and Sodium (well F01, E01) emerging as the primary contributors.

Table 3.4 Univariate analysis of osmolyte stress tolerance showing significant differences ($p < 0.05$) between TR_{34}/L98H and c*yp51a* wildtype *A. fumigatus*. Statistical tests used include t-tests and Mann-Whitney tests.

Wells	test	t statistic	p-value
H07 (10mM Sodium Nitrite)	Mann-Whitney	20	0.004
G07 (100mM Sodium Benzoate + pH 5.2)	Mann-Whitney	28	0.02
D07 (4% Sodium Sulfate)	Mann-Whitney	29	0.03
D08 (5% Sodium Sulfate)	Mann-Whitney	30	0.03
E11 (6% Urea)	Mann-Whitney	31	0.04
D05 (2% Sodium Sulfate)	Mann-Whitney	32	0.04
G05 (20mM Sodium Benzoate + pH 5.2)	t-test	-2.1	0.04

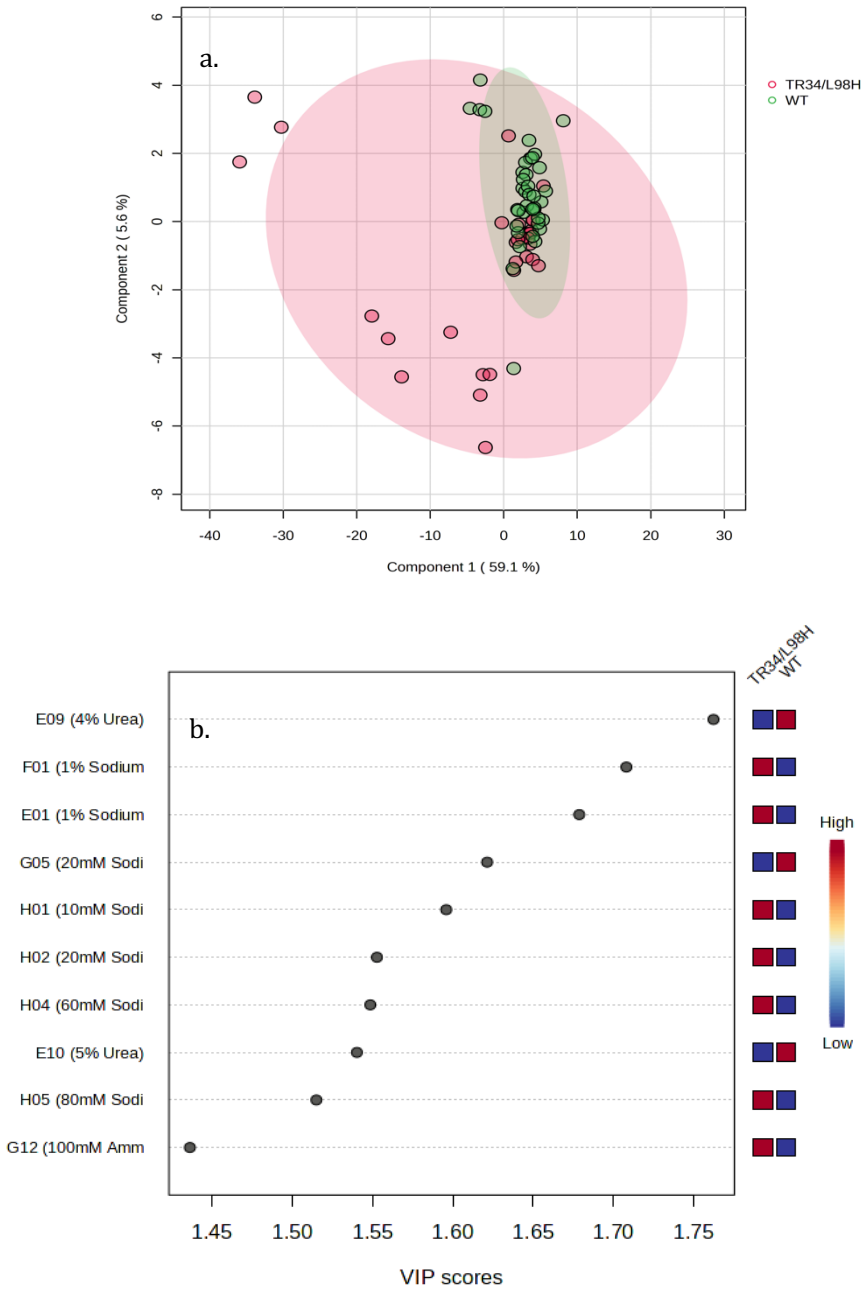


Figure 3.12. **PLS-DA of osmolyte response kinetics.** Distribution of TR_{34}/L98H (pink circles) and WT (wildtype, green circles) samples along the first two principal components (PC1 and PC2) (a). Each point represents an individual isolate, with ellipses indicating the 95% confidence intervals for each group. VIP scores plot showing the most significant osmolyte differentiation in TR_{34}/L98H and *cyp51a* wildtypes based on the PLS-DA analysis with higher scores representing greater importance (b). The utilisation levels for TR_{34}/L98H and WT isolates are shown with colour gradients from blue (low utilisation) to red (high utilisation).

3.4.5.4 pH

Significant differences in pH tolerance between TR_{34}/L98H and wildtype strains were observed in 8 conditions, particularly at acidic pH levels 4.5 and 5.5 and alkaline pH 9.5 (Table 3.5). Cross-validation revealed poor model performance (permutations $n = 2000$ $p > 0.05$) prompting the use of PCA instead

(Figure 3.13). Clustering of wildtype isolates indicate a homogenous metabolic profile, with core metabolic features also present within the TR_{34}/L98H. Although some dispersion in the TR_{34}/L98H isolates, the majority overlap substantially with the wildtype isolates, suggesting there is no distinct separation in osmolyte metabolite profiles between the two groups along the primary principal components (PC1 and PC2).

Table 3.5. Univariate analysis of pH stress tolerance showing significant differences ($p < 0.05$) between TR_{34}/L98H and *cyp51a* wildtype *A. fumigatus* isolates. Statistical tests used include t-tests and Mann-Whitney tests

Wells	test	t-statistic	P-value
A03 (pH 4.5)	Mann-Whitney	20	0.004
B01 (pH 4.5)	Mann-Whitney	21	0.005
A05 (pH 5.5)	Mann-Whitney	23	0.008
A11 (pH 9.5)	Mann-Whitney	26	0.01
F06 (L-Tryptophan + pH 9.5)	Mann-Whitney	27	0.02
G09 (Tyramine + pH 9.5)	t-test	-2.61	0.02
D01 (Anthranilic Acid + pH 4.5)	Mann-Whitney	31	0.04
D05 (p-Amino-Benzoic Acid + pH 4.5)	Mann-Whitney	32	0.04

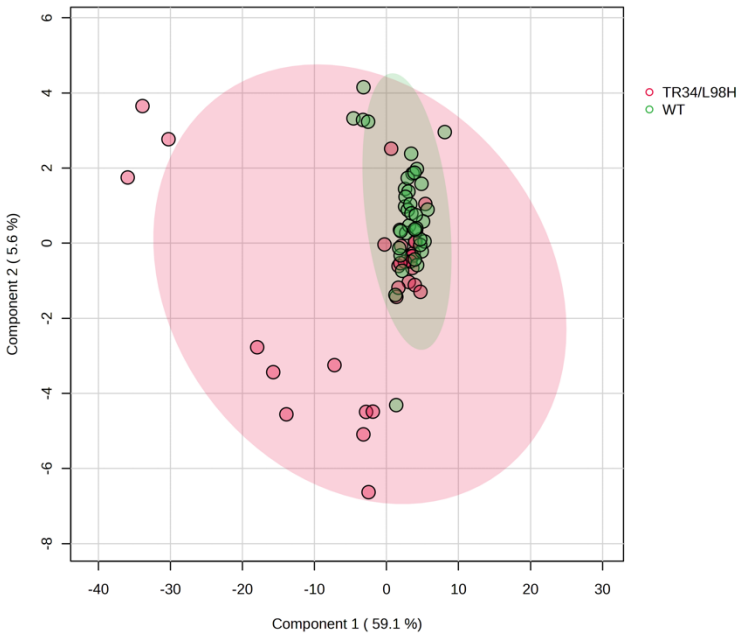


Figure 3.13 **PCA of pH response kinetics.** Distribution of TR_{34}/L98H (pink circles) and WT (wildtype, green circles) isolates along the first two principal components (PC1 and PC2). Each point represents an individual isolate, with ellipses indicating the 95% confidence intervals for each group.

3.4 Discussion

This study provides a comprehensive analysis of the genetic and phenotypic diversity of *A. fumigatus* isolates across the United Kingdom, with a particular focus on the TR_{34}/L98H resistance mechanism. Using WGS and high-throughput phenotyping, this study investigated the evolutionary adaptations and phenotypic characteristics associated with azole resistance and virulence in *A. fumigatus*. TR_{34}/L98H isolates exhibited a higher accumulation of nsSNPs in genes related to toxins, secondary metabolites, cell wall integrity, nutrient acquisition, and stress response, suggesting an enhanced adaptive potential to environmental stressors and antifungal treatments. These findings align with previous studies on *A. fumigatus* diversity, reinforcing the idea that secondary metabolism genes exhibit the greatest variability among virulence-associated genes (387,393)

The TR_{34}/L98H genotypes had significantly more nsSNPs in eight genes related to toxins and secondary metabolite production, including three cytochrome P450 monooxygenases (easK, CYP5081B1, CYP5081A1), *osc3*, *fumR*, *tpcA, tpcB*, and *gliZ.* Cytochrome P450 enzymes are essential for diverse biochemical processes, such as the oxidation of steroids and fatty acids and the detoxification of xenobiotics like polycyclic aromatic hydrocarbons (PAHs), pesticides, and insecticides, which may facilitate adaptation to hostile environments (394–401).

Mutations in *osc3* (*erg7*), encodes oxidosqualene:protostadienol cyclase, which diverts 2,3-epoxysqualene from ergosterol production to helvolic acid synthesis (402), could increase the availability of 2,3-epoxysqualene for ergosterol production, potentially enhancing azole resistance (Furukawa et al. 2020). *FumR* (*fapR*) regulates fumagillin biosynthesis (404,405), an anti-angiogenic compound that inhibits endothelial proliferation and blood vessel formation (163,406,407). Upregulation of fumR during infection suggests a strategic role in facilitating invasion and adaptation within the host (408). Notably, Barber *et al*., (387), observed an absence of *fumR* in 49% of isolates, although the specific genotypes lacking *fumR* were not specified. *GliZ* regulates gliotoxin biosynthesis, a critical virulence factor that facilitates immune evasion and enhances infection establishment, ultimately increasing its chances of survival and proliferation in host (409–411). High impact variants

in *gliZ* were also detected by Barber et al. (387). *TpcA*, encoding O-methyltransferase, promotes *hapX* expression, enhancing siderophore synthesis crucial for iron regulation and virulence (412,413). *HapX* disruption has been linked to increased *cyp51A* expression and azole resistance, independent of iron levels (414). Adaptation to iron starvation is crucial for virulence, given the limited iron during infection (415,416). *TpcB* regulates trypacidin, which induces necrosis-induced lung cell death, contributing to pathogenicity (417). Moreover, absence of trypacidin has been shown to increases phagocytosis by murine alveolar macrophages but reduced phagocytosis by amoebas, highlighting its dual role in enhancing virulence and defending against environmental predators (418).

Additional nsSNPs in the *mfsC* and *RodA* genes in TR_{34}/L98H isolates may enhance resistance to antifungals and immune responses. Sharma *et al*., (2019) (419) observed the overexpression of *mfsC* in non-*cyp51a* resistant isolates, with WGS identifying a large number of SNPs in *mfsC*, which could potentially explain the observed overexpression. The additional nsSNPs could optimise MFS transporter function, acting as an efflux pump to expel antifungal agents, thus enhancing multidrug resistance Additional nsSNPs in *RodA* may impact rodlet formation, masking fungal cell wall components from immune detection (146,147,420). This dual advantage of increased drug resistance and enhanced immune evasion would enable TR_{34}/L98H isolates to survive and persist more effectively in hostile environments, contributing to their success and prevalence.

Genes associated with allergens, *csn* and *aspHS*, show significant nsSNP differences between TR_{34}/L98H and wildtype isolates. The *csn* gene encodes chitosanases from the glycosyl hydrolase family 75 (GH75), which hydrolyse chitosan, a deacetylated form of chitin. Although GH75 chitosanases, particularly those of fungal origin, have been relatively understudied, the conversion of chitin to chitosan likely modulates fungal cell wall structure (421). Increased nsSNPs in *csn* may impact immune evasion in TR_{34}/L98H isolates. As humans do not synthesize chitin, GH75 chitosanases are promising antifungal drug targets (422), however, targeting the entire chitin synthase family is not a viable option due to predicted differences in structure and the membrane bound location of the proteins (423). Additional nsSNPs in *aspHS,* encoding cytotoxic asp-hemolysin may also influence the

ability of *A. fumigatus* to evade immune defences and impact toxicity to macrophages and endothelial cells (424), potentially supporting infection success (425). These genetic changes may give TR_{34}/L98H isolates a selective advantage under immune pressure and antifungal treatment, contributing to their enhanced virulence and pathogenic success.

Four genes related to signalling and regulation, *FOS-1, GprC, GprD,* and *mpkA*, show significant differences between TR_{34}/L98H and wildtype isolates. *FOS-1* encodes a putative histidine kinase involved in responses to osmotic stress, dicarboximide fungicides, and cell wall assembly. While deletion of *FOS-1* does not affect growth or morphology, it delays conidiation and increases dicarboximide fungicide resistance, suggesting adaptive advantages under stress (426). The additional nsSNPs in *FOS-1* in TR_{34}/L98H could impact resistance to fungicides targeting cell wall integrity. *GprC* and *gprD* mediate thermal adaptation, with *gprC* being particularly crucial at elevated temperatures (427). The lower TR_{34}/L98H mutation rate in *gprC* suggests selective pressure to preserve heat adaptation, while higher *gprD* mutations may enable flexibility in cooler temperatures. Transcriptomic shifts from primary to secondary metabolism upon deletion of either *gprC* or *gprD* indicate an evolved capacity for metabolic reprogramming (427). This flexibility could allow TR_{34}/L98H to prioritise the production of secondary metabolites, in response to environmental stresses. Mutations in *mpkA* could optimise responses to oxidative stress, reduce antifungal susceptibility, and increase virulence by refining gliotoxin control, given the role of *mpkA* in gliotoxin regulation, self-protection, cell wall integrity, and response to reactive oxygen species (ROS) (428,429).

The TR_{34}/L98H variant of *A. fumigatus* displays a significantly higher number of nsSNPs in genes related to cell wall integrity, such as *och1*, *Ecm33*, and *chsA*, compared to the wildtype. Polymorphisms in *och1* may affect conidial formation under calcium stress potentially impacting virulence (430). Similarly, variations in *Ecm33* might alter cell wall stability, potentially affecting resistance to antifungal agents and the host's immune defences (431). Additionally, increased nsSNPs in *chsA,* a

gene essential for chitin synthesis and the oxidative stress response (432), suggest potential changes in cell wall structure or regulation that could improve resistance to environmental stressor.

The TR_{34}/L98H exhibits more nsSNPs in genes associated with nutrient acquisition and stress response, including *ddpIV*, *pkaC2*, and *ctsD*, potentially enhancing its ecological and pathogenic success in nutrient-limited settings. For instance, *DppIV* is known to facilitate tissue invasion and immune evasion (433), additional nsSNPs could influence its function to strengthen invasive capabilities. Mutations in *pkaC2*, which plays a role in regulating oxidative metabolism and conidial germination (434), may enhance oxidative stress resistance, supporting survival in the host environment. Lastly, alterations in *ctsD*, a protease upregulated during infection, might increase nutrient acquisition, thereby promoting growth and virulence (435).

The phenotypic analysis of wildtype and TR_{34}/L98H azole resistant *A. fumigatus* isolates reveals significant metabolic adaptability, enabling survival across diverse environmental conditions. While growth differences are evident, OmniLog data highlight overlapping metabolic profiles, suggesting nuanced, context-specific adaptations. Compared to TR_{34}/L98H, wildtype isolates efficiently utilise alternative carbon sources such as N-acetyl-D-glucosamine (GlcNAc), D-trehalose, D-maltose, Gly-Pro, and L-asparagine, reflecting their ability to adapt to fluctuating environments. Although glucose serves as the primary energy source (436), limited glucose availability in host environments necessitates the shift to alternative sources like GlcNAc (437)**.** Notably, GlcNAc exposure induces changes in cell wall composition, decreasing glucan and galactomannan while increasing chitin and mannan, thereby heightening susceptibility to cell wall-targeting antifungals (383). Despite metabolic flexibility, wildtype strains may exhibit increased vulnerability to cell wall stress. In contrast, TR_{34}/L98H isolates may prioritise alternative carbon sources, minimising the risks associated with GlcNAc utilisation and enhancing survival under azole induced stress.

During early germination, it is hypothesised that d-trehalose provides energy for conidial germination and cell wall biosynthesis (438,439). However, TR_{34}/L98H may shift energy metabolism away from

d-trehalose to alternative carbon sources as an adaptive response to azole stress. Additionally, cell wall modifications in TR_{34}/L98H strains might lower their dependence on d-trehalose making their germination process less energy-intensive. This shift could lead to delayed conidiation since they are not efficiently using d-trehalose for rapid energy release.

The distinction between wildtype and TR_{34}/L98H *A. fumigatus* strains becomes more pronounced when analysing nitrogen utilisation, with 21 metabolites showing significant variation between the two *cyp51a* genotypes. Metabolites such as L-glutamine and L-alanine emerge as key differentiators in nitrogen metabolism. The differences in nitrogen and carbon utilisation align with the concept of catabolite repression which enables fungi to prioritize specific substrates to optimize growth and survival under nutrient-limiting conditions (10). This regulatory mechanism may explain the distinct nitrogen and carbon utilisation profiles of TR_{34}/L98H strains. These metabolic shifts likely represent an adaptive response to environmental stressors, allowing strains to efficiently exploit alternative nitrogen and carbon sources when preferred nutrients are scarce.

Among the 10 osmolytes differentiating TR_{34}/L98H from wildtype *A. fumigatus*, seven were significantly utilised by TR_{34}/L98H, reflecting an enhanced osmotic stress tolerance that likely confers increased survival and competitiveness in environments with fluctuating osmotic conditions. Araújo et al. (2020) (440), suggest that fungi inhabiting dynamic environments often exhibit robust stress response systems, and the improved osmotic tolerance observed in TR_{34}/L98H isolates likely contributes to their persistence and dissemination in biophysically complex settings. In the context CF lung environments, which are characterised by fluctuating osmotic conditions, altered pH, and nutrient limitations due to thick mucus and recurrent infections (441,442), these metabolic and stress response differences between TR_{34}/L98H and wildtype *A. fumigatus* isolates are particularly relevant. The enhanced osmotic stress tolerance in TR_{34}/L98H isolates likely confers a selective advantage in conditions where osmotic pressures vary due to mucus dehydration and solute concentration, promoting the persistence of TR_{34}/L98H strains. In contrast, wildtype isolates demonstrated superior growth across a broad pH range (4.5 to 9.5) compared to TR_{34}/L98H strains, suggesting that wildtype

strains possess greater metabolic flexibility. This adaptability may enable wildtype isolates to colonise various niches within the CF lung, where pH levels fluctuate in response to infection and inflammation, potentially contributing to their ecological fitness and persistence in the lung environment.

These findings reveal that the TR_{34}/L98H genotype of *A. fumigatus* has evolved extensive genetic and metabolic adaptations that may enhance both azole resistance and virulence, demonstrating the pathogen's remarkable ability to thrive under environmental pressures. The accumulation of nsSNPs in genes related to toxin production, immune evasion, and nutrient acquisition underscores the multifaceted functional potential of TR_{34}/L98H isolates. While this study does not include direct expression analysis, the implications of these genetic variations warrant further exploration to understand their potential roles in enhancing the pathogenicity of *A. fumigatus.* The metabolic profiles observed in carbon and nitrogen utilisation and stress tolerance highlights the capacity for metabolic reprogramming. However, while the TR_{34}/L98H allele may influence specific aspects of metabolism, these changes do not produce a distinct metabolic profile. This points to a multifaceted adaptation strategy where metabolic flexibility plays a critical role in environmental resilience rather than drastic shifts in metabolic pathways. This phenotypic characterisation underscores the metabolic versatility of *A. fumigatus* while also highlighting specific sources that may be critical for its growth and pathogenicity.

Machine learning classifiers, such as random forest models, could be applied to mutation profiles to predict the TR_{34}/L98H genotype and identify the most predictive mutations. However, the functional consequences of these mutations remain uncertain without comprehensive SNP impact annotation, protein modelling, expression data, and functional validation studies. By focusing solely on single nucleotide changes, this approach may overlook structural variations, such as insertions, deletions, and copy number changes, that could influence phenotypic diversity. Additionally, the quality and reliability of alignments are influenced by the accuracy and completeness of the reference genome, with errors or gaps potentially leading to misalignments or obscuring genetic variations in the sample data.

Experimental approaches, such as site-directed mutagenesis and gene knockout/overexpression studies using isogenic lines, are essential for determining whether these mutations confer adaptive advantages or alter gene function. Assessing potential trade-offs in growth, fitness, and antifungal susceptibility as well as using animal models and co-culture experiments with host cells will be fundamental to understanding the broader biological implications of these mutations.

Fungal phenotypic plasticity, driven by the immediate growth environment (443), complicates data interpretation in PM assays. This plasticity, potentially influenced by epigenetic mechanisms, can alter metabolic profiles, adding a layer of complexity when trying to link genotype to phenotype. Examining epigenetic modifications, such as DNA methylation and histone changes, could provide valuable insights into how metabolic plasticity is regulated and improve the predictive accuracy of PM assays. However, integrating PM data with genomic, transcriptomic, and epigenomic information poses significant challenges due to the complexity of multi-omics analysis. Advanced computational tools are required to handle the scale of these datasets and to fully understand how genetic and epigenetic factors shape metabolic pathways and influence phenotypic expression. Lastly, metabolic diversity among fungal isolates complicates efforts to draw consistent conclusions, as phenotypic plasticity varies across isolates. Larger sample sizes are essential to capture the full range of metabolic adaptability, as small samples may overlook key variations.

Conclusion

In conclusion, the TR_{34}/L98H genotype of *A. fumigatus* exhibits extensive genetic and metabolic adaptations that likely enhance both azole resistance and virulence. The accumulation of nsSNPs in key genes related to toxins, immune evasion, and nutrient acquisition highlights its multifaceted adaptive potential. While metabolic flexibility appears central to environmental resilience, further functional validation is required to determine the exact roles of these mutations.

Chapter 4 Epidemiology of azole resistant *A. fumigatus* in a respiratory disease cohort

4.1 Abstract

Azole resistance in A. fumigatus poses a major challenge in managing chronic respiratory diseases, where long-term antifungal therapy is often required. Prospective surveillance of 55 individuals revealed a 25% prevalence of azole resistance, with resistance strongly associated with CF and CPA. WGS of 178 isolates from 15 individuals identified TR34/L98H as a predominant resistance mechanism in 26.6% of cases, while the TR46/Y121F/T289A allele was detected in one individual, highlighting its emergence in respiratory disease cohorts in London. The inclusion of retrospective WGS data expanded the study to include 300 isolates from 83 individuals collected between 2015 and 2022. Phylogenomic and population diversity analysis showed extensive genetic diversity among isolates, including mixed colonisations, distinct subpopulations, and potential signs of recombination, revealing the persistence of certain resistant strains within hosts alongside evidence of external introductions. Remote sampling methods adapted during COVID-19 facilitated high patient engagement and enabled a comprehensive longitudinal dataset. This work highlights the complexity of azole resistance dynamics in *A. fumigatus*, underscoring the need for advanced surveillance strategies that incorporate high-throughput sampling and WGS to accurately capture intraspecific diversity and emerging resistance mechanisms.

4.2 Introduction

Opportunistic pathogens such as *A. fumigatus* have evolved extraordinary adaptability, allowing them to thrive across diverse environmental niches under a wide range of abiotic and biotic stressors (133,337). This adaptability is largely driven by the acquisition of advantageous traits through spontaneous mutations and recombination. During prolonged infections, *A. fumigatus* continually adapts to survive in the human host, an environment vastly different from its typical ecological niches, such as decaying organic matter (263). In-host fungal adaptation can be evidenced by macroscopic

abnormalities, such as reduced sporulation and slower growth in sample cultures from chronically colonised patients (223,263). These adaptations are shaped by a dynamic interplay between the pathogen and the host immune system, where immune defences are insufficient to fully eradicate the infecting the fungi (444). This allows the pathogen to persist, adapt and evolve under constant selective pressures (235).

In chronic respiratory diseases, where persistent fungal colonisations can endure for months, repeated azole therapy is often necessary. The prolonged exposure to azoles creates a potent selective environment favouring the survival of resistant *A. fumigatus* colonies (265,445–447). Triazoles antifungal agents, including itraconazole, voriconazole, and posaconazole, have long been the cornerstone of therapeutic management for aspergillosis. However, the global emergence of triazole-resistant *A. fumigatus* strains has profoundly reduced the efficacy of the treatments, thereby constraining therapeutic options and worsening clinical outcomes (294). Clinically derived azole resistance is frequently associated with nsSNPs in the coding region of the drug target *cyp51a,* which encodes the enzyme, 14α-sterol demethylase (CYP51A). These nsSNPs are often located in specific genetic "hotspots" that confer resistance. Notable examples include polymorphisms at the M220 position, such as M220I (methionine to isoleucine) and M220V (methionine to valine), which are linked to itraconazole resistance and variable resistance to voriconazole and posaconazole (448). Similarly, mutations at position G54, such as G54W (glycine to tryptophan) and G54E (glycine to glutamic acid), are implicated in itraconazole resistance (449). These mutations effectively reconfigure the binding pocket of the CYP51A enzyme, diminishing drug binding and efficacy and precipitating therapeutic failure (450,451). Many of these mutations can result in resistance to multiple triazoles (252,260)

Previous studies have described in host acquisition (260,264,354), offering key insights into the adaptive changes that occur under antifungal pressure. Genotypically distinct colonies of *A. fumigatus* can emerge within a single patient, each exhibiting distinct mutations, suggesting a high level of evolutionary potential within the infecting fungal population. A classic example of in host *de-*

novo azole resistance development was observed in patients with chronic granulomatous disease. A study by Ballard *et al*., (354) utilised WGS to examine the microevolution of *A. fumigatus* in a patient over two years, isolating 13 strains that exhibited 248 non-synonymous polymorphisms. Initially, these strains were azole susceptible, but later isolates demonstrated resistance to itraconazole, voriconazole, and/or posaconazole. The progression illustrated the development of both *cyp51A*-dependent and independent resistance mechanisms, facilitating fungal persistence even under sustained antifungal therapy. In chronic respiratory diseases, this in-host evolution occurs against a mosaic of microenvironments, characterised by substantial variability in immune responses, oxygen and nutrient availability and pharmacokinetic and pharmacodynamic profiles (452). This spatial heterogeneity can promote the evolution and long-term stability of population diversity during infection (453). Additionally, individuals can acquire azole resistant *A. fumigatus* strains from the environment, such as TR_{34}/L98H and TR_{46}/Y121F/T289A, further contributing to the complexity of azole resistant population dynamics (254,272,454–456). Consequently, studies isolating a limited number of colonies may fail to capture the full spectrum of resistance mechanisms across patient populations. Comprehensive *in vitro* susceptibility testing should involve multiple colonies, as single colony assessments risk underestimating the diversity of azole resistant *A. fumigatus* within hosts (457,458).

Surveillance at the Royal Brompton and Harefield NHS Foundation Trust (RBHT) identified a ~13% prevalence of triazole-resistant isolates among individuals with chronic respiratory diseases. Notably, 40% of these resistant isolates contained the environmentally acquired TR_{34}/L98H (301), indicating that environmental transmission substantially contributes to the epidemiology of resistance in this vulnerable cohort. Targeted surveillance studies are essential to assess the prevalence of both *de novo* and environmental resistance. Despite extensive azole resistance surveillance, comprehensive longitudinal studies examining in-host diversity of *A. fumigatus* in chronic respiratory disease patients are lacking.

4.3 Methods

4.3.1 Impact of COVID-19 on Prospective Clinical Surveillance

Initially, patients were scheduled to provide sputum samples during routine outpatient visits. However, following national guidelines for the prevention of COVID-19, outpatient visits were restricted, and at-risk patients were advised to remain at home under shielding measures. To ensure the continuity of the study, the sampling approach was adapted: patients were provided with remoted sampling kits, enabling them to safely collect and submit sputum samples from their homes. This modification adhered to public health recommendations and facilitated uninterrupted data collection throughout the pandemic.

4.3.2 Remote sputum sample collection

Each month, participants were provided with a remote sampling kit, which included a sterile 30 ml sample collection tube (Thermo Scientific™, Sterilin™), the necessary UN3373-compliant pre-paid return packaging (Appendix 6). A detailed sampling instruction leaflet provided step-by-step guidance on how to properly collect, package, and mail the sputum sample to the Imperial College London laboratories (Appendix 7). Participants were instructed to record their unique patient identification number and the date of sputum collection on the sample tube to ensure traceability of each sample.

4.3.3 Sputum sample processing

Sputum samples were processed upon receipt or stored at 4°C for up to 72 hours. Sample details, including receipt dates, sputum production, appearance, and volume were recorded in the RedCap® (Research Electronic data capture) data collection platform hosted at Imperial College London, UK (360,361). An equal volume (1:1 ratio) of Mucolyse Sputum Digestant (Pro-Lab diagnostics, UK) was added to the sample tube and incubated at room temperature for 20 minutes to liquify the sample and enhance the isolation of fungal species. Aliquots of the liquified sample were inoculated on to three

culture plates containing Sabouraud dextrose agar (SDA, Oxoid Ltd, UK) supplemented with chloramphenicol (50 mg/L) to supress bacterial growth. For high volume cultures, 200µl of liquefied sample was inoculated on to two culture plates and distributed with a sterile L-shaped spreader. One plate was incubated at 28°C for 7 days for the isolation of culturable fungi associated with the sputum, and the second was incubated at 45°C for 7 days for the isolation of *A. fumigatus*. A third plate, inoculated with 100 µl of concentrated cells (centrifuged at 3000rpm for 10 minutes) was incubated at 28°C for up to 4 weeks to allow for the isolation of slower growing fungi such as *Exophiala spp*. and *Scedosporidium spp*.

4.3.4 Isolation of *A. fumigatus* colonies

To capture sample diversity, a subset of up to 5 colonies per morphology were sub-cultured onto SDA plates using the 3-spot method as detailed in section 2.4.3. Conidia from pure cultures were cryopreserved at -80°C according to section 2.4.5.

4.3.5 Antifungal susceptibility screening

All (n = 321) *A. fumigatus* isolates were screened for susceptibility to the three clinical azoles, itraconazole (4 mg/L), voriconazole (2 mg/L) and posaconazole (0.5 mg/L) and the agricultural azole tebuconazole as per section 2.8.

4.3.6 Retrospective clinical isolate collection

Fungal cultures from respiratory samples are routinely processed at the RBH Microbiology Laboratory, adhering to established local protocols. Under the supervision of Professor Darius-Armstrong James, longitudinal clinical isolates of yeasts and moulds have been preserved on SDA slopes (Oxoid Ltd, UK) as part of an ongoing research initiative*. A. fumigatus* isolates from a 2019 collection were accessed to enhance the longitudinal *A. fumigatus* prospective collection. Fungal isolates had previously been identified as per local standard procedures at the RBH microbiology laboratory. In total, 164 were labelled as *A. fumigataus* and subsequently sub-cultured. Of these, 43 were discarded due to possible contamination or failed to grow. Patient ID numbers were matched to

the 121 revived isolates, with 13 matched to participants in the prospective RBH respiratory disease cohort. Isolate retrieval was facilitated by Clinical Scientist Ali Nuh and Professor Darius Armstrong-James. Conidia were harvested from the original culture as per section 2.4.3. Plates were incubated at 45°C for 3-5 days and visually inspected for uniform morphology to ensure purity. Pure colonies were stored at 4°C until processing for downstream analysis or cryopreservation at -80°C as per section 2.4.5.

4.3.7 DNA extraction and quantification

Clinical isolates were systematically selected to capture the genotypic diversity of *A. fumigatus* within each patient sample. Priority was given to longitudinal isolates from patients with more than three culture-positive samples. Isolates were cultured from glycerol stocks at 45°C for 2-5 days as described in section 2.5.3 followed by gDNA extraction and WGS (as per section 2.9 and 2.10 respectively).

4.3.8 Next Generation Sequencing & Bioinformatic analysis

Genomic DNA underwent WGS at the Earlham Institute, utilising the Illumina NovaSeq sequencing platform as described in section 2.10.1. Whole genome sequence alignments were processed as per sections 2.10.3 - 2.10.4. Genotypic characterisation was performed as per sections 2.10.6.

4.3.9 Incorporation of 118 RBH retrospective genomes

The retrospective genomic library (section 2.10.2) includes the raw FASTA files of 118 previously sequenced *A. fumigatus* isolates originating from the RBH respiratory disease cohort (collected between 2015-2016). Patient identification numbers and clinical demographics were matched to prospective patient isolates to further enhance the longitudinal data set. Isolates ordinated from 74 individuals diagnosed with ABPA (n = 8), Aspergillus bronchitis (*n* = 2), Aspergillus colonisation (*n* = 3), Bronchiectasis (*n* = 2), CF (*n* = 50) and CPA (*n* = 7) and 2 patients with an 'unknown diagnosis'. WGS alignments were processed as per section 2.10.3. VCFannotator (Broad Institute) was used to identify nsSNPs within the cyp51a coding region as described in section 2.10.6.

4.3.10 Phylogenomic analysis

Phylogenetic trees were inferred from whole genome sequences using RAxML-NG (370) as described in section 2.12. Bootstrap replicates were concatenated with the inferred trees until convergence was achieved (n = 250 bootstraps). Phylogenetic trees were visualised in R 4.3.1 using the ggTree (371) and ggTreeExtra (372) packages and uploaded as an interactive Microreact project (Appendix 2).

4.3.11 Calculating pairwise SNPs

To explore genomic diversity and identify closely related *A. fumigatus* isolates, pairwise unique SNPs were calculated between VCF files and visualised as histograms as described in section 2.13.

4.3.12 Multivariate analysis of genomic data

Multivariate genomic analysis was conducted in R version 4.3.1 using the adegenet package version 2.1.10 following established protocols (373–376) as per section 2.14.

4.3.13 Genetic diversity

Nucleotide diversity (π), defined as the average pairwise nucleotide differences between sequences in a population (459) was assessed to evaluate intra-genetic diversity. Tajima's D, which is a measure of deviation from neutral evolution (460), was used to assess the evolutionary dynamics and selective pressures acting on the *A. fumigatus* populations. Diploid SNPs were identified using GATK HaplotypeCaller (version 4.0), with sequencing reads aligned to the AF293 reference genome (365). Variants were called using a minimum base quality of 20, a confidence threshold of 30, and exclusion of repeat regions. SNPs were selected with GATK SelectVariants and filtered using VariantFiltration based on quality metrics (QD < 2.0, FS > 60.0, MQ < 40.0, MQRankSum < -12.5, ReadPosRankSum < -8.0, SQR > 4.0, DP < 10). Only variants marked PASS in the VCF file were retained for downstream analyses.

4.3.14 Statistical analysis

The association between diagnosis and azole resistance was assessed using chi-square tests and logistic regression, with categorical variables including gender, age group, and diagnosis. Logistic regression modelled resistance based on diagnosis, age, and gender, with predicted probabilities visualised through confidence intervals. Analyses were performed in R (version 4.3.1) and visualised using ggplot2 (v3.5.1). Nucleotide diversity (π) and Tajima's D was compared using non-parametric methods due to non-normality, with bootstrapped mean diversity and 95% confidence intervals (1,000 iterations). Group differences were assessed with the Kruskal-Wallis test, followed by Dunn's test with Bonferroni adjustment for pairwise comparisons.

4.4 Results

4.4.1 Patient participation and sputum sample collection

Between September 2020 and April 2022, 296 sample kits were distributed to 55 individuals (Appendix 8). Of these, 235 sputum samples were returned for processing, resulting in a 79% sample return rate. (Figure 4.1a). Among the participants, four returned only one sample, while 35 patients demonstrated higher engagement by providing three or more consecutive samples. All participants resided in the UK, particularly in urban areas around London (Figure 4.1b). In total, 321 serial *A. fumigataus* isolates and 760 yeasts and moulds were collected from patients diagnosed with the following underlying conditions: CF (*n* = 9, 16.4%), CPA (*n* = 21, 38.2%), ABPA (*n* = 23, 41.8%), *A. fumigatus* colonisation (*n* = 1, 1.8%), and COPD (*n* = 1, 1.8%) (Figure 4.1c). During the course of the study, 4 participants verbally opted out due to declining health, and unfortunately, 3 participants passed away.

4.4.2 Azole resistance detected in 146/321 of prospective clinical isolates.

A total of 321 serial *A. fumigatus* colonies from 55 patients were screened for azole susceptibility. Of these, 45.5% (*n* = 146) demonstrated resistance to at least one clinical azole. Voriconazole (2 mg/L) exhibited the highest efficacy among clinical azoles, with 18.4% (*n* = 59) displaying resistance, compared to 32.1% (*n* = 103) and 35.8% (*n* = 115) resistant to itraconazole (4 mg/L) and

posaconazole (0.5 mg/L), respectively. Resistance to the agricultural azole tebuconazole was also observed, with 26.2% (*n* = 84) demonstrating resistance at 6 mg/L, and 12.1% (*n* = 39) exhibiting resistance at concentrations up to 16 mg/L.

a.

Total Participants	Total sample kits provided	Total samples returned	Total sputum samples processed	Isolates colleted	
				Aspergillus fumigatus	Other
55	296	235	235	321	760



Figure 4.1 **Geographical distribution and clinical diagnosis of individuals participating in prospective clinical surveillance**. Table providing an overview of the number of sample kits provided and returned for processing and total number of isolates collected (a). Geographical distribution of participants in the prospective surveillance study across the UK, indicated by coloured points corresponding to clinical diagnoses (CF, CPA, ABPA, COPD and *A. fumigatus* colonization) (b). The inset bar chart shows the number of participants per clinical diagnoses (c).

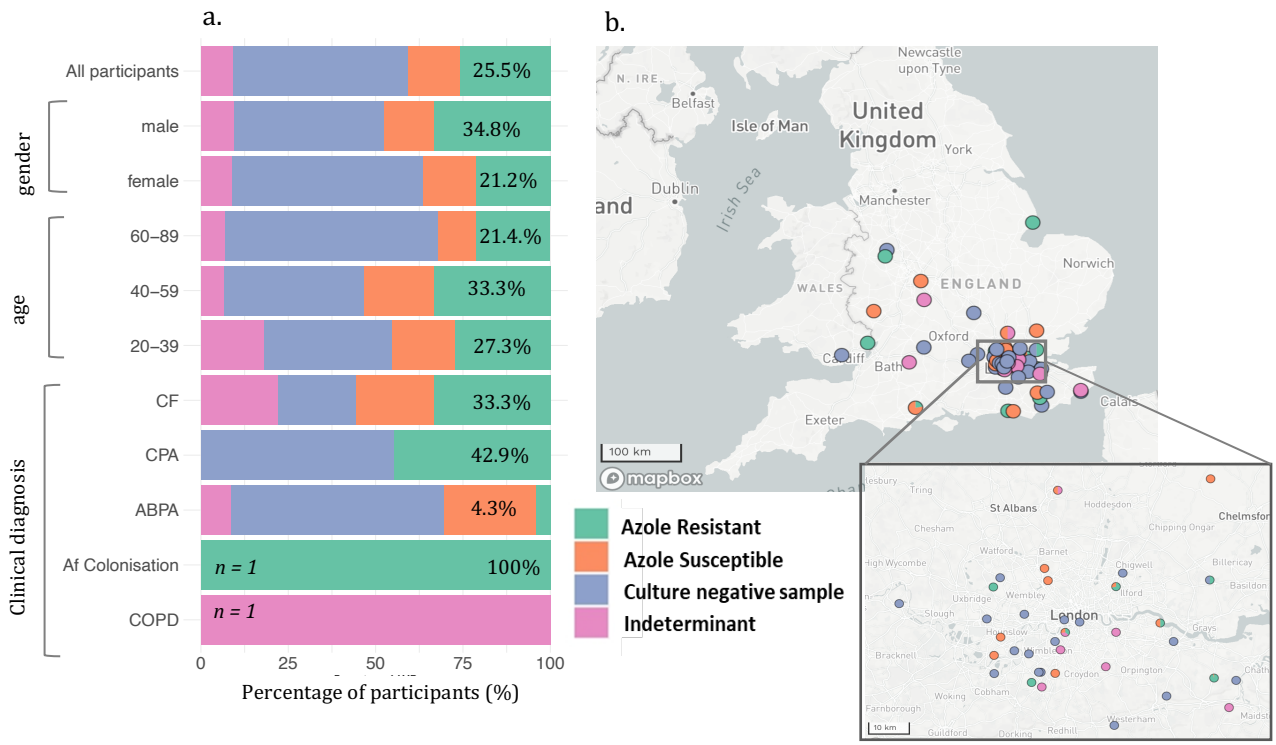


Figure 4.2. **Azole resistance prevalence across the prospective chronic respiratory disease cohort**. Prevalence of azole resistance among participants in the respiratory disease cohort who had at least one azole-resistant isolate in longitudinal samples (a). Resistance prevalence is further categorised by gender, age, and clinical diagnosis. UK distribution of participants with at least one azole resistant isolate detected in longitudinal samples (b).

4.4.3 Azole resistance detected in 25% of the RBH respiratory disease cohort

Of the 55 participants, 25.5% had at least one isolate that exhibited resistance to at least one clinical azole (Figure 4.2a). Resistance prevalence was higher in the 40-59 age group. Among the 21 CPA participants, 100% of culture positive samples contained at least one azole resistant isolate, resulting in a resistance prevalence of 42.9%. Participants with CF had a resistance prevalence of 33.3%, notably higher than those diagnosed with ABPA (4.3%). The geographical distribution of clinical azole resistance in the UK is shown in Figure 4.2b.

4.4.4 Association of azole resistance with clinical diagnosis and demographics

Azole resistance was significantly associated with clinical diagnosis and patient demographics, with clinical diagnosis showing the strongest association ($\chi^2 = 61.2$, df = 2, $p < 0.0001$; Appendix 9). Patients

with CPA exhibited a positive association with resistance (χ^2 = 22.7, df = 2, p < 0.0001, standardised residual = 6.3; Appendix 9), and multivariate logistic regression confirmed CPA as a strong independent predictor of resistance (Figure 4.3a). Conversely, ABPA was associated with a significantly lower likelihood of resistance (χ^2 = 38.4, p < 0.0001, standardised residual = -4.1). Regarding patient demographics, gender initially appeared to be associated with resistance (p < 0.05, Appendix 9); however, after adjusting for other factors, logistic regression revealed no significant difference between genders (Figure 4.3b). Age demonstrated varying associations with resistance: in univariate analysis, the 20–39 age group showed a negative association (χ^2 = 5.4, p < 0.05, standardised residual -1.7, Appendix 9), the 40–59 group exhibited a positive association (χ^2 = 4.6, p < 0.05, standardized residual = 1.4), and no significant association was observed in the 60–89 group (χ^2 = 0.01, p = 0.9). However, when accounting for diagnosis and gender, multivariate logistic regression identified a significant increase in the probability of resistance with age, particularly in the 60–89 group (p < 0.001) (Figure 4.3c).

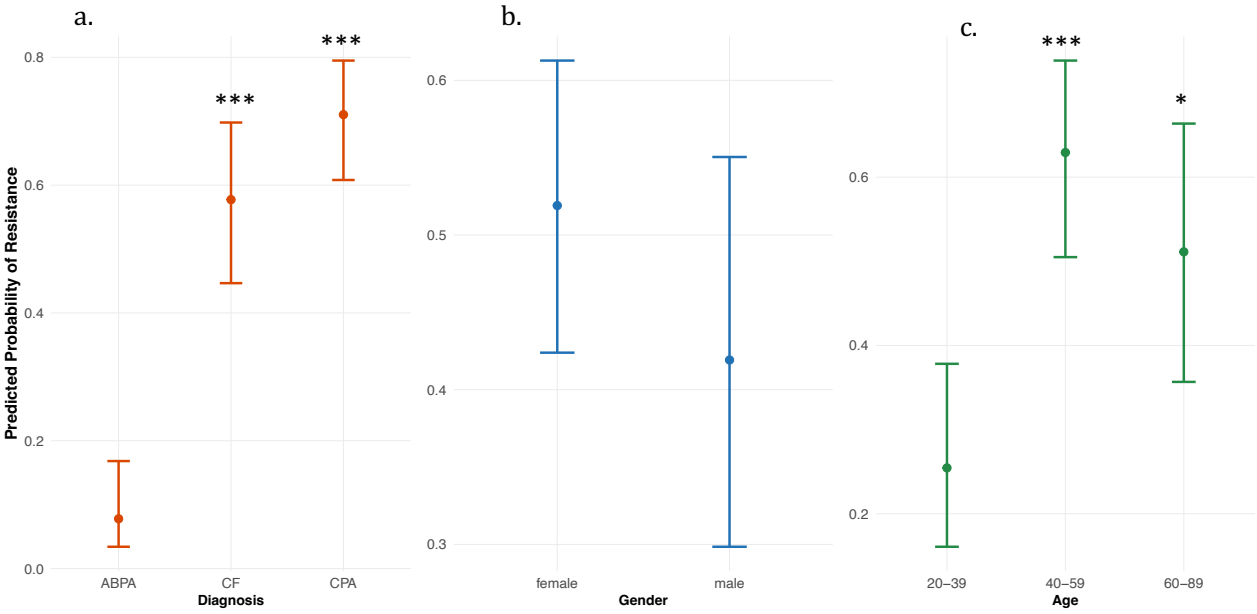


Figure 4.3. **Effect of clinical diagnosis, gender and age on predicted probability of resistance.** Effect plots from a logistic regression model showing the predicted probability of resistance for diagnosis (a), gender (b) and age (c). Error bars represent the 95% confidence intervals for the predicted probabilities. Significant codes: p= <0.001 '***', 0.01 '*'.

4.4.5 WGS of 182 longitudinal *A. fumigatus* isolates

The sequencing panels consisted of 178 prospective isolates from 15 individuals and 4 retrospective isolates from 4 individuals in the Royal Brompton respiratory disease cohort (Appendix 10). Of these, 112 demonstrated resistance to at least one of the clinical azoles. These isolates originated from 11 individuals diagnosed with ABPA (*n* = 3), CF (*n* = 3) and CPA (*n* = 5). Azole susceptible isolates (n = 70) originated from 11 individuals diagnosed with ABPA (*n* = 6), Bronchiectasis (*n* = 1), CF (*n* = 4) and CPA (*n* = 5). Isolates were considered azole-susceptible based on the absence of growth in azole-containing wells in VIPcheck™ plates (Mediaproducts BV, Netherlands) during the screening procedure described in section 2.8.1. Alignments of the sequenced genomes are summarised in Appendix 5.

4.4.6 Genotypic characterisation of clinical *A. fumigatus* isolates

Genotypic characterisation of isolates from the prospective cohort identified 16 distinct genotypes (Appendix 10 & Figure 4.4). Among these, three individuals (Cases 36, 37, and 40) exclusively harboured wildtype isolates. Notably, all isolates from Case 40 were azole susceptible, while some wildtype isolates from Cases 36 and 37, both diagnosed with ABPA, exhibited azole resistance. In Case 44 and Case 41, azole susceptible isolates with wildtype *cyp51a* and D262Y polymorphisms coexisted. Case 42 presented one isolate harbouring M172V/F46Y that remained susceptible to clinical azoles, alongside *cyp51A* wildtype isolates, two of which exhibited resistance to tebuconazole (6mg/L). Of the 64 *cyp51a* wildtypes, 14% (*n* = 9) demonstrated resistance to at least one clinical azole, and 7.8% (*n* = 5) exhibited susceptibility to clinical azoles but were resistant to tebuconazole at 6 mg/L. The G448S polymorphism was predominant in Case 33, with isolates demonstrating variable azole resistance profiles. In contrast, the G54 hotspot polymorphism was prevalent in Case 35, also with CPA, where all but one isolate demonstrated resistance to itraconazole (4 mg/L) and posaconazole (0.5 mg/L). In Case 30, an individual with CF, a 120-bp tandem repeat (TR_{120}) was detected, along with associated nsSNPs, correlating with azole resistance. Among the 15 individuals, the TR_{34}/L98H allele was identified in 26.6% (*n* = 4), while TR_{46}/Y121F/T289A was detected in one isolate from Case 32.

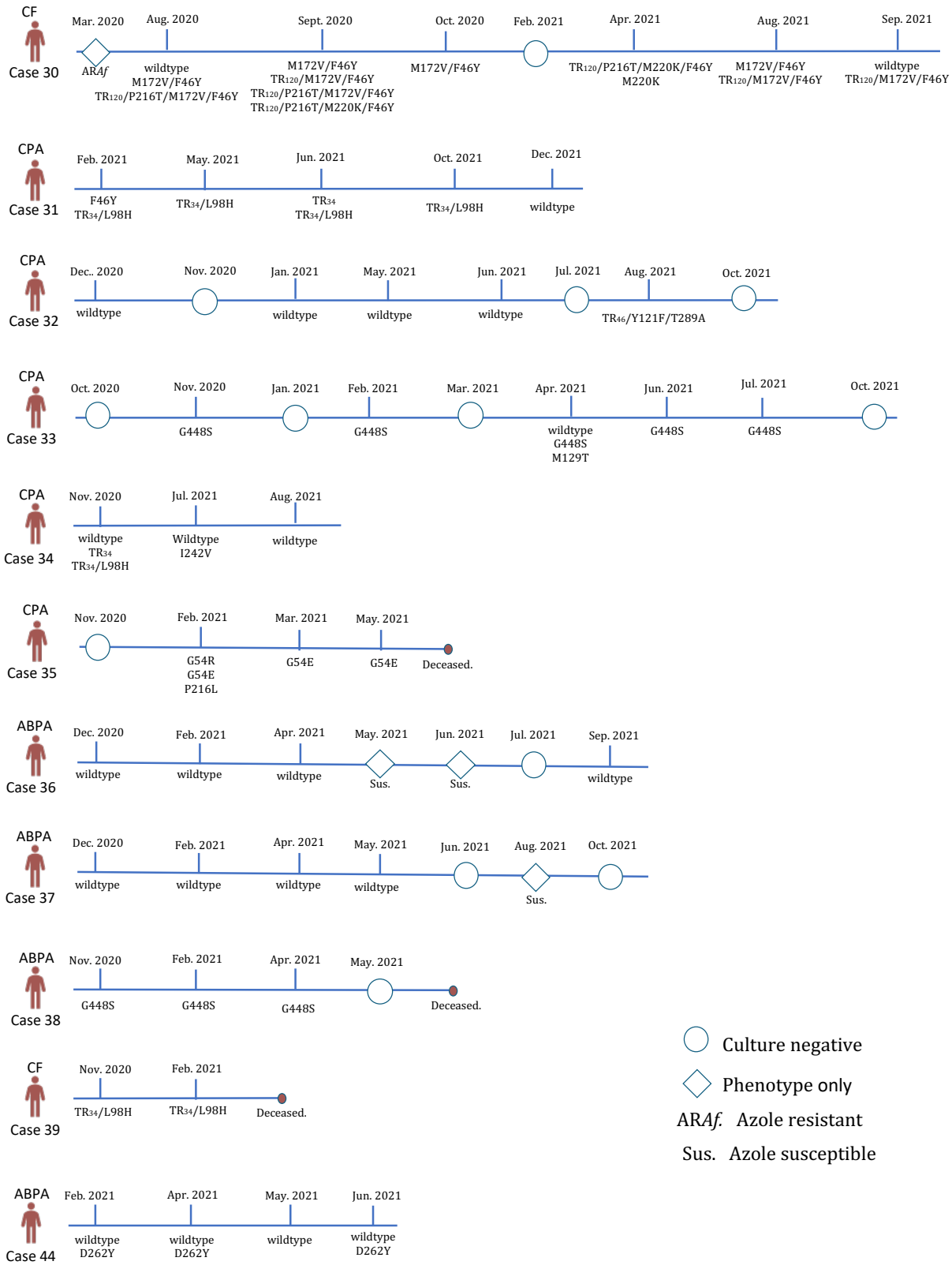


Figure 4.4. **Distribution of *cyp51a* polymorphisms detected during prospective surveillance of individuals diagnosed with chronic respiratory diseases.**

4.4.7 Genetic diversity of *A. fumigatus* isolates from the prospective chronic respiratory disease cohort.

Nucleotide diversity (π) (Figure 4.5a), and Tajima's D (Figure 4.5b), were analysed across individual cases of ABPA, CF, and CPA revealing significant differences in π across all cases ($p < 0.05$). Among ABPA cases, the highest nucleotide diversity was observed in Cases 37 and 38 ($\pi = 6.3 \times 10^{-4}$ and 1.53×10^{-4}, respectively), while Case 44 exhibited the lowest diversity ($\pi = 5.1 \times 10^{-5}$). In CF, a broader range of diversity was seen, with Case 30 showing the lowest median nucleotide diversity ($\pi = 7.69 \times 10^{-6}$), and Case 39 displaying much higher diversity ($\pi = 4.4 \times 10^{-4}$). CPA cases exhibited the greatest variability, with Case 33 having the highest nucleotide diversity among all 11 cases ($\pi = 1.1 \times 10^{-3}$), while Case 31 showed the lowest median value ($\pi = 8.3 \times 10^{-6}$), indicating substantial heterogeneity within the CPA group. All ABPA cases exhibited positive median Tajima's D values (0.48 - 2.43). Among CF cases, Case 30 showed a negative Tajima's D value (-1.10), whereas Case 39 had a positive Tajima's D (1.79). CPA cases demonstrated varying Tajima's D values, with Case 31 showing a strongly negative value (-1.47), while Cases 33 had positive medians (2.8).

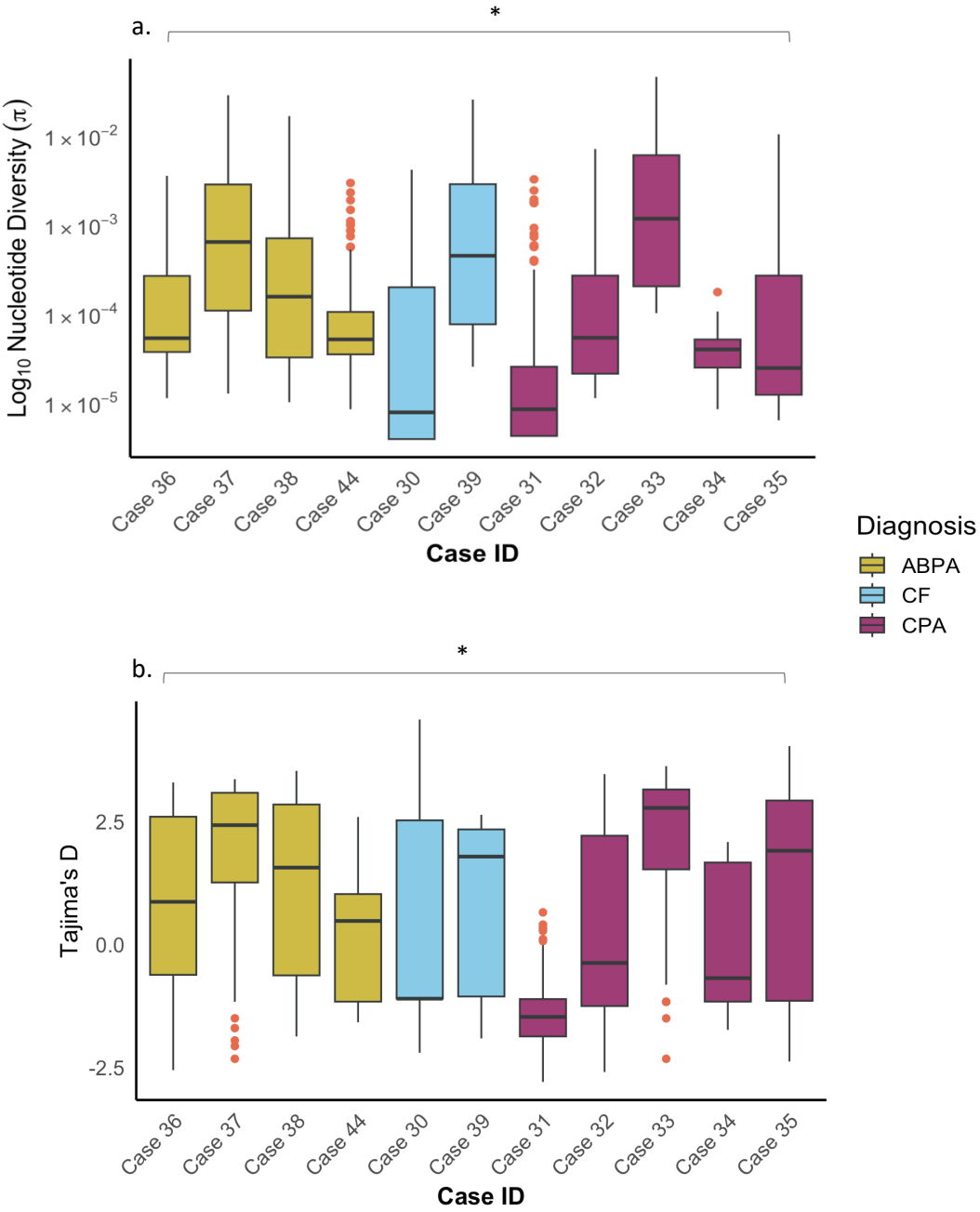


Figure 4.5. **Genetic diversity of *A. fumigatus* isolates from the prospective chronic respiratory disease cohort.** Nucleotide diversity (π) values for *A. fumigatus* isolates from patients with ABPA (yellow), CF (blue), and CPA (purple). Each boxplot represents the range and distribution of diversity across isolates for each case (a). Tajima's D values for the same cases, reflecting the allele frequency (b). Significant code: $p < 0.05$ '*'

4.4.8 Phylogenomic and population structure analysis of *A. fumigatus* in chronic respiratory disease cohorts

Retrospective clinical WGS data from the RBH cohort were integrated into genomic pipelines, enhancing the RBH clinical dataset to a total of 300 isolates from 83 individuals diagnosed with chronic respiratory diseases. Genotypic characterisation of these isolates is summarised in Figure 4.6. Phylogenomic analysis of whole-genome sequences revealed three genetic clusters, with median bootstrap support of 92% (Appendix 5), with azole-resistant strains distributed across all three clusters (Figure 4.6). Several individuals harboured serial isolates with high genetic similarity, indicating the stability and persistence of specific strains over time. In contrast, isolates from certain individuals, such as Cases 34 and 36, were dispersed across all three clusters, reflecting substantial genetic diversity within a single host. The TR_{34}/L98H polymorphisms were primarily restricted to Cluster 1 (C1), which encompassed isolates from multiple patients. The M172V/F46Y and TR_{120} polymorphisms were confined to Cluster 2 (C2). Cluster 3 (C3), lacking tandem repeats, harboured several point mutations, including G448S, G54 (E, W, R), M129T, P109T, M220K, P216L, D262Y, and M172V/F46Y. In summary, a clear clustering of azole resistant *A. fumigatus* with TR_{34}/L98H in comparison to azole susceptible isolates was evident and most azole resistant strains segregated into genetic clusters according to their respective polymorphism. DAPC was employed to further investigate the genetic relationships among isolates within the context of clinical diagnoses. DAPC analysis of whole-genome SNP data revealed genetic differentiation among patients with ABPA, CF, CPA, and non-CF conditions, suggesting the presence of distinct genetic markers or signatures associated with each disease group (Figure 4.7). Nucleotide diversity (π) within the *A. fumigatus* populations was assessed across these groups (Figure 4.8), revealing significant differences in diversity ($p < 0.05$) between all populations. The CF group exhibited the lowest nucleotide diversity compared to non-CF, ABPA, and CPA groups, while the CPA group had the highest diversity, significantly exceeding both the CF and ABPA group.

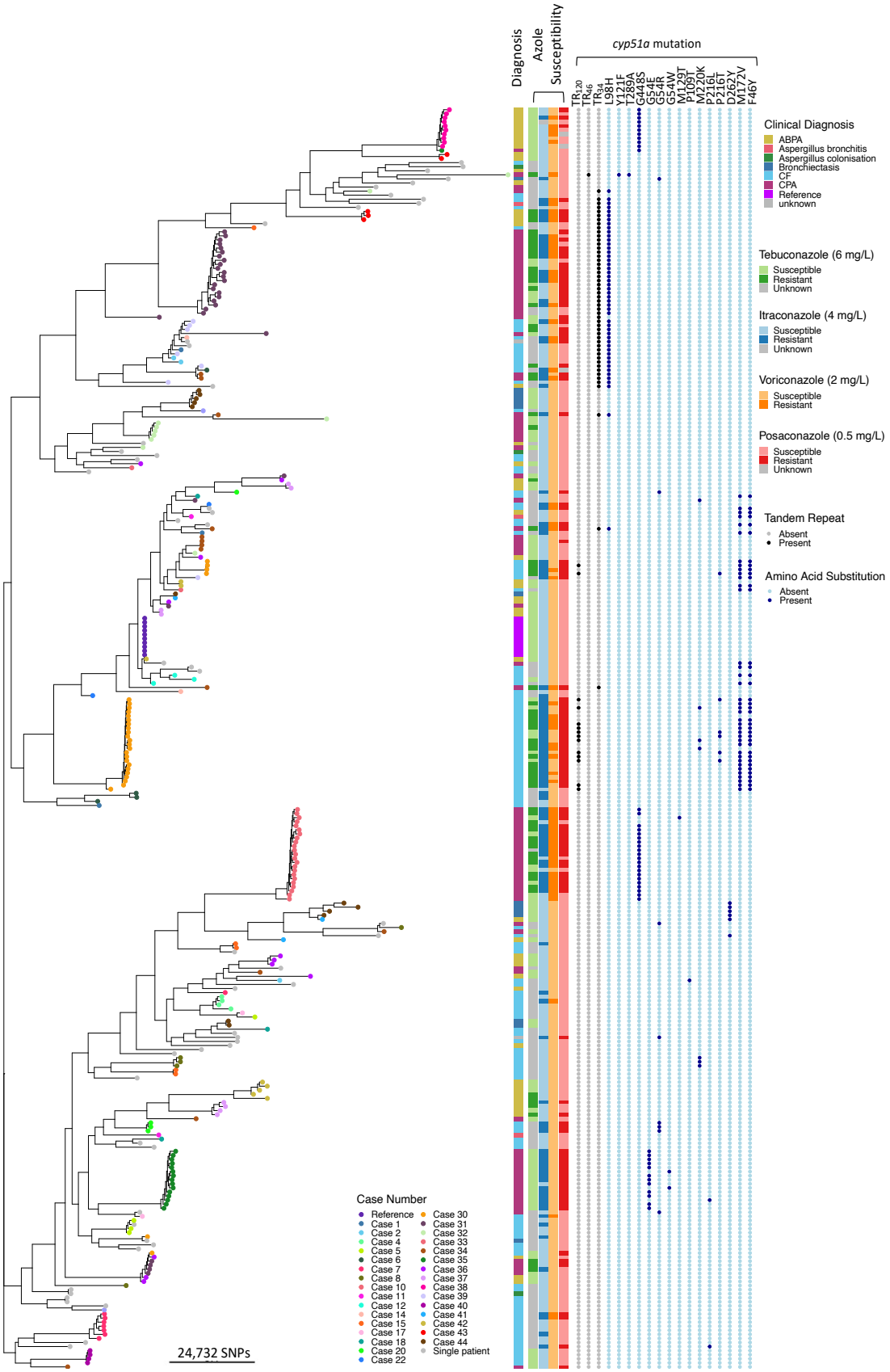


Figure 4.6. **Phylogenetic tree illustrating the evolutionary relationships of *A. fumigatus* isolates from individuals diagnosed chronic respiratory diseases.** Coloured circles on the branches represent the Case ID. The heatmaps indicate disease diagnosis and susceptibility profiles for tebuconazole and the clinical azoles, with darker colours representing resistance. *Cyp51a* polymorphisms are indicated by grey (TR_s) and blue points (amino acid substitutions).

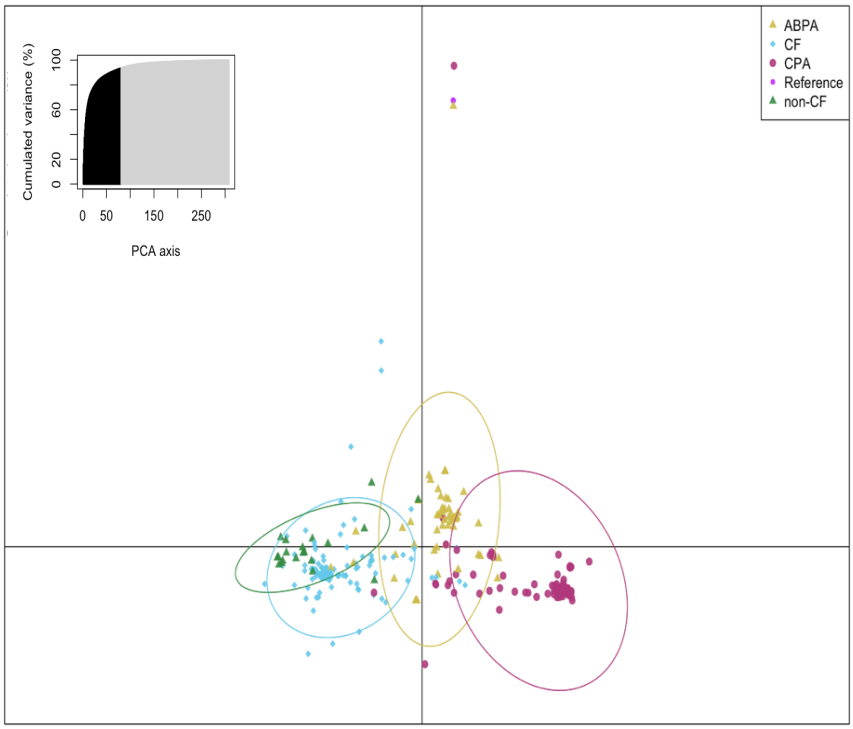


Figure 4.7 **DAPC based on SNP variants of 300 *A. fumigatus* isolates from individuals with ABPA, CF, non-CF and CPA**.

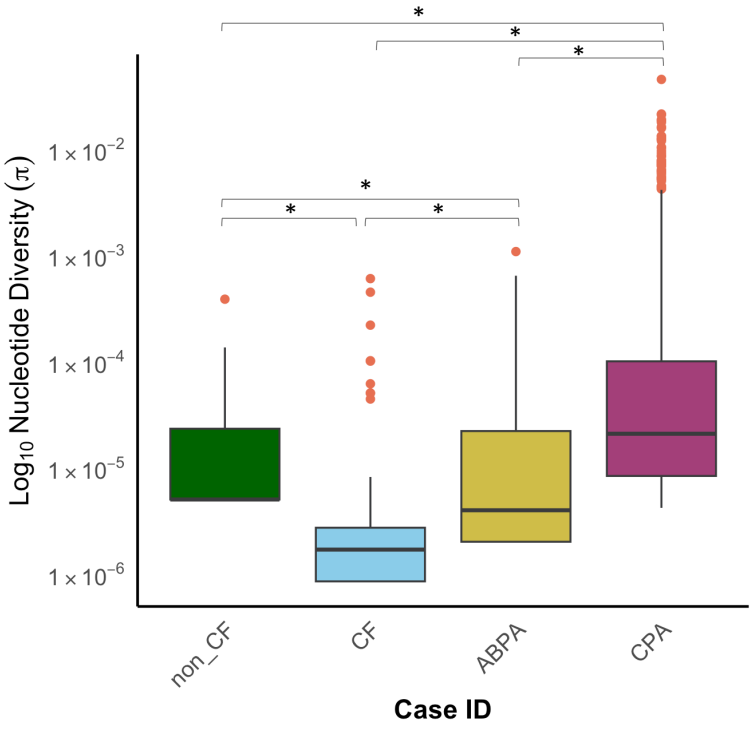


Figure 4.8. **Nucleotide diversity (π) of 300 *A. fumigatus* isolates from individuals with ABPA, CF, and CPA.** Each boxplot represents the range and distribution of diversity across isolates for each diagnosis. Significant code: $p < 0.05$ '*'.

4.5 Discussion

This study provides a genotypic analysis of 300 A*. fumigatus* isolates collected from 83 individuals between 2015 and 2022, demonstrating a high prevalence of azole resistance in a chronic respiratory disease cohort. The TR_{34}/L98H allele, was identified as a major driver of resistance. WGS revealed considerable genetic diversity within hosts and clinical diagnostics, underscoring the intricate interplay between environmental pressures, adaptive responses, and the host immune system in shaping *A. fumigatus* populations

Azole resistance in *A. fumigatus* is increasingly observed among patients with chronic respiratory diseases. In the prospective surveillance cohort (2020–2021), a 25% prevalence of phenotypic azole resistance was observed, with logistic regression indicating a strong association between resistance and conditions such as CF and CPA.WGS revealed that 31.3% (5/16) of individuals had environmentally associated resistance mechanisms, with four carrying TR_{34}/L98H, and one individual carrying TR_{46}/Y121F/T289A, highlighting the heightened risk of environmental acquisition. The high incidence of TR_{34}/L98H in this cohort is consistent with its status as a globally dominant resistance mechanism (280,337,352,352,353,461,461,462). Notably, national surveillance in the Netherlands has shown a doubling of TR_{34}/L98H incidence over the past decade, accounting for nearly half of azole resistant cases in CF patients by 2018, reinforcing its growing clinical significance (463). The detection of the TR_{46}/Y121F/T289A allele in Case 32 signals its emergence in the UK, echoing reports from Europe (268,464–467), Asia (468–470) and Africa (471). Although first identified in a clinical isolate in Manchester in 2017 (472), retrospective surveillance from 1998–2017 found no cases among 1,469 isolates in London (473). The first environmental detection in 2019, involving six isolates from soil, compost, and hospital flower beds in London, confirmed local TR_{46}/Y121F/T289A presence (474). By 2023, a national surveillance study found TR_{46}/Y121F/T289A in 6% of aerosolised *A. fumigatus* isolates conferring resistance associated polymorphisms, compared to 59% for TR_{34}/L98H (359). This emergence points to a potential for broader dissemination, mirroring the trajectory of TR_{34}/L98H. These findings highlight the urgency for enhanced national surveillance to monitor further expansion

Several cases exhibited serial isogenic strains, indicating that certain azole resistant strains can persist and proliferate within the host rather than being supplanted by distinct strains. This supports the hypothesis of long-term colonisation by a single strain. (354,357). Detailed analysis of these cases offers valuable insights into the in-host evolutionary dynamics of antifungal resistance. A TR_{120} allele, along with associated polymorphisms, was detected in isolates from Case 30, an individual diagnosed with CF. The TR_{120} was first reported in the Netherlands in 2019 in a fatal case of aspergillosis identified, via WGS and STR*Af* typing, emerging after prolonged triazole therapy (475). In this study, phylogenetic analysis confirmed the isolates from Case 30 were closely related (100% bootstrap support), showing resistance to itraconazole and posaconazole, and displaying various combinations of nsSNPs, even in the absence of TR_{120}. Notably, one TR_{120} isolate remained azole susceptible, indicating heterogeneity in resistance mechanisms. In *A. fumigatus*, particularly among CF patients, such patterns may be driven by parasexual recombination, a process that facilitates genetic variation and the rapid adaptation to antifungal therapy (235). Case 30 exhibited a low nucleotide diversity (7.69×10^{-6}) among patients, alongside a negative Tajima's D value (-1.10), possibly indicating a selective sweep that favoured resistance mutations. These findings further challenge the notion that all TR mutations originate solely from environmental sources, highlighting the significant role of in-host evolution in driving antifungal resistance (296,475).

In Case 31, involving an individual with CPA, *A. fumigatus* isolates carrying the TR_{34}/L98H mutation exhibited high phylogenetic relatedness (100% bootstrap support), dating back to 2016. The CPA lung environment, characterised by chronic inflammation, cavitations and tissue damage, provides a niche conducive to fungal growth and asexual sporulation, facilitating persistence and adaptation (260). This setting allows for repeated cycles of asexual reproduction, enhancing the potential for clonal expansion. The observed low nucleotide diversity ($\pi = 8.3 \times 10^{-6}$) and negative Tajima's D value (-1.47) are indicative of recent clonal expansion, likely driven by selective pressures, resulting in the dominance of resistant clones. While the low nucleotide diversity and negative Tajima's D values in both cases are consistent with clonal expansion, alternative scenarios should be considered. For instance, limited gene flow within the host environment could restrict genetic diversity, promoting

the persistence of specific clones, while purifying selection may further reduce diversity by eliminating deleterious mutations. These dynamics highlight the complexity of in-host evolution, where selective pressures shape resistance through a combination of clonal persistence, genetic variation, and the unique ecological conditions within the host.

Additionally, an isolate carrying the TR_{34} mutation without the L98H substitution was detected in Case 31, representing the first clinical report of this allele. This unlinked TR_{34} mutation challenges the assumption that TR_{34}/L98H emerged solely *de novo* and suggests the possibility of intragenic recombination, aligning with previous reports of unlinked TR_{34} in environmental isolates (353,359). Since the discovery of the sexual cycle in *A.* fumigatus (224), evidence increasingly shows that recombination drives the emergence of resistance alleles in environmental settings (34,231,341). Auxier *et al*., (2023) (476) independently demonstrated that *A. fumigatus* has one of the highest recombination rates among eukaryotes, allowing TR_{34}/L98H progeny to form from parental strains with separate TR_{34} and L98H mutations. This process likely contributes to the emergence of isolates with combined mutations linked to distinct *cyp51A* tandem repeats. The phylogenetic relatedness between TR_{34} and TR_{34}/L98H isolates in Case 31 suggests that recombination may have occurred, either via sexual recombination in the environment, where the patient had repeated exposure, or through in-host genetic recombination, highlighting the adaptive potential of *A. fumigatus* within the lung environment and the risk of further resistance development. However, the absence of an isolated L98H mutation leaves the exact mechanism unclear. In Case 34, a TR_{34} mutation unlinked from L98H was also identified, with this isolate being phylogenetically distinct from others in the study. This finding indicates either incomplete sampling of the *A. fumigatus* population or an independent acquisition from an environmental source rather than in-host recombination.

In contrast to cases dominated by a single strain, a more diverse population structure of *A. fumigatus* was observed in certain patients, indicating mixed infections with multiple strains. For instance, in Case 39, a CF patient who sadly passed away, TR_{34}/L98H isolates exhibited greater phylogenetic diversity than those in Case 30. Case 39 showed higher nucleotide diversity and a

positive Tajima's D, indicating a mixed infection likely caused by the acquisition of strains from different environmental sources. Given that *A. fumigatus* isolates can persist in CF lungs over time, this could present multiple opportunities for resistance to emerge independently in different strains, further complicating treatment. The presence of diverse strains across multiple cases further highlights that a single sample may not represent the full fungal population in the lung (467,477).

The incorporation of retrospective genomes enhanced the statistical power of the study, allowing for clearer identification of genetic diversity patterns in *A. fumigatus* across different clinical conditions. DAPC revealed partial clustering between CPA, CF, and ABPA isolates, indicating a shared genetic background, while also highlighting distinct disease-specific differentiation, particularly between CPA and CF. The reduced diversity in CF is likely driven by strong selective pressures, including thick mucus and robust immune responses, which create genetic bottlenecks and support the persistence of clonal *A. fumigatus* strains (478). In contrast, CPA exhibited greater genetic diversity, likely due to its more variable environment and less restrictive selection pressures, allowing for the coexistence of multiple genotypes (479). These findings emphasise the adaptation of *A. fumigatus* to disease-specific respiratory niches.

The patient sampling methodology, utilising remote sputum kits with prepaid return packaging, proved highly effective, achieving an impressive 79% return rate. This high level of patient engagement, combined with the study's longitudinal design, enabled the collection of a comprehensive dataset, encompassing over 300 serial *A. fumigatus* isolates and more than 700 additional yeasts and moulds from 55 participants. Remote sampling kits, increasingly favoured for their convenience and non-invasive nature, facilitate routine monitoring and clinical trial participation without the need for frequent hospital visits, thereby expanding surveillance efforts to diverse and geographically remote populations. Recent studies have also validated the reliability of posted CF sputum samples for culture-based microbiology, even after prolonged delays at ambient temperatures, further supporting the utility of these kits in remote surveillance initiatives (480). Traditional surveillance approaches typically analyse a single isolate per patient, which, while valuable for broad epidemiological insights,

often overlook the genetic and phenotypic diversity present within individual hosts. In contrast, our high-throughput methodology, which examined multiple colonies per patient, provided a more nuanced and detailed understanding of the resistance landscape. Through this in-depth analysis of intraspecific diversity within our prospective cohort, significant variations in genetic diversity were identified across multiple individuals, highlighting distinct evolutionary trajectories of resistance. This approach offers a more comprehensive perspective on the adaptive mechanisms at play, enhancing our understanding of *A. fumigatus* resistance development within the host environment.

These findings have significant implications for the management of *A. fumigatus* infections, particularly in patients with chronic respiratory diseases such as CF and CPA. The high prevalence of azole resistance, driven by both in-host evolutionary processes and environmental acquisition, underscores the necessity for comprehensive, integrated surveillance strategies. The detection of emerging resistance mechanisms, including TR_{46}/Y121F/T289A, suggests a diversification of resistance profiles that could spread more extensively in clinical and environmental contexts, paralleling the global rise of TR_{34}/L98H. These observations reinforce the need for coordinated national and international surveillance to detect and respond to emerging resistance patterns. The identification of mixed infections and extensive genetic diversity within individual hosts challenges the utility of traditional single-isolate sampling methods, which risk underestimating the true extent of resistance. High-throughput sampling approaches that capture intraspecific diversity offer a more accurate reflection of the resistance landscape, enabling more effective antifungal interventions. This is particularly relevant for CF and CPA patients, where prolonged azole exposure imposes strong selective pressures, accelerating the evolution of resistant strains. Additionally, the success of remote sputum sampling in maintaining high patient engagement demonstrates its utility as a scalable tool for long-term surveillance of azole resistance, particularly in populations with restricted access to healthcare. Such strategies could enhance the early detection of resistance, informing treatment decisions and mitigating the spread of resistant *A. fumigatus* strains. Collectively, these findings emphasise the urgent need for sophisticated, patient-centred surveillance frameworks and a more

nuanced understanding of the ecological and evolutionary dynamics underpinning azole resistance in *A. fumigatus*.

The prospective cohort was primarily drawn from a single geographic region and healthcare setting, which may limit the generalisability of the findings to broader populations. Although retrospective data were incorporated to enhance the longitudinal analysis, expanding the geographical and demographic scope of future studies would provide a more comprehensive understanding of azole resistance trends across different regions and patient populations. The 25% phenotypic azole resistance observed in our cohort is notably higher than previous rates reported at RBHT (13.3%) (301). This difference may partly stem from sampling bias, as repeated sampling in a smaller cohort could inflate resistance prevalence. However, the consistent detection of resistant strains underscores their persistence in the host environment and the significant challenges they pose for treatment. Although sputum sampling was effective and achieved high patient engagement, it may not fully capture the *A. fumigatus* population within the lungs, particularly in cases of lower respiratory tract colonisation where sampling efficiency is variable. Incorporating bronchoalveolar lavage (BAL) in future studies could provide a more comprehensive assessment of fungal diversity, especially in patients with limited or absent sputum production. Additionally, limiting the analysis to a subset of colonies (up to five per sample) may still underestimate the true genetic diversity. Given the rapid emergence of azole resistance and the potential for multiple clonal populations within a single host, more exhaustive sampling or deep sequencing would offer a more accurate representation of in-host diversity. The study's reliance on culture-based methodologies may introduce bias toward more readily culturable strains, potentially excluding less abundant or slow-growing variants. For example, PCR-based diagnostics have identified a 55% prevalence of TR_{34}/L98H in culture-negative sputum samples (481), suggesting that molecular techniques may reveal higher resistance rates than those reported in this study. The integration of culture-independent methods, such as PCR-based diagnostics, with traditional approaches could provide a more complete characterisation of the fungal community and the resistance landscape.

Another limitation is the focus on *cyp51A* mutations as the primary resistance mechanism. Although *cyp51A*-independent resistance was acknowledged, the study's design did not extensively investigate other genetic pathways or mechanisms contributing to azole resistance. This may overlook key factors such as efflux pump activation, biofilm formation, or mutations in other genes associated with resistance. Additionally, the longitudinal aspect of the study was impacted by the COVID-19 pandemic, which limited patient interactions and sample collection opportunities. Although remote sputum kits proved effective, it is possible that certain fluctuations in fungal populations or resistance dynamics were missed during periods of reduced patient contact. Future studies would benefit from consistent sampling intervals and real-time monitoring to capture the full spectrum of in-host evolution. The phylogenetic analyses and genotyping in this study provided insights into evolutionary trajectories of resistance but were unable to fully delineate the dynamics of recombination events or the specific genetic exchanges occurring within the host environment. Employing long-read sequencing technologies, such as PacBio or Oxford Nanopore, in future studies could enhance the resolution of recombination events, structural variations, and horizontal gene transfer, offering a deeper understanding of in-host adaptation and resistance evolution.

Conclusions

This study reveals significant genetic diversity and dual mechanisms of azole resistance in *A. fumigatus*, driven by both in-host evolution and environmental acquisition. The emergence of resistance variants, such as TR_{46}/Y121F/T289A, underscores the need for expanded surveillance and advanced molecular techniques. High-throughput sampling and remote sputum kits offer scalable tools for monitoring resistance, while future research should leverage culture-independent methods and long-read sequencing to further elucidate resistance dynamics.

ACKNOWLEDGEMNETS: I would like to acknowledge Rodrigo Monteirinho-Leitao (Imperial College London) for his support with prospective isolate collection, antifungal susceptibility testing, and sputum sample processing. I would also like to acknowledge Ali Nuh (Imperial College London/RBHT)

and Professor Darius Armstrong-James for their assistance with accessing retrospective isolate collections.

Chapter 5 Environmental reservoirs of azole-resistant *A. fumigatus* detected in a Hospital setting

5.1 Abstract

Nosocomial *A. fumigatus* infections, exacerbated by the increasing prevalence of azole resistance, present a critical challenge within healthcare environments, especially among immunocompromised patients. However, the acquisition of azole resistance in the context of chronic respiratory diseases remains poorly understood. WGS data were integrated with extensive environmental sampling to elucidate potential pathways of azole resistance acquisition in clinical settings. Air and soil samples collected from multiple hospital sites were screened for azole-resistant *A. fumigatus*, and WGS was utilised to characterize resistance mechanisms, population structure, and transmission dynamics. The analysis identified a widespread presence of *A. fumigatus* in the hospital environment, with 63.8% of air and 85.7% of soil samples culture positive testing positive. Azole resistance was detected in 4.5% of air and 3.4% of soil isolates, predominantly involving the TR_{34}/L98H allele. Spatial analysis identified contamination hotspots in outpatient areas, basements, and the hospital reception, indicating potential environmental reservoirs for resistant strains. Phylogenomic analysis revealed genetic relatedness between clinical and environmental isolates, suggesting direct or indirect transmission pathways within the hospital. These findings underscore the need for comprehensive fungal surveillance in healthcare settings to mitigate the risks of exposure to azole-resistant strains, particularly in patients with chronic respiratory conditions. By leveraging high-resolution WGS data, this study provides critical insights into the transmission dynamics and genetic diversity of *A. fumigatus* in hospital environments, advocating for enhanced infection control measures, targeted environmental monitoring, and optimized antifungal stewardship.

5.2 Introduction

A. fumigatus has emerged as a prevalent pathogen in nosocomial invasive fungal infections. Given the growing recognition by global health authorities (16), enhancing fungal surveillance and control measures are critical to mitigating the impact of fungal pathogens in healthcare settings. Highly related genotypes of azole-resistant *A. fumigatus* have been identified in both clinical and environmental samples, signalling a concerning rise in human exposure to aerosolised spores with pre-existing azole resistance mechanisms (337,353). This poses a particular risk in healthcare environments, where azole-resistant *A. fumigatus* significantly compromises available treatment options for vulnerable patient populations. (271,327,482).

The emergence of azole-resistant *A. fumigatus* strains in healthcare settings is reported globally, indicating widespread environmental contamination and patient infections. A notable example from a French University Hospital revealed an increasing incidence of azole-resistant *A. fumigatus* among patients, with resistance rates reaching 16% by 2017 (483). Intensive environmental surveillance uncovered that 71% of soil and numerous air samples contained isolates with the TR_{34}/L98H mutation, highlighting the extensive environmental prevalence and raising questions about the role of ornamental plants in healthcare environments (483). Similarly, a multicentre study in Iran reported a striking 55% prevalence of azole resistance in soil samples, with the TR_{34}/L98H mutation detected in all resistant isolates (484). In Spain, resistant strains isolated from a patient's hospital bathroom were isogenic with clinical strains from the same patient, exhibiting identical MIC resistance profiles and the TR_{34}/L98H genotype, suggesting possible environmental acquisition (286). Furthermore, the utilisation of the STR*Af* assay has demonstrated nosocomial isolates with pre-adapted azole resistance mechanisms have the potential to infect susceptible hosts (254). However, a critical issue identified in multiple case studies is the absence of high-resolution genomic data, combined with fragmented surveillance and inconsistent genotypic and phenotypic characterisation. Genotyping studies have been pivotal in shaping prevention strategies for healthcare-associated aspergillosis, particularly during hospital renovations, by providing crucial insights into transmission dynamics and infection control recommendations (210,485). Many studies employ short tandem repeats to trace

environmental sources of *A. fumigatus*. However, the genetic variability within the *A. fumigatus* population may complicate the precise linkage of clinical isolates to specific environmental origins, thus limiting the effectiveness of STRs in accurately mapping possible transmission pathways. Consequently, environmental sources and reservoirs of azole resistant *A. fumigatus* in the hospital setting remains poorly characterised. Understanding genome variability in *A. fumigatus* populations within high-exposure environments is essential for phylogenomic analysis to determine strain relatedness, assess distribution patterns, and identify potential common sources (479). Furthermore, current nosocomial surveillance in healthcare settings typically prioritise the most at-risk patient groups, are often conducted prospectively following the identification of an outbreak or infection and often prioritise specific prokaryotic pathogens (486,487). This targeted approach can result in the inadvertent neglect of fungal acquisitions affecting non-target patient cohorts. As a result, significant nosocomial fungal acquisitions may go undetected, compromising patient safety. Such oversights are particularly prevalent in hospitals with limited resources or without established reporting systems, where the true incidence of nosocomial infections is unclear (488,489).

Transmission dynamics of *A. fumigatus* within healthcare environments share notable parallels with other respiratory pathogens, underscoring the potential for similar environmental contamination. Studies have demonstrated that bacterial pathogens such as *Pseudomonas aeruginosa* and *Staphylococcus aureus*, including multidrug-resistant strains, frequently contaminate healthcare settings through aerosolization and direct contact, thereby increasing the potential for nosocomial transmission (490–492). For example, Zuckerman *et al*., (492) identified a 13.6% contamination rate of these bacteria in inpatient environments, with pathogens predominantly detected on patients' hands, in the air, and on various surfaces. Similarly, Ferroni *et al*., (490) observed significant contamination with *P. aeruginosa* in bedroom air and shower surfaces following patient presence, with 50% of colonised individuals harbouring identical *P. aeruginosa* strains in both their sputum and bedroom air samples, indicating aerosol transmission as a major route of environmental contamination. Tanner *et al*., (491) further confirmed the persistence of multidrug-resistant organisms in 13% of patient rooms, highlighting the potential for sustained pathogen survival in

healthcare settings. These bacterial transmission dynamics have direct implications for *A. fumigatus*, as spores recovered from cough aerosols of colonised CF patients suggest a parallel transmission pathway (289). The inherent resilience and environmental persistence of *A. fumigatus* conidia enable them to survive within healthcare environments, posing a considerable risk to vulnerable cohorts. This transmission is further facilitated by compensatory evolution, where secondary mutations mitigate the fitness costs of resistance, enhancing the survival of *A. fumigatus* in azole-exposed environments. Individuals with chronic respiratory diseases, who often receive prolonged azole therapy and harbour high levels of azole-resistant strains, can release these resistant spores into their surroundings through coughing or exhalation. While in-host evolution often results in fitness costs, such as reduced sporulation and slower growth (223,263), compensatory evolution could restore the fitness of these strains, allowing them to adapt and thrive in hospital settings, on surfaces, in the air, or in soil within hospital environments. Furthermore, exposure to residual azole antifungals commonly used in these environments, can exert selective pressure, favouring the survival and proliferation of resistant strains, which then establish themselves as environmental reservoirs.

In individuals with chronic respiratory conditions, who frequently experience microbial colonisation and exhibit a high prevalence of azole resistance (~13%) (301) understanding resistance acquisition pathways is essential. To address this, 'real-time' epidemiological surveillance of *A. fumigatus* was conducted in a central London hospital over a two-year period. WGS data from isolates obtained from patients attending the central London hospital were integrated into a comprehensive WGS dataset of hospital environmental isolates to assess the burden of azole resistance, identify potential environmental sources, and explore routes of acquisition in high-exposure settings. Comparative isolates from a UK-wide clinical and environmental dataset were included to enhance discriminatory power for phylogenomic analysis and DAPC in order to identify distinct genetic backgrounds of clonal strains. This high-resolution WGS approach allowed differentiation between clinical and environmental strains, providing valuable insights into azole resistance acquisition pathways and informing strategies for targeted interventions and improved public health measures.

5.3 Methods

5.3.1 Impact of COVID-19 on environmental surveillance

From November 2020 to June 2021, access to some hospital areas were strictly controlled in response to the COVID-19 pandemic. This included limited public access to hospitals and outpatient areas, with a complete closure of certain areas during peak transmission periods. From November 2020-February 2021, environmental surveillance was conducted during hospital closure times to adhere to health and safety guidelines. Access to the intensive care units was restricted to reduce potential contamination risks. Consequently, environmental surveillance was adapted to these constraints.

5.3.2 Hospital sampling locations

To assess the level of culturable *A. fumigatus* and explore potential transmission risks of environmentally acquired azole resistant *A. fumigataus* in the clinic, seasonal air and soil samples were systematically collected from the Royal Brompton Hospital, London. Air samples were collected from locations with potential air quality issues and soil samples were collected from indoor and outdoor flower beds, including public waiting areas (Figure 5.1). The Royal Brompton and Harefield Trust make up the largest heart and lung specialist medical centres in the United Kingdom, serving approximately 216,000 outpatient visits and 40,000 inpatient admissions between 2019-2020 (493). The Royal Brompton Hospital, situated in Chelsea, west London includes several stand-alone buildings. The original Victorian building, 'Site A,' constructed in 1882 as an extension of the original 'Hospital for Consumption and Diseases,' is still in use today and consists of several outpatient clinics. Air samples were collected from five locations within 'Site A,' including an Outpatients, Ambulatory and CT department, a staff office, and the hospital basement. Additionally, air samples were collected from an external staff carpark area at the back of the hospital which served as an 'external control' (Figure 5.1i). Soil samples were collected from internal flower beds adjacent to the Outpatients clinic and external flower beds located outside the staff entrance. The modern 'Site B' building, constructed in 1991, contains multiple inpatient wards specialising in respiratory and cardiac conditions. Air

samples were collected from four locations within 'Site B,' including two inpatient wards, the Intensive Care Unit (ICU), hospital Reception. Soil samples were collected from internal and external flower beds at the hospital Reception and from two external courtyards. Soil samples were collected from a private park which served as the 'control' soil samples.



Figure 5.1. **Hospital sampling locations**. Soil and air samples were collected from multiple locations within the hospital to assess the presence and distribution of *A. fumigatus*. Soil samples were collected from indoor and outdoor potted plants and garden spaces, including patient waiting areas (a-c), a reception area (d) and outdoor courtyards (e-f). Air samples were also collected from locations with potential air quality issues, including areas with signs of dampness or old air conditioning units: ceiling with water damage (g) and a window-mounted old air conditioning unit (h). External control located at the back of the hospital in a staff car park (i).

5.3.3 Hospital Air Surveillance

Air samples were collected using a 'SAS Super 180' (Cherwell Laboratories, UK) air sampler (Figure 5.2a), positioned at approximately 1.2 meters height. Contact plates (90 mm) containing SDA media supplemented with antibiotics (16 mg/L penicillin and 16 mg/L streptomycin) were placed on the aspirating head. The sample time was set to 5 minutes to collect 1000L (1 m^3) of air, with technical replicates performed at each location. Post-sampling, the plates were immediately sealed with parafilm, stored in individual ziplock bags, and the aspirating head was sterilised with 10% Chemegene HLD4 disinfectant (Medimark International) to prevent cross-contamination between locations. In the laboratory, plates were incubated at 45°C for up to 5 days and monitored daily for fungal growth (Figure 5.2b-e). Identification and isolation of *A. fumigatus* colonies were based on their macro and microscopic characteristics and isolated according to the protocols detailed in sections 2.4.3 and 2.5.1.

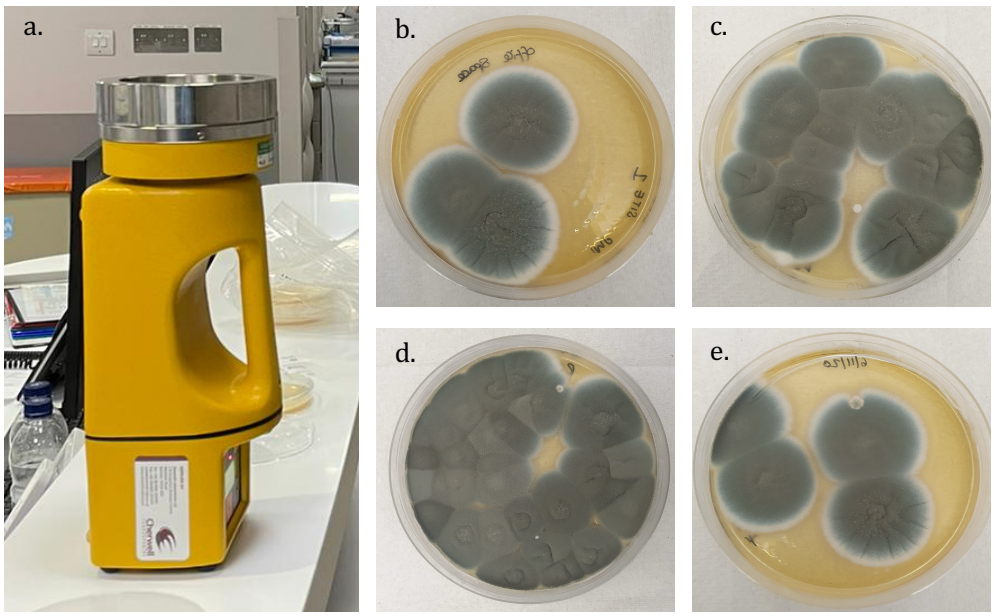


Figure 5.2. **Hospital air surveillance method**. The SAS 180 air sampler (a) used for capturing aerosolised A. fumigatus conidia from the hospital environment and representative contact plates displaying the growth of *A. fumigatus* from air samples collected at four different hospital locations after incubation (b-e).

5.3.4 Hospital Soil Surveillance

Surface soil was collected from internal and external hospital flower beds into a 5 ml Eppendorf tube (Eppendorf AG, Hamburg, Germany). To isolate *A. fumigatus*, 2 g of soil was suspended in 8 ml of sterile suspension buffer containing 0.85% NaCl plus 0.5% Tween®-20 (ThermoFisher Scientific) as previously described (494) Briefly, 200 µl of supernatant was aliquoted on to duplicate culture plates containing SDA media supplemented with antibiotics (16 mg/L penicillin and 16 mg/L streptomycin). Culture plates were incubated at 45°C and checked daily for *A. fumigatus* colony growth. Colonies were identified based on macroscopic characteristics and isolated as per section 2.4.3 and 2.5.1.

5.3.5 Spatiotemporal distribution of *A. fumigatus* CFUs

Colony counts from air and soil samples were recorded to assess spatiotemporal patterns and distribution of *A. fumigatus* CFUs, along with potential environmental impact factors, at 'Site A' and 'Site B.'

5.3.6 Isolation of *A. fumigatus* colonies

Up to 5 colonies per morphology were sub-cultured onto SDA plates using the 3-spot method as detailed in section 2.4.3. Sub-cultures were cryopreserved at -80°C according to section 2.4.5.

5.3.7 Antifungal susceptibility testing

All *A. fumigatus* isolates (n = 388) were screened for susceptibility to the agricultural azole tebuconazole and three clinically relevant azoles using VIPCheck™ plates (Mediaproducts BV, Netherlands), following the methodologies outlined in section 2.8. Conidia were harvested either directly from primary subcultures or from secondary subcultures derived from glycerol stocks as described in section 2.5.3.

5.3.8 gDNA extraction and quantification

Isolates from the hospital environment were systematically chosen to represent the spatiotemporal distribution of both azole resistant and azole susceptible strains from air and soil samples within the hospital (section 2.9.1). Isolates were cultured from glycerol stocks at 45°C for 2-5 days as described in section 2.5.3 and gDNA extracted following the protocol outlined in section 2.9.2. DNA quantity and purity were assessed prior to sequencing as per section 2.9.4.

5.3.9 Next Generation sequencing & Bioinformatic Analysis

Genomic DNA underwent WGS at the Earlham Institute, utilising the Illumina NovaSeq sequencing platform as described in section 2.10.1. WGS alignments were processed as per sections 2.10.3-4. Genotypic characterisation was performed as per sections 2.10.6.

5.3.10 Investigating a potential vector of azole resistance

Multi-triazole resistance strains containing the TR_{34}/L98H genotype were found in both air and soil samples in the hospital environment. To investigate a possible vector of the TR_{34}/L98H strains, the hospital estates depart was contacted regarding the compost used in the ornamental soil beds. Almost one-year after the hospital environmental surveillance had concluded, a compost bag of the same brand was purchased and subsequently sampled for *A. fumigatus*. Soil samples were processed as described in section 5.3.4 and cultured *A. fumigatus* colonies were screened for susceptibility as per section 2.8. Isolates were sub cultured as per section 2.5.3 for gDNA extraction and WGS (as per section 2.9 and 2.10 respectively).

5.3.11 Incorporation of clinical WGS from RBH respiratory disease cohort and the UK dataset

To investigate possible routes of transmission, 182 WGS derived from the RBH respiratory disease cohort (section 4.4.1.5) were incorporated into the hospital environment dataset. An additional 626

comparator clinical and environmental WGS were included to confirm epidemiological links within the broader UK dataset.

5.3.12 Phylogenomic analysis

Phylogenetic trees were inferred from WGS using RAxML-NG (370) as described in section 2.12. Additional bootstrap replicates (*n* = 500 bootstraps) were concatenated with the inferred trees until convergence was achieved. Phylogenetic trees were visualised in R version 4.3.1 using the ggTree (371) and ggTreeExtra (372) packages and uploaded as an interactive Microreact project (Appendix 2).

5.3.14 Calculating unique pairwise SNPs

To explore genomic diversity and identify closely related *A. fumigatus strains,* pairwise unique SNPs were calculated between VCF files as described in section 2.13. Pairwise unique SNPs were visualized as a histogram in R version 4.3.1 to illustrate genetic variation withing the population. Isolates pairs sharing less than 6% of the total SNP diversity were subset to identify clonal groups.

5.3.15 Multivariate analysis of genomic data

Multivariate genomic analysis was conducted in R version 4.3.1 using the adegenet package version 2.1.10 following established protocols (373–376) as per section 2.14.

5.3.16 Statistical Analysis

Data analysis was conducted in R version 4.3.1, with variables reported as counts across categories. A significance level of $p < 0.05$ was used. The Shapiro-Wilk test assessed normality, and for non-normally distributed data, the Kruskal-Wallis test identified significant differences, followed by Dunn's post-hoc test for pairwise comparisons.

5.4 Results

5.4.1 Sample Collection

Air samples (*n* = 136) and soil samples (*n* = 77) were collected between November 2020 and February 2022 across two hospital sites; an original Victorian building (Site A) and a newer hospital building constructed in 1991 (Site B) (Table 5.1) From site A, 66 air samples were collected from an outpatient area, Ambulatory, CT, hospital basement and staff office. An additional 6 air samples were collected during fine scale surveillance of the Outpatients area for the purpose of azole resistance detection only. From Site B, 50 air samples were collected from two inpatient wards, a public Reception area and an ICU. Only 8 samples were collected from the ICU from March 2021 – November 2021due to COVID-19 restrictions. A further 14 air samples were collected from an external carpark which served as an external control. Soil samples were collected both internally (*n* =26) and externally (*n* =51) across the hospital. Of the indoor soil samples collected, the majority (*n* = 17/26) were collected from Site A within an Outpatients area. Only 1 indoor flower bed was located and subsequently sampled within Site B, the main public Reception area. No planted beds or pots were found in corridors or wards in Site B. The remaining Site B soil samples were collected from outside flower beds either within the hospital courtyards or the Reception entrance.

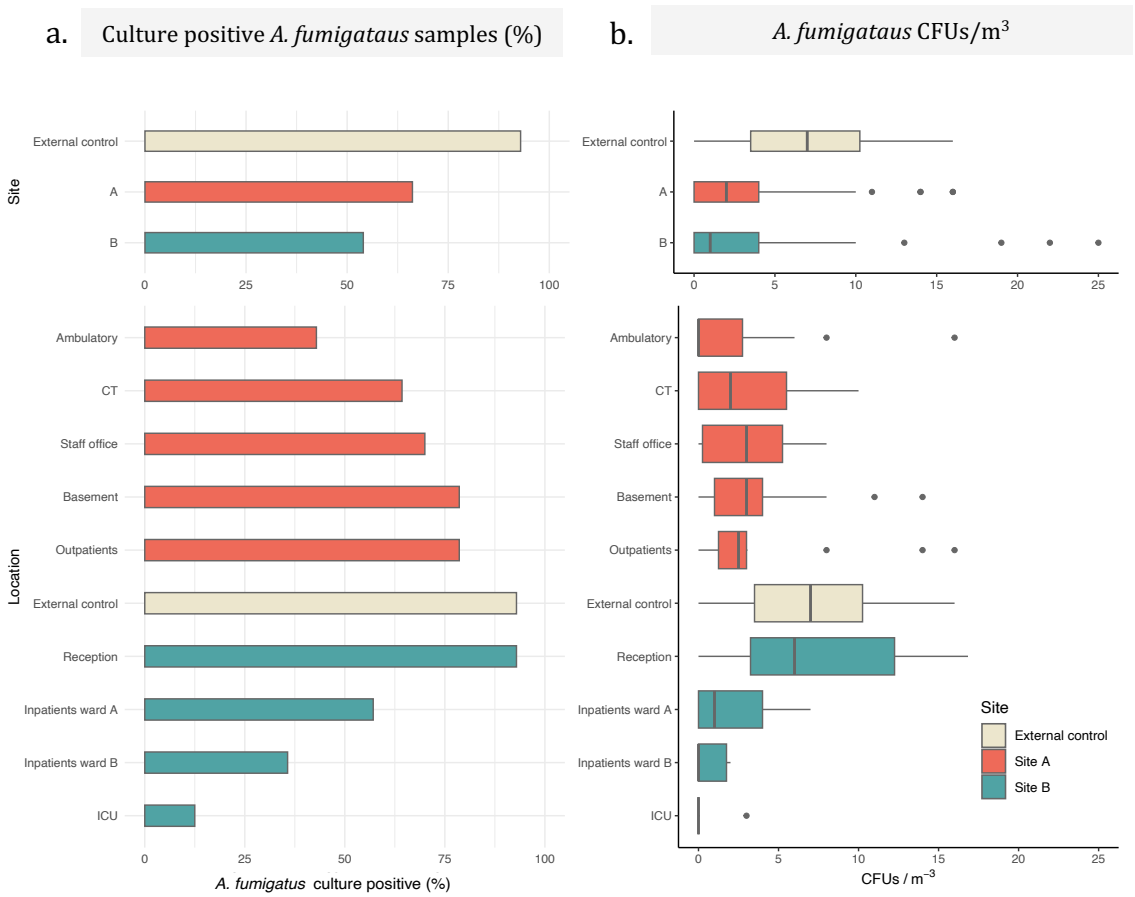
Table 5.1. Summary of sampling effort for hospital surveillance, including the number of air and samples collected

Sample date	No. of air samples	No. of soil samples	Total
6th November 2020	18	16	36
14th December 2020	18	14	32
9th February 2021	18	17	35
7th March 2021	20	n.a	20
12th June 2021	20	12	32
10th September 2021	18	n.a	18
8th November 2021	18	18	36
9th February 2022	6	n.a	6
Total	**136**	**77**	**215**

5.4.2 Spatial distribution of CFUs

5.5.2.1 Air Surveillance

Out of 130 indoor air samples, 63.85% (*n* = 83) were culture positive for *A. fumigatus,* yielding a total of 387 CFUs (median = 2 CFUs/m^3). The spatial distribution of *A. fumigatus* in the air at the Royal Brompton Hospital varied across hospital sites and specific internal locations (Figure 5.3). The external control, utilised to benchmark external conditions, exhibited the highest percentage of culture-positive samples at 92.9%, (median = 7 CFUs/m^3), surpassing both Site A and Site B. The Victorian-era 'Site A' showed a higher percentage of culture positive samples (65.15%) compared to the modern 'Site B' (54%). However, a post hoc Dunn's test revealed no significant differences in CFUs between these two sites. The concentration of CFUs varied significantly across the sampled locations. Among the internal sites, the Reception area recorded the highest fungal load, with a median concentration of 6 CFUs/m^3. This was followed by the basement and staff office, both with a median concentration of 3 CFUs/m^3, and the outpatient department with a median concentration of 2.5 CFUs/m^3, indicating potential fungal contamination hotspots. Significant differences were observed between the Reception area and both Inpatient Ward B (adj*. p-value* < 0.005) and the ICU (adj*. p-value* < 0.005) (Appendix 11), highlighting the heterogenous distribution of viable *A. fumigatus* conidia within hospital environments. Additionally, significant differences were detected between the external control and three internal sites: the Ambulatory care unit (adj. *p-value* < 0.05), Inpatient Ward B (adj*. p-value* < 0.005) and the ICU (adj*. p-value* < 0.005), suggesting effective environmental control in these areas. No significant differences were observed between CFU counts of the external control and all other sites.



*Fi*gure 5.3. **Spatial distribution of *A. fumigatus* in the air at the Royal Brompton Hospital.** The percentage of *A. fumigatus* culture-positive air samples from two hospital sites, the Victorian-era site A (red) and the modern site B (blue), including an external control (beige) (a). Locations within these sites include ambulatory, CT, staff office, basement, cardiomyopathy, reception, inpatients ward A, inpatients ward B, and ICU. Colony-forming units per cubic meter (CFUs/m^3) of *A. fumigatus* in air samples from the same sites (b). Box plots illustrate the distribution of CFUs, indicating the median, interquartile range, and outliers.

5.4.2.2 Soil Surveillance

The distribution of *A. fumigatus* in soil samples at the RBH was assessed from internal and external flower beds (Figure 5.4). Of the 77 soil samples, 85.71% (n = 66) were *A. fumigatus* culture positive, yielding a total of 884 CFUs, translating to a median density of 2 CFUs/g of soil. The Kruskal-Wallis test revealed no significant differences in CFUs between soil samples from internal and external flower beds ($p > 0.05$). However, internal samples exhibited a greater range and variability in CFU counts (sd = 21.5) compared to external samples (sd = 4.2) and the private park 'control' samples (sd = 3.2), suggesting increased heterogeneity in fungal contamination within the internal flower beds. The external Reception Courtyard exhibited the highest median CFU concentration across all flower beds (median = 4.5 CFUs/g). Among the internal sites, the Reception flower bed exhibited the highest

concentrations, recording the maximum CFU count of 75 CFUs/g and the highest median CFU concentration of 3.5 CFUs/g. Within the Outpatients department, a flower bed designated 'Outpatients 1' had a median CFU concentration of 2.5 CFUs/g, while the flower bed designated 'Outpatients 2' demonstrated considerable variability in CFU counts, including an extreme outlier of 61.5 CFUs/g, indicating significant fluctuations in fungal contamination levels.

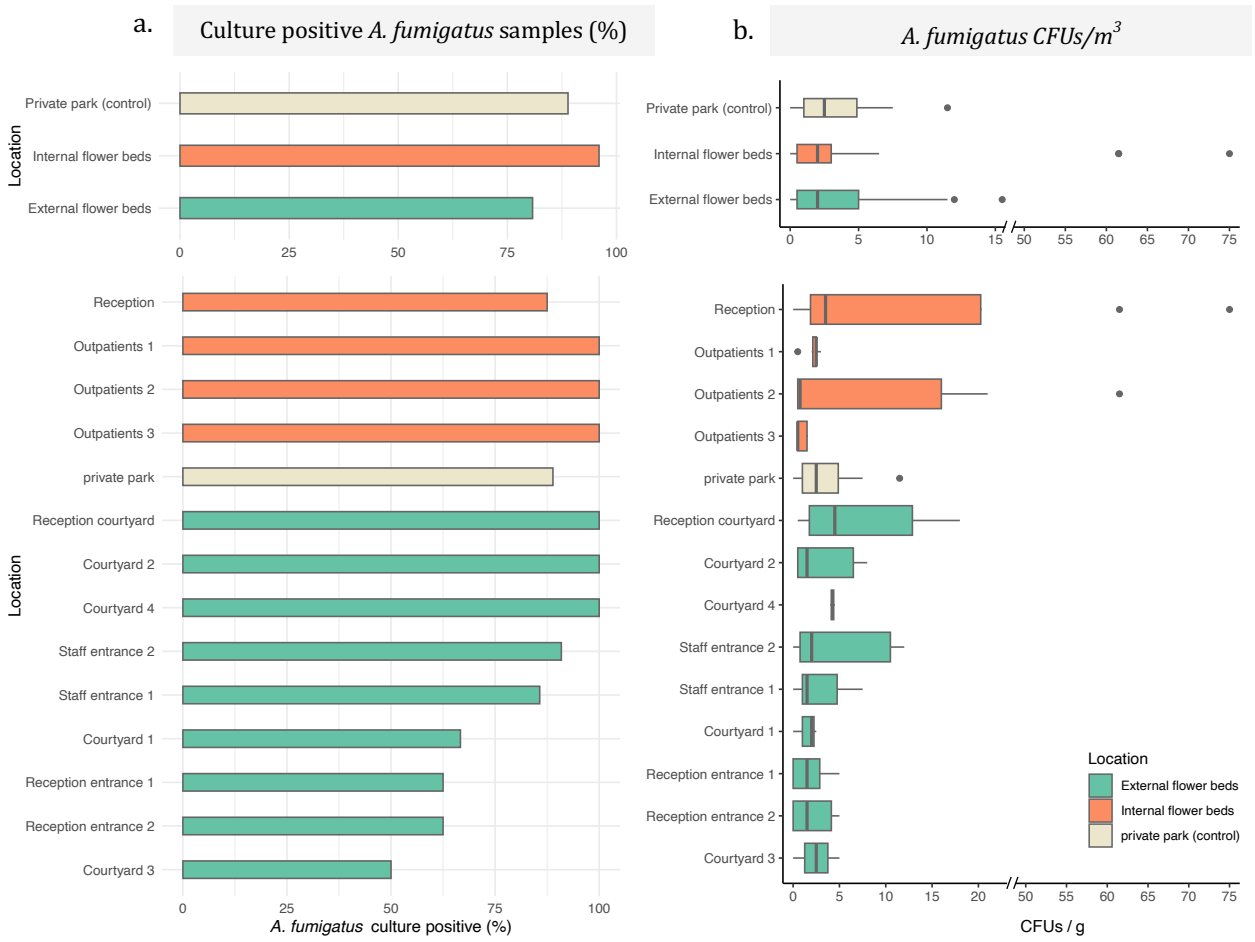


Figure 5.4. **Spatial distribution of *A. fumigatus* in soils at the Royal Brompton Hospital.** Percentage of *A. fumigatus* culture-positive samples across internal (orange) and external (green) soil beds at the hospital, including samples collected from a private park in London as a control (beige) (a). Internal locations include areas such as the reception, cardiomyopathy wards, staff entrances, and various courtyards. Colony-forming units per gram (CFUs/g) of *A. fumigatus* in soil samples from the same locations (b). Box plots illustrate the distribution of CFUs, indicating the median,

5.4.3 Temporal distribution of colony forming units

5.4.3.1 Air Surveillance

Temporal variability in airborne CFU concentrations was monitored from November 2020 to November 2021 (Figure 5.5a). A non-parametric Kruskal-Wallis test was conducted to evaluate

differences in CFU counts over time between Site A and Site B (Appendix 11). For the external control, no significant temporal differences in CFU counts were observed ($p > 0.05$). Despite visually apparent differences, the lack of statistical significance is likely attributable to the limited sample size ($n = 2$ per sampling date). Although CFUs fluctuated across different dates and sites, statistically significant ($p < 0.05$) temporal variations were detected only at Site A (Appendix 11).

5.4.3.2 Soil Surveillance

Soil samples obtained from both internal and external locations demonstrated temporal variations of CFUs (Figure 5.5b). However, only the private park 'control' and external hospital flower beds showed significant temporal variability ($p < 0.05$ and $p < 0.005$ respectively) (Appendix 11), reflecting potential environmental influences on *A. fumigatus* fungal loads.

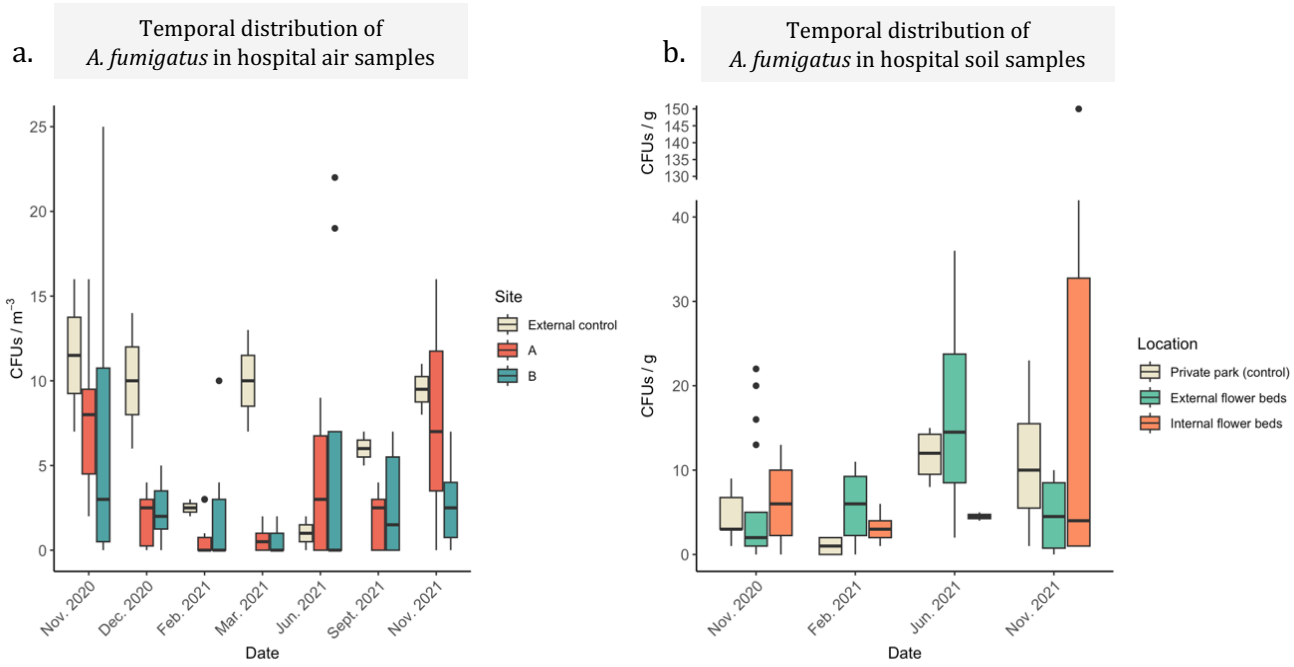


Figure 5.5. **Temporal distribution of *A. fumigatus* in air and soil samples at the Royal Brompton Hospital.** Concentration of A. fumigatus CFUs/m^3 collected in air samples from site A, B and an external control across all sample time points from November 2020 to November 2021 (a). Concentration of A. fumigatus CFUs/g in soil samples from external and internal flower beds and a private park which served as a control (b). Outliers are shown as individual points.

5.4.4 Pan-azole resistance detected within the hospital environment.

A total of 363 *A. fumigatus* colonies were isolated from internal and external air and soil samples. Resistance to at least one clinical azole (itraconazole (4mg/L), voriconazole (2 mg/L), posaconazole (0.5mg/L)) was detected in 2.7% (*n* = 5) of isolates cultured from air samples and 1.12% (*n* = 2) of isolates cultured from soil samples. All isolates exhibiting clinical azole resistance also demonstrated resistance to tebuconazole at concentrations of at least 6 mg/L. Overall, tebuconazole resistance was confirmed in 7% (*n* = 13) of isolates cultured from air samples and 4.5% (*n* = 8) isolates cultured from soil samples. Azole resistant isolates were identified throughout the year, consistently emerging from localised areas such as the hospital basement and Outpatients department in Site A, and the Reception area in Site B. Fine scale air surveillance of the Outpatients department in February 2022 identified tebuconazole resistance in 20% (*n* = 5) of isolates, with 8% (n = 2) also exhibiting resistance to at least 2 clinical azoles.

5.4.5 WGS of 102 *A. fumigatus* isolates from the hospital environment

The sequencing panel included 51 isolates from air samples, 47 from soil, and 4 from swabs collected during fine scale surveillance of the Outpatients department. Isolates selected for WGS are summarised in Appendix 12. In total, 19 tebuconazole resistant *A. fumigatus* isolates were included for WGS. These isolates originated from either air or soil samples from the hospital Basement (*n* = 2), CT (*n* = 1), Outpatients department (*n* = 11), Inpatients ward B (*n* = 1), Reception (*n* = 3), External air control (*n* = 1) and External courtyards (*n* = 1). Alignments of the sequenced genomes are summarised in Appendix 5.

5.4.6 Genotypic characterisation confirmed presence of *cyp51a* alleles

Isolates were genotypically characterised to determine the frequency and distribution of azole resistant associated *cyp51a* alleles revealing, the presence of 8 distinct *cyp51a* alleles (Appendix 12). All *cyp51a* wildtypes were susceptible to the clinical azoles. However, seven isolates exhibited resistance to tebuconazole, indicating the presence of non-*cyp51a* resistance mechanisms.

Nonsynonymous point mutations such as M172V/F46Y (*n* = 16), G448S (*n* = 2), D262Y (*n* = 3), and I242V (*n* =1) were also detected in air and soil samples from multiple sampling locations. With the exception of M172V/F46Y, all isolates containing G448S, D262Y and I242V were triazole susceptible. Of the 16 isolates containing the M172V/F46Y mutation, 75% (*n* = 12) were susceptible to the triazoles, however 25% (*n* = 4) exhibited tebuconazole resistance (6mg/L), of which two were also resistant to posaconazole. An isolate containing TR_{120} was recovered from a CT air sample and demonstrated resistance to tebuconazole (6 mg/L). The presence of TR_{34}/L98H was confirmed in 7.8% (*n* = 8) of the observed *cyp51a* genotypes. Of these, 6 were isolated from air samples collected from the hospital basement, Outpatients, and Reception area, while 2 were from soil samples collected from the Reception area. Notably, the Outpatients area accounted for half of the TR_{34}/L98H genotypes, with all four isolates recovered on different sampling dates, highlighting a possible persistent environmental contamination. All isolates containing TR_{34}/L98H, exhibited resistance to tebuconazole up to 16mg/L and were resistant to at least one clinical azole.

5.4.7 Genetic diversity and population structure of *A. fumigatus* in the hospital environment

Pairwise SNP analysis of 102 *A. fumigatus* isolates from the hospital environment revealed a median divergence of 47,971 SNPs between isolates (Figure 5.6). To investigate the spatiotemporal distribution of genetically similar isolates, pairs sharing less than 3% of the observed genetic diversity (<1,399 SNPs) were identified (Table 5.6). Of the 10 pairs, four originated from the same samples (Outpatients soil, November 2021, and Compost, July 2022), suggesting possible clonal replication during culture. The remaining six pairs were collected from different locations or times, indicating a broad spatiotemporal distribution of clonal isolates. Among isolate pairs sharing less than 6% genetic diversity (<2,798 SNPs), six contained the TR_{34}/L98H genotype. One of these pairs was from the same sample (outpatients' air, September 2021), while the others were distributed across various locations and time points within the hospital. Additionally, a pair of azole susceptible isolates with the G448S mutation also demonstrated broad spatiotemporal distribution. These results indicate that genetically similar *A. fumigatus* isolates, including those with resistance-associated mutations, are widely

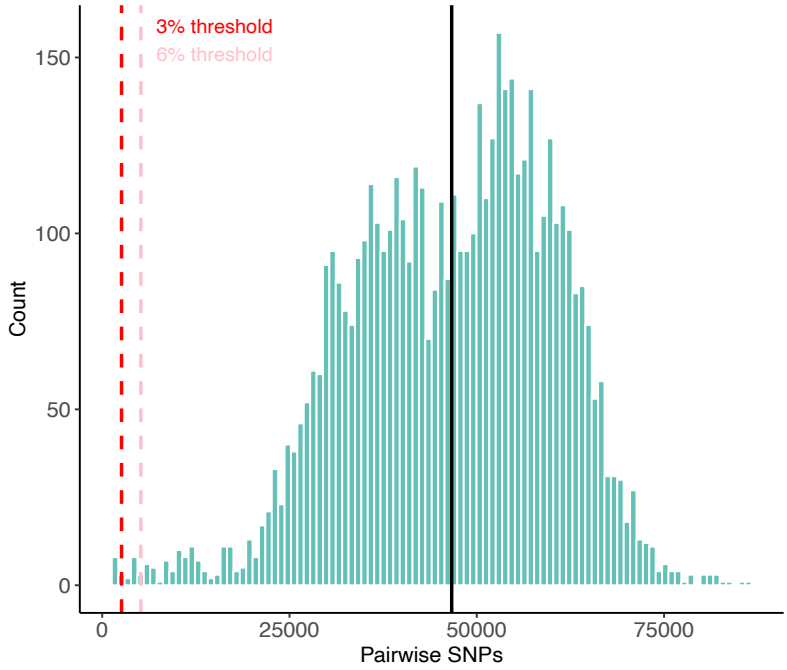


Figure 5.6. **Distribution of pairwise unique SNPs among *A. fumigatus* isolates collected from the hospital environment.** The histogram illustrates the frequency of unique SNPs between isolate pairs, with counts ranging from 0 to over 75,000 SNPs. The solid black line marks the median number of pairwise SNPs across the dataset. The dashed red lines indicate the 3% and 6% genetic distance thresholds, representing commonly used cutoffs for defining population structure

Table 5.2. Summary of genetically similar isolate pairs in the hospital environment sharing <6% of the observed genetic diversity.

	Isolate Pair 1					Isolate pair 2				
Threshold (%)	Isolate	Location	Source	*cyp51a* allele	Date	Isolate	Location	Source	*cyp51a* allele	Date
3%	FN046	Outpatients	Soil	wildtype	Nov. 2021	FN089	Outpatients	Soil	wildtype	Nov. 2021
	FN087	Outpatients	Soil	wildtype	Nov. 2021	FN046	Outpatients	Soil	wildtype	Nov. 2021
	FN087	Outpatients	Soil	wildtype	Nov. 2021	FN089	Outpatients	Soil	wildtype	Nov. 2021
	FN052	Reception	Soil	wildtype	Nov. 2021	FN089	Outpatients	Soil	wildtype	Nov. 2021
	FN052	Reception	Soil	wildtype	Nov. 2021	FN046	Outpatients	Soil	wildtype	Nov. 2021
	FN059	External control	Air	wildtype	Jun. 2021	FN038	Basement	Air	wildtype	Nov. 2021
	FN068	Private park	soil	wildtype	Feb. 2021	FN055	Reception	Air	wildtype	Nov. 2021
	FN060	Ambulatory	Air	wildtype	Dec. 2020	FN065	Inpatients Ward A	Air	wildtype	Mar. 2021
	FC001	Compost	Compost	TR34/L98H	Jul. 2022	FC002	Compost	Compost	TR34/L98H	Jul. 2022
	FN002	Outpatients	Air	TR34/L98H	Nov. 2021	FC002	Compost	Compost	TR34/L98H	Jul. 2022
6%	FN078	Office	Air	G448S	Dec. 2020	FN099	Ambulatory	Air	G448S	Mar. 2021
	FN030	Inpatients Ward B	Air	M172/F46Y	Dec. 2020	FN092	External control	Air	M172/F46Y	Feb . 2021
	FN002	Outpatients	Air	TR34/L98H	Nov. 2021	FN017	Reception	Air	TR34/L98H	Jun. 2021
	FN019	Reception	Soil	TR34/L98H	Jun. 2021	FN017	Reception	Air	TR34/L98H	Jun. 2021
	FN022	Outpatients	Air	TR34/L98H	Sep. 2021	FN098	Basement	Air	TR34/L98H	Jun. 2021
	FN072	Reception	Soil	M172/F46Y	Jun. 2021	FN018	Office: External	Soil	M172/F46Y	Jun. 2021
	FN093	Inpatients Ward A	Air	M172/F46Y	Dec. 2020	FN051	Outpatients	Soil	M172/F46Y	Jun. 2021
	FN002	Outpatients	Air	TR34/L98H	Nov. 2021	FN019	Reception	Soil	TR34/L98H	Jun. 2021
	FC001	Compost	Compost	TR34/L98H	Jul. 2022	FN019	Reception	Soil	TR34/L98H	Jun. 2021
	FC002	Compost	Compost	TR34/L98H	Jul. 2022	FN019	Reception	Soil	TR34/L98H	Jun. 2021

dispersed throughout the hospital environment over time. This was further demonstrated with phylogenetic analysis (Figure 5.7) and DAPC (Figure 5.8). Phylogenetic analysis demonstrated strong bootstrap support over 70% (Appendix 5). This analysis, incorporating susceptibility profiles, *cyp51a* genotypes, and sampling locations, revealed a distinct spatiotemporal distribution of genetically related *A. fumigatus* isolates and highlighted patterns of azole resistance. Notably, MTR resistant isolates carrying the TR_{34}/L98H mutation were consistently detected across different locations, such as the Outpatients department, Reception, and Basement area, at multiple time points. These findings indicate the persistent presence of a TR_{34}/L98H reservoir within the hospital setting, maintained over an extended period. DAPC showed that isolates, irrespective of source or location were highly clustered, suggesting limited genetic differentiation.

5.4.7.3 Investigating a possible vector of azole resistance

Isolates containing the TR_{34}/L98H genotypes, cultured from a compost bag supplied by the same vendor used in the hospital beds, were incorporated into genomic pipelines for comprehensive analysis. Phylogenetic analysis (Figure 5.7) and DAPC (Figure 5.8) highlighted that these compost-derived isolates, sampled a year after the conclusion of hospital surveillance, clustered with isolates from the hospital environment. Pairwise SNP counts (Table 5.6) further indicated that these compost isolates are genetically similar to isolates collected from the Reception soil samples and an Outpatients air sample.

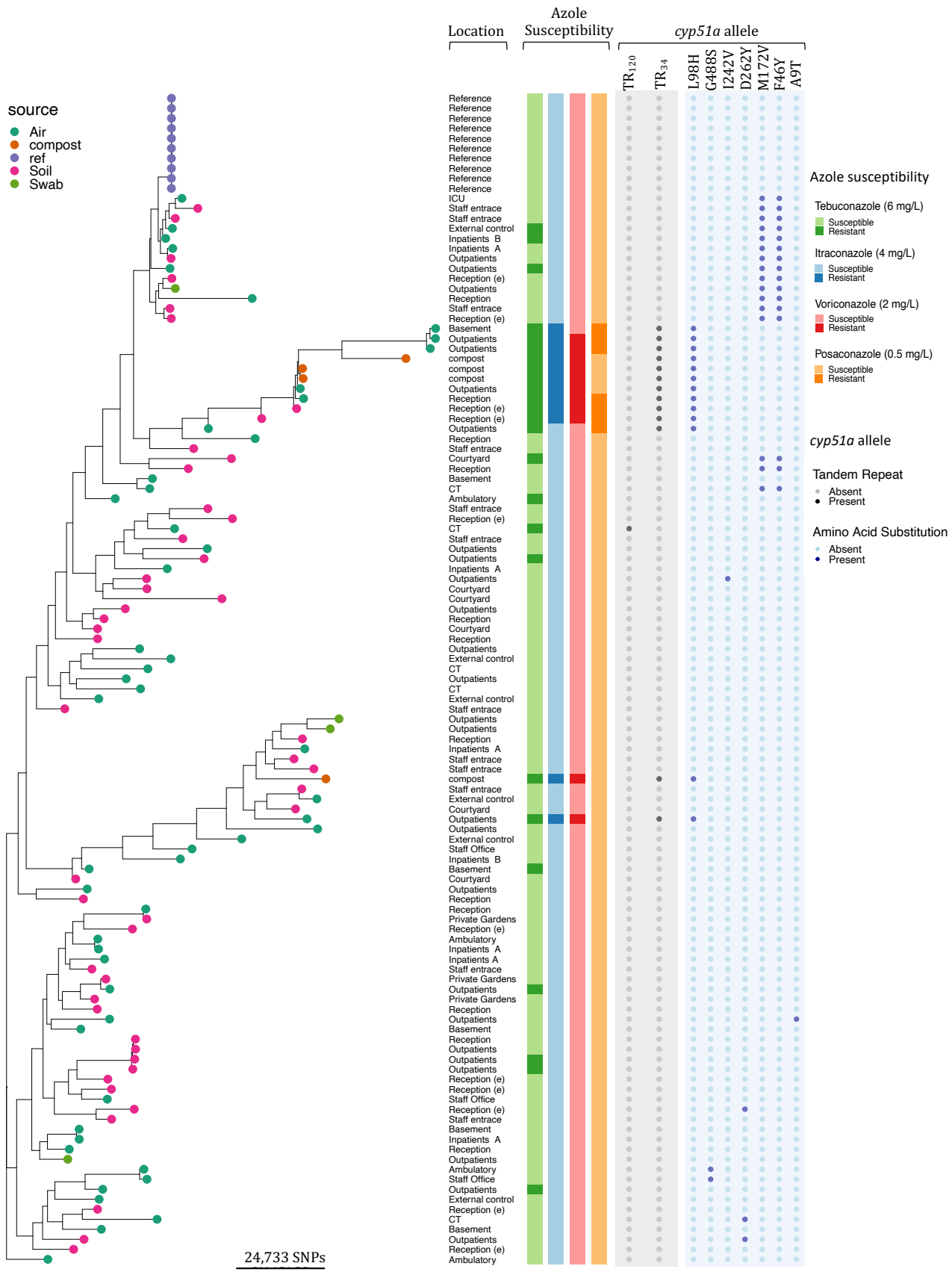


Figure 5.7. **Phylogenetic tree illustrating the evolutionary relationships of environmental *A. fumigatus* isolates from the Royal Brompton Hospital.** Coloured circles on the branches represent the source of the isolate. Adjacent to the tree is location from which the sample was collected. The heatmaps indicate susceptibility profiles for tebuconazole and the clinical azoles, with darker colours representing resistance. Cyp51a polymorphisms are indicated by grey (TR_s) and blue points (amino acid substitutions).

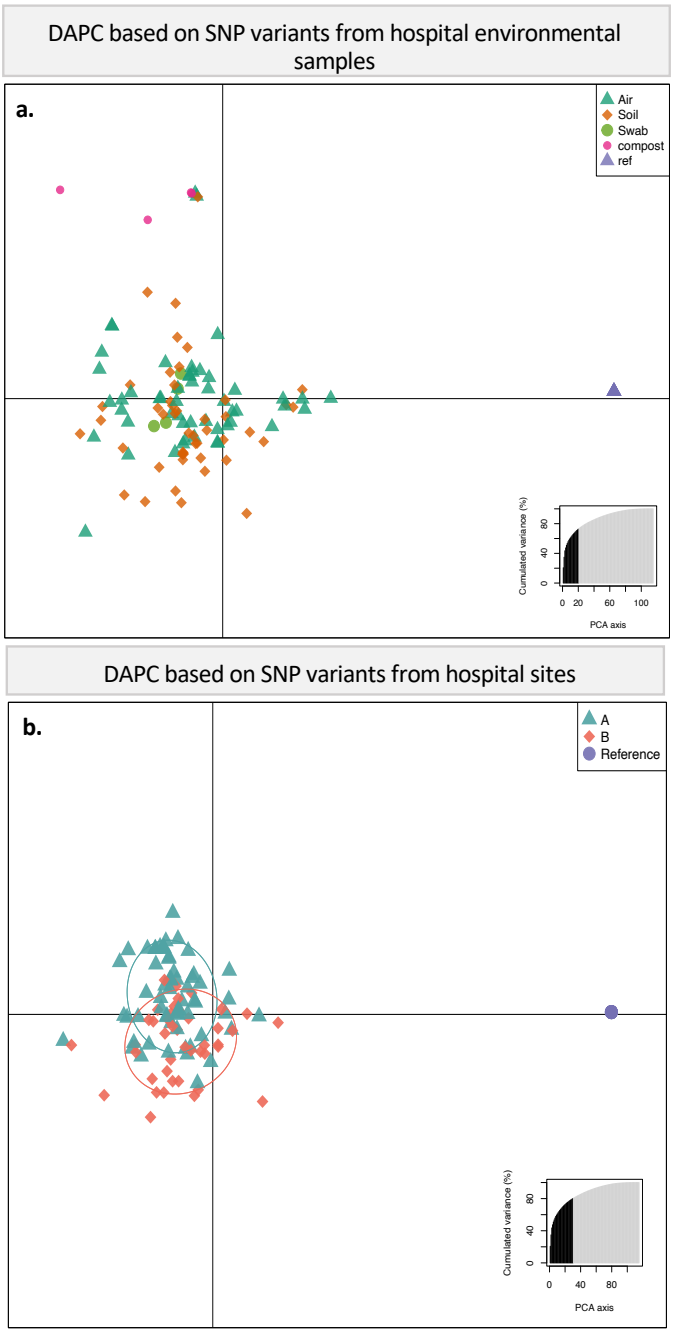


Figure 5.8 **DAPC based on SNP variants from hospital environmental samples.** Samples from environmental sources include air (green triangles), soil (orange diamonds), swab (green circles), and compost (pink circles) (a.). Samples collected from the Victorian-era Site A (red diamonds) and modern building Site B (blue triangles) (b.). The AF293 refence samples (n = 10) are shown as purple points. The inset shows the cumulative variance explained by the PC axes, indicating the proportion of total variance captured by the analysis. The separation of clusters demonstrates the genetic diversity between different environmental samples within the hospital.

5.4.9 Epidemiological links between clinical and environmental isolates

A fine-scale phylogenetic analysis of 284 prospective clinical isolates from the RBH respiratory disease cohort and RBH environment identified multiple instances of closely related strains (Figure 5.9) with median bootstrap support of over 70% (Appendix 5). The outer rings of the phylogeny, which depict tebuconazole and clinical azole resistance, illustrates the overlap of resistant isolates across clinical and hospital environmental samples, particularly those containing the TR_{34}/L98H allele. The incorporation of the broader UK dataset, which included an additional 118 retrospective clinical genomes from RBH, 151 clinical isolates from the wider UK clinical cohort and 347 environmental isolates from across the UK, further corroborated epidemiological links (Figure 5.10a). These findings highlight the potential for transmission from high-exposure environments, such as hospital settings.

5.4.9.1 Case studies of environmental routes of transmission

Sub-phylogenies within the UK wide phylogeny (Figure 5.10.b-d), with 100% bootstrap support, highlight key clusters associated with environmental transmission. These clusters were mapped across three distinct sub-phylogenies, further reinforcing the role of the hospital environment as a possible reservoir of resistance. The sub-phylogeny in Figure 5.10.b highlights Case 33, an individual diagnosed with CPA with isolates containing the G448S mutation collected over period of approximately 8 months from November 2020 – July 2021. The isolates, which demonstrated resistance to both clinical azoles and the agricultural azole tebuconazole, were phylogenetically clustered and highly related. The hospital isolates were cultured from air samples in December 2020 and March 2021 and contained the G448S mutation but were azole susceptible. The Sub-phylogenies presented in Figure 5.10.c-d highlight possible acquisition of the TR_{34}/L98H genotype. However, while the TR_{34}/L98H isolates from the hospital environment displayed genetic similarity to those from the RBH clinical cohort, they were also closely related to 5 clinical isolates from the broader UK population and 4 environmental isolates from across the UK.

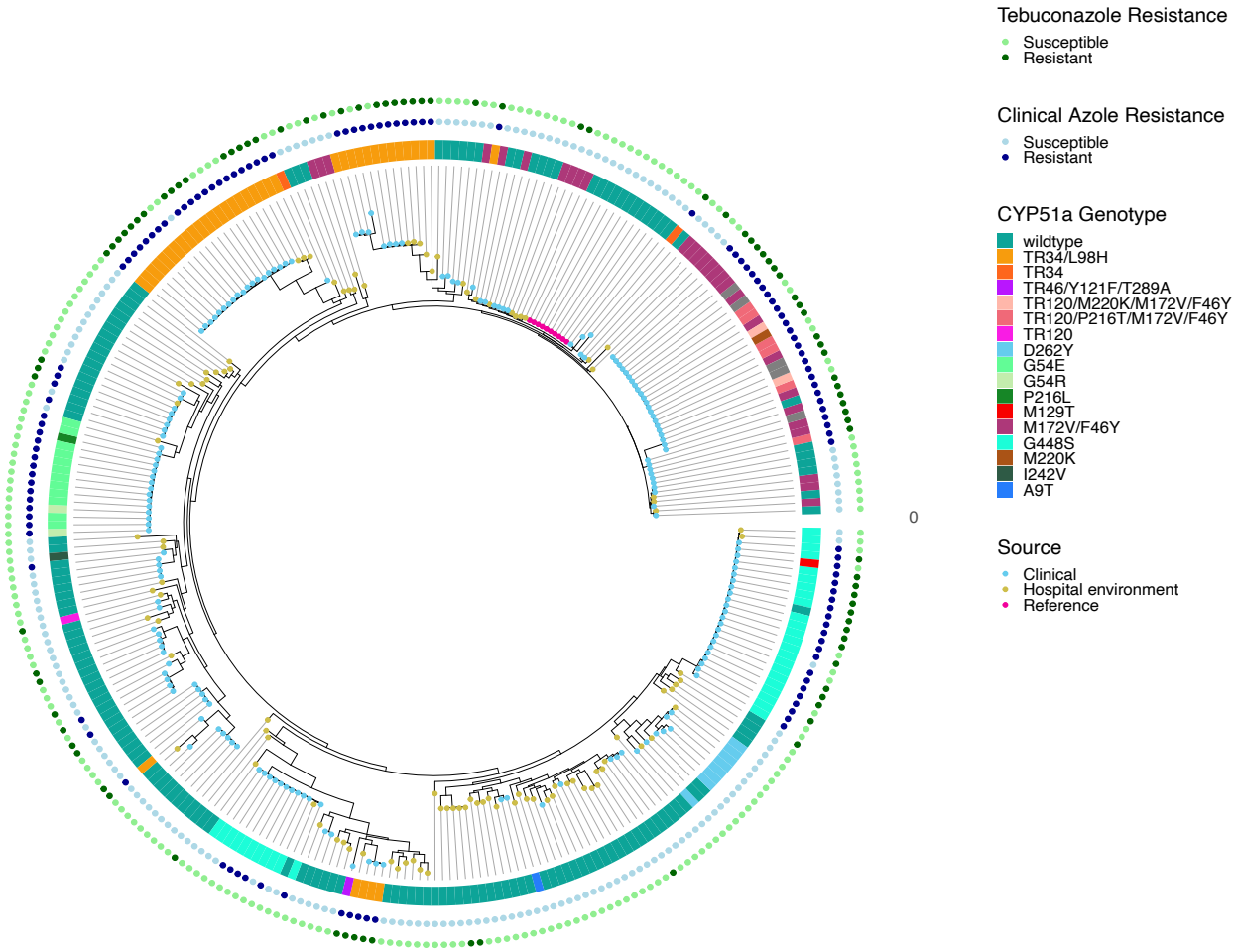


Figure 5.9 **Phylogenetic tree illustrating the evolutionary relationships of environmental *A. fumigatus* isolates from the Royal Brompton Hospital and clinical isolates from the RBH respiratory disease cohort.** Coloured circles on the branches represent the source of the isolate. The inner circle indicates *cyp51a* genotypes and the outer data points indicate tebuconazole resistance (dark green) and clinical azole resistance (dark blue).

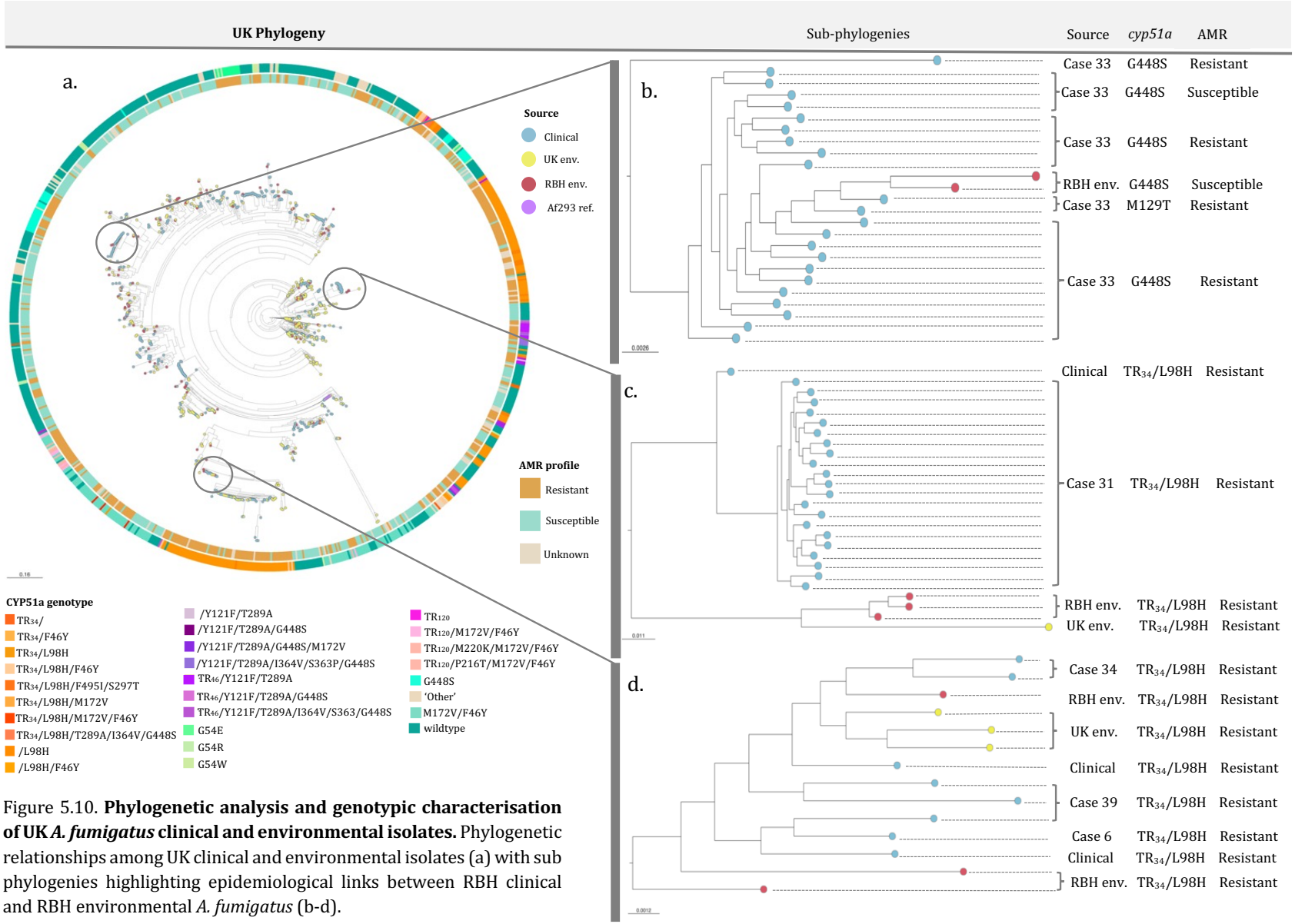
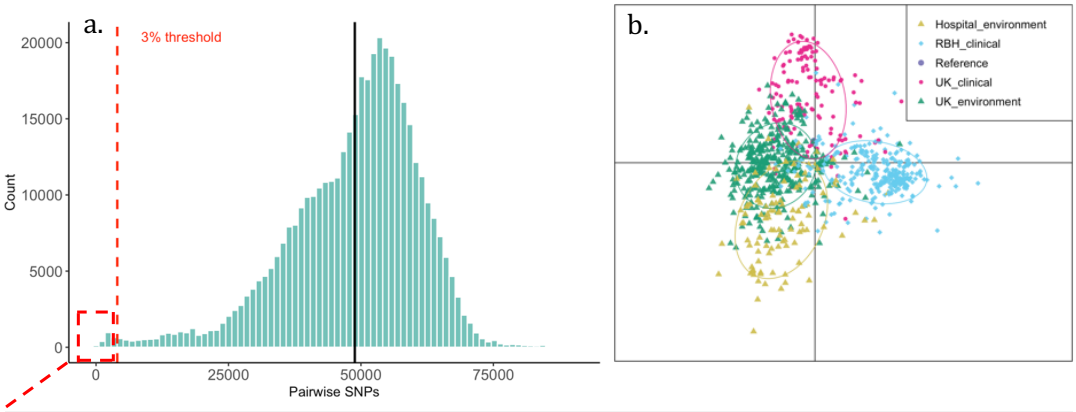


Figure 5.10. **Phylogenetic analysis and genotypic characterisation of UK *A. fumigatus* clinical and environmental isolates.** Phylogenetic relationships among UK clinical and environmental isolates (a) with sub phylogenies highlighting epidemiological links between RBH clinical and RBH environmental *A. fumigatus* (b-d).

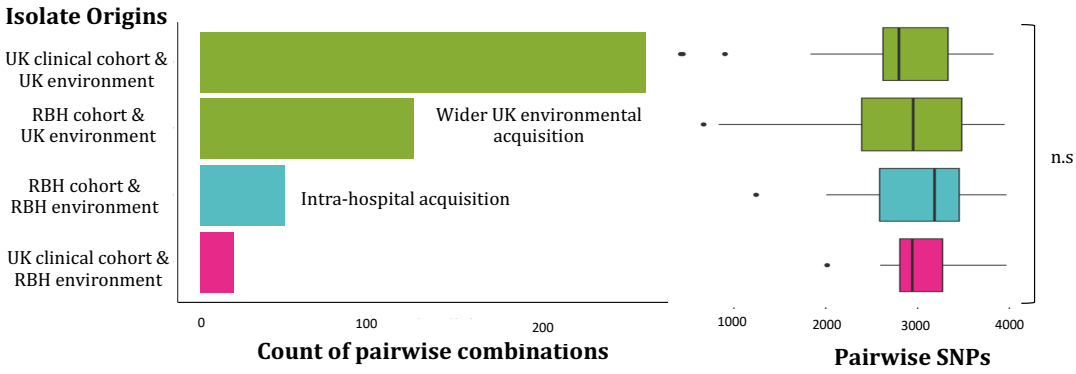
5.4.9.2 Multivariate analysis and pairwise relationships

To further investigate the genetic relationships, pairwise SNP comparisons and DAPC analyses were performed. Within the UK dataset, pairs of isolates were, on average, separated by 49,156 unique SNPs (Figure 5.11.a). DAPC revealed clear genetic links between clinical and environmental clusters (Figure 5.11.b), with a notable overlap between hospital environment and UK environmental isolates, highlighting that the hospital isolates are drawn from the broader UK environmental population. While the UK clinical and RBH clinical isolates formed distinct clusters, possibly due to sampling bias introduced through longitudinal surveillance of multiple strains, both groups exhibited unique genetic characteristics compared to environmental isolates. However, some proximity to the environmental clusters was evident, supporting the hypothesis of a shared origin for these isolates. The origins and counts of pairwise combinations sharing less than 3% (< 1,474 SNPs) of the observed population diversity are shown in Figure 5.11.c, no significant difference was observed in SNP diversity across the combinations. The majority of RBH clinical isolate pairs were genetically closely related to those from the wider UK environment (*n* = 143 isolate pairs), indicating the broader environment as the primary reservoir for *A. fumigatus.* However, 49 pairs of RBH environment and RBH clinical isolates suggest possible intra-hospital transmission. Of the RBH cohort, 41% (*n* = 7) harboured isolates that were genetically similar to the hospital environment only, while 35% (*n* = 6) had isolates genetically linked to the wider UK environment (Figure 5.11d). Additionally, 25% of patients carried mixed strains from both the hospital and UK environment, predominantly with the TR_{34}/L98H genotype. These findings highlight the complexity of transmission dynamics, involving both broader environmental reservoirs and potential intra-hospital acquisition.

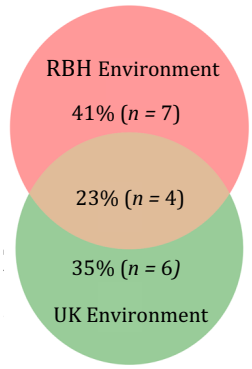
Distribution of UK *A. fumigatus* pairwise SNPs and DAPC based on SNP variants



c. Distribution of *A. fumigatus* pairwise combinations sharing <3% UK genomic diversity



d. Origins of isolate pairs: RBH vs. UK environment



Case ID	Transmission Route	Environment Genotypes	Clinical Genotypes
Case 8	RBH environment	wildtype	wildtype
RB001	RBH environment	wildtype	wildtype
RB014	RBH environment	wildtype	wildtype
RB008	RBH environment	G488S	G488S
RB008	RBH environment	G448S	M129T
RB019	RBH environment	M172V/F46Y	wildtype
RB029	RBH environment	D246Y	D246Y
RB036	RBH environment	D246Y	D246Y
RB002	RBH environment	wildtype	wildtype
RB002	RBH environment	wildtype	M172V/F46Y
RB002	UK environment	TR_{34}/L98H	TR_{34}/L98H
RB009	RBH environment	TR_{34}/L98H	TR_{34}/L98H
RB009	RBH environment	M172V/F46Y	wildtype
RB009	RBH environment	I242V	wildtype
RB009	UK environment	TR_{34}/L98H	TR_{34}/L98H
RB009	UK environment	M172V/F46Y	TR_{34}/L98H
RB023	RBH environment	TR_{34}/L98H	TR_{34}/L98H
RB023	UK environment	TR_{34}/L98H	TR_{34}/L98H
Case 6	RBH environment	TR_{34}/L98H	TR_{34}/L98H
Case 6	UK environment	TR_{34}/L98H	TR_{34}/L98H
Case 12	UK environment	M172V/F46Y	M172V/F46Y
Case 14	UK environment	TR_{34}/L98H	TR_{34}/L98H
Case 19	UK environment	TR_{34}/L98H	TR_{34}/L98H
Case 7	UK environment	D430G	wildtype
RB027	UK environment	wildtype	wildtype
RB032	UK environment	TR_{34}/L98H	TR_{34}/L98H
RB032	UK environment	L98H	TR_{34}/L98H

Figure 5.11 **Distribution of *A. fumigatus* pairwise SNPs and genomic clustering.** Histogram of pairwise SNPs among UK isolates, with a 3% genomic diversity threshold (a). DAPC plot showing genetic clusters of hospital, RBH clinical, UK environment, and reference isolates (b). Pairwise combinations with <3% genomic diversity, including their sources, with boxplots showing variation (c). Venn diagram of isolate overlap between RBH and UK environments, highlighting the distribution of shared genotypes between clinical and environmental samples (d)

5.5 Discussion

This study offers valuable insights into the epidemiology of azole resistant *A. fumigatus* in a high-exposure healthcare setting, particularly with respect to azole resistance acquisition in patients with chronic respiratory diseases. Leveraging WGS for 'real-time' surveillance, *A. fumigatus* isolates were collected from air, soil, and clinical samples over a two-year period, revealing considerable genetic diversity, recurrent instances of azole resistance and potential epidemiological links between environmental and clinical isolates. These findings highlight the need for enhanced fungal surveillance and control strategies, particularly in healthcare environments, where vulnerable patient populations are at increased risk of acquiring resistant fungal infections.

The results highlight a concerning environmental reservoir of azole resistant *A. fumigatus* within the hospital setting. Triazole resistance was detected in 4.5% of air isolates and 3.4% of soil isolates, aligning with reported UK prevalence rates of 3–6% for azole resistance in *A. fumigatus* (277,359,474,495). Azole-resistant TR_{34}/L98H isolates exhibited distinct spatiotemporal distribution within the hospital, persisting in key areas such as the basement, Outpatients are, and Reception. These locations may serve as transmission hotspots, contributing to ongoing contamination and repeated patient exposure.

The detection of the TR_{34}/L98H allele in hospital air and soil samples mirrors global reports of environmental contamination and patient infections (254,286,483,484). Such findings raise the possibility that individuals with chronic respiratory diseases may acquire azole resistant *A. fumigatus* from contaminated hospital spaces during visits or stays. WGS data further support this, revealing genetic links between clinical and environmental isolates, indicating possible direct or indirect transmission routes (496). These observations align with previous reports of pan-azole resistant *A. fumigatus* occurring on clonal backgrounds in both environmental and clinical settings (353).

A substantial proportion of *A. fumigatus* culture-positive samples were detected in both air (63.85%) and soil (85.71%), highlighting the ubiquitous presence of *A. fumigatus* within the hospital

environment. This extensive presence mirrors earlier reports of widespread *A. fumigatus* distribution in healthcare settings, even in areas with stringent protective measures (496–500). WGS revealed significant genetic diversity, with DAPC showing substantial genetic overlap between indoor air and soil samples. Hospital soils likely serve as reservoirs, contributing to the spread of aerosolised conidia and impacting air quality. The genetic similarity among isolates from various time points and locations suggests that the *A. fumigatus* can persist in the hospital environment. Under selective pressure from residual azoles, resistant strains are favoured, leading to the establishment of azole-resistant *A. fumigatus* within the hospital setting and heightening the potential risk of transmission to vulnerable patients.

The detection of the TR_{120} allele within the hospital environment, previously reported only in clinical isolates from patients undergoing long-term azole therapy in the Netherlands (475), raises the possibility of patient-derived spores in the hospital. Two CF patients in the RBH cohort harboured TR_{120} alleles with associated SNPs, suggesting patient-to-environment transmission. Given that CF patients can aerosolise *A. fumigatus* spores (289), it is plausible that patient-to-environment transmission contributes to the ongoing presence and persistence of resistant strains, with compensatory evolutionary processes supporting their survival and spread within the hospital environment. However, the clinical TR_{120} isolates were genetically distinct from the environmental TR_{120} isolates, suggesting either independent evolution in the environment or challenging the assumption that TR_{120} mutations arise exclusively within the host. This distinction may also indicate that the full genetic diversity of the *A. fumigatus* population in the hospital setting has not been fully captured. The lack of a reliable molecular clock for *A. fumigatus* complicates the determination of transmission directionality, making it difficult to discern whether transmission occurs from patient-to-environment, environment-to-patient, or through independent evolutionary events.

Genomic analysis identified multiple *cyp51a* alleles, including M172V/F46Y, G448S, and D262Y, in both clinical and environmental A. fumigatus isolates. While point mutations are often linked to long-term azole therapy in patients, independent studies have reported such point mutations in

environmental samples (501–506), suggesting that resistance can develop outside clinical settings. These findings indicate that azole-resistant strains may evolve due to environmental azole exposure, blurring the distinction between patient- and environment-driven resistance pathways (295,505).

The distribution of *A. fumigatus* in soil samples varied considerably, with high concentrations in the Outpatients (61.5 CFUs/g) and Reception areas (75 CFUs/g), particularly in indoor flower beds. These elevated fungal loads may be influenced by plant maintenance practices and suggest that external sources, such as compost, could introduce resistant strains into the hospital environment. Compost used in hospital flower beds may act as a vector for azole resistant *A. fumigatus*, as isolates from compost samples showed genetic similarity to hospital environmental isolates. However, due to the widespread clonal dissemination of the TR_{34}/L98H genotype, determining the direct source remains challenging. This underscores the importance of monitoring external environmental inputs like compost as potential sources of resistance in healthcare settings.

This study highlights the growing prevalence of azole resistant *A. fumigatus*, which is becoming increasingly embedded in our environments, emphasising the urgent need for infection control strategies that address both temporal and spatial variations in antifungal resistance. Patients with chronic respiratory diseases, are particularly susceptible to *A. fumigatus* colonisation, with high rates of azole resistance documented in these populations (301). Here, WGS has precisely identified epidemiological links between hospital environmental isolates and clinical strains, suggesting that patients may acquire resistant infections during hospital visits. The findings highlight the dynamic nature of *A. fumigatus* populations in healthcare settings and the importance of integrating high-resolution genomic data with clinical surveillance to monitor azole resistance, especially in areas frequented by high-risk patients. However, the study's focus on a single hospital site may limit the broader applicability of the findings. Expanding the research to a multi-centre study across diverse healthcare settings would provide a more comprehensive understanding of regional azole resistance patterns. Collaborative efforts could establish standardised guidelines and improve patient outcomes through access to broader data. However, accessing regulated hospital spaces remains challenging

due to ethical and logistical constraints, particularly exacerbated during the COVID-19 pandemic, which may have led to an underrepresentation of resistant strains. Future surveillance should prioritise comprehensive sampling across all hospital areas, focusing on vulnerable patients and investigating seasonal variations in fungal load and resistance profiles to better understand transmission dynamics.

Given the ubiquitous presence of *A. fumigatus* in various environments, protecting susceptible cohorts from exposure is particularly challenging. While interventions are more feasible in controlled indoor hospital environments, areas with high human traffic, such as outpatient clinics, remain difficult to regulate. Integration of remote patient surveillance, such as at-home testing, offers a promising avenue to reduce the need for hospital visits, thereby minimising patient exposure to potentially contaminated environments and reducing the risk of patient-to-patient transmission.

Despite the strengths of WGS, an element of uncertainty remains in our conclusions. The clonal expansion of globally distributed TR_{34}/L98H genotypes, and the complex, multifactorial transmission dynamics of *A. fumigatus* suggest intricate global interconnections that are not yet fully explored (507). While environmental acquisition of azole resistance has been strongly suggested in previous studies, the direct impact of environmental reservoirs of TR_{34}/L98H on clinical cases remain circumstantial. Although our findings support the role of hospitals as potential reservoirs for these resistant strains, more extensive temporal and spatial genomic surveillance is needed to conclusively link environmental sources with clinical cases. Integrating real-time WGS surveillance into routine infection control poses logistical challenges due to its complexity and resource demands. Automating WGS analysis pipelines with machine learning algorithms could greatly enhance the speed and accuracy of outbreak detection, resistance tracking, and intervention strategies. Machine learning can analyse complex datasets, identifying patterns and risk factors for azole resistance, improving predictive accuracy, and guiding targeted interventions. By addressing these limitations and integrating advanced genomic tools into surveillance efforts, healthcare systems can be better equipped to combat the emerging threat of azole-resistant *A. fumigatus* in both clinical and environmental contexts.

In conclusion, this surveillance study, incorporating high-resolution 'real-time' genomic epidemiology, underscores the clinical implications of azole resistant *A. fumigatus* in hospital environments, particularly for patients with chronic respiratory conditions. The clonal dissemination of multi-triazole-resistant strains, particularly those with the TR_{34}/L98H resistance allele, highlights the significant risk posed by environmental reservoirs to individuals with chronic respiratory diseases. Addressing this emerging public health threat will require coordinated efforts to enhance fungal surveillance, minimise environmental contamination, and optimise antifungal stewardship.

ACKNOWLEDGEMNETS: I would like to acknowledge Rodrigo Monteirinho-Leitao (Imperial College London) for his support with prospective isolate collection, antifungal susceptibility testing and gDNA extraction. Special thanks to Dr. Anand Shah for his assistance with hospital surveillance.

Chapter 6 Characterising azole resistant *A. fumigatus* in home environments of chronic respiratory disease cohorts.

6.1 Abstract

A citizen science approach to investigate the presence and distribution of azole-resistant *A. fumigatus* within home environments across the UK, focusing on households of patients with conditions such as cystic fibrosis and chronic pulmonary aspergillosis. Participants collected air, soil, dust, and swab samples over a one-year period, resulting in a comprehensive dataset of 438 isolates. WGS of 101 isolates identified multiple *cyp51A*polymorphisms, including TR_{34}/L98H, unlinked L98H, and Y121F/T289A, as well as novel combinations of nonsynonymous SNPs, indicating a diverse range of resistance mechanisms in the home environment. The study revealed that soil samples were the primary source of resistant isolates, contributing 70.5% of the detected azole-resistant *A. fumigatus* strains. Despite the presence of resistant strains in 60% of surveyed homes, WGS analysis showed no direct genetic links between clinical and environmental isolates, suggesting that patients may acquire resistant strains from multiple sources. A comparison with hospital environments revealed a significantly higher prevalence of resistance in clinical settings, likely reflecting the extensive use of azole antifungals in healthcare. These findings emphasize the role of residential environments as potential reservoirs for resistant *A. fumigatus* and highlight the utility of citizen science in environmental surveillance.

6.2 Introduction

First documented in the 19th century, fungal contamination in residential environments was described as a “terrible calamity,” highlighting issues such as “wetness in walls,” “constant dampness” and mouldiness affecting furniture,” and the widespread presence of “white, green, and grey moulds found on woodwork and plaster” (508). The adverse building conditions led to concerns about the impact of indoor mould exposure on the development of diphtheria and residents well-being. The awareness of mould-related health risks has significantly evolved since the 19th century, driven by

advancements in housing construction, improved ventilation, and increased scientific understanding of indoor air quality. However, contemporary cases such as the tragic death of a two-year-old boy from prolonged exposure to *Stachybotrys spp.*, commonly known as "black mould" and associated with "sick house syndrome", has brought the issue of indoor air quality to the forefront of public attention.

In modern society, where individuals spend 70% to 90% of their time indoors, exposure to airborne fungi can have considerable adverse health effects, including allergies, infection and inflammation (509–511). Individuals with pre-existing respiratory conditions such as asthma or COPD are particularly vulnerable. Chronic inhalation of fungal spores can exacerbate symptoms, leading to increased respiratory distress and the development of fungal infections. Fungi are abundant in both indoor and outdoor environments, but under optimal conditions, such as temperature and humidity they can proliferate excessively (512,513). Factors such as building characteristics, occupant behaviours, air conditioning systems, and aerosolization of microorganisms from carpets, as well as outdoor fungal spore concentrations, significantly influence indoor fungal communities (514,515). Common indoor fungi include *Aspergillus spp.*, *Penicillum spp.*, *Cladosporium spp.*, and *Stachybotrys spp.* (516–518), which frequently colonise materials when conditions are favourable. Species of the genus *Clodosporium*, *Penicillium*, *Stachybotrys* and *Trichoderma* are particularly prevalent on all wood materials (519), while *Aspergillus* have a propensity to colonise ceiling tiles, concrete (520,521), and woodchip and modified wood products (519). In damp and water-damaged environments, which are especially prone to fungal growth, *A. fumigatus* is commonly found on substrates such wallpaper and paint, which support colonisation until subsequent aerosolization (522). It has also been detected in a wide variety of everyday food products, including baked goods, tea, biscuits, spices, cereals, beans, nuts, fruits, and dairy items, easily entering households through a variety of commonly consumed foods (205,206,523). Routine activities such as potting plants and household chores like vacuuming and dusting, can stir up and spread *A. fumigatus* spores into the air (197,214), making exposure to *A. fumigatus* a common aspect of everyday life. While regular cleaning and disinfecting can reduce fungal contamination, the extensive use of azole-containing products, such as household cleaners, paints, and sealants, as biocides can inadvertently contribute to the development of azole-resistant *A. fumigatus*.

A study by Paluch *et al.,* (524) identified high concentrations of *A. fumigatus*, including azole-resistant strains carrying the TR_{34}/L98H resistance allele, in the home of a CF patient. Similarly, Lavergne *et al*., (525) reported a fatal case of invasive aspergillosis caused by an isolate with the TR_{46}/Y121F/T289A resistance mechanism, with the patient's home and surrounding outdoor environment identified as the likely source of infection. These findings underscore the potential for domestic settings to serve as reservoirs for azole-resistant *A. fumigatus.* Furthermore, recent evidence suggests that patients infected with *A. fumigatus* may release spores into their surroundings through coughing or exhalation (289). Spores can settle on surfaces, remain airborne, or enter the soil within the home, creating a potential cycle of environmental contamination and re-exposure.

Azole resistance in *A. fumigatus* has been well-documented in UK clinical and environmental settings, yet data within residential environments remains scarce, complicating the identification of primary reservoirs and transmission routes. This knowledge gap is particularly concerning for individuals with chronic respiratory conditions, who exhibit a high prevalence of azole resistance (~13%) (301). However, mycological surveillance in residential settings poses significant logistical and ethical challenges, including coordinating access, ensuring consistent sampling, and addressing privacy concerns. To address these limitations, a citizen science approach was employed, building on large-scale studies where participants across the UK collected environmental samples (277,359). By adopting these established protocols, mycological surveillance was conducted to assess the burden of azole resistance in households of patients with chronic respiratory diseases. High-resolution WGS analysis enabled the differentiation between clinical and environmental strains, providing key insights into resistance acquisition routes.

6.3 Methods

6.3.1 Participant selection for home surveillance

A citizen science-based approach was employed to assess culturable *A. fumigatus* levels in the homes of participants from the MRC FREAL respiratory disease cohort (section 2.2) and to investigate potential environmental transmission routes of azole resistance. Participants were selected based on the number of *A. fumigatus* isolates identified during the prior clinical surveillance study, prioritising those with three or more culture-positive sputum samples to increase the likelihood of detecting genetically related isolates. Two participants with consecutive culture-negative samples were selected to assess the burden of *A. fumigatus* for comparative analysis. At-home surveillance kits were distributed to 13 participants diagnosed with the following respiratory disorders: CF (n = 1), CPA (n = 7), ABPA (n = 4), and bronchiectasis (n = 1). Participants were contacted *via* phone or email prior to the study to explain its purpose and determine their interest in participating. Participants homes were located in both rural and urban areas, including London, Surrey, Hertfordshire, Sussex, Dorset, and Wales.

6.3.2 Fine scale home surveillance: Case 34

To compare azole resistance exposure between the hospital and home environments, a detailed surveillance study was conducted in which Case 34 agreed to participate. This study employed a fine-scale surveillance strategy, ensuring that the sampling techniques and procedures used in the hospital setting (sections 5.3.4 – 5.3.5) were replicated in the home environment to maintain methodological uniformity.

6.3.3 Remote environmental surveillance

Surveillance kits included materials for collecting indoor air, soil, dust, and swab samples, along with prepaid return packaging and a detailed instruction leaflet (Appendix 13). The leaflet provided step-by-step guidance on sample collection, packaging, and mailing to Imperial College

London laboratories. Pre-labelled materials ensured traceability, with participants recording sample locations. Kits were sent every three months to capture seasonal variation. Samples collected between January to February were classified as winter, from April to May as spring, from June to July as summer, and from October to November as autumn. Returned samples were processed immediately or stored at 4°C until processing

6.3.4 Sample Collection

Air Surveillance

Recognising that microbial recovery can be partially lost during extraction (526), it is often recommended to use multiple sampling techniques (527). To maximize *A. fumigatus* recovery, participants were provided with two types of passive air samplers, both previously validated for capturing airborne *A. fumigatus* (359,528,529). The samplers included a MicroAmp™ clear adhesive film (Thermo Fisher Scientific, UK) and an electrostatic dust collector (EDC) (Liefheit, UK), sterilised by autoclaving in aluminium foil at 121°C for 15 minutes prior to distribution. Each sampling kit contained two of each sampler, which participants were instructed to place in separate locations within their homes at approximately 1.2 meters in height to simulate breathing zone exposure. The adhesive side of the film and the EDC were exposed to the indoor air environment for 14 days to allow for particulate matter to settle. After the sampling period, participants re-covered the adhesive film, placed the EDC in a sterile zip-lock bag, and returned the samplers using the prepaid packaging provided in the kit.

Soil Surveillance

Surface soil samples were collected into sterile 50 ml Falcon tubes from indoor potted plants or outdoor soil beds. The Falcon tubes were placed in zip-lock bags to prevent cross-sample contamination during transit. All sampling kits included disposable FFP2 NR face masks (Medisave, UK) to protect against spore inhalation and latex-free disposable gloves for use during soil collection.

Settled dust surveillance

To adequately reflect the level of microbial contamination in indoor environments, settled dust was collected from floors or carpets using a vacuum cleaner. Participants were instructed to secure the EDC to the end of the vacuum nozzle with an elastic band and vacuum a section of the floor for up to 5 minutes. Afterward, the EDC was removed and placed into a sterile zip-lock bag. Participants were also given the option to collect dust from surfaces by gently sweeping the EDC across a surface before placing in a sterile zip lock bag.

Surface swabs

Surface swab samples were collected by swabbing indoor sites prone to moisture and mould accumulation, such as washing machine seals, bathroom sills, and kitchen sills. Participants were instructed to locate problematic areas and gently swab the areas using the sterile environmental collection swabs provided (Steriswab™, Medical Wire, UK).

6.3.5 Fungal cultivation

Viable *Aspergillus* conidia bioburden was analysed using culture-based methods. Rose Bengal media supplemented with chloramphenicol (Millipore, Merck) was employed to enhance the sensitivity of *A. fumigatus* cultures and suppress the growth of rapidly spreading species such as Mucor, which can otherwise outcompete *A. fumigatus.*

6.3.6 Sample Processing

MicroAmp™ adhesive air samplers

A. fumigatus colonies were isolated from MicroAmp™ (Applied Biosystems™, UK) adhesive air samplers following previously described protocols (359). Briefly, the adhesive side of the MicroAmp™ film was pressed directly onto the culture media in 120 mm square petri dishes and incubated at 45°C for 24 hours to select for *A. fumigatus* growth. After the initial 24-hour period, the MicroAmp™ film was removed from the agar and discarded, and the plates were incubated for an additional 48 hours.

Colonies were identified based on macroscopic characteristics and isolated as per section 2.4.3 and 2.5.1.

EDC air and dust samples

All EDC samples were washed in 50 ml of 0.85% NaCl with 0.05% Tween-80 by orbital shaking at 250 rpm for 60 minutes at room temperature. The suspension was then centrifuged to pellet the debris and concentrate the cells. The supernatant was removed, and the pellet resuspended. Aliquots of 150 µl were inoculated on to 90 mm culture plates in triplicate and distributed with an L-shaped spreader. Culture plates were left to dry in the safety cabinet before incubation at 45°C for 2-3 days. Colonies were identified based on macroscopic characteristics and isolated as per section 2.4.3 and 2.5.1.

Surface swabs

Surface swab samples were washed with 1ml of 0.85% NaCl with 0.05% Tween®-80 by vortex mixing for 1 minute. Aliquots of 200 µl were inoculated on to 90 mm culture plates in triplicate and distributed with an L-shaped spreader. Culture plates were left to dry in the safety cabinet before incubation at 45°C for 2-3 days. Colonies were identified based on macroscopic characteristics and isolated as per section 2.4.3 and 2.5.1.

Soil samples

To isolate *A. fumigatus*, 2 g of soil was suspended in 8 ml of sterile suspension buffer containing 0.85% NaCl plus 0.5% Tween®-20 (ThermoFisher Scientific) as previously described (495). From this suspension, 200 µl of supernatant was aliquoted on to 90 mm culture plates in triplicate and distributed with an L-shaped spreader. Plates were left to dry in the hood. The plates were incubated at 45°C and checked daily for *A. fumigatus* colony growth. Colonies were identified based on macroscopic characteristics and isolated as per section 2.4.3 and 2.5.1.

6.3.7 Spatiotemporal distribution of *A. fumigatus* CFUs

Colony counts were recorded per sample to assess the spatiotemporal distribution of *A. fumigatus* within the participants home environment.

6.3.8 Isolation of *A. fumigatus* colonies

Up to 5 colonies per morphology were sub-cultured onto SDA plates using the 3-spot method as detailed in section 2.4.3. Sub-cultures were cryopreserved at -80°C according to section 2.4.5.

6.3.9 Antifungal susceptibility testing

All *A. fumigatus* isolates (*n* = 438) were screened for susceptibility to three clinically relevant azoles using VIPCheck™ plates (Mediaproducts BV, Netherlands), and to the agricultural azole tebuconazole as described in section 2.8. Conidia were harvested either directly from primary subcultures or from secondary subcultures derived from glycerol stocks as described in section 2.5.3.

6.3.10 gDNA extraction and quantification

Isolates from the home environment were systematically chosen to represent the spatiotemporal distribution of both azole-resistant and azole susceptible strains. Isolates were cultured from glycerol stocks at 45°C for 2-5 days as described in section 2.5.3. Genomic DNA was extracted and quantified as described in sections 2.9.2 and 2.9.4 respectively.

6.3.11 Next Generation sequencing & Bioinformatic Analysis

Genomic DNA underwent WGS as described in section 2.10.1. Whole genome sequence alignments were processed as per section 2.10.3 – 2.10.4. Genotypic characterisation was performed as per section 2.10.6.

6.3.12 Phylogenomic analysis

Phylogenetic trees were inferred from WGS from the home environment using RAxML-NG (370) as described in section 2.12. Additional bootstrap replicates (n = 350) were concatenated with the inferred trees until convergence was achieved. Phylogenetic trees were visualised in R version 4.3.1 using the ggTree (371) and ggTreeExtra (372) packages and uploaded as an interactive Microreact project (Appendix 2).

6.3.13 Calculating pairwise SNPs

To explore genomic diversity within home environments and identify closely related *A. fumigatus* strains, pairwise unique SNPs were calculated between VCF files as described in section 2.13. Pairwise unique SNPs were visualised as a histogram in R version 4.3.1 to illustrate genetic variation within the population.

6.3.14 Incorporation of RBH clinical WGS

To explore potential transmission routes, 110 clinical genomes obtained from the RBH prospective surveillance of home participants (section 4.3.2) were integrated into the home environment dataset.

6.3.15 Multivariate analysis of genomic data

Multivariate genomic analysis was conducted in R version 4.3.1 using the adegenet package version 2.1.10 following established protocols (373–376) as per section 2.14.

6.3.16 Statistical Analysis

Spearman's rank correlation was applied to assess the relationship between *A. fumigatus* CFU counts in the home environment and sputum samples, using a non-parametric approach to account for non-normal data distribution. Analyses were performed using R version 4.3.1, with statistical significance defined as $p < 0.05$.

6.5 Results

6.5.1 Patient participation and sample collection

Between May 2020 and October 2023, 48 home surveillance kits were distributed to 13 participants. Of these, 19 kits were returned for processing by 10 patients, resulting in a 40% sample return rate. Among the participants, only 2 returned a sample kit for each sampling round. During the course of the surveillance study, 1 participant was undergoing regular inpatient visits to the RBH and consequently verbally opted out and unfortunately, 3 participants passed away.

6.5.2 Spatial distribution of CFUs

The distribution of *A. fumigatus* CFUs was assessed across environmental sources from each home. In total, 6,309 CFUs were cultured from 506 environmental samples, with soils exhibiting the highest *A. fumigatus* bioburden with an average of 49 CFUs/g (Figure 6.1) and median of 12 CFUs/g. After soils, floor and dust samples collected using EDCs averaged up to 5 CFUs per sample, with a median CFU counts of 0. Swab and air samples, collected using MicroAmp™ adhesive film and EDCs, had the lowest counts, averaging less than 1 CFU per sample. The bioburden of *A. fumigatus* varied across homes (Figure 6.2). Case 42 had the highest average CFU count, largely driven by soil samples exceeding an average of 130 CFUs, followed by Case 33, where soil averaged over 90 CFUs. Cases 37, 38, and 32 had progressively lower averages, with soil remaining the predominant source. In contrast, the lowest CFU counts were observed in Cases 35, 36, and 31, similar to Cases 60 and 61. A Spearman's correlation test was conducted to evaluate the relationship between *A. fumigatus* bioburden in the home environment and CFU counts in sputum samples. A weak positive correlation (rho = 0.267) between home bioburden and sputum CFUs was noted, but this was not statistically significant ($p = 0.455$).

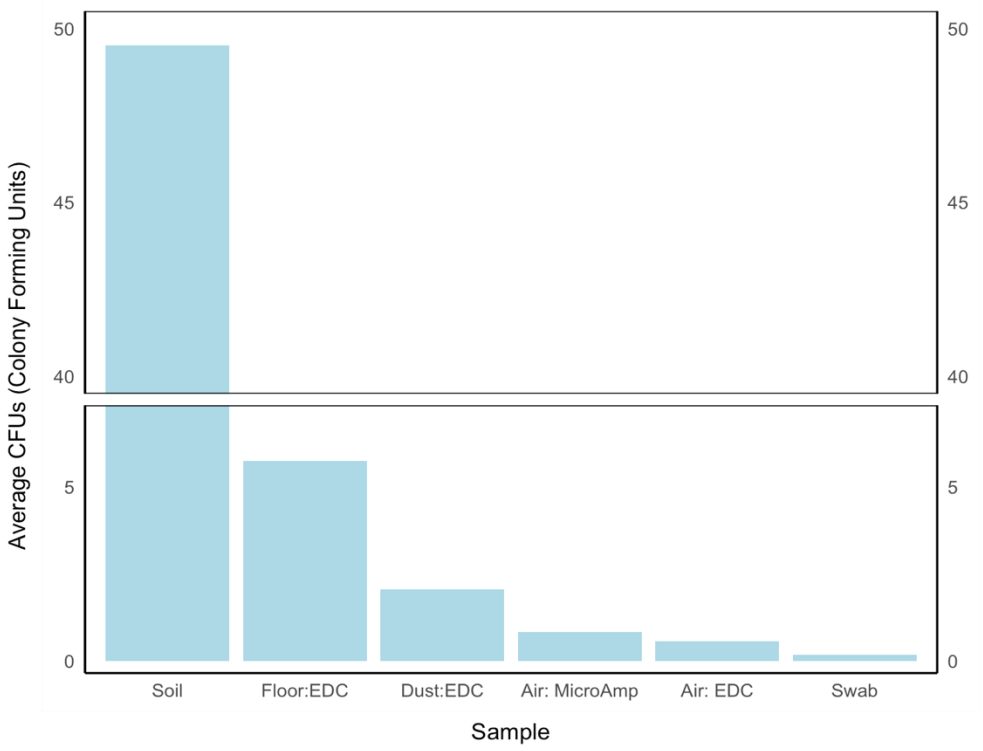


Figure 6.1. **Average CFU counts from samples collected in participant homes**

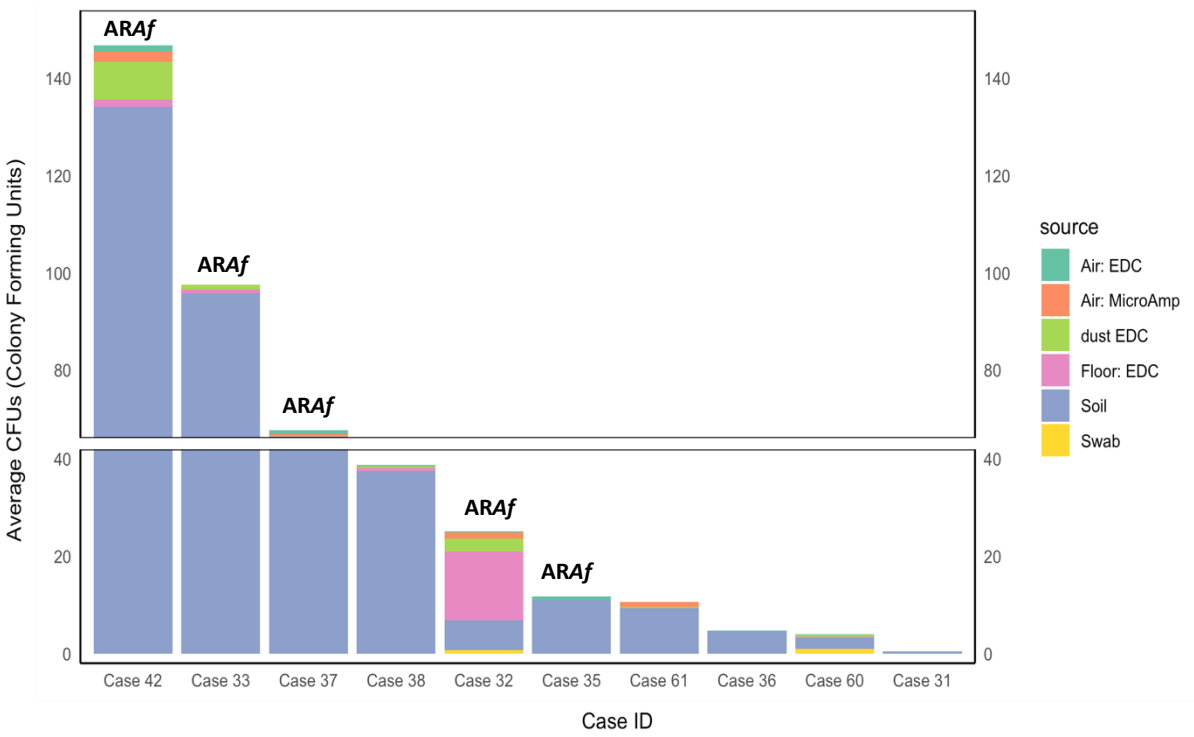


Figure 6.2. **Average CFU counts across participating home environments**

In total 438 *A. fumigatus* isolates were collected from air (*n* = 55) soil (*n* = 291), swabs (*n* = 4) and floor and surface dust (*n* = 89) samples from the home environment. Tebuconazole resistance (6 mg/L) was confirmed in 3.8% (*n* = 17) isolates across 6 homes. Of the 17 tebuconazole resistant isolates, 70.5% (*n* = 12) were sourced from soil samples from 3 participant homes, 17.6% (*n* = 3) originated from air samples from 1 home and 11.7% (*n* = 2) were sourced from dust samples from 1 home. Cross resistance to at least one of the clinical azoles (itraconazole, voriconazole and posaconazole) was observed in 76.5% (*n* = 13) of the tebuconazole resistant isolates.

6.5.4 Comparison of azole resistance in environmental *A. fumigatus* isolates from participants homes and the hospital

A total of 8 air and 8 soil samples were collected from the home of Case 34, all of which were culture-positive for *A. fumigatus*, yielding 76 viable *A. fumigatus* colonies. Air samples had a median concentration of 8.5 CFUs/m^3, notably higher than the median of 2 CFUs/m^3 observed in the hospital environment. Soil samples from the home yielded a median of 3 CFUs/g, comparable to the counts observed in the hospital soil samples (2 CFUs/g). All 76 isolates underwent azole susceptibility testing, revealing a resistance rate of 1.3% (*n* = 1), in contrast to a 7.2% resistance rate (26/337) observed in isolates from the hospital environment. A direct comparison between isolates from the home of Case 34 and the hospital was performed, with sampling standardized by the number of sampling dates to account for the longitudinal nature of hospital surveillance. Given the detection of only a single resistant isolate in the home, a Fisher's exact test was conducted, showing no significant difference in resistance rates between the two environments ($p > 0.05$) (Figure 6a). Nonetheless, the estimated odds ratio of 0.173 (95% CI: 0.004–1.089) indicates a possible trend toward lower resistance in the home, although this trend was not statistically supported. However, when all isolates from home environments were considered, statistical analysis using a Chi-square test revealed a significantly higher prevalence of azole resistance in hospital derived isolates compared to those from home environments ($p < 0.05$) (Figure 6b).

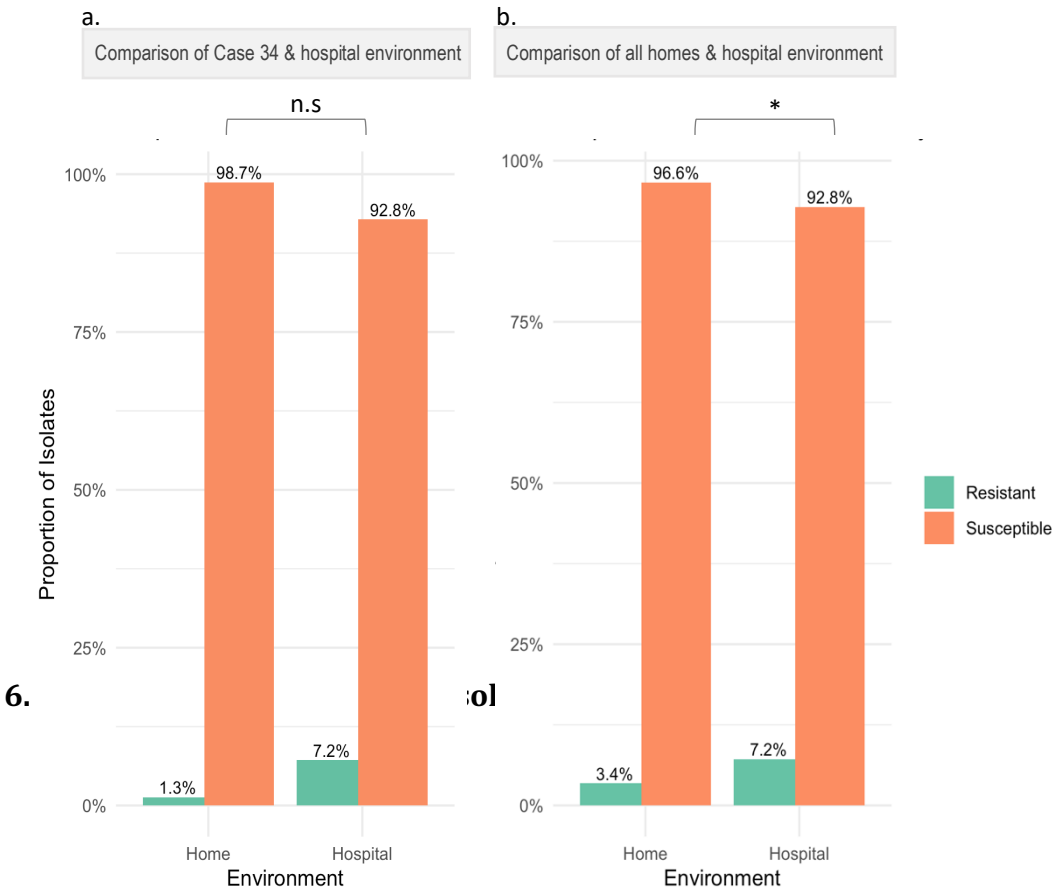


Figure 2.3 **Comparison of azole resistance prevalence of hospital and home environments.** No significant difference was observed in resistance rates between the hospital and home environment of Case 34 (a), However, when all home environments were considered collectively, a significant difference emerged between the homes and the hospital (b)

The sequencing panel included 101 isolates collected from the homes of 9 individuals (Appendix 14). The number of isolates sequenced per household ranged from 1 – 22. Isolates originated from air (*n* = 23), dust (*n* = 16), and soil (*n* = 62). In total, 15 tebuconazole resistant (6 mg/L) isolates were included from 6 homes, of which 9 also exhibited resistance to at least one of the 3 clinical azoles. Alignments of the sequenced genomes are summarised in Appendix 5.

6.5.6 Genotypic Characterisation

Isolates were genotypically characterised to determine the frequency and distribution of azole resistant associated *cyp51a* genotypes in the home environment. All wildtypes were azole susceptible with the exception of one isolate from an air sample which exhibited resistance to tebuconazole (6 mg/L), suggesting a non-*cyp51a* associated resistance mechanism. Among the M172V/F46Y

polymorphisms, 5/21 isolates showed resistance to tebuconazole (6 mg/L), with one also resistant to posaconazole. Additional nonsynonymous *cyp51a* polymorphisms, including D262Y (*n* = 1) and I242V (*n* = 2), were detected in air and soil samples, respectively, with all isolates susceptible to azoles. A novel combination of nonsynonymous SNPs (G448S/Y121F/T289A/I364V/S363P) was identified in outdoor soil and compost bin samples from Case 42, collected in January and October 2023. An isolate from an outdoor soil sample provided by Case 35 exhibited tebuconazole resistance (16 mg/L) and carried the Y121F/T289A polymorphism but lacked the associated TR_{46} tandem repeat. A TR_{34}/L98H isolate was recovered from an air sample from Case 35, displaying resistance to tebuconazole (16 mg/L) and three clinical azoles: itraconazole (4 mg/L), voriconazole (2 mg/L), and posaconazole (0.5 mg/L). Another isolate from Case 35, obtained from an indoor soil sample, carried the L98H mutation without TR_{34}. The L98H polymorphism, in the absence of TR_{34}, was further detected in two other instances: from an air sample provided by Case 32 in July 2023, and a dust sample from Case 34 in January 2023. All three L98H isolates, lacking TR_{34}, exhibited resistance to tebuconazole (6 mg/L), itraconazole (4 mg/L), and posaconazole (0.5 mg/L).

6.5.7 Genetic diversity and population structure of *A. fumigatus* across home environments

A. fumigatus isolates from the home environment demonstrated a median pairwise divergence of 52,207 SNPs (Figure 6.4a). DAPC analysis showed minimal genetic differentiation among isolates, regardless of their environmental source (Figure 6.4b). To further explore the spatiotemporal distribution of genetically similar isolates, pairs sharing less than 3% of the observed genetic diversity (<1,453 SNPs) were identified (Table 6.2). Of the 18 pairs, 7 originated from the same home environment while 11 originated from different homes highlighting the cosmopolitan distribution of *A. fumigatus.* This was further demonstrated by phylogenomic and DAPC analysis. Phylogenetic analysis demonstrated median bootstrap support of 98% (Appendix 5), and revealed significant genetic diversity, with isolates from individual homes distributed across multiple branches (Figure 6.5). Cluster 3 (C3) contained azole-resistant isolates, including those with *cyp51a* polymorphisms, such as G448S/Y121F/T289A/I364V/S363P, found in soil and compost bin samples from the home of

Case 42, along with the TR_{34}/L98H allele recovered from an air sample. Additionally, three L98H point mutations were identified in isolates from dust, air, and soil samples from different homes (Case 32, Case 34, and Case 35), all within C3 and demonstrating resistance to itraconazole (4mg/L). In contrast, azole-susceptible wild-type isolates were primarily grouped in Cluster 2 (C2), which also included an azole susceptible isolate with the I242V variant. Cluster 1 (C1) mostly comprised azole-susceptible isolates with M172V/F46Y variants, except for one tebuconazole and posaconazole resistant isolate from a soil sample from the home of Case 42.

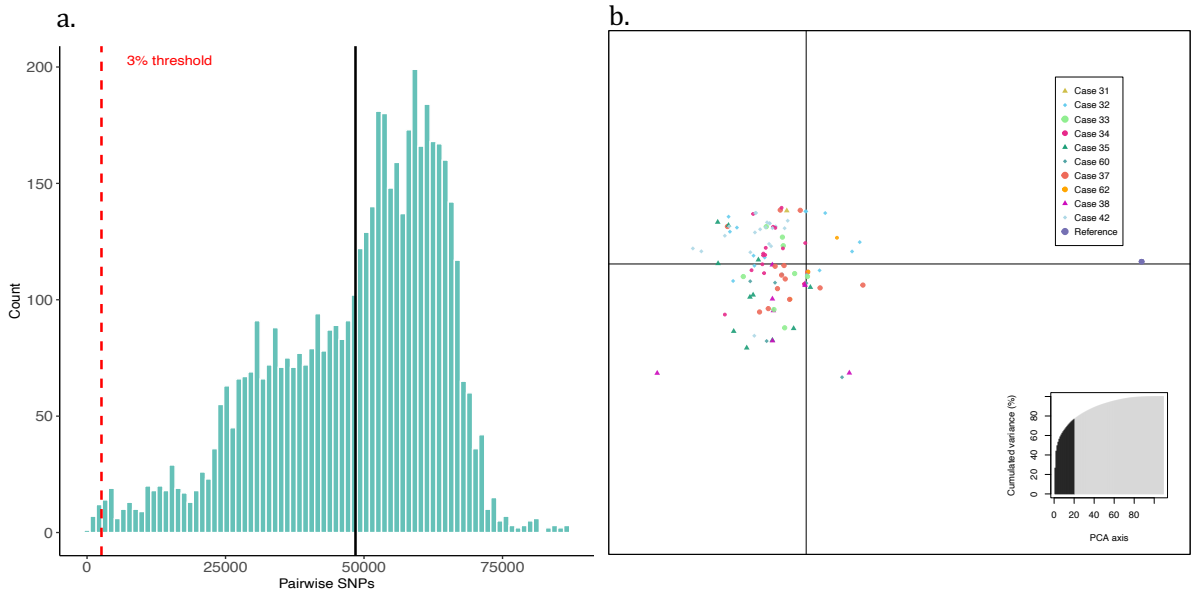


Figure 6.4 **Population diversity of *A. fumigatus* from the home environments of individuals with chronic respiratory diseases.** Histogram of pairwise SNPs among isolates, with a 3% genomic diversity threshold (a). DAPC based on SNP variants from home environmental samples (b). Samples collected from air, soil and dust of participant homes. Coloured points represent the homes of each Case ID. The AF292 refence samples (n = 10) are shown as purple points. The inset shows the cumulative variance explained by the principal component axes, indicating the proportion of total variance captured by the analysis. The separation of clusters demonstrates the genetic diversity between different environmental samples within the hospital.

Table 6.1 Summary of genetically similar isolate pairs from home environments sharing <3% of the observed genetic diversity.

Isolate Pair 1						Isolate pair 2				
Threshold (%)	Isolate	Case ID	Source	*cyp51a* allele	Date	Isolate	Case ID	Source	*cyp51a* allele	Date
3%	FH057	Case 37	Soil	M172V/F46Y	May 2022	FH055	Case 61	Air	M172V/F46Y	May 2022
	FH030	Case 33	Soil	M172V/F46Y	May 2023	FH022	Case 32	Soil	M172V/F46Y	May 2022
	FH082	Case 38	Soil	I242V	May 2022	FH062	Case 35	Soil	I242V	Feb. 2023
	FH020	Case 32	dust	wildtype	May 2022	FH016	Case 32	dust	wildtype	May 2022
	FH067	Case 42	Soil	G448S/Y121F/ T289A/I364V/S363P	Jan. 23	FH037	Case 42	Soil	G448S/Y121F/ T289A/I364V/S363P	Jan. 23
	FH025	Case 38	Soil	M172V/F46Y	May 2022	FH050	Case 34	Soil	M172V/F46Y	Jul. 2023
	FH102	Case 42	Dust	wildtype	Oct. 2023	FH094	Case 33	Dust	wildtype	Nov. 23
	FH002	Case 42	Dust	wildtype	Jan. 2023	FH006	Case 42	Air	wildtype	Jan. 2023
	FH093	Case 42	Soil	M172V/F46Y	Jan. 2023	FH052	Case 42	Soil	M172V/F46Y	Jan. 2023
	FH087	Case 42	Air	wildtype	Jan. 2023	FH006	Case 42	Air	wildtype	Jan. 2023
	FH002	Case 42	Dust	wildtype	Jan. 2023	FH087	Case 42	Air	wildtype	Jan. 2023
	FH070	Case 42	Soil	G448S/Y121F/ T289A/I364V/S363P	Oct. 2023	FH100	Case 42	Soil	G448S/Y121F/ T289A/I364V/S363P	Oct. 2023
	FH015	Case 32	Soil	wildtype	May 2022	FH075	Case 37	Soil	wildtype	Jan. 2023
	FH064	Case 34	Air	wildtype	Jul. 2023	FH087	Case 42	Air	wildtype	Jan. 2023
	FH030	Case 33	Soil	M172V/F46Y	May 2023	FH050	Case 34	Soil	M172V/F46Y	Jul. 2023
	FH025	Case 38	Soil	M172V/F46Y	May 2022	FH030	Case 33	Soil	M172V/F46Y	May 2023
	FH050	Case 34	Soil	M172V/F46Y	Jul. 2023	FH022	Case 32	Soil	M172V/F46Y	May 2022
	FH066	Case 37	Dust	M172V/F46Y	Jan. 2023	FH050	Case 34	Soil	M172V/F46Y	Jul. 2023

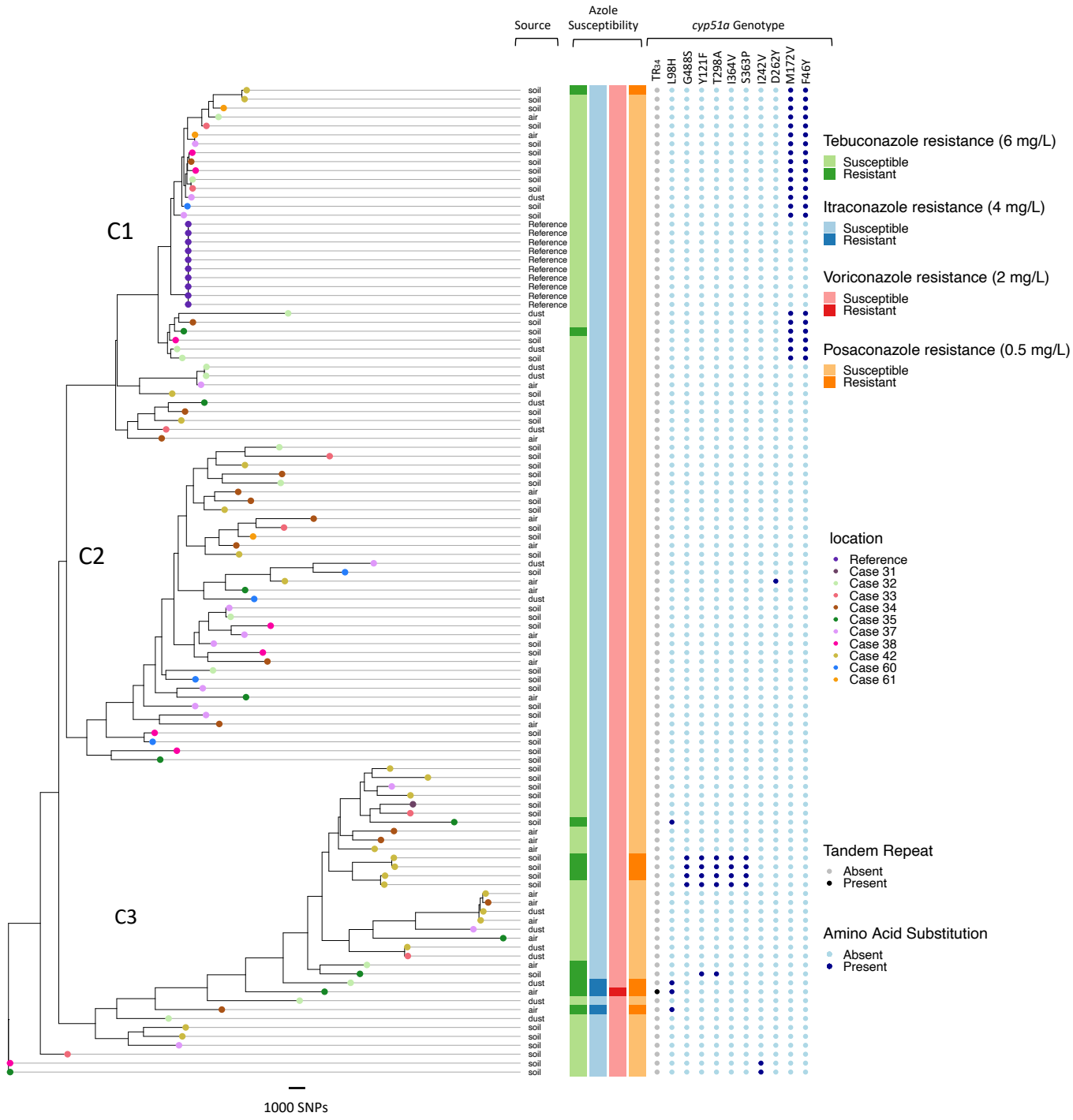


Figure 6.5. **Phylogenetic tree illustrating the evolutionary relationships of environmental *A. fumigatus* isolates from participants home environments.** Coloured circles on the branches represent the participant homes (Case ID). Adjacent to the tree the sample ID. The heatmaps indicate susceptibility profiles for tebuconazole and the clinical azoles, with darker colours representing resistance. *Cyp51a* polymorphisms are indicated by grey (TR_s) and blue points (amino acid substitutions).

6.5.8 No epidemiological links between home and clinical isolates

Clinical WGS data from the prospective surveillance cohort were included to assess potential transmission pathways between patients and their home environments, resulting in a dataset of 211 WGS from both patients and their residential environments. Phylogenetic analysis, supported by median bootstrap support of 98% across all branches (Appendix 5), revealed that clinical isolates clustered according to their respective patients. However, isolates from home environments showed no consistent clustering with patient-specific clinical isolates, indicating substantial genetic heterogeneity between patients' isolates and those from their home environments (Figure 6.6).

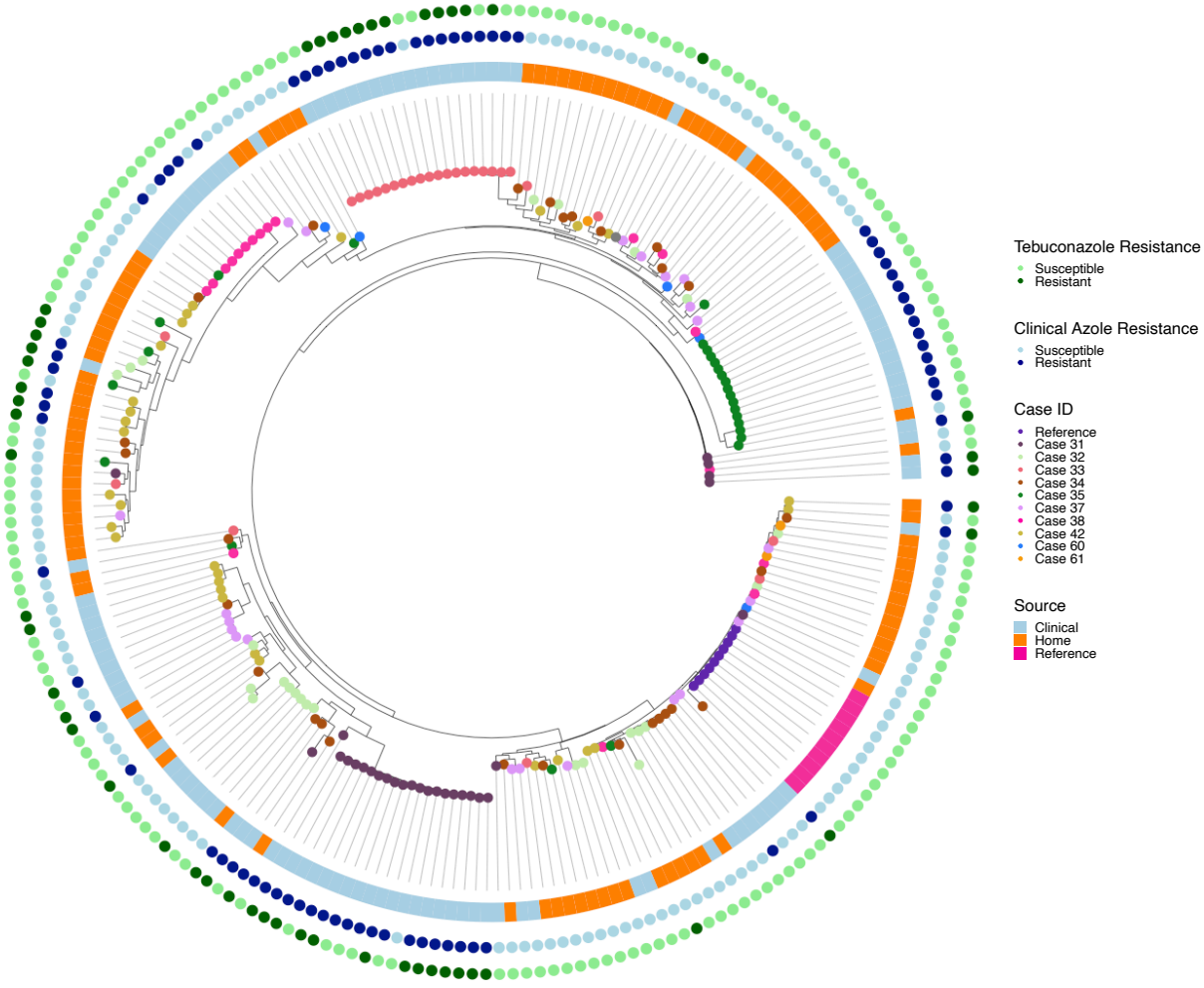


Figure 6.6 **Phylogenetic tree showing evolutionary relationships between A. fumigatus isolates from participant homes and corresponding clinical samples.** Coloured circles on the branches represent the source of the isolate (Case ID). The inner circle indicates the source, either clinical or home environment. The outer rings indicate susceptibility profiles for tebuconazole (green) and the clinical azoles (blue), with darker colours representing resistance.

6.6 Discussion

A citizen science approach was employed to characterise azole resistant *A. fumigatus* within the home environments of individuals with chronic respiratory diseases. Over a one-year sampling period, participants collected air, dust, swab, and soil samples, resulting in the isolation of azole resistant *A. fumigatus* in 60% of surveyed homes. WGS of 101 isolates identified *cyp51A* polymorphisms, including TR_{34}/L98H, unlinked L98H and Y121F/T289A, and novel combinations of *cyp51A* SNPs. Despite detecting resistant strains in homes, WGS revealed no direct genetic links between clinical and environmental isolates, highlighting the genetic diversity of *A. fumigatus* populations across different settings.

The presence of *A. fumigatus* in domestic settings highlights the widespread nature of azole-resistant strains in the environment. Of all samples collected, soil yielded the highest CFU counts and subsequently yielded 70.5% (n = 12) of the detected azole resistant isolates. The frequent detection of azole-resistant isolates in residential soil signifies a critical health risk, as these environmental reservoirs can lead to direct exposure during gardening and potting activities. As noted by Lavergne et al. (525), such exposure can have severe consequences, including fatal aspergillosis linked to resistant strains from domestic settings. Polymorphisms such as Y121F/T289A and Y121F/T289A/S363P/I364V/G448S were identified in soil samples without the TR_{46} tandem repeat, contrasting with earlier reports from plant waste in the Netherlands, where these mutations co-occurred with TR_{46} (530). Additionally, L98H without TR_{34} was detected in air and dust samples, consistent with recent reports of unlinked TR_{34} and L98H mutations in the UK (353,359). The emergence of these novel polymorphisms indicates a diversification of azole resistance mechanisms within environmental *A. fumigatus* populations, suggesting that these mutations may arise and persist independently in specific UK environments. Continuous monitoring of resistance patterns is crucial for tracking changes in resistance dynamics and understanding the evolution of azole resistance in *A. fumigatus.*

Dust samples collected using EDCs exhibited an average of up to 5 CFUs per sample, with a median of 0, while air samples using EDCs showed an average of 0.5 CFUs and a median of 0. These levels are notably lower than those reported in a French study using EDCs to assess indoor mould, where *A. fumigatus* was detected in 49% of samples, with median values ranging from 0.6 to 11 CFU (531). Differences in geographical location, ventilation, moisture levels, and cleaning practices likely explain the observed variability in CFU counts between households, as these factors significantly influence fungal growth dynamics (532). Despite the detection of *A. fumigatus* in residential environments, the low concentrations observed align with previous studies, which have reported its limited prevalence in indoor settings (533,534). The lack of a significant correlation between environmental CFU levels and respiratory colonisation (Spearman's correlation: rho = 0.267, $p > 0.05$) indicates that environmental exposure alone may not directly contribute to colonisation. This finding aligns with earlier studies that also failed to identify a direct link between the presence of *A. fumigatus* in homes and IgG levels in sputum (531). However, transient colonisation remains a complicating factor, as low-dose exposures to pathogenic *A. fumigatus* may have a greater impact than higher concentrations of non-pathogenic fungi (531,535).

Sampling was primarily conducted by individuals in stable health, which may introduce bias and limit the detection of *A. fumigatus* in households with more severe disease states. The low CFU counts observed, particularly in air and dust samples, likely reflect cooler indoor temperatures and reduced humidity, which are less favourable for fungal growth compared to warmer, more humid conditions. The limited number of isolates per household, combined with the high genetic divergence among isolates, complicates the identification of specific transmission pathways. Variability in environmental factors such as ventilation, moisture, and cleaning practices further influence CFU counts, making cross-household comparisons challenging.

While passive sampling techniques, commonly employed in large-scale studies, offer practicality, they likely influence the accuracy of spore distribution data. Adhesive films and EDCs are less effective at capturing transient airborne spore spikes compared to active methods like volumetric air sampling.

Furthermore, the reliance on culture-based methods, which exclude non-culturable or slow-growing strains and risk microbial loss during sample extraction (526), likely underestimates the genetic diversity of *A. fumigatus*. Metagenomic sequencing could offer a more comprehensive view of fungal community. Addressing these methodological factors is essential for interpreting the spatial distribution of azole-resistant *A. fumigatus* in residential environments, highlighting the importance of integrating both passive and active sampling approaches in future studies. Although WGS provides high-resolution genotypic data, the limited number of isolates per household and the inherent genetic diversity of *A. fumigatus* complicate the identification of specific transmission pathways. High pairwise divergence among isolates indicates that patients may acquire azole-resistant *A. fumigatus* from diverse sources, including those beyond their immediate environments.

A comparison between hospital and participant home environments revealed a significantly higher prevalence of azole-resistant *A. fumigatus* in hospitals (chi-square test, $p < 0.05$). This difference likely results from the extensive use of azole antifungals in clinical settings, which promotes the amplification of resistant strains. Routine application of azole-based treatments for patient care and infection control favours the persistence of resistant *A. fumigatus* populations. In contrast, home environments, with less frequent and lower levels of azole exposure, exhibit a reduced incidence of resistance. Hospitals may thus act as reservoirs for resistant strains, increasing exposure risk for immunocompromised and vulnerable individuals, which can lead to a higher likelihood of colonisation or infection by resistant *A. fumigatus*. However, no significant difference was observed between the home environment of Case 34 and the hospital, despite using the same sampling methods. However, the limited number of isolates and the small scale of home surveillance limit the ability to draw definitive conclusions. Larger studies with more extensive sampling are needed to better understand the relationship between environmental sources and transmission of resistance. For clinicians, the possibility of patients being exposed to azole resistance in their own homes should be considered when managing cases of recurrent infections or treatment failures. Integrating environmental assessments into clinical management strategies could enhance understanding of potential exposure

sources. Moreover, this study underscores the need for increased public awareness regarding fungal exposure risks in domestic settings.

Conclusions.

This study reveals that azole-resistant *A. fumigatus* is present in a substantial proportion of residential environments, particularly within soil samples. Although no direct genetic transmission between home and clinical isolates was observed, the findings highlight the role of environmental reservoirs in contributing to exposure risks. The higher prevalence of resistance observed in hospitals compared to homes emphasises the potential for healthcare settings to serve as amplification sites for resistant strains. While the limitations of passive sampling and the need for larger-scale studies are acknowledged, this study demonstrates the effectiveness of citizen science in filling critical surveillance gaps.

Chapter 7 Concluding Remarks

The overall aim of this thesis was to provide a detailed characterisation of resistance acquisition pathways, offering insights into the dynamics of azole exposure and resistance development in chronic respiratory diseases. This chapter highlights the key findings, presenting a comprehensive analysis of the genetic backgrounds contributing to azole resistance in the UK.

7.1 Genotypic and phenotypic characterisation reveals adaptive potential of the globally dominant TR_{34}/L98H azole resistance mechanism

The substantial genetic variation observed across 210 virulence genes in 155 azole resistant TR_{34}/L98H isolates, and 428 azole susceptible *cyp51a* wildtypes highlights the dynamic functional potential of azole resistant *A. fumigatus.* Genes associated with toxin production and secondary metabolism exhibited particularly high frequencies of nsSNPs in TR_{34}/L98H isolates, leading to amino acid substitutions within protein-coding regions. These mutations contribute to genetic diversity and

likely play a crucial role in adaptation. Bottery *et al.*, (536), detected the *msh6* hypermutator variant, found in 88% of TR_{34}/L98H isolates and linked to a 4-9-fold increase in mutation rates, which may explain the high genetic diversity observed here. Compromised mismatch repair systems allow unchecked replication errors, including base pair mismatches and indels, to accumulate, accelerating mutation rates. This increased evolutionary capacity promotes genetic variation, potentially offering adaptive advantages that enhance survival under environmental pressures. Non-*cyp51A* mutations in genes such as *hapE* and *hmg1* (355,419,537), along with the involvement ABC and MFS transporters (419,445,538,539), further highlights the multifaceted nature of azole resistance, which extends beyond target site mutations. While this Thesis has identified virulence genes potentially linked to enhanced adaptability, the functional impact can range from negligible to profound, with some amino acid substitutions being conservative and having minimal effect. As a result, the specific virulence potential and adaptive mechanisms of these mutations remain uncertain. Future research on genetic variations beyond *cyp51A*, including functional analyses, predictive modelling, and variant impact studies, will be essential for advancing our understanding of *A. fumigatus* resistance and pathogenicity.

The phenotypic analysis of wildtype and TR_{34}/L98H *A. fumigatus* isolates revealed significant metabolic adaptability, enabling survival across diverse environmental conditions. Wildtype isolates efficiently utilised alternative carbon sources such as N-acetyl-D-glucosamine and d-trehalose, reflecting their ability to thrive in fluctuating environments where glucose availability is limited. However, this metabolic flexibility may increase their susceptibility to cell wall-targeting antifungals. In contrast, TR_{34}/L98H isolates may prioritise alternative energy sources, reducing reliance on d-trehalose during early germination, possibly as an adaptive response to lower energy expenditure, offering a survival advantage in azole-rich environments. Additionally, TR_{34}/L98H demonstrated specific adaptations to nitrogen utilisation, aligning with catabolite repression. These shifts may enhance the ability of TR_{34}/L98H strains to exploit alternative nitrogen and carbon sources under nutrient-limiting conditions. Furthermore, TR_{34}/L98H isolates exhibited enhanced osmotic stress tolerance, which may provide TR_{34}/L98H isolates with a selective advantage, facilitating their

persistence and dissemination, particularly in the CF lung. Conversely, wildtype isolates demonstrated broader pH adaptability, suggesting their metabolic flexibility enables colonisation and persistence within various niches of the CF lung. These findings highlight the importance of metabolic adaptability in *A. fumigatus* resistance, especially in azole-resistant TR_{34}/L98H isolates. The identification of nsSNPs in virulence genes further reveals the complexity of resistance mechanisms. Addressing both metabolic flexibility and genetic resistance will be essential for developing more effective antifungal treatments.

7.2 High burden of azole resistance with dominance of TR_{34}/L98H in individuals with chronic respiratory diseases.

Prospective surveillance using remote sampling techniques revealed azole resistance in 25% of individuals within a respiratory disease cohort, with higher prevalence among those with CF and CPA. Genotypic characterisation revealed that 31.3% of patients harboured environmentally associated resistant genotypes, specifically TR_{34}/L98H and TR_{46}/Y121F/T289A. The detection of TR_{34}/L98H aligns with a previous report from a London specialist cardiothoracic centre, which identified its prevalence in approximately one-third of induvial (301). However, the identification of TR_{46}/Y121F/T289A, first reported in Manchester in 2017 (472), is new to London cohorts. The presence of TR_{46}/Y121F/T289A in 6% of UK environmental samples, including London soils (277,359,474) indicates an environmental acquisition. The emergence of voriconazole resistant TR_{46}/Y121F/T289A in UK clinical settings raises concerns regarding its potential to follow the trajectory of TR_{34}/L98H, emphasising the urgency for continued surveillance. The genetic heterogeneity and population diversity of *A. fumigatus* across respiratory disease cohorts have significant clinical and biological implications. The presence of heteroresistant subpopulations within genetically diverse infections may reduce the efficacy of standard therapies and mixed infections can lead to persistent disease despite treatment. Advanced diagnostic tools, such as WGS, combined with routine phenotypic resistance characterisation can facilitate more personalised antifungal therapies. Expanding surveillance to other respiratory disease cohorts is key to understanding genetic diversity within infections. In cases of high genetic diversity, therapeutic drug monitoring, combination

therapies, or alternative antifungals may be necessary. In contrast, reduced genetic diversity indicates infection by a genetically uniform population or single strain. Selective sweeps driven by positive selection pressures, such as antifungal drug exposure, can further homogenize the population. Although this uniformity may lead to the dominance of resistant strains, it also offers predictability in disease progression. Understanding the complexities of *A. fumigatus* infections and their impact on treatment outcomes across diverse patient populations remains an important area for future research. Longitudinal analyses provide valuable insights into the diversification of *A. fumigatus* populations over time, enhancing knowledge of the evolutionary processes that drive infection persistence and antifungal resistance.

7.3 Healthcare settings can act as environmental reservoirs for azole resistant *A. fumigatus*, increasing the risk of patient exposure and infection

Azole resistant *A. fumigatus* in healthcare environments poses significant risks to vulnerable populations, including individuals with chronic respiratory diseases. This Thesis provides a comprehensive epidemiological assessment of *A. fumigatus* in a high-exposure healthcare setting, emphasising the significant risk posed by azole resistant strains, particularly TR_{34}/L98H, to vulnerable patient populations. The identification of MTR genotypes, such as TR_{34}/L98H, in both air and soil samples highlights the widespread contamination in key hospital areas, including outpatient departments and the hospital reception, which raises concerns about the persistence of resistant *A. fumigatus* in environments where vulnerable cohorts are frequently exposed. The role of compost and other external sources in introducing resistant strains into healthcare settings suggests the need for greater consideration of external inputs into hospital environments. These findings align with global reports of environmental acquisition and patient infections, (254,286,483,484), reinforcing the significance of hospital environments in the persistence and spread of azole-resistant strains.

By integrating WGS with environmental and clinical surveillance, this study revealed high-resolution epidemiological links between clinical and environmental *A. fumigatus* isolates, confirming the role of hospital environments as reservoirs for resistant strains. The observed genetic similarity between

these isolates indicates bidirectional transmission, where patients may acquire resistant strains from the hospital environment and simultaneously contribute to its contamination by dispersing resistant conidia through respiratory activities such as coughing (289). This likely facilitates the persistence and dissemination of azole resistant strains within hospital air and soil. Expanding to multi-centre surveillance, combined with real-time WGS, would offer valuable insights into regional resistance patterns and improve transmission tracking. Future efforts should integrate environmental, clinical, and genomic data to guide targeted antifungal interventions and reduce patient exposure to resistant strains. Ultimately, addressing the emerging threat of azole-resistant *A. fumigatus* will require coordinated strategies, integrating advanced genomic tools with routine infection control. By mitigating environmental contamination and refining antifungal stewardship, healthcare systems can better protect at-risk patient populations and reduce the burden of invasive fungal infections in clinical settings.

7.4 Azole-resistant *A. fumigatus* persists at low levels in homes but is more prevalent in hospitals, reflecting different resistance dynamics across environments.

The detection of azole-resistant *A. fumigatus* in 60% of surveyed homes indicates its growing entrenchment within our built environments, potentially heightening exposure risks for vulnerable individuals. Despite its presence, the spore abundance remains low, air samples consistently show median CFUs of 0, aligning with earlier findings where the *A. fumigatus* bioburden is typically lower than that of other sporulating fungi, such as *Penicillium* and *Cladosporium*. This raises certain ecological questions: Why do homes harbour lower *A. fumigatus* concentrations despite its widespread distribution? How does spore presence interact with host immune responses to drive colonization or clearance of fungal strains? Are there broader synergistic interactions with other fungal species that influence its persistence? What are the clinical implications of these dynamics? The transient nature of *A. fumigatus* colonisation adds complexity to exposure dynamics, as even minimal exposure to pathogenic strains can significantly affect host-pathogen interactions compared to higher concentrations of non-pathogenic fungi. The capacity of *A. fumigatus* to adapt and persist under low-abundance conditions suggests that sporadic inhalation of resistant spores could still result in

colonisation events. This risk is particularly acute for immunocompromised individuals, where even low-level exposure can lead to severe, life-threatening infections.

Phylogenomic analyses revealed high-resolution genetic similarity between clinical and hospital environment isolates, supported by strong bootstrap values (>70%), suggesting potential transmission pathways between patients and hospital environments. The absence of epidemiological links between patient isolates and their home environments further supports the hypothesis that patients may both acquire and transmit resistant strains within hospital settings, facilitating cross-exposure among vulnerable populations. Moreover, the higher prevalence of resistance observed in high-exposure hospital settings compared to residential environments indicates that hospitals may act as reservoirs of resistance, posing a significant public health challenge. The potential for persistent patient-to-environment transmission of resistant strains, capable of thriving through compensatory evolution, suggests that hospitals may act as reservoirs of drug resistance. This environment, shaped by increased azole use and recurrent transmission, could foster the recombination and persistence of highly adapted strains. The global rise of resistant variants like TR_{34}/L98H, which may possess heightened pathogenicity and virulence, exacerbates this threat, amplifying exposure risks for those most vulnerable. These dynamics underscore the urgency for targeted environmental surveillance to detect and characterise low-level spore presence and to elucidate mechanisms driving transient colonisation in both clinical and residential settings. Advanced surveillance techniques, integrating spatial and temporal population dynamics, are crucial for identifying the threshold levels that initiate colonisation, guiding effective management strategies for azole-resistant *A. fumigatus* in high-risk populations.

7.5 Future directions

The global emergence of azole resistant *A. fumigatus* has emphasised the role of environmental selection pressures, particularly through the use of environmental azole fungicides in agriculture, in driving clinically significant resistance. This context is especially relevant as new antifungal agents, such as olorofim, are introduced into clinical practice. Olorofim targets dihydroorotate dehydrogenase

(DHODH), a key enzyme in the pyrimidine synthesis pathway, which prevents conidial germination and induces morphological changes leading to cell lysis pathway (540–543). Currently in phase III clinical trials for invasive aspergillosis, olorofim has shown efficacy against azole-resistant strains, representing the first new antifungal mechanism in over 20 years and offering a promising option for combating drug-resistant fungal infections (544). Despite its therapeutic potential, concerns about the long-term efficacy of olorofim have emerged following the approval of ipfluenoquin by the US Environmental Protection Agency (EPA) for agricultural use (545), a fungicide that also targets DHODH. The use of ipflufenoquin, under review in other regions, risks selecting DHODH-resistant *A. fumigatus* strains, potentially compromising olorofim efficacy and paralleling *cyp51a*-mediated azole resistance linked to agricultural fungicide use (546). Additionally, interactions between the ergosterol and pyrimidine biosynthesis pathways, highlighted in a recent study (541) suggest potential complications in combining azoles with olorofim. Azoles may upregulate pyrimidine biosynthesis, potentially counteracting the inhibitory effects of olorofim on DHODH. Therefore, precise dosing in combination therapy, particularly for TR_{34}/L98H strains, is critical to preserve therapeutic efficacy. As olorofim nears clinical deployment, applying insights gained from the challenges of managing azole resistance can ensure the sustained efficacy of this novel antifungal. To avoid similar pitfalls, a proactive approach is needed, emphasising early implementation of nationwide, cross-sectional surveillance programs. High-throughput WGS and longitudinal surveillance will be crucial for tracking resistance evolution and identifying alternative resistance mechanisms. Monitoring in-host population dynamics is vital for understanding resistance evolution and persistence within patients. This approach can track genetic shifts during infection, revealing the emergence of minor resistant subpopulations that can become dominant under antifungal pressure.

The complexity of antifungal resistance necessitates rapid, precise diagnostics to guide treatment. Integrating advanced molecular methods, such as PCR and next-generation sequencing into clinical practice can significantly improve detection. Portable platforms like the Oxford MinION enable real-time sequencing, even in resource-limited settings, allowing for the rapid identification of resistance markers (547–549). Longitudinal sampling and real-time sequencing, can identify emerging

resistance patterns early, guiding adaptive treatment strategies. Combining WGS data with patient treatment histories helps elucidate the selective pressures shaping resistance, aiding in the identification of transmission networks and informing targeted interventions. Although real-time sequencing of fungal pathogens is still evolving, its potential to monitor resistance patterns and manage outbreaks could transform antifungal stewardship (550).

Utilising the *A. fumigatus* COFUN genome-wide knockout collection (551) and the COFUN transcription factor-specific library (552) in high-throughput screening, such as Omnilog® platform, could identify genes that influence antifungal resistance and stress adaptation. This approach can identify critical pathways influencing susceptibility to drugs like olorofim and azoles, offering a clearer understanding of the genetic basis of drug tolerance and virulence. Developing advanced in vitro and in vivo models is also vital for exploring the complex interactions between *A. fumigatus*, host immunity, and environmental pressures. Systems such as organ-on-chip models can replicate the human lung environment, providing insights into fungal-host interactions and enabling drug testing at clinically relevant concentrations (553). Fungi-on-a-Chip microfluidic technologies can simulate host-environment interactions, allowing precise drug efficacy screening to support targeted therapies and preserve the effectiveness of new antifungals (554).

Effective monitoring of indoor environments for *A. fumigatus* requires an understanding of airflow dynamics and the characteristics of indoor spaces. The airborne dispersal of *A. fumigatus* spores in indoor environments plays a crucial role in the spread of fungal infections, especially in healthcare settings where immunocompromised patients are particularly vulnerable. The prolonged suspension of spores is influenced by factors like ventilation efficiency, building design, and human activity, which create "well-mixed" zones where spores can accumulate and circulate (555). These areas may act as reservoirs of airborne spores, heightening exposure risks. By mapping these zones and understanding air movement in indoor environments, targeted interventions such as optimising air filtration placement and controlling airflow patterns can be implemented. Integrating these insights into

surveillance protocols enables precise environmental management to minimise spore exposure in high-risk areas.

Conclusions

This thesis provides a comprehensive analysis of the genetic and phenotypic factors contributing to azole resistance in *A. fumigatus* across the UK. The findings highlight the adaptive potential of resistant strains like TR_{34}/L98H, the role of environmental reservoirs, and the complex dynamics of resistance transmission between hospital and home environments. The emergence of novel antifungal agents such as olorofim offers hope, but the risk of resistance evolution underscores the need for proactive surveillance and precise antifungal stewardship. Integrating advanced molecular diagnostics and targeted environmental management is crucial for mitigating the spread of azole-resistant *A. fumigatus* and safeguarding vulnerable populations.

References

1. Hawksworth DL, Lücking R. Fungal diversity revisited: 2.2 to 3.8 million species. *Microbiology Spectrum*. 2017;5(4):10–1128.

2. Brown GD, Ballou ER, Bates S, Bignell EM, Borman AM, Brand AC, et al. The pathobiology of human fungal infections. *Nature Reviews Microbiology*. 2024;1–18.

3. Fisher MC, Henk DA, Briggs CJ, Brownstein JS, Madoff LC, McCraw SL, et al. Emerging fungal threats to animal, plant and ecosystem health. *Nature*. 2012;484(7393):186–94.

4. Sinsabaugh RS. Enzymic analysis of microbial pattern and process. *Biology and Fertililty of Soils*. 1994;17:69–74.

5. Richards TA, Talbot NJ. Osmotrophy. *Current Biology*. 2018;28(20):R1179–80.

6. Gancedo JM. Yeast carbon catabolite repression. *Microbiology and molecular biology reviews*. 1998;62(2):334–61.

7. Adnan M, Zheng W, Islam W, Arif M, Abubakar YS, Wang Z, et al. Carbon catabolite repression in filamentous fungi. *International Journal of Molecular Sciences*. 2017;19(1):48.

8. Magasanik B, Kaiser CA. Nitrogen regulation in Saccharomyces cerevisiae. *Gene*. 2002;290(1–2):1–18.

9. Snoeijers SS, Pérez-García A, Joosten MHAJ, De Wit PJGM. The effect of nitrogen on disease development and gene expression in bacterial and fungal plant pathogens. *European Journal of Plant Pathology*. 2000;106:493–506.

10. Nair A, Sarma SJ. The impact of carbon and nitrogen catabolite repression in microorganisms. *Microbiological Research*. 2021;251:126831.

11. Bills GF, Gloer JB. Biologically active secondary metabolites from the fungi. *Microbiology Spectrum*. 2016;4(6):10–1128.

12. Zain ME. Impact of mycotoxins on humans and animals. *Journal of Saudi chemical society*. 2011;15(2):129–44.

13. Brown GD, Denning DW, Gow NAR, Levitz SM, Netea MG, White TC. Hidden killers: Human fungal infections. *Science Translational Medicine*. 2012;4(165):165rv13-165rv13.

14. Kudymowa, J., Hu, J., & Hird, T. Fungal diseases: Health burden, neglectedness, and potential interventions. Rethink Priorities. 2024. https://rethinkpriorities.org/publications/fungal-diseases. [Accessed 1st September 2024]

15. Bongomin F, Gago S, Oladele RO, Denning DW. Global and multi-national prevalence of fungal diseases—estimate precision. *Journal of Fungi*. 2017;3(4):57.

16. WHO. WHO fungal priority pathogens list to guide research, development and public health action. Geneva: World Health Organization; 2022. Licence: CC BY-NC-SA 3.0 IGO.

17. Editorial. Stop neglecting fungi. Nature Microbiology. 2017;25;2:17120.

18. Nnadi NE, Carter DA. Climate change and the emergence of fungal pathogens. *PLoS Pathogens.* 2021;17(4):e1009503.

19. Lindsey R, Dahlman L. Climate change: Global temperature. 2016. *https://www.climate.gov/news-features/understanding-climate/climate-change-global-temperature*. [Date Accessed: 15th April 2024]

20. Van Rhijn N, Bromley M. The consequences of our changing environment on life threatening and debilitating fungal diseases in humans. *Journal of Fungi*. 2021;7(5):367.

21. Granados DP, Castañeda E. Influence of climatic conditions on the isolation of members of the *Cryptococcus neoformans* species complex from trees in Colombia from 1992–2004. *FEMS Yeast Research*. 2006;6(4):636–44.

22. Seidel D, Wurster S, Jenks JD, Sati H, Gangneux JP, Egger M, et al. Impact of climate change and natural disasters on fungal infections. *Lancet Microbe*. 2024;5(6):e594-e605.

23. Kumar R, Kumar A, Saikia P. Deforestation and forests degradation impacts on the environment. In: Environmental Degradation: Challenges and Strategies for Mitigation. Springer. Switzerland; 2022. p. 19–46.

24. Tazerji SS, Nardini R, Safdar M, Shehata AA, Duarte PM. An overview of anthropogenic actions as drivers for emerging and re-emerging zoonotic diseases. *Pathogens*. 2022;11(11):1376.

25. Rauseo AM, Coler-Reilly A, Larson L, Spec A. Hope on the horizon: novel fungal treatments in development. *Open Forum Infectious Diseases*. 2020;7(2):ofaa016.

26. Denning DW. Antifungal drug resistance: an update. *European Journal of Hospital Pharmacy*. 2022;29(2):109–12.

27. Wiederhold NP. Antifungal resistance: current trends and future strategies to combat. *Infection and Drug Resistance*. 2017;249–59.

28. Dhasarathan P, AlSalhi MS, Devanesan S, Subbiah J, Ranjitsingh AJA, Binsalah M, et al. Drug resistance in *Candida albicans* isolates and related changes in the structural domain of Mdr1 protein. *Journal of Infection and Public Health*. 2021;14(12):1848–53.

29. Russo TP, Santaniello A. Tackling antibiotic and antifungal resistance in domestic animals, synanthropic species, and wildlife: a global health imperative. *Antibiotics*. 2023;17;12(11):1632

30. Brauer VS, Rezende CP, Pessoni AM, De Paula RG, Rangappa KS, Nayaka SC, et al. Antifungal agents in agriculture: Friends and foes of public health. *Biomolecules*. 2019;9(10):521.

31. Monapathi ME, Oguegbulu JC, Adogo L, Klink M, Okoli B, Mtunzi F, et al. Pharmaceutical pollution: azole antifungal drugs and resistance of opportunistic pathogenic yeasts in wastewater and environmental water. *Applied and Environmental Soil Science*. 2021;2021(1):9985398.

32. Ostrosky-Zeichner L, Casadevall A, Galgiani JN, Odds FC, Rex JH. An insight into the antifungal pipeline: selected new molecules and beyond. *Nature Reviews Drug Discovery*. 2010;9(9):719–27.

33. Perfect JR. The antifungal pipeline: A reality check. *Nature Reviews Drug Discovery*. 2017;16(9):603–16.

34. Fisher MC, Hawkins NJ, Sanglard D, Gurr SJ. Worldwide emergence of resistance to antifungal drugs challenges human health and food security. *Science*. 2018;18;360(6390):739-742.

35. Pathadka S, Yan VKC, Neoh CF, Al-Badriyeh D, Kong DCM, Slavin MA, et al. Global consumption trend of antifungal agents in humans from 2008 to 2018: data from 65 middle-and high-income countries. *Drugs*. 2022;82(11):1193–205.

36. FAOSTAT. Food and Agriculture Organization of the United Nations. 2024. *https://www.fao.org/faostat/en/#home*. [Date Accessed: 5th June 2024].

37. Pimentão AR, Cuco AP, Pascoal C, Cássio F, Castro BB. Current trends and mismatches on fungicide use and assessment of the ecological effects in freshwater ecosystems. *Environmental Pollution*. 2024;123678.

38. Sharma A, Kumar V, Shahzad B, Tanveer M, Sidhu GPS, Handa N, et al. Worldwide pesticide usage and its impacts on ecosystem. *SN Applied Sciences*. 2019;1:1–16.

39. European Centre for Disease Prevention and Control. Risk assessment on the impact of environmental usage of triazoles on the development and spread of resistance to medical triazoles in Aspergillus species. Stockholm: *ECDC*. 2013.

40. WHO. WHO fungal priority pathogens list to guide research, development and public health action. Geneva: World Health Organization; 2022. Licence: CC BY-NC-SA 3.0 IGO.

41. WHO Bacterial Priority Pathogens List, 2024: bacterial pathogens of public health importance to guide research, development and strategies to prevent and control antimicrobial resistance. Geneva: World Health Organization; 2024. Licence: CC BY-NC-SA 3.0 IGO.

42. Richardson MD. Changing patterns and trends in systemic fungal infections. Journal of Antimicrobial Chemotherapy. 2005;56:i5-i11.

43. Wu C, Chen X, Cai Y, Xia J, Zhou X, Xu S, et al. Risk Factors Associated with Acute Respiratory Distress Syndrome and Death in Patients with Coronavirus Disease 2019 Pneumonia in Wuhan, China. *JAMA International Medicine*. 2020;180(7):934–43.

44. Zhu X, Ge Y, Wu T, Zhao K, Chen Y, Wu B, et al. Co-infection with respiratory pathogens among COVID-2019 cases. *Virus Research*. 2020;285:198005.

45. Koehler P, Cornely OA, Böttiger BW, Dusse F, Eichenauer DA, Fuchs F, et al. COVID-19 associated pulmonary aspergillosis. *Mycoses*. 2020;63(6):528–34.

46. Hoenigl M. Invasive Fungal Disease Complicating Coronavirus Disease 2019: When It Rains, It Spores. Clinical Infectious Diseases. 2020;73(7):e1645-8

47. Heard KL, Hughes S, Mughal N, Moore LSP. COVID-19 and fungal superinfection. *Lancet Microbe*. 2020;1(3):e107.

48. Armstrong-James D, Youngs J, Bicanic T, Abdolrasouli A, Denning DW, Johnson E, et al. Confronting and mitigating the risk of COVID-19 associated pulmonary aspergillosis. *European Respiratory Journal*. 2020;56(4).

49. Dagenais TRT, Keller NP. Pathogenesis of *Aspergillus fumigatus* in invasive aspergillosis. *Clinical Microbiology Reviews*. 2009;22(3):447–65.

50. Zupančič J, Novak Babič M, Zalar P, Gunde-Cimerman N. The black yeast *Exophiala dermatitidis* and other selected opportunistic human fungal pathogens spread from dishwashers to kitchens. *PLoS One*. 2016;11(2):e0148166.

51. Hiruma M, Kawada A, Ohata H, Ohnishi Y, Takahashi H, Yamazaki M, et al. Systemic phaeohyphomycosis caused by *Exophiala dermatitidis*. *Mycoses*. 1993;36(1–2):1–7.

52. Ajanee N, Alam M, Holmberg K, Khan J. Brain abscess caused by Wangiella dermatitidis: Case report. *Clinical Infectious Diseases*. 1996;23(1):197–8.

53. Ozawa Y, Suda T, Kaida Y, Kato M, Hasegaw H, Fujii M, et al. A case of bronchial infection of *Wangiella dermatitidis*. *Nihon Kokyuki Gakkai Zasshi*. 2007;45(11):907–11.

54. Alabaz D, Kibar F, Arikan S, Sancak B, Celik U, Aksaray N, et al. Systemic phaeohyphomycosis due to *Exophiala (Wangiella)* in an immunocompetent child. *Medical Mycology*. 2009;47(6):653–7.

55. Chang X, Li R, Yu J, Bao X, Qin J. Phaeohyphomycosis of the central nervous system caused by *Exophiala dermatitidis* in a 3-year-old immunocompetent host. *Journal of Child Neurology*. 2009;24(3):342–5.

56. Suzuki K, Nakamura A, Fujieda A, Nakase K, Katayama N. Pulmonary infection caused by *Exophiala dermatitidis* in a patient with multiple myeloma: A case report and a review of the literature. *Medical Mycology Case Reports*. 2012;1(1):95–8.

57. Griffard EA, Guajardo JR, Cooperstock MS, Scoville CL. Isolation of *Exophiala dermatitidis* from pigmented sputum in a cystic fibrosis patient. *Paediatric Pulmonology*. 2010;45(5):508–10.

58. Kondori N, Lindblad A, Welinder-Olsson C, Wennerås C, Gilljam M. Development of IgG antibodies to *Exophiala dermatitidis* is associated with inflammatory responses in patients with cystic fibrosis. *Journal of Cystic Fibrosis*. 2014;13(4):391–9.

59. Silva WC, Gonçalves SS, Santos DWCL, Padovan ACB, Bizerra FC, Melo ASA. Species diversity, antifungal susceptibility and phenotypic and genotypic characterisation of *Exophiala spp*. infecting patients in different medical centres in Brazil. *Mycoses*. 2017;60(5):328–37.

60. Badali H, De Hoog GS, Sudhadham M, Meis JF. Microdilution in vitro antifungal susceptibility of *Exophiala dermatitidis*, a systemic opportunist. *Medical Mycology*. 2011;49(8):819–24.

61. Malo ME, Schultzhaus Z, Frank C, Romsdahl J, Wang Z, Dadachova E. Transcriptomic and genomic changes associated with radioadaptation in *Exophiala dermatitidis*. Computational and Structural Biotechnology Journal. 2021;19:196–205.

62. Song Y, Du M, Menezes da Silva N, Yang E, Vicente VA, Sybren de Hoog G, et al. Comparative Analysis of Clinical and Environmental Strains of Exophiala spinifera by Long-Reads Sequencing and RNAseq Reveal Adaptive Strategies. *Frontiers in Microbiology*. 2020;11:1880.

63. Rougeron A, Giraud S, Alastruey-Izquierdo A, Cano-Lira J, Rainer J, Mouhajir A, et al. Ecology of Scedosporium Species: Present Knowledge and Future Research. *Mycopathologia.* 2018;183(1):185–200.

64. Chen M, Zeng J, De Hoog GS, Stielow B, Gerrits Van Den Ende AHG, Liao W, et al. The 'species complex' issue in clinically relevant fungi: A case study in *Scedosporium apiospermum*. *Fungal Biology*. 2016;120(2):137–46.

65. Cimon B, Carrère J, Vinatier JF, Chazalette JP, Chabasse D, Bouchara JP. Clinical significance of Scedosporium apiospermum in patients with cystic fibrosis. *European Journal of Clinical Microbiology and Infectious Diseases.* 2000;19(1):53–6.

66. Bouchara JP, Le Govic Y, Kabbara S, Cimon B, Zouhair R, Hamze M, et al. Advances in understanding and managing *Scedosporium* respiratory infections in patients with cystic fibrosis. *Expert Review of Respiratory Medicine*. 2020;14(3):259–73.

67. De Jong CCM, Slabbers L, Engel TGP, Yntema JB, van Westreenen M, Croughs PD, et al. Clinical relevance of *Scedosporium spp*. and *Exophiala dermatitidis* in patients with cystic fibrosis: A nationwide study. *Medical Mycology*. 2020;58(7):859–66.

68. Iribarren ME, Moreno RMG, Cáceres LD, Sanz MTP, Moreno BB, Cavero TA, et al. Study of a cohort of patients with cystic fibrosis and isolation of *Scedosporium spp*. *Archivos de Bronconeumología (English Edition)*. 2019;55(11):559–64.

69. Devoto TB, Pola S, Rubeglio E, Finquelievich J, Gamarra S, García-Effron G, et al. Prevalence of fungal colonization in cystic fibrosis: a retrospective study over 3 years in Buenos Aires, Argentina. *International Journal of Infectious Diseases*. 2018;73:279–80.

70. Blyth CC, Harun A, Middleton PG, Sleiman S, Lee O, Sorrell TC, et al. Detection of occult Scedosporium species in respiratory tract specimens from patients with cystic fibrosis by use of selective media. *Journal of Clinical Microbiology*. 2010;48(1):314–6.

71. Lu Q, van den Ende AHGG, Bakkers J, Sun J, Lackner M, Najafzadeh MJ, et al. Identification of *Pseudallescheria* and *Scedosporium* species by three molecular methods. *Journal of Clinical Microbiology*. 2011;49(3):960–7.

72. Cuenca-Estrella M, Ruiz-Díez B, Martínez-Suárez J V, Monzón A, Rodríguez-Tudela JL. Comparative in-vitro activity of voriconazole (UK-109,496) and six other antifungal agents against clinical isolates of *Scedosporium prolificans* and *Scedosporium apiospermum*. *Journal of Antimicrobial Chemotherapy*. 1999;43(1):149–51.

73. Sedlacek L, Graf B, Schwarz C, Albert F, Peter S, Würstl B, et al. Prevalence of *Scedosporium* species and *Lomentospora prolificans* in patients with cystic fibrosis in a multicenter trial by use of a selective medium. *Journal of Cystic Fibrosis*. 2015;14(2):237–41.

74. Gilgado F, Serena C, Cano J, Gené J, Guarro J. Antifungal susceptibilities of the species of the *Pseudallescheria boydii* complex. *Antimicrobial Agents and Chemotherapy*. 2006;50(12):4211–3.

75. Carrillo AJ, Guarro J. In Vitro Activities of Four Novel Triazoles against *Scedosporium spp*. *Antimicrobial Agents and Chemotherapy*. 2001;45(7):2151–3.

76. Lackner M, De Hoog GS, Verweij PE, Najafzadeh MJ, Curfs-Breuker I, Klaassen CH, et al. Species-specific antifungal susceptibility patterns *of Scedosporium* and *Pseudallescheria* species. *Antimicrobial Agents and Chemotherapy*. 2012;56(5):2635–42.

77. Tortorano AM, Richardson M, Roilides E, van Diepeningen A, Caira M, Munoz P, et al. ESCMID and ECMM joint guidelines on diagnosis and management of hyalohyphomycosis: Fusarium spp., Scedosporium spp. and others. *Clinical Microbiology and Infection*. 2014;20(S3):27–46.

78. Lackner M, Klaassen CH, Meis JF, van den Ende AHGG, De Hoog GS. Molecular identification tools for sibling species of *Scedosporium* and *Pseudallescheria*. *Sabouraudia*. 2012;50(5):497–508.

79. Schwarz C, Brandt C, Melichar V, Runge C, Heuer E, Sahly H, et al. Combined antifungal therapy is superior to monotherapy in pulmonary scedosporiosis in cystic fibrosis. *Journal of Cystic Fibrosis*. 2019;18(2):227–32.

80. Sigera LSM, Denning DW. A systematic review of the therapeutic outcome of mucormycosis. *Open Forum Infectious Diseases*. 2024;30:ofad704.

81. Prakash H, Chakrabarti A. Global epidemiology of mucormycosis. *Journal of Fungi*. 2019;5(1):26.

82. Jeong W, Keighley C, Wolfe R, Lee WL, Slavin MA, Kong DCM, et al. The epidemiology and clinical manifestations of mucormycosis: a systematic review and meta-analysis of case reports. *Clinical Microbiology and Infection*. 2019;25(1):26–34.

83. Roden MM, Zaoutis TE, Buchanan WL, Knudsen TA, Sarkisova TA, Schaufele RL, et al. Epidemiology and outcome of zygomycosis: A review of 929 reported cases. *Clinical Infectious Diseases.* 2005;41(5):634–53.

84. Farmakiotis D, Kontoyiannis DP. Mucormycoses. *Infectious Disease Clinics North America*. 2016;30(1):143–63.

85. Chamilos G, Marom EM, Lewis RE, Lionakis MS, Kontoyiannis DP. Predictors of pulmonary zygomycosis versus invasive pulmonary aspergillosis in patients with cancer. *Clinical Infectious Diseases.* 2005;41(1):60–6.

86. Cornely OA, Alastruey-Izquierdo A, Arenz D, Chen SCA, Dannaoui E, Hochhegger B, et al. Global guideline for the diagnosis and management of mucormycosis: an initiative of the European Confederation of Medical Mycology in cooperation with the Mycoses Study Group Education and Research Consortium. *Lancet Infectious Diseases*. 2019;19(12):e405–21.

87. Singh AK, Singh R, Joshi SR, Misra A. Mucormycosis in COVID-19: A systematic review of cases reported worldwide and in India. Diabetes & Metabolic Syndrome: *Clinical Research & Reviews*. 2021;6(4):265.

88. Holzel H, Macqueen S, MacDonald A, Alexander S, Campbell CK, Johnson EM, et al. *Rhizopus microsporus* in wooden tongue depressors: a major threat or minor inconvenience? *Journal of Hospital Infection*. 1998;38(2):113–8.

89. Mitchell SJ, Gray J, Morgan MEI, Hocking MD, Durbin GM. Nosocomial infection with Rhizopus microsporus in preterm infants: association with wooden tongue depressors. *The Lancet*. 1996;348(9025):441–3.

90. Christiaens G, Hayette MP, Jacquemin D, Melin P, Mutsers J, De Mol P. An outbreak of Absidia corymbifera infection associated with bandage contamination in a burns unit. *Journal of Hospital Infection*. 2005;61(1).

91. Duffy J, Harris J, Gade L, Sehulster L, Newhouse E, O'Connell H, et al. Mucormycosis outbreak associated with hospital linens. *The Paediatric Infectious Disease Journal*. 2014;33(5):472–6.

92. Srinivas C, Devi DN, Murthy KN, Mohan CD, Lakshmeesha TR, Singh B, et al. *Fusarium oxysporum f. sp. lycopersici* causal agent of vascular wilt disease of tomato: Biology to diversity–A review. *Saudi Journal of Biological Sciences*. 2019;26(7):1315–24.

93. Legrand F, Picot A, Cobo-Díaz JF, Chen W, Le Floch G. Challenges facing the biological control strategies for the management of Fusarium Head Blight of cereals caused by *F. graminearum. Biological control*. 2017;113:26–38.

94. Xie SY, Ma T, Zhao N, Zhang X, Fang B, Huang L. Whole-genome sequencing and comparative genome analysis of *Fusarium solani-melongenae* causing Fusarium root and stem rot in sweet potatoes. *Microbiology Spectrum*. 2022;10(4):e00683-22.

95. Miedaner T, Bolduan C, Melchinger AE. Aggressiveness and mycotoxin production of eight isolates each of *Fusarium graminearum* and *Fusarium verticillioides* for ear rot on susceptible and resistant early maize inbred lines. *European Journal of Plant Pathology*. 2010;127:113–23.

96. Goswami RS, Kistler HC. Heading for disaster: Fusarium graminearum on cereal crops. *Molecular Plant Pathology*. 2004;5(6):515–25.

97. Nelson PE, Dignani MC, Anaissie EJ. Taxonomy, biology, and clinical aspects of *Fusarium* species. *Clinical Microbiology Reviews*. 1994;7(4):479–504.

98. Correll DP, Luzi SA, Nelson BL. Allergic Fungal Sinusitis. *Head and Neck Pathology*. 2015;9(4):488–91.

99. Kurien M, Anandi V, Raman R, Brahmadathan KN. Maxillary sinus fusariosis in immunocompetent hosts. *Journal of Laryngology and Otology*. 1992;106(8):733–6.

100. Sevestre J, Kopec L. Disseminated fusariosis. *New England Journal of Medicine*. 2020;382(21):e64.

101. Horn DL, Freifeld AG, Schuster MG, Azie NE, Franks B, Kauffman CA. Treatment and outcomes of invasive fusariosis: review of 65 cases from the PATH Alliance® registry. *Mycoses.* 2014;57(11):652–8.

102. Campo M, Lewis RE, Kontoyiannis DP. Invasive fusariosis in patients with hematologic malignancies at a cancer center: 1998–2009. *Journal of Infection*. 2010;60(5):331–7.

103. Nucci M, Garnica M, Gloria AB, Lehugeur DS, Dias VCH, Palma LC, et al. Invasive fungal diseases in haematopoietic cell transplant recipients and in patients with acute myeloid leukaemia or myelodysplasia in Brazil. *Clinical Microbiology and Infection*. 2013;19(8):745–51.

104. Hof H. The medical relevance of *Fusarium spp*. *Journal of fungi*. 2020;6(3):117.

105. Sassi C, Stanzani M, Lewis RE, Vianelli N, Tarsi A, Poerio A, et al. Radiologic findings of Fusarium pneumonia in neutropenic patients. *Mycoses*. 2017;60(2):73–8.

106. Al-Hatmi AMS, Bonifaz A, Ranque S, Sybren de Hoog G, Verweij PE, Meis JF. Current antifungal treatment of fusariosis. *Internation Journal Antimicrobial Agents*. 2018;51(3):326–32.

107. Homa M, Galgóczy L, Manikandan P, Narendran V, Sinka R, Csernetics Á, et al. South Indian isolates of the *Fusarium solani* species complex from clinical and environmental samples: Identification, antifungal susceptibilities, and virulence. *Frontiers in Microbiology*.2018;23;9:1052

108. Dalhoff A. Does the use of antifungal agents in agriculture and food foster polyene resistance development? A reason for concern. *Journal of Global Antimicrobial Resistance*. 2018;13:40–8.

109. Price CL, Parker JE, Warrilow AG, Kelly DE, Kelly SL. Azole fungicides - understanding resistance mechanisms in agricultural fungal pathogens. *Pest Management Science*. 2015;71(8):1054–8.

110. Sharma S, Das S, Virdi A, Fernandes M, Sahu SK, Koday NK, et al. Re-appraisal of topical 1% voriconazole and 5% natamycin in the treatment of fungal keratitis in a randomised trial. British *Journal of Ophthalmology*. 2015;99(9):1190–5.

111. Anaissie EJ, Kuchar RT, Rex JH, Francesconi A, Kasai M, Müller FMC, et al. Fusariosis associated with pathogenic Fusarium species colonization of a hospital water system: A new paradigm for the epidemiology of opportunistic mold infections. *Clinical Infectious Diseases*. 2001;33(11):1871–8.

112. Levitz SM. The ecology of Cryptococcus neoformans and the epidemiology of cryptococcosis. *Reviews of Infectious Diseases*. 1991;13(6):1163–9.

113. Bartlett KH, Kidd SE, Kronstad JW. The emergence of *Cryptococcus gattii* in British Columbia and the Pacific Northwest. *Current Infectious Disease Reports*. 2008;10(1):58–65.

114. Gugnani HC, Mitchell TG, Litvintseva AP, Lengeler KB, Heitman J, Kumar A, et al. Isolation of *Cryptococcus gattii* and *Cryptococcus* neoformans var. grubii from the flowers and bark of Eucalyptus trees in India. *Medical Mycology*. 2005;43(6):565–9.

115. Datta K, Bartlett KH, Baer R, Byrnes E, Galanis E, Heitman J, et al. Spread of *Cryptococcus gattii* into Pacific Northwest region of the United States. *Emerging Infectious Diseases*. 2009;15(8):1185.

116. Kozubowski L, Heitman J. Profiling a killer, the development of *Cryptococcus neoformans*. *FEMS Microbiology Reviews*. 2012;36(1):78–94.

117. Desnos-Ollivier M, Patel S, Spaulding AR, Charlier C, Garcia-Hermoso D, Nielsen K, et al. Mixed infections and in vivo evolution in the human fungal pathogen *Cryptococcus neoformans*. *mBio.* 2010;1(1):10–1128.

118. Su X, Li W, Liu J, Wang Y, Liu J, Xu X, et al. Comparison of features and outcomes between HIV-negative patients with *Cryptococcus gattii* meningitis and *Cryptococcus neoformans* meningitis in South China. *Mycoses*. 2022;65(9):887–96.

119. Baddley JW, Chen SCA, Huisingh C, Benedict K, DeBess EE, Galanis E, et al. MSG07: an international cohort study comparing epidemiology and outcomes of patients with *Cryptococcus neoformans* or *Cryptococcus gattii* infections. *Clinical Infectious Diseases*. 2021;73(7):1133–41.

120. Tugume L, Ssebambulidde K, Kasibante J, Ellis J, Wake RM, Gakuru J, et al. *Cryptococcal meningitis*. *Nature Reviews Disease Primers*. 2023;9(1):62.

121. Cogliati M. Global molecular epidemiology of *Cryptococcus neoformans* and *Cryptococcus gattii*: an atlas of the molecular types. *Scientifica (Cairo).* 2013;2013(1):675213.

122. Lin CK, Tsai YH, Huang CC. Disseminated *Cryptococcosis* with acute respiratory distress syndrome in a patient with newly diagnosed systemic lupus erythematosus - a case report. *Thorax Medicine.* 2002;17(4):425-429

123. Orsini J, Blaak C, Tam E, Rajayer S, Morante J. Disseminated cryptococcal infection resulting in acute respiratory distress syndrome (ARDS) as the initial clinical presentation of AIDS. *Internal Medicine*. 2016;55(8):995–8.

124. Setianingrum F, Rautemaa-Richardson R, Denning DW. Pulmonary cryptococcosis: a review of pathobiology and clinical aspects. *Medical Mycology*. 2019;57(2):133–50.

125. Hsiao PJ, Cheng H, Kao YH, Wang YH, Chiu CC, Chiang WF, et al. Comparison of laboratory diagnosis, clinical manifestation, and management of pulmonary cryptococcosis: Report of the clinical scenario and literature review. *Clinica Chimica Acta*. 2022;524:78–83.

126. French N, Gray K, Watera C, Nakiyingi J, Lugada E, Moore M, et al. Cryptococcal infection in a cohort of HIV-1-infected Ugandan adults. *Aids*. 2002;16(7):1031–8.

127. Rajasingham R, Govender NP, Jordan A, Loyse A, Shroufi A, Denning DW, et al. The global burden of HIV-associated cryptococcal infection in adults in 2020: a modelling analysis. *Lancet Infectious Diseases*. 2022;22(12):1748–55.

128. Rajasingham R, Smith RM, Park BJ, Jarvis JN, Govender NP, Chiller TM, et al. Global burden of disease of HIV-associated cryptococcal meningitis: an updated analysis. *Lancet Infectious Diseases*. 2017;17(8):873–81.

129. Coussement J, Heath CH, Roberts MB, Lane RJ, Spelman T, Smibert OC, et al. Current epidemiology and clinical features of Cryptococcus infection in patients without HIV infection: a multicentre study in 46 hospitals from Australia and New Zealand. *Clinical Infectious Diseases*. 2023;77(7):976-986

130. Rhodes JC. Aspergillus fumigatus: Growth and virulence. *Medical Mycology*. 2006;44(1):S77-81

131. Tekaia F, Latgé JP. *Aspergillus fumigatus*: Saprophyte or pathogen?. Current Opinion in Microbiology. 2005;8(4):385-92

132. Van De Veerdonk FL, Gresnigt MS, Romani L, Netea MG, Latgé JP. *Aspergillus fumigatus* morphology and dynamic host interactions. *Nature Reviews Microbiology*. 2017;15(11):661-674.

133. Pringle A, Baker DM, Platt JL, Wares JP, Latgé JP, Taylor JW. Cryptic speciation in the cosmopolitan and clonal human pathogenic fungus *Aspergillus fumigatus. Evolution (N Y).* 2005;59(9):1886–99.

134. Baltussen TJH, Zoll J, Verweij PE, Melchers WJG. Molecular mechanisms of conidial germination in *Aspergillus spp*. *Microbiology and Molecular Biology Reviews*. 2020;84(1):10–1128.

135. Gonçalves VN, Amorim SS, da Costa MC, de Assis Santos D, Convey P, Rosa LH. Pathogenic potential of an environmental *Aspergillus fumigatus* strain recovered from soil of *Pygoscelis papua* (Gentoo penguins) colony in Antarctica. *Brazilian Journal of Microbiology*. 2024;1–8.

136. Abdel-Hafez SII. Thermophilic and thermotolerant fungi in the desert soils of Saudi Arabia. *Mycopathologia*. 1982;80(1):15–20.

137. Zhdanova NN, Zakharchenko VA, Vember V V, Nakonechnaya LT. Fungi from Chernobyl: mycobiota of the inner regions of the containment structures of the damaged nuclear reactor. *Mycological Research*. 2000;104(12):1421–6.

138. Knox BP, Blachowicz A, Palmer JM, Romsdahl J, Huttenlocher A, Wang CCC, et al. Characterization of *Aspergillus fumigatus* isolates from air and surfaces of the international space station. *mSphere*. 2016;1(5):10–1128.

139. Samson RA, Visagie CM, Houbraken J, Hong SB, Hubka V, Klaassen CHW, et al. Phylogeny, identification and nomenclature of the genus *Aspergillus. Studies in Mycology*. 2014;78(1):141–73.

140. Sugui JA, Kwon-Chung KJ, Juvvadi PR, Latgé JP, Steinbach WJ. *Aspergillus fumigatus* and related species. *Cold Spring Harbour Perspectives in Medicine*. 2015;5(2):a019786.

141. Ullmann AJ, Aguado JM, Arikan-Akdagli S, Denning DW, Groll AH, Lagrou K, et al. Diagnosis and management of Aspergillus diseases: executive summary of the 2017 ESCMID-ECMM-ERS guideline. Clinical Microbiology and Infection. 2018;1:e1-e38

142. Wasylnka JA, Moore MM. Adhesion of *Aspergillus* species to extracellular matrix proteins: evidence for involvement of negatively charged carbohydrates on the conidial surface. *Infection and Immunity*. 2000;68(6):3377–84.

143. Latgé JP. *Aspergillus fumigatus* and Aspergillosis. *Clinical Microbiology Reviews.* 1999;12(2):310-50

144. Abad A, Fernández-Molina JV, Bikandi J, Ramírez A, Margareto J, Sendino J, et al. What makes *Aspergillus fumigatus* a successful pathogen? Genes and molecules involved in invasive aspergillosis. *Revista Iberoamericana de Micología*. 2010;27(4):155–82.

145. Cramer RA, Rivera A, Hohl TM. Immune responses against *Aspergillus fumigatus*: what have we learned? *Current Opinion in Infectious Diseases*. 2011;24(4):315–22.

146. Aimanianda V, Bayry J, Bozza S, Kniemeyer O, Perruccio K, Elluru SR, et al. Surface hydrophobin prevents immune recognition of airborne fungal spores. *Nature*. 2009;460(7259):1117–21.

147. Paris S, Debeaupuis JP, Crameri R, Carey M, Charles F, Prévost MC, et al. Conidial hydrophobins of *Aspergillus fumigatus*. *Applied and Environmental Microbiology*. 2003;69(3):1581–8.

148. Medzhitov R, Janeway Jr CA. Innate immunity: impact on the adaptive immune response. *Current Opinion in Immunology*. 1997;9(1):4–9.

149. Wanner A, Salathé M, O'Riordan TG. Mucociliary clearance in the airways. *American Journal of Respiratory and Critical Care Medicine*. 1996;154(6):1868–902.

150. Schleimer RP, Berdnikovs S. Etiology of epithelial barrier dysfunction in patients with type 2 inflammatory diseases. *Journal of Allergy and Clinical Immunology*. 2017;139(6):1752–61.

151. Crameri R, Blaser K. Allergy and immunity to fungal infections and colonization. *European Respiratory Journal*. 2002;19(1):151–7.

152. Regnis JA, Robinson M, Bailey DL, Cook P, Hooper P, Chan HK, et al. Mucociliary clearance in patients with cystic fibrosis and in normal subjects. *American Journal of Respiratory and Critical Care Medicine*. 1994;150(1):66–71.

153. Stevens DA, Moss RB, Kurup VP, Knutsen AP, Greenberger P, Judson MA, et al. Allergic bronchopulmonary Aspergillosis in cystic fibrosis - state of the art: cystic fibrosis foundation consensus conference. *Clinical Infectious Diseases*. 2003;37(3):S225-64

154. Haase G, Skopnik H, Groten T, Kusenbach G, Posselt HG. Long-term fungal cultures from sputum of patients with cystic fibrosis. *Mycoses*. 2009;34(9–10):373–6.

155. Rapaka RR, Kolls JK. Pathogenesis of allergic bronchopulmonary aspergillosis in cystic fibrosis: Current understanding and future directions. *Medical. Mycology. 2009;.*47(Suppl. 1)**:** S331-S337.

156. Saunders R v., Modha DE, Claydon A, Gaillard EA. Chronic *Aspergillus fumigatus* colonization of the pediatric cystic fibrosis airway is common and may be associated with a more rapid decline in lung function. *Medical Mycology*. 2016;54(5):537–43.

157. Anstead M, Saiman L, Mayer-Hamblett N, Lands LC, Kloster M, Goss CH, et al. Pulmonary exacerbations in CF patients with early lung disease. *Journal of Cystic Fibrosis*. 2014;13(1):74–9.

158. Chai LYA, Vonk AG, Kullberg BJ, Verweij PE, Verschueren I, Van Der Meer JWM, et al. *Aspergillus fumigatus* cell wall components differentially modulate host TLR2 and TLR4 responses. *Microbes and Infection*. 2011;13(2):151–9.

159. Latgé J. Tasting the fungal cell wall. *Cell Microbiology*. 2010;12(7):863–72.

160. Latgé JP, Mouyna I, Tekaia F, Beauvais A, Debeaupuis JP, Nierman W. Specific molecular features in the organization and biosynthesis of the cell wall of *Aspergillus fumigatus*. *Medical Mycology*. 2005;43(sup.1):15–22.

161. Hohl TM, Van Epps HL, Rivera A, Morgan LA, Chen PL, Feldmesser M, et al. *Aspergillus fumigatus* triggers inflammatory responses by stage-specific β-glucan display. *PLoS Pathogogens*. 2005;1(3):e30.

162. Garcia-Rubio R, de Oliveira HC, Rivera J, Trevijano-Contador N. The fungal cell wall: *Candida, Cryptococcus*, and *Aspergillus* species. *Frontiers in Microbiology*. 2020;10:2993.

163. Ito JI. Enhancing angiogenesis in invasive aspergillosis: a novel therapeutic approach. *The Journal of infectious diseases*. 2013;207(7):1031-3

164. Kamai Y, Chiang LY, Lopes Bezerra LM, Doedt T, Lossinsky AS, Sheppard DC, et al. Interactions of *Aspergillus fumigatus* with vascular endothelial cells. *Medical Mycology*. 2006;44(1):S115–7.

165. Ben-Ami R, Albert ND, Lewis RE, Kontoyiannis DP. Proangiogenic growth factors potentiate in situ angiogenesis and enhance antifungal drug activity in murine invasive aspergillosis. *Journal of Infectious Diseases*. 2013;207(7):1066–74.

166. Waring P, Eichner RD, Müllbacher A, Sjaarda A. Gliotoxin induces apoptosis in macrophages unrelated to its antiphagocytic properties. *Journal of Biological Chemistry*. 1988;263(34):18493–9.

167. Mitchell CG, Slight J, Donaldson K. Diffusible component from the spore surface of the fungus *Aspergillus fumigatus* which inhibits the macrophage oxidative burst is distinct from gliotoxin and other hyphal toxins. *Thorax*. 1997;52(9):796–801.

168. Amitani R, Taylor G, Elezis EN, Llewellyn-Jones C, Mitchell J, Kuze F, et al. Purification and characterization of factors produced by *Aspergillus fumigatus* which affect human ciliated respiratory epithelium. *Infection and Immunity*. 1995;63(9):3266–71.

169. Bünger J, Westphal G, Mönnich A, Hinnendahl B, Hallier E, Müller M. Cytotoxicity of occupationally and environmentally relevant mycotoxins. *Toxicology*. 2004;202(3):199–211.

170. Kosmidis C, Denning DW. The clinical spectrum of pulmonary aspergillosis. Thorax. 2015;70(3):270–7.

171. Agarwal R, Chakrabarti A. Allergic bronchopulmonary aspergillosis in asthma: epidemiological, clinical and therapeutic issues. *Future Microbiology*. 2013;8(11):1463–74.

172. Agarwal R, Chakrabarti A, Shah A, Gupta D, Meis JF, Guleria R, et al. Allergic bronchopulmonary aspergillosis: Review of literature and proposal of new diagnostic and classification criteria. *Clinical and Experimental Allergy*. 2013;43(8):850–73.

173. Song P, Adeloye D, Salim H, Dos Santos JP, Campbell H, Sheikh A, et al. Global, regional, and national prevalence of asthma in 2019: a systematic analysis and modelling study. *Journal of Global Health*. 2022;12.

174. Denning DW, Pleuvry A, Cole DC. Global burden of allergic bronchopulmonary aspergillosis with asthma and its complication chronic pulmonary aspergillosis in adults. *Medical Mycology*. 2013;51(4):361–70.

175. Denning DW. Global incidence and mortality of severe fungal disease. *Lancet Infectious Diseases*. 2024;24(7) E428-E438

176. Ray A, Aayilliath K A, Banerjee S, Chakrabarti A, Denning DW. Burden of serious fungal infections in India. In: *Open Forum Infectious Diseases.* 2022;9(12):ofac603

177. Soundappan K, Muthu V, Dhooria S, Sehgal IS, Prasad KT, Rudramurthy SM, et al. Population prevalence of allergic bronchopulmonary aspergillosis in asthma: An epidemiological study of 43,261 participants from North India. *Clinical & Experimental Allergy*. 2023;53(7).

178. Janahi IA, Rehman A, Al-Naimi AR. Allergic bronchopulmonary aspergillosis in patients with cystic fibrosis. *Annals of Thoracic Medicine*. 2017;12(2):74–82.

179. Denning DW, Cadranel J, Beigelman-Aubry C, Ader F, Chakrabarti A, Blot S, et al. Chronic pulmonary aspergillosis: Rationale and clinical guidelines for diagnosis and management. *European Respiratory Journal*. 2016;47(1):45–68.

180. Denning DW. Diagnosing pulmonary aspergillosis is much easier than it used to be: a new diagnostic landscape. *The International Journal of Tuberculosis and Lung Disease*. 2021;25(7):525–36.

181. Denning DW, Cole DC, Ray A. New estimation of the prevalence of chronic pulmonary aspergillosis (CPA) related to pulmonary TB–a revised burden for India. *IJID regions*. 2023;6:7–14.

182. Bongomin F, Asio LG, Baluku JB, Kwizera R, Denning DW. Chronic pulmonary aspergillosis: notes for a clinician in a resource-limited setting where there is no mycologist. *Journal of Fungi*. 2020;6(2):75.

183. Denning DW, Pleuvry A, Cole DC. Global burden of chronic pulmonary aspergillosis as a sequel to pulmonary tuberculosis. *Bulletin of the World Health Organization*. 2011;89(12):864–72.

184. Walsh TJ, Anaissie EJ, Denning DW, Herbrecht R, Kontoyiannis DP, Marr KA, et al. Treatment of aspergillosis: clinical practice guidelines of the Infectious Diseases Society of America. *Clinical infectious diseases*. 2008;46(3):327–60.

185. Denning DW, Morgan EF. Quantifying deaths from aspergillosis in HIV positive people. *Journal of Fungi*. 2022;8(11):1131.

186. Segal BH. Aspergillosis. *New England Journal of Medicine*. 2009;360(18):1870–84.

187. Levesque E, Ait-Ammar N, Dudau D, Clavieras N, Feray C, Foulet F, et al. Invasive pulmonary aspergillosis in cirrhotic patients: analysis of a 10-year clinical experience. *Annals of Intensive Care*. 2019;9:1–9.

188. Douwes J, Pearce N. Invited commentary: Is indoor mold exposure a risk factor for asthma? Americann Journal of Epidemiology. 2003;158(3):203–6.

189. Denning DW, O'Driscoll BR, Powell G, Chew F, Atherton GT, Vyas A, et al. Randomized controlled trial of oral antifungal treatment for severe asthma with fungal sensitization: The Fungal Asthma Sensitization Trial (FAST) study. American Journal Respiratory Critical Care Medicine. 2009;179(1):11–8.

190. Patterson TF, Thompson III GR, Denning DW, Fishman JA, Hadley S, Herbrecht R, et al. Practice guidelines for the diagnosis and management of aspergillosis: 2016 update by the Infectious Diseases Society of America. Clinical infectious diseases. 2016;63(4):e1–60.

191. Alastruey-Izquierdo A, Cadranel J, Flick H, Godet C, Hennequin C, Hoenigl M, et al. Treatment of chronic pulmonary aspergillosis: current standards and future perspectives. Respiration. 2018;96(2):159–70.

192. Schauwvlieghe AFAD, Rijnders BJA, Philips N, Verwijs R, Vanderbeke L, Van Tienen C, et al. Invasive aspergillosis in patients admitted to the intensive care unit with severe influenza: a retrospective cohort study. Lancet Respir Med. 2018;6(10):782–92.

193. Herbrecht R, Denning DW, Patterson TF, Bennett JE, Greene RE, Oestmann JW, et al. Voriconazole versus amphotericin B for primary therapy of invasive aspergillosis. New England Journal of Medicine. 2002;347(6):408–15.

194. Mullins J, Harvey R, Seaton A. Sources and incidence of airborne *Aspergillus fumigatus* (Fres). *Clinical & Experimental Allergy*. 1976;6(3):209–17.

195. O'Gorman CM. Airborne *Aspergillus fumigatus* conidia: a risk factor for aspergillosis. *Fungal Biology Reviews*. 2011;25(3):151–7.

196. Hudson HJ. Thermophilous and thermotolerant fungi in the air-spora at Cambridge. *Transactions of the British Mycological Society*. 1973;60(3):596-8.

197. Millner PD, Olenchock SA, Epstein E, Rylander R, Haines J, Walker J, et al. Bioaerosols associated with composting facilities. *Compost Science & Utilization.* 1994;2(4):8-57.

198. Recer GM, Browne ML, Horn EG, Hill KM, Boehler WF. Ambient air levels of *Aspergillus fumigatus* and thermophilic actinomycetes in a residential neighbourhood near a yard-waste composting facility. *Aerobiologia (Bologna).* 2001;17:99–108.

199. Lis DO, Ulfig K, Wlazło A, Pastuszka JS. Microbial air quality in offices at municipal landfills. *Journal of Occupational and Environmental Hygiene*. 2004;1(2):62–8.

200. Bünger J, Schappler-Scheele B, Hilgers R, Hallier E. A 5-year follow-up study on respiratory disorders and lung function in workers exposed to organic dust from composting plants. *International Archives of Occupational and Environmental Health.* 2007;80:306–12.

201. Millner PD, Bassett DA, Marsh PB. Dispersal of Aspergillus fumigatus from sewage sludge compost piles subjected to mechanical agitation in open air. *Applied and Environmental Microbiology*. 1980;39(5):1000–9.

202. Allmers H, Huber H, Baur X. Two year follow-up of a garbage collector with allergic bronchopulmonary aspergillosis (ABPA). *American Journal of Industrial Medicine*. 2000;37(4):438–42.

203. Mehta SK, Sandhu RS. Immunological significance of *Aspergillus fumigatus* in cane-sugar mills. *Archives of Environmental Health: An International Journal*. 1983;38(1):41–6.

204. Akiyama K. ABPA as an occupational Disease. Aspergillosis: *From Diagnosis to Prevention*. 2010;689–93.

205. Bouakline A, Lacroix C, Roux N, Gangneux JP, Derouin F. Fungal contamination of food in hematology units. *Journal of Clinical Microbiology*. 2000;38(11):4272–3.

206. De Bock R, Gyssens I, Peetermans M, Nolard N. *Aspergillus* in pepper. *The Lancet*. 1989;334(8658):331–2.

207. Verweij PE, Kerremans JJ, Voss A, Meis JFGM. Fungal contamination of tobacco and marijuana. *JAMA*. 2000;284(22):2875.

208. Pini G, Faggi E, Donato R, Sacco C, Fanci R. Invasive pulmonary aspergillosis in neutropenic patients and the influence of hospital renovation. *Mycoses*. 2008;51(2):117–22.

209. Wirmann L, Ross B, Reimann O, Steinmann J, Rath PM. Airborne *Aspergillus fumigatus* spore concentration during demolition of a building on a hospital site, and patient risk determination for invasive aspergillosis including azole resistance. *Journal of Hospital Infection*. 2018;100(3):e91–7.

210. Talento AF, Fitzgerald M, Redington B, O'Sullivan N, Fenelon L, Rogers TR. Prevention of healthcare-associated invasive aspergillosis during hospital construction/renovation works. *Journal of Hospital Infection*. 2019;103(1):1–12.

211. Haiduven D. Nosocomial aspergillosis and building construction. *Medical Mycology*. 2009;47(Suppl.1):S210–6.

212. Prezant B, Weekes DM, Miller JD (eds). Recognition, evaluation, and control of indoor mold. *American Industrial Hygiene Association*; 2008.

213. Review of fungal outbreaks and infection prevention in healthcare settings during construction and renovation. *Clinical Infectious Diseases*. 2015;61(3):433-44.

214. Rhame FS, Streifel AJ, Kersey Jr JH, McGlave PB. Extrinsic risk factors for pneumonia in the patient at high risk of infection. *American Journal of Medicine*. 1984;76(5):42–52.

215. Lutz BD, Jin J, Rinaldi MG, Wickes BL, Huycke MM. Outbreak of invasive *Aspergillus* infection in surgical patients, associated with a contaminated air-handling system. *Clinical Infectious Diseases.* 2003;37(6):786–93.

216. Lee LD, Berkheiser M, Jiang Y, Hackett B, Hachem RY, Chemaly RF, et al. Risk of bioaerosol contamination with Aspergillus species before and after cleaning in rooms filtered with high-efficiency particulate air filters that house patients with hematologic malignancy. *Infection Control and Hospital Epidemiology*. 2007;28(9):1066–70.

217. Diba K, Jangi F, Makhdoomi K, Moshiri N, Mansouri F. *Aspergillus* diversity in the environments of nosocomial infection cases at a university hospital. *Journal of Medicine and Life*. 2019;12(2):128.

218. McCarty JM, Flam MS, Pullen G, Jones R, Kassel SH. Outbreak of primary cutaneous aspergillosis related to intravenous arm boards. *The Journal of pediatrics* 1986;108(5 Pt 1):721-4.

219. Anaissie EJ, Stratton SL, Dignani MC, Summerbell RC, Rex JH, Monson TP, et al. Pathogenic *Aspergillus* species recovered from a hospital water system: a 3-year prospective study. *Clinical Infectious Diseases*. 2002;34(6):780–9.

220. Schmitt HJ, Blevins A, Sobeck K, Armstrong D. *Aspergillus* species from hospital air and from patients. *Mycoses*. 1990;33(11–12):539–41.

221. Brakhage AA, Langfelder K. Menacing mold: the molecular biology of *Aspergillus fumigatus*. *Annual Reviews in Microbiology*. 2002;56(1):433–55.

222. Zhang J, Debets AJM, Verweij PE, Melchers WJG, Zwaan BJ, Schoustra SE. Asexual sporulation facilitates adaptation: The emergence of azole resistance in *Aspergillus fumigatus*. *Evolution (N Y).* 2015;69(10):2573–86.

223. Zhang J, Snelders EE, Zwaan BJ, Schoustra SE, Kuijper EJ, Arendrup MC, et al. Relevance of heterokaryosis for adaptation and azole-resistance development in *Aspergillus fumigatus. Proceedings of the Royal Society B*. 2019;286(1896):20182886.

224. O'Gorman CM, Fuller HT, Dyer PS. Discovery of a sexual cycle in the opportunistic fungal pathogen *Aspergillus fumigatus*. *Nature*. 2009;457(7228):471–4.

225. Dyer PS, Ingram DS, Johnstone K. The control of sexual morphogenesis in the Ascomycotina. *Biological Reviews*. 1992;67(4):421–58.

226. Barton NH, Charlesworth B. Why sex and recombination? *Science*. 1998;281(5385):1986-90.

227. McDonald MJ, Rice DP, Desai MM. Sex speeds adaptation by altering the dynamics of molecular evolution. *Nature*. 2016;531(7593):233–6.

228. Turgeon BG, Yoder OC. Proposed nomenclature for mating type genes of filamentous ascomycetes. *Fungal Genetics and Biology*. 2000;1(31):1-5.

229. Coppin E, Debuchy R, Arnaise S, Picard M. Mating types and sexual development in filamentous ascomycetes. *Microbiology and molecular biology reviews*. 1997;61(4):411–28.

230. Lee SC, Ni M, Li W, Shertz C, Heitman J. The evolution of sex: a perspective from the fungal kingdom. *Microbiology and molecular biology reviews*. 2010;74(2):298–340.

231. Zhang J, Snelders E, Zwaan BJ, Schoustra SE, Meis JF, Van Dijk K, et al. A novel environmental azole resistance mutation in *Aspergillus fumigatus* and a possible role of sexual reproduction in its emergence. *mBio*. 2017;8(3):10-128

232. Zhang J, Debets AJM, Verweij PE, Snelders E. Azole-resistance development; how the *Aspergillus fumigatus* lifecycle defines the potential for adaptation. *Journal of Fungi*. 2021;7(8):599.

233. Pontecorvo G. Non-random distribution of multiple mitotic crossing-over among nuclei of heterozygous diploid *Aspergillus*. *Nature*. 1952;170(4318):204–5.

234. Strømnæs Ø, Garber ED. Heterocaryosis and the parasexual cycle in *Aspergillus fumigatus. Genetics*. 1963;48(5):653.

235. Engel T, Verweij PE, Van Den Heuvel J, Wangmo D, Zhang J, Debets AJM, et al. Parasexual recombination enables *Aspergillus fumigatus* to persist in cystic fibrosis. *ERJ Open Research*. 2020;6(4):20-20.

236. Saupe SJ. Molecular genetics of heterokaryon incompatibility in filamentous ascomycetes. *Microbiology and molecular biology reviews*. 2000;64(3):489–502.

237. Bhargava V, Tomashefski Jr JF, Stern RC, Abramowsky CR. The pathology of fungal infection and colonization in patients with cystic fibrosis. *Human Pathology*. 1989;20(10):977–86.

238. Kaur S, Singh S. Biofilm formation by *Aspergillus fumigatus*. *Medical Mycology*. 2014;52(1):2–9.

239. Meletiadis J, Antachopoulos C, Stergiopoulou T, Pournaras S, Roilides E, Walsh TJ. Differential fungicidal activities of amphotericin B and voriconazole against *Aspergillus* species determined by microbroth methodology. *Antimicrobial Agents and Chemotherapy*. 2007;51(9):3329–37.

240. Carolus H, Pierson S, Lagrou K, Van Dijck P. Amphotericin B and other polyenes—Discovery, clinical use, mode of action and drug resistance. *Journal of Fungi*. 2020;6(4):321.

241. Harbarth S, Pestotnik SL, Lloyd JF, Burke JP, Samore MH. The epidemiology of nephrotoxicity associated with conventional amphotericin B therapy. *American Journal of Medicine*. 2001;111(7):528–34.

242. Wingard JR, Kubilis P, Lee L, Yee G, White M, Louise W, et al. Clinical significance of nephrotoxicity in patients treated with amphotericin B for suspected or proven aspergillosis. *Clinical infectious diseases*. 1999;29(6):1402–7.

243. Deray G. Amphotericin B nephrotoxicity. Journal of antimicrobial chemotherapy. 2002;49:37–41

244. Fanos V, Cataldi L. Amphotericin B-induced nephrotoxicity: a review. *Journal of chemotherapy*. 2000;12(6):463–70.

245. Heykants J, Van Peer A, Van de Velde V, Van Rooy P, Meuldermans W, Lavrijsen K, et al. The clinical pharmacokinetics of itraconazole: an overview. *Mycoses*. 1989;32:67–87.

246. Tucker RM, Denning DW, Arathoon EG, Rinaldi MG, Stevens DA. Itraconazole therapy for nonmeningeal coccidioidomycosis: clinical and laboratory observations. *Journal of the American Academy of Dermatology*. 1990;23(3):593–601.

247. Denning DW, Venkateswarlu K, Oakley KL, Anderson MJ, Manning NJ, Stevens DA, et al. Itraconazole resistance in *Aspergillus fumigatus*. *Antimicrobial Agents and Chemotherapy*. 1997;41(6):1364–8.

248. Alqahtani MS, Kazi M, Alsenaidy MA, Ahmad MZ. Advances in oral drug delivery. *Frontiers in Pharmacology*. 2021;12:618411.

249. Verweij PE, Arendrup MC, Alastruey-Izquierdo A, Gold JAW, Lockhart SR, Chiller T, et al. Dual use of antifungals in medicine and agriculture: How do we help prevent resistance developing in human pathogens? *Drug Resistance Updates*. 2022;65:100885.

250. Kharb R, Sharma PC, Yar MS. Pharmacological significance of triazole scaffold. *Journal of Enzyme Inhibition and Medicinal Chemistry.* 2011;26(1):1–21.

251. Nywening A V, Rybak JM, Rogers PD, Fortwendel JR. Mechanisms of triazole resistance in *Aspergillus fumigatus. Environmental Microbiology*. 2020;22(12):4934–52.

252. Verweij PE, Chowdhary A, Melchers WJG, Meis JF. Azole resistance in aspergillus fumigatus: Can we retain the clinical use of mold-active antifungal azoles? *Clinical Infectious Diseases*. 2016; 1;62(3):362-8.

253. Verweij PE, Snelders E, Kema GH, Mellado E, Melchers WJ. Azole resistance in Aspergillus fumigatus: a side-effect of environmental fungicide use? *The Lancet Infectious Diseases*. 2009. 1;9(12):789-95.

254. Snelders E, Huis In't Veld RAG, Rijs AJMM, Kema GHJ, Melchers WJG, Verweij PE. Possible environmental origin of resistance of *Aspergillus fumigatus* to medical triazoles. *Applied and Environmental Microbiology*. 2009 Jun 15;75(12):4053–7.

255. Parker JE, Warrilow AGS, Price CL, Mullins JGL, Kelly DE, Kelly SL. Resistance to antifungals that target CYP51. *Journal of Chemical Biology*. 2014;7:143–61.

256. Bossche H Vanden, Koymans L, Moereels H. P450 inhibitors of use in medical treatment: Focus on mechanisms of action. *Pharmacology and Therapeutics*. 1995;67(1):79-100.

257. Guegan H, Prat E, Robert-Gangneux F, Gangneux JP. Azole resistance in *Aspergillus fumigatus*: a five-year follow up experience in a tertiary hospital with a special focus on cystic fibrosis. *Frontiers in Cellular Infection and Microbiology*. 2021;10:613774.

258. Livengood SJ, Drew RH, Perfect JR. Combination therapy for invasive fungal infections. *Current Fungal Infection Reports*. 2020;14:40–9.

259. Chen SCA, Slavin MA, Sorrell TC. Echinocandin antifungal drugs in fungal infections: a comparison. *Drugs*. 2011;71:11–41.

260. Camps SMT, van der Linden JWM, Li Y, Kuijper EJ, van Dissel JT, Verweij PE, et al. Rapid induction of multiple resistance mechanisms in Aspergillus fumigatus during azole therapy: a case study and review of the literature. *Antimicrobial Agents and Chemotherapy*. 2012;56(1):10–6.

261. Howard SJ, Cerar D, Anderson MJ, Albarrag A, Fisher MC, Pasqualotto AC, et al. Frequency and evolution of azole resistance in *Aspergillus fumigatus* associated with treatment failure. *Emerging Infectious Diseases*. 2009;15(7):1068.

262. Chen J, Li H, Li R, Bu D, Wan Z. Mutations in the cyp51A gene and susceptibility to itraconazole in *Aspergillus fumigatus* serially isolated from a patient with lung aspergilloma. *Journal of Antimicrobial Chemotherapy*. 2005;55(1):31–7.

263. Verweij PE, Zhang J, Debets AJM, Meis JF, van de Veerdonk FL, Schoustra SE, et al. In-host adaptation and acquired triazole resistance in *Aspergillus fumigatus*: a dilemma for clinical management. *Lancet Infectious Diseases*. 2016;16(11):e251–60.

264. Howard SJ, Pasqualotto AC, Anderson MJ, Leatherbarrow H, Albarrag AM, Harrison E, et al. Major variations in *Aspergillus fumigatus* arising within aspergillomas in chronic pulmonary aspergillosis. *Mycoses*. 2013;56(4):434–41.

265. Di Paolo M, Hewitt L, Nwankwo E, Ni M, Vidal-Diaz A, Fisher MC, et al. A retrospective 'real-world' cohort study of azole therapeutic drug monitoring and evolution of antifungal resistance in cystic fibrosis. *JAC Antimicrobial Resistance*. 2021;3(1):dlab026.

266. Dauchy C, Bautin N, Nseir S, Reboux G, Wintjens R, Le Rouzic O, et al. Emergence of *Aspergillus fumigatus* azole resistance in azole-naïve patients with chronic obstructive pulmonary disease and their homes. *Indoor Air*. 2018;28(2):298–306.

267. van der Linden JWM, Snelders E, Kampinga GA, Rijnders BJA, Mattsson E, Debets-Ossenkopp YJ, et al. Clinical implications of azole resistance in Aspergillus fumigatus, The Netherlands, 2007-2009. *Emerging Infectious Diseases*. 2011;17(10):1846

268. van der Linden JWM, Camps SMT, Kampinga GA, Arends JPA, Debets-Ossenkopp YJ, Haas PJA, et al. Aspergillosis due to voriconazole highly resistant Aspergillus fumigatus and recovery of genetically related resistant isolates from domiciles. *Clinical infectious diseases*. 2013;57(4):513–20.

269. Steinmann J, Hamprecht A, Vehreschild M, Cornely OA, Buchheidt D, Spiess B, et al. Emergence of azole-resistant invasive aspergillosis in HSCT recipients in Germany. *Journal of Antimicrobial Chemotherapy*. 2015;70(5):1522–6.

270. Chowdhary A, Sharma C, Kathuria S, Hagen F, Meis JF. Prevalence and mechanism of triazole resistance in Aspergillus fumigatus in a referral chest hospital in Delhi, India and an update of the situation in Asia. *Frontiers in Microbiology*. 2015;6:428.

271. Lestrade PP, Bentvelsen RG, Schauwvlieghe AFAD, Schalekamp S, van der Velden WJFM, Kuiper EJ, et al. Voriconazole resistance and mortality in invasive aspergillosis: a multicenter retrospective cohort study. *Clinical Infectious Diseases*. 2019;68(9):1463–71.

272. Snelders E, Camps SMT, Karawajczyk A, Schaftenaar G, Kema GHJ, van der Lee HA, et al. Triazole fungicides can induce cross-resistance to medical triazoles in Aspergillus fumigatus. *PLoS One*. 2012;7(3):e31801.

273. Jørgensen LN, Heick TM. Azole use in agriculture, horticulture, and wood preservation–is it indispensable? *Frontiers in Cellular and Infection Microbiology*. 2021;11:730297.

274. Fungicide Resistance Action Committee. www.frac.info [Date Accessed: 28th May 2022]

275. Martínez-Matías N, Rodríguez-Medina JR. Fundamental concepts of azole compounds and triazole antifungals: A beginner's review. *Puerto Rico Health Sciences Journal*. 2018;37(3).

276. Chen ZF, Ying GG, Ma YB, Lai HJ, Chen F, Pan CG. Typical azole biocides in biosolid-amended soils and plants following biosolid applications. *Journal of Agricultural and Food Chemistry*. 2013;61(26):6198–206.

277. Shelton JMG, Collins R, Uzzell CB, Alghamdi A, Dyer PS, Singer AC, et al. Citizen science surveillance of triazole-resistant *Aspergillus fumigatus* in United Kingdom residential garden soils. *Applied and Environmental Microbiology*. 2022;88(4):e02061-21.

278. Rivero-Menendez O, Alastruey-Izquierdo A, Mellado E, Cuenca-Estrella M. Triazole resistance in Aspergillus spp.: a worldwide problem? *Journal of Fungi*. 2016;2(3):21.

279. Chowdhary A, Sharma C, Meis JF. Azole-resistant aspergillosis: Epidemiology, molecular mechanisms, and treatment. *Journal of Infectious Diseases*. 2017;216(3):S436–44.

280. Burks C, Darby A, Gómez Londoño L, Momany M, Brewer MT. Azole-resistant *Aspergillus fumigatus* in the environment: Identifying key reservoirs and hotspots of antifungal resistance. *PLoS Pathogogens*. 2021;17(7):e1009711.

281. Resendiz Sharpe A, Lagrou K, Meis JF, Chowdhary A, Lockhart SR, Verweij PE, et al. Triazole resistance surveillance in *Aspergillus fumigatus*. *Medical Mycology*. 2018;56(suppl.1):S83–92.

282. Meis JF, Chowdhary A, Rhodes JL, Fisher MC, Verweij PE. Clinical implications of globally emerging azole resistance in *Aspergillus fumigatus*. *Philosophical Transactions of the Royal Society B*: *Biological Sciences*. 2016;371(1709):20150460.

283. Rocchi S, Daguindau E, Grenouillet F, Deconinck E, Bellanger AP, Garcia-Hermoso D, et al. Azole-resistant *Aspergillus fumigatus* isolate with the TR_{34}/L98H mutation in both a fungicide-sprayed field and the lung of a hematopoietic stem cell transplant recipient with invasive aspergillosis. *Journal of Clinical Microbiology*. 2014;52(5):1724–6.

284. Jeanvoine A, Rocchi S, Reboux G, Grenouillet F, Benassarou M, Chirouze C, et al. Sinus aspergillosis due to an azole-resistant *Aspergillus fumigatus* strain carrying the TR_{34}/L98H mutation in immunocompetent host. *Infectious Diseases*. 2016;48(10):765–6.

285. Monzo-Gallo P, Alastruey-Izquierdo A, Chumbita M, Aiello TF, Gallardo-Pizarro A, Peyrony O, et al. Report of three azole-resistant *Aspergillus fumigatus* cases with TR_{34}/L98H mutation in hematological patients in Barcelona, Spain. *Infection*. 2024;1–6.

286. Gonzalez-Jimenez I, Lucio J, Menéndez-Fraga MD, Mellado E, Peláez T. Hospital environment as a source of azole-resistant *Aspergillus fumigatus* strains with TR_{34}/L98H and G448S *cyp51a* mutations. *Journal of Fungi*. 2021;7(1):22.

287. Risum M, Hare RK, Gertsen JB, Kristensen L, Johansen HK, Helweg-Larsen J, et al. Azole-resistant *Aspergillus fumigatus* among Danish cystic fibrosis patients: increasing prevalence and dominance of TR_{34}/L98H. *Frontiers inf Microbiology*. 2020;11:1850.

288. Lemaire B, Normand AC, Forel JM, Cassir N, Piarroux R, Ranque S. Hospitalized patient as source of *Aspergillus fumigatus*, 2015. *Emerging Infectious Diseases*. 2018;24(8):1524.

289. Engel TGP, Erren E, Vanden Driessche KSJ, Melchers WJG, Reijers MH, Merkus P, et al. Aerosol transmission of *Aspergillus fumigatus* in cystic fibrosis patients in the Netherlands. *Emerging Infectious Diseases.* 2019;25(4):797–9.

290. Pegues DA, Lasker BA, McNeil MM, Hamm PM, Lundal JL, Kubak BM. Cluster of cases of invasive aspergillosis in a transplant intensive care unit: evidence of person-to-person airborne transmission. *Clinical infectious diseases*. 2002;34(3):412–6.

291. Arastehfar A, Gabaldón T, Garcia-Rubio R, Jenks JD, Hoenigl M, Salzer HJF, et al. Drug-resistant fungi: an emerging challenge threatening our limited antifungal armamentarium. *Antibiotics.* 2020;9(12):877.

292. Bueid A, Howard SJ, Moore CB, Richardson MD, Harrison E, Bowyer P, et al. Azole antifungal resistance in *Aspergillus fumigatus*: 2008 and 2009. *Journal of Antimicrobial Chemotherapy*. 2010;65(10):2116–8.

293. Buil JB, Snelders E, Denardi LB, Melchers WJG, Verweij PE. Trends in azole resistance in *Aspergillus fumigatus*, the Netherlands, 1994–2016. *Emerging Infectious Diseases*. 2019;25(1):176.

294. Lestrade PPA, Meis JF, Melchers WJG, Verweij PE. Triazole resistance in *Aspergillus fumigatus:* recent insights and challenges for patient management. *Clinical Microbiology and Infection.* 2019;25(7):799–806.

295. Wiederhold NP. Epidemiology and Prevalence of Azole-Resistant *Aspergillus fumigatus*: What Is Our Understanding of the Situation? *Current Fungal Infect Reports*. 2023;17(3):177–87.

296. Van der Linden JWM, Arendrup MC, Warris A, Lagrou K, Pelloux H, Hauser PM, et al. Prospective multicenter international surveillance of azole resistance in *Aspergillus fumigatus. Emerging Infectious Diseases*. 2015;21(6):1041.

297. Pfaller MA, Carvalhaes CG, Messer SA, Rhomberg PR, Castanheira M. In vitro activity of posaconazole and comparators versus opportunistic filamentous fungal pathogens globally collected during 8 years. *Diagnostic Microbiology and Infectious Diseases*. 2021;101(3):115473.

298. Vermeulen E, Lagrou K, Verweij PE. Azole resistance in *Aspergillus fumigatus*: A growing public health concern. *Current Opinion in Infectious Diseases*. 2013;26(6):493–500.

299. Snelders E, van der Lee HAL, Kuijpers J, Rijs AJMM, Varga J, Samson RA, et al. Emergence of azole resistance in *Aspergillus fumigatus* and spread of a single resistance mechanism. *PLoS Medicine.* 2008;5(11):e219.

300. Heo ST, Tatara AM, Jiménez-Ortigosa C, Jiang Y, Lewis RE, Tarrand J, et al. Changes in in vitro susceptibility patterns of *Aspergillus* to triazoles and correlation with aspergillosis outcome in a tertiary care cancer center, 1999–2015. *Clinical Infectious Diseases*. 2017;65(2):216–25.

301. Abdolrasouli A, Scourfield A, Rhodes J, Shah A, Elborn JS, Fisher MC, et al. High prevalence of triazole resistance in clinical *Aspergillus fumigatus* isolates in a specialist cardiothoracic centre. *International Journal of Antimicrobial Agents*. 2018 Nov 1;52(5):637–42.

302. Lestrade PPA, Buil JB, van Der Beek MT, Kuijper EJ, van Dijk K, Kampinga GA, et al. Paradoxal trends in azole-resistant Aspergillus fumigatus in a national multicenter surveillance program, the Netherlands, 2013–2018. *Emerging Infectious Diseases.* 2020;26(7):1447.

303. Public Health England. English surveillance programme for antimicrobial utilisation and resistance (ESPAUR). 2017;1–143.

304. Lavergne RA, Morio F, Danner-Boucher I, Horeau-Langlard D, David V, Hagen F, et al. One year prospective survey of azole resistance in *Aspergillus fumigatus* at a French cystic fibrosis reference centre: prevalence and mechanisms of resistance. *Journal of Antimicrobial Chemotherapy.* 2019;74(7):1884–9.

305. Seufert R, Sedlacek L, Kahl B, Hogardt M, Hamprecht A, Haase G, et al. Prevalence and characterization of azole-resistant Aspergillus fumigatus in patients with cystic fibrosis: a prospective multicentre study in Germany. *Journal of Antimicrobial Chemotherapy*. 2018;73(8):2047–53.

306. Amorim A, Guedes-Vaz L, Araujo R. Susceptibility to five antifungals of *Aspergillus fumigatus* strains isolated from chronically colonised cystic fibrosis patients receiving azole therapy. *International Journal of Antimicrobial Agents*. 2010;35(4):396–9.

307. Burgel PR, Baixench MT, Amsellem M, Audureau E, Chapron J, Kanaan R, et al. High prevalence of azole-resistant *Aspergillus fumigatus* in adults with cystic fibrosis exposed to itraconazole. *Antimicrobial Agents and Chemotherapy*. 2012;56(2):869–74.

308. Tseng HK, Perfect JR. Strategies to manage antifungal drug resistance. *Expert Opinion in Pharmacotherapy*. 2011;12(2):241–56.

309. Arvanitis M, Anagnostou T, Fuchs BB, Caliendo AM, Mylonakis E. Molecular and nonmolecular diagnostic methods for invasive fungal infections. Clin Microbiol Rev. 2014;27(3):490–526.

310. Miyazaki T, Kohno S, Mitsutake K, Maesaki S, Tanaka K ichi, Ishikawa N, et al. Plasma (1--> 3)-beta-D-glucan and fungal antigenemia in patients with candidemia, aspergillosis, and cryptococcosis. J Clin Microbiol. 1995;33(12):3115–8.

311. Klont RR, Mennink-Kersten MASH, Verweij PE. Utility of *Aspergillus* antigen detection in specimens other than serum specimens. *Clinical Infectious Diseases*. 2004;39(10):1467–74.

312. Martin-Souto L, Buldain I, Areitio M, Aparicio-Fernandez L, Antoran A, Bouchara JP, et al. ELISA test for the serological detection of Scedosporium/Lomentospora in Cystic Fibrosis patients. Front Cell Infect Microbiol. 2020;10:602089.

313. Page ID, Baxter C, Hennequin C, Richardson MD, van Hoeyveld E, van Toorenenbergen AW, et al. Receiver operating characteristic curve analysis of four Aspergillus-specific IgG assays for the diagnosis of chronic pulmonary aspergillosis. Diagn Microbiol Infect Dis. 2018;91(1):47–51.

314. Ramanan P, Wengenack NL, Theel ES. Laboratory diagnostics for fungal infections: a review of current and future diagnostic assays. Clin Chest Med. 2017;38(3):535–54.

315. Andes DR, Ghannoum MA, Mukherjee PK, Kovanda LL, Lu Q, Jones ME, et al. Outcomes by MIC values for patients treated with isavuconazole or voriconazole for invasive aspergillosis in the phase 3 SECURE and vital trials. Antimicrobial Agents and Chemotherapy. 2019;63(1):10-128.

316. Buil JB, Van Der Lee HAL, Rijs AJMM, Zoll J, Hovestadt JAMF, Melchers WJG, et al. Single-center evaluation of an agar-based screening for azole resistance in *Aspergillus fumigatus* by using VIPcheck. *Antimicrobial Agents and Chemotherapy*. 2017;61(12).

317. Langridge PJ, Sheehan RL, Denning DW. Microbial yield from physiotherapy assisted sputum production in respiratory outpatients. *BMC Pulmonary Medicine*. 2016;16:1–8.

318. Morton CO, White PL, Barnes RA, Klingspor L, Cuenca-Estrella M, Lagrou K, et al. Determining the analytical specificity of PCR-based assays for the diagnosis of IA: What is *Aspergillus*? *Medical Mycology.* 2017;55(4):402–13.

319. White PL, Alanio A, Brown L, Cruciani M, Hagen F, Gorton R, et al. An overview of using fungal DNA for the diagnosis of invasive mycoses. *Expert Reviews in Molecular Diagnostics*. 2022;22(2):169–84.

320. Carvalho-Pereira J, Fernandes F, Araújo R, Springer J, Loeffler J, Buitrago MJ, et al. Multiplex PCR based strategy for detection of fungal pathogen DNA in patients with suspected invasive fungal infections. *Journal of Fungi*. 2020;6(4):308.

321. Ross IL, Weldhagen GF, Kidd SE. Detection and identification of dermatophyte fungi in clinical samples using a commercial multiplex tandem PCR assay. *Pathology*. 2020;52(4):473–7.

322. Sabino R, Simões H, Veríssimo C. Molecular detection of *Aspergillus*: application of a real-time PCR multiplex assay in tissue samples. *Journal of Fungi*. 2020;6(1):11.

323. Dannaoui E, Gabriel F, Gaboyard M, Lagardere G, Audebert L, Quesne G, et al. Molecular diagnosis of invasive aspergillosis and detection of azole resistance by a newly commercialized PCR kit. *Journal of Clinical Microbiology*. 2017;55(11):3210–8.

324. Pelzer BW, Seufert R, Koldehoff M, Liebregts T, Schmidt D, Buer J, et al. Performance of the AsperGenius® PCR assay for detecting azole resistant *Aspergillus fumigatus* in BAL fluids from allogeneic HSCT recipients: A prospective cohort study from Essen, West Germany. *Medical Mycology.* 2020;58(2):268–71.

325. Singh A, Sharma B, Mahto KK, Meis JF, Chowdhary A. High-frequency direct detection of triazole resistance in *Aspergillus fumigatus* from patients with chronic pulmonary fungal diseases in India. *Journal of Fungi*. 2020;6(2):67.

326. Scharmann U, Kirchhoff L, Hain A, Buer J, Koldehoff M, Steinmann J, et al. Evaluation of three commercial PCR assays for the detection of azole resistant *Aspergillus fumigatus* from respiratory samples of immunocompromised patients. *Journal of Fungi*. 2021;7(2):132

327. Patterson TF, Thompson III GR, Denning DW, Fishman JA, Hadley S, Herbrecht R, et al. Practice guidelines for the diagnosis and management of aspergillosis: 2016 update by the Infectious Diseases Society of America. *Clinical Infectious Diseases*. 2016;63(4):e1–60.

328. Egger M, Jenks JD, Hoenigl M, Prattes J. Blood Aspergillus PCR: the good, the bad, and the ugly. *Journal of Fungi*. 2020;6(1):18.

329. Guegan H, Chevrier S, Belleguic C, Deneuville E, Robert-Gangneux F, Gangneux JP. Performance of molecular approaches for Aspergillus detection and azole resistance surveillance in cystic fibrosis. *Frontiers in Microbiology*. 2018;9(MAR):531.

330. de Groot T, Puts Y, Berrio I, Chowdhary A, Meis JF. Development of Candida auris microsatellite typing and its application on a global collection of isolates*. bioRxiv*. 2019;11(1).

331. de Valk HA, Meis JFGM, Klaassen CHW. Microsatellite based typing of Aspergillus fumigatus: strengths, pitfalls and solutions. *Journal of Microbiological Methods*. 2007;69(2):268–72.

332. Klaassen CHW. MLST versus microsatellites for typing *Aspergillus fumigatus* isolates. *Medical Mycology*. 2009;47(sup1):S27–33.

333. Klaassen CHW, Osherov N. *Aspergillus* strain typing in the genomics era. *Studies in Mycology*. 2007;59:47–51.

334. Duarte-Escalante E, Zúñiga G, Nava Ramírez O, Córdoba S, Refojo N, Arenas R, et al. Population structure and diversity of the pathogenic fungus *Aspergillus fumigatus* isolated from different sources and geographic origins. *Memórias do Instituto Oswaldo Cruz*. 2009;104:427–33.

335. Ashu EE, Hagen F, Chowdhary A, Meis JF, Xu J. Global population genetic analysis *of Aspergillus fumigatus. mSphere*. 2017;2(1):10–1128.

336. Klaassen CHW, Gibbons JG, Fedorova ND, Meis JF, Rokas A. Evidence for genetic differentiation and variable recombination rates among Dutch populations of the opportunistic human pathogen *Aspergillus fumigatus*. Molecular Ecology. 2012;21(1):57–70.

337. Sewell TR, Zhu J, Rhodes J, Hagen F, Meis JF, Fisher MC, et al. Nonrandom distribution of azole resistance across the global population of *Aspergillus fumigatus*. *mBio.* 2019;10(3):e00392-19.

338. Pinholt M, Larner-Svensson H, Littauer P, Moser CE, Pedersen M, Lemming LE, et al. Multiple hospital outbreaks of vanA *Enterococcus faecium* in Denmark, 2012–13, investigated by WGS, MLST and PFGE. *Journal of Antimicrobial Chemotherapy*. 2015;70(9):2474–82.

339. Garcia-Rubio R, Gonzalez-Jimenez I, Lucio J, Mellado E. *Aspergillus fumigatus* Cross-Resistance between Clinical and Demethylase Inhibitor Azole Drugs. *Applied and Environmental Microbiology*. 2021;87(5):1–12.

340. Rhodes J, Abdolrasouli A, Farrer RA, Cuomo CA, Aanensen DM, Armstrong-James D, et al. Genomic epidemiology of the UK outbreak of the emerging human fungal pathogen *Candida auris*. *Emerging Microbes and Infection*. 2018;7(1):1–12.

341. Abdolrasouli A, Rhodes J, Beale MA, Hagen F, Rogers TR, Chowdhary A, et al. Genomic context of azole resistance mutations in *Aspergillus fumigatus* determined using whole-genome sequencing. *mBio*. 2015;6(3):e00536.

342. Vandeputte P, Ghamrawi S, Rechenmann M, Iltis A, Giraud S, Fleury M, et al. Draft genome sequence of the pathogenic fungus *Scedosporium apiospermum*. *Genome Announcements.* 2014;2(5):10–1128.

343. Duvaux L, Shiller J, Vandeputte P, de Bernonville TD, Thornton C, Papon N, et al. Draft genome sequence of the human-pathogenic fungus Scedosporium boydii. *Genome Announcements*. 2017;5(37).

344. Shiller J, Duvaux L, Vandeputte P, Lemaire C, Rougeron A, De Bernonville TD, et al. Draft genome sequence of the environmental fungus *Scedosporium dehoogii*. *Mycopathologia.* 2021;186:889–92.

345. Venice F, Spina F, Davolos D, Ghignone S, Varese GC. The genomes of *Scedosporium* between environmental challenges and opportunism. *IMA Fungus*. 2023;14(1):25.

346. Rhodes J, Beale MA, Vanhove M, Jarvis JN, Kannambath S, Simpson JA, et al. A population genomics approach to assessing the genetic basis of within-host microevolution underlying recurrent cryptococcal meningitis infection. *G3: Genes, Genomes, Genetics*. 2017;7(4):1165–76.

347. Billmyre RB, Clancey SA, Heitman J. Natural mismatch repair mutations mediate phenotypic diversity and drug resistance in *Cryptococcus deuterogattii*. *Elife.* 2017;6:e28802.

348. Stone NRH, Rhodes J, Fisher MC, Mfinanga S, Kivuyo S, Rugemalila J, et al. Dynamic ploidy changes drive fluconazole resistance in human cryptococcal meningitis. *The Journal of Clinical Investigation.* 2019;129(3):999–1014.

349. Farrer RA, Borman AM, Inkster T, Fisher MC, Johnson EM, Cuomo CA. Genomic epidemiology of a *Cryptococcus neoformans* case cluster in Glasgow, Scotland, 2018. *Microbial Genomics*. 2021; *7*(3):000537.

350. Marek C, Croxen MA, Dingle TC, Bharat A, Schwartz IS, Wiens R, et al. The use of genome sequencing to investigate an outbreak of hospital-acquired mucormycosis in transplant patients. *Transplant Infectious Disease*. 2019;21(5):e13163.

351. Garcia-Hermoso D, Criscuolo A, Lee SC, Legrand M, Chaouat M, Denis B, et al. Outbreak of invasive wound mucormycosis in a burn unit due to multiple strains of *Mucor circinelloides f. circinelloides* resolved by whole-genome sequencing. *mBio*. 2018;9(2):e00573-18.

352. Chowdhary A, Kathuria S, Xu J, Sharma C, Sundar G, Singh PK, et al. Clonal Expansion and emergence of environmental multiple-triazole-resistant *Aspergillus fumigatus* strains carrying the TR_{34}/L98H mutations in the *cyp51* gene in India. *PLoS One*. 2012. 28;7(12):e52871

353. Rhodes J, Abdolrasouli A, Dunne K, Sewell TR, Zhang Y, Ballard E, et al. Population genomics confirms acquisition of drug-resistant *Aspergillus fumigatus* infection by humans from the environment. *Nature Microbiology*. 2022;7(5):663–74.

354. Ballard E, Melchers WJG, Zoll J, Brown AJP, Verweij PE, Warris A. In-host microevolution of *Aspergillus fumigatus*: A phenotypic and genotypic analysis. *Fungal Genetics and Biology*. 2018;113:1–13.

355. Souza ACO, Ge W, Wiederhold NP, Rybak JM, Fortwendel JR, Rogers PD. hapE and hmg1 mutations are drivers of cyp51A-independent pan-triazole resistance in an *Aspergillus fumigatus* clinical isolate. *Microbiology Spectrum*. 2023;11(3):e05188-22.

356. Lucio J, Gonzalez-Jimenez I, Roldan A, Amich J, Alcazar-Fuoli L, Mellado E. Importance of the *Aspergillus fumigatus* Mismatch Repair Protein Msh6 in antifungal resistance development. *Journal of Fungi*. 2024;10(3):210.

357. Misas E, Deng JZ, Gold JAW, Gade L, Nunnally NS, Georgacopoulos O, et al. Genomic description of human clinical *Aspergillus fumigatus* isolates, California, 2020. *Medical Mycology*. 2023;61(2):myad012.

358. Hiel SJP, Hendriks ACA, Eijkenboom JJA, Bosch T, Coolen JPM, Melchers WJG, et al. *Aspergillus* outbreak in an Intensive Care Unit: Source analysis with whole genome sequencing and short tandem repeats. *Journal of Fungi*. 2024;10(1):51.

359. Shelton JMG, Rhodes J, Uzzell CB, Hemmings S, Brackin AP, Sewell TR, et al. Citizen science reveals landscape-scale exposures to multiazole-resistant *Aspergillus fumigatus* bioaerosols. *Science Advances*. 2023;9(29):eadh8839.

360. Harris PA, Taylor R, Minor BL, Elliott V, Fernandez M, O'Neal L, et al. The REDCap consortium: building an international community of software platform partners. *Journal of Biomedical Information*. 2019;95:103208.

361. Harris PA, Taylor R, Thielke R, Payne J, Gonzalez N, Conde JG. Research electronic data capture (REDCap)—a metadata-driven methodology and workflow process for providing translational research informatics support. *Journal of Biomedical Information*. 2009;42(2):377–81.

362. Zymo Research. Zymo Research. Genomic DNA Clean & Concentrator®-25 Clean and concentrate large-sized DNA from any enzymatic reaction or impure preparation. Zymo Research. https://files.zymoresearch.com/protocols/_d4064_d4065_genomic_dna_clean_concentrator-25.pdf [Date Accessed 9th March 2022]

363. *GENEWIZ from azenta*. https://www.genewiz.com/en-GB/Public/Services/Sanger-Sequencing/ [Accessed 18th January 2022].

364. Brackin AP, Shelton JMG, Abdolrasouli A, Fisher MC, Sewell TR. A low-cost tebuconazole-Based screening test for azole-resistant *Aspergillus fumigatus*. *Current Protocols in Microbiology.* 2020;58(1):e112.

365. Nierman WC, Pain A, Anderson MJ, Wortman JR, Kim HS, Arroyo J, et al. Genomic sequence of the pathogenic and allergenic filamentous fungus *Aspergillus fumigatus*. *Nature.* 2005;438(7071):1151–6.

366. McKenna A, Hanna M, Banks E, Sivachenko A, Cibulskis K, Kernytsky A, et al. The Genome Analysis Toolkit: a MapReduce framework for analyzing next-generation DNA sequencing data. *Genome Research*. 2010;20(9):1297–303.

367. Li H, Durbin R. Fast and accurate short read alignment with Burrows–Wheeler transform. *Bioinformatics*. 2009;25(14):1754–60.

368. Li H, Handsaker B, Wysoker A, Fennell T, Ruan J, Homer N, et al. The sequence alignment/map format and SAMtools. *Bioinformatics*. 2009;25(16):2078–9.

369. Nash A, Sewell T, Farrer RA, Abdolrasouli A, Shelton JMG, Fisher MC, et al. MARDy: Mycology Antifungal Resistance Database. *Bioinformatics*. 2018;34(18):3233-4.

370. Kozlov AM, Darriba D, Flouri T, Morel B, Stamatakis A. RAxML-NG: a fast, scalable and user-friendly tool for maximum likelihood phylogenetic inference. *Bioinformatics*. 2019;35(21):4453–5.

371. Yu G, Smith DK, Zhu H, Guan Y, Lam TT. ggtree: an R package for visualization and annotation of phylogenetic trees with their covariates and other associated data. *Methods in Ecology and Evolution*. 2017;8(1):28–36.

372. Xu S, Dai Z, Guo P, Fu X, Liu S, Zhou L, et al. ggtreeExtra: compact visualization of richly annotated phylogenetic data. *Molecular Biology and Evolution*. 2021;38(9):4039–42.

373. Jombart T, Kamvar ZN, Collins C, Lustrik R, Beugin MP, Knaus BJ, et al. Package 'adegenet'. Github repository:< https://github com/thibautjombart/adegenet. 2018; [Date Accessed: 28th May 2022]

374. Jombart T. adegenet: a R package for the multivariate analysis of genetic markers. *Bioinformatics.* 2008;24(11):1403–5.

375. Jombart T, Collins C. A tutorial for Discriminant Analysis of Principal Components (DAPC) using adegenet 2.1. 0. Imperial College London; 2015.

376. Jombart T, Collins C. Analysing genome-wide SNP data using adegenet 2.0. 0. 2015.

377. Keller NP. Heterogeneity confounds establishment of "a" model microbial strain. *mBio.* 2017; 8;8(1):10-128.

378. Ries LNA, Steenwyk JL, De Castro PA, De Lima PBA, Almeida F, De Assis LJ, et al. Nutritional heterogeneity among *Aspergillus fumigatus* strains has consequences for virulence in a strain- And host-dependent manner. *Frontiers in Microbiology*. 2019;10:854

379. Kowalski CH, Beattie SR, Fuller KK, McGurk EA, Tang YW, Hohl TM, et al. Heterogeneity among isolates reveals that fitness in low oxygen correlates with *Aspergillus fumigatus* virulence. *mBio.* 2016;7(5):10-1128.

380. Fedorova ND, Khaldi N, Joardar VS, Maiti R, Amedeo P, Anderson MJ, et al. Genomic islands in the pathogenic filamentous fungus Aspergillus fumigatus*. PLoS Genetics*. 2008;4(4):e1000046.

381. Askew DS. Aspergillus fumigatus: virulence genes in a street-smart mold. *Current Opinion in Microbiology*. 2008;11(4): 331-337

382. Johns LE, Goldman GH, Ries LNA, Brown NA. Nutrient sensing and acquisition in fungi: mechanisms promoting pathogenesis in plant and human hosts. *Fungal Biology Reviews*. 2021;36:1–14.

383. He R, Wei P, Odiba AS, Gao L, Usman S, Gong X, et al. Amino sugars influence *Aspergillus fumigatus* cell wall polysaccharide biosynthesis, and biofilm formation through interfering galactosaminogalactan deacetylation. *Carbohydrate Polymers*. 2024;324:121511.

384. Ene I V, Adya AK, Wehmeier S, Brand AC, MacCallum DM, Gow NAR, et al. Host carbon sources modulate cell wall architecture, drug resistance and virulence in a fungal pathogen*. Cell Microbiology.* 2012;14(9):1319–35.

385. Rizzetto L, Giovannini G, Bromley M, Bowyer P, Romani L, Cavalieri D. Strain dependent variation of immune responses to *A. fumigatus*: definition of pathogenic species. *PLoS One.* 2013;8(2):e56651.

386. Kale SD, Ayubi T, Chung D, Tubau-Juni N, Leber A, Dang HX, et al. Modulation of immune signaling and metabolism highlights host and fungal transcriptional responses in mouse models of invasive pulmonary aspergillosis. *Scientific Reports*. 2017;7(1):17096.

387. Barber AE, Sae-Ong T, Kang K, Seelbinder B, Li J, Walther G, et al. *Aspergillus fumigatus* pan-genome analysis identifies genetic variants associated with human infection. *Nature Microbiology*. 2021;6(12):1526–36.

388. Puértolas-Balint F, Rossen JWA, Oliveira dos Santos C, Chlebowicz MMA, Raangs EC, Van Putten ML, et al. Revealing the virulence potential of clinical and environmental *Aspergillus fumigatus* isolates using whole-genome sequencing. *Frontiers in Microbiology*. 2019;10:1970.

389. Arendrup M, Guinea J, Cuenca-Estrella M, Meletiadis J, Mouton J, Lagrou K, et al. EUCAST definitive document e. def 9.3. Method for the determination of broth dilution minimum inhibitory concentrations of antifungal agents for conidia forming moulds*Clinical Microbiology* and *Infection.* 2015;14(10):982–4.

390. Vaas LAI, Sikorski J, Hofner B, Fiebig A, Buddruhs N, Klenk HP, et al. Opm: An R package for analysing OmniLog® phenotype microarray data. *Bioinformatics*. 2013;29(14):1823–4.

391. Kolde R, Kolde MR. Package 'pheatmap'. *R package*. 2015;1(7):790.

392. Pang Z, Chong J, Zhou G, de Lima Morais DA, Chang L, Barrette M, et al. MetaboAnalyst 5.0: narrowing the gap between raw spectra and functional insights. *Nucleic Acids Research.* 2021;49(W1):W388–96.

393. Lind AL, Wisecaver JH, Lameiras C, Wiemann P, Palmer JM, Keller NP, et al. Drivers of genetic diversity in secondary metabolic gene clusters within a fungal species. *PLoS Biology.* 2017;15(11):e2003583.

394. Esteves F, Rueff J, Kranendonk M. The central role of cytochrome P450 in xenobiotic metabolism—a brief review on a fascinating enzyme family. *Journal of Xenobiotics*. 2021;11(3):94–114.

395. Chigu NL, Hirosue S, Nakamura C, Teramoto H, Ichinose H, Wariishi H. Cytochrome P450 monooxygenases involved in anthracene metabolism by the white-rot basidiomycete Phanerochaete chrysosporium. *Applied Microbiology and Biotechnology*. 2010;87:1907–16.

396. Van Bogaert INA, Groeneboer S, Saerens K, Soetaert W. The role of cytochrome P450 monooxygenases in microbial fatty acid metabolism. *FEBS Journal*. 2011;278(2):206–21.

397. Babot ED, Del Río JC, Cañellas M, Sancho F, Lucas F, Guallar V, et al. Steroid hydroxylation by basidiomycete peroxygenases: a combined experimental and computational study. *Applied and Environmental Microbiology*. 2015;81(12):4130–42.

398. Lah L, Podobnik B, Novak M, Korošec B, Berne S, Vogelsang M, et al. The versatility of the fungal cytochrome P450 monooxygenase system is instrumental in xenobiotic detoxification. *Molecular Microbiology* 2011;81(5):1374–89.

399. Joo SH, Keum YS. Oxidative metabolism of quinazoline insecticide fenazaquin by *Aspergillus niger*. *Applied Biological Chemistry*. 2018;61(6):681–7.

400. Bokade P, Purohit HJ, Bajaj A. Myco-remediation of chlorinated pesticides: insights into fungal metabolic system. *Indian Journal of Microbiology*. 2021;61:237–49.

401. Singh N, Kumar A, Sharma B. Role of fungal enzymes for bioremediation of hazardous chemicals. *Recent Advancement in White Biotechnology Through Fungi: Volume 3: Perspective for Sustainable Environments.* 2019;237–56.

402. Kimura M, Kushiro T, Shibuya M, Ebizuka Y, Abe I. Protostadienol synthase from Aspergillus fumigatus: Functional conversion into lanosterol synthase. *Biochemical and Biophysical Research Communications*. 2010;391(1):899–902.

403. Furukawa T, Van Rhijn N, Fraczek M, Gsaller F, Davies E, Carr P, et al. The negative cofactor 2 complex is a key regulator of drug resistance in *Aspergillus fumigatus*. *Nature Communications*. 2020;11(1):427.

404. Wiemann P, Guo CJ, Palmer JM, Sekonyela R, Wang CCC, Keller NP. Prototype of an intertwined secondary-metabolite supercluster. *Proceedings of the National Academy of Sciences*. 2013;110(42):17065–70.

405. Dhingra S, Lind AL, Lin HC, Tang Y, Rokas A, Calvo AM. The fumagillin gene cluster, an example of hundreds of genes under veA control in *Aspergillus fumigatus*. *PLoS One*. 2013;8(10):e77147.

406. Kanno T, Uehara T, Osawa M, Fukumoto H, Mine S, Ueda K, et al. Fumagillin, a potent angiogenesis inhibitor, induces Kaposi sarcoma-associated herpesvirus replication in primary effusion lymphoma cells. *Biochemical and Biophysical Research Communications*. 2015;463(4):1267–72.

407. Ingber D, Fujita T, Kishimoto S, Sudo K, Kanamaru T, Brem H, et al. Synthetic analogues of fumagillin that inhibit angiogenesis and suppress tumour growth. *Nature*. 1990;348(6301):555–7.

408. Guruceaga X, Ezpeleta G, Mayayo E. A possible role for fumagillin in cellular damage during host infection by Aspergillus. *Virulence.* 2018;9(1):1548-1561

409. Bok JW, Chung D, Balajee SA, Marr KA, Andes D, Nielsen KF, et al. GliZ, a transcriptional regulator of gliotoxin biosynthesis, contributes to *Aspergillus fumigatus* virulence. *Infection and Immunity*. 2006;74(12):6761–8.

410. Sutton P, Newcombe NR, Waring P, Müllbacher A. In vivo immunosuppressive activity of gliotoxin, a metabolite produced by human pathogenic fungi. *Infection and Immunity*. 1994;62(4):1192–8.

411. Fitzpatrick LR, Wang J, Le T. In vitro and in vivo effects of gliotoxin, a fungal metabolite. *Digestive Diseases and Sciences*. 2000;45:2327–36.

412. Li H, Dai J, Shi Y, Zhu X, Jia L, Yang Z. Molecular regulatory mechanism of the iron-ion-promoted asexual sporulation of *Antrodia cinnamomea* in submerged fermentation revealed by comparative transcriptomics. *Journal of Fungi*. 2023;9(2):235.

413. Misslinger M, Hortschansky P, Brakhage AA, Haas H. Fungal iron homeostasis with a focus on *Aspergillus fumigatus*. *Biochimica et Biophysica Acta (BBA) - Molecular Cell Research*. 2021;1868(1):118885.

414. Kühbacher A, Peiffer M, Hortschansky P, Merschak P, Bromley MJ, Haas H, et al. Azole resistance-associated regulatory motifs within the promoter of cyp51A in *Aspergillus fumigatus*. *Microbiology Spectrum*. 2022;10(3):e01209-22.

415. Nairz M, Dichtl S, Schroll A, Haschka D, Tymoszuk P, Theurl I, et al. Iron and innate antimicrobial immunity—depriving the pathogen, defending the host. *Journal of Trace Elements in Medicine and Biology.* 2018;48:118–33.

416. Schrettl M, Haas H. Iron homeostasis—Achilles' heel of *Aspergillus fumigatus*? *Current Opinion in Microbiology* 2011;14(4):400–5.

417. Gauthier T, Wang X, Sifuentes Dos Santos J, Fysikopoulos A, Tadrist S, Canlet C, et al. Trypacidin, a spore-borne toxin from *Aspergillus fumigatus*, is cytotoxic to lung cells. *PLoS One*. 2012;7(2):e29906.

418. Mattern DJ, Schoeler H, Weber J, Novohradská S, Kraibooj K, Dahse HM, et al. Identification of the antiphagocytic trypacidin gene cluster in the human-pathogenic fungus *Aspergillus fumigatus*. *Applied Microbiology and Biotechnology*. 2015;99:10151–61.

419. Sharma C, Nelson-Sathi S, Singh A, Pillai MR, Chowdhary A. Genomic perspective of triazole resistance in clinical and environmental *Aspergillus fumigatus* isolates without cyp51A mutations. *Fungal Genetics and Biology*. 2019;132:103265.

420. Thau N, Monod M, Crestani B, Rolland C, Tronchin G, Latge JP, et al. Rodletless mutants of *Aspergillus fumigatus*. *Infection and Immunity*. 1994;62(10):4380–8.

421. Tsigos I, Martinou A, Kafetzopoulos D, Bouriotis V. Chitin deacetylases: new, versatile tools in biotechnology. *Trends in Biotechnology*. 2000;18(7):305–12.

422. Hoell IA, Vaaje-Kolstad G, Eijsink VGH. Structure and function of enzymes acting on chitin and chitosan. *Biotechnology & Genetic Engineering Reviews*. 2010;27(1):331–66.

423. Tada R, Latge JP, Aimanianda V. Undressing the fungal cell wall/cell membrane-the antifungal drug targets. *Current Pharmaceutical Design*. 2013;19(20):3738–47.

424. Rementeria A, López-Molina N, Ludwig A, Vivanco AB, Bikandi J, Pontón J, et al. Genes and molecules involved in *Aspergillus fumigatus* virulence. *Revista Iberoamericana de Micología*. 2005;22(1):1–23.

425. Gravelat FN, Doedt T, Chiang LY, Liu H, Filler SG, Patterson TF, et al. In vivo analysis of *Aspergillus fumigatus* developmental gene expression determined by real-time reverse transcription-PCR. *Infection and Immunity*. 2008;76(8):3632–9.

426. Pott GB, Miller TK, Bartlett JA, Palas JS, Selitrennikoff CP. The isolation of FOS-1, a gene encoding a putative two-component histidine kinase from *Aspergillus fumigatus*. *Fungal Genetics and Biology*. 2000;31(1):55–67.

427. Gehrke A, Heinekamp T, Jacobsen ID, Brakhage AA. Heptahelical receptors GprC and GprD of *Aspergillus fumigatus* are essential regulators of colony growth, hyphal morphogenesis, and virulence. *Applied and Environmental Microbiology*. 2010;76(12):3989–98.

428. Alves de Castro P, Figueiredo Pinzan C, Dos Reis TF, Valero C, Van Rhijn N, Menegatti C, et al. *Aspergillus fumigatus* mitogen-activated protein kinase MpkA is involved in gliotoxin production and self-protection. *Nature Communications*. 2024;15(1):33.

429. Jain R, Valiante V, Remme N, Docimo T, Heinekamp T, Hertweck C, et al. The MAP kinase MpkA controls cell wall integrity, oxidative stress response, gliotoxin production and iron adaptation in *Aspergillus fumigatus*. *Molecular Microbiology*. 2011;82(1):39–53.

430. Kotz A, Wagener J, Engel J, Routier FH, Echtenacher B, Jacobsen I, et al. Approaching the secrets of N-glycosylation in *Aspergillus fumigatus*: characterization of the AfOch1 protein. *PLoS One*. 2010;5(12):e15729.

431. Romano J, Nimrod G, Ben-Tal N, Shadkchan Y, Baruch K, Sharon H, et al. Disruption of the Aspergillus fumigatus ECM33 homologue results in rapid conidial germination, antifungal resistance and hypervirulence. *Microbiology*. 2006;152(7):1919–28.

432. Zhu Y, Liu T, Wang Y, Chen G, Fang X, Zhou G, et al. ChsA, a Class Ⅱ Chitin Synthase, Contributes to Asexual Conidiation, Mycelial Morphology, Cell Wall Integrity, and the Production of Enzymes and Organic Acids in *Aspergillus niger*. *Journal of Fungi*. 2023;9(8):801.

433. Kamath MM, Lightfoot JD, Adams EM, Kiser RM, Wells BL, Fuller KK. The *Aspergillus fumigatus* UPR is variably activated across nutrient and host environments and is critical for the establishment of corneal infection. *PLoS Pathogens*. 2023;19(10):e1011435.

434. Morelli KA, Kerkaert JD, Cramer RA. *Aspergillus fumigatus* biofilms: Toward understanding how growth as a multicellular network increases antifungal resistance and disease progression. *PLoS Pathogens*. 2021;17(8):e1009794.

435. Vickers I, Reeves EP, Kavanagh KA, Doyle S. Isolation, activity and immunological characterisation of a secreted aspartic protease, CtsD, from *Aspergillus fumigatus*. *Protein Expression and Purification.* 2007;53(1):216–24.

436. Beattie SR, Mark KMK, Thammahong A, Ries LNA, Dhingra S, Caffrey-Carr AK, et al. Filamentous fungal carbon catabolite repression supports metabolic plasticity and stress responses essential for disease progression. *PLOS Pathogens*. 2017;13(4):e1006340.

437. Ansari S, Kumar V, Bhatt DN, Irfan M, Datta A. N-acetylglucosamine sensing and metabolic engineering for attenuating human and plant pathogens. *Bioengineering*. 2022;9(2):64.

438. d'Enfert C, Bonini BM, Zapella PDA, Fontaine T, Da Silva AM, Terenzi HF. Neutral trehalases catalyse intracellular trehalose breakdown in the filamentous fungi *Aspergillus nidulans* and *Neurospora crassa*. *Molecular Microbiology*. 1999;32(3):471–83.

439. Krijgsheld P, Bleichrodt R v, Van Veluw GJ, Wang F, Müller WH, Dijksterhuis J, et al. Development in Aspergillus. Studies in Mycology. 2013;74(1):1–29.

440. Araújo CAS, Ferreira PC, Pupin B, Dias LP, Avalos J, Edwards J, et al. Osmotolerance as a determinant of microbial ecology: A study of phylogenetically diverse fungi. *Fungal Biology*. 2020;124(5):273–88.

441. Massip-Copiz MM, Santa-Coloma TA. Extracellular pH and lung infections in cystic fibrosis. *European Journal of Cell Biology*. 2018;97(6):402–10.

442. Morrison CB, Markovetz MR, Ehre C. Mucus, mucins, and cystic fibrosis. *Pediatric Pulmonology*. 2019;54:S84–96.

443. Rohlfs M. Fungal secondary metabolite dynamics in fungus–grazer interactions: novel insights and unanswered questions. *Frontiers in Microbiology*. 2015;5:788.

444. Faure E, Kwong K, Nguyen D. Pseudomonas aeruginosa in Chronic Lung Infections: How to Adapt Within the Host? *Frontiers in Immunology*. 2018;22;9:2416

445. Hokken MWJ, Zoll J, Coolen JPM, Zwaan BJ, Verweij PE, Melchers WJG. Phenotypic plasticity and the evolution of azole resistance in *Aspergillus fumigatus*; an expression profile of clinical isolates upon exposure to itraconazole. *BMC Genomics*. 2019;20:1–17.

446. Takeda K, Suzuki J, Watanabe A, Arai T, Koiwa T, Shinfuku K, et al. High detection rate of azole-resistant *Aspergillus fumigatus* after treatment with azole antifungal drugs among patients with

chronic pulmonary aspergillosis in a single hospital setting with low azole resistance. *Medical Mycology*. 2021;59(4):327–34.

447. Blair JMA, Webber MA, Baylay AJ, Ogbolu DO, Piddock LJV. Molecular mechanisms of antibiotic resistance. *Nature Reviews Microbiology*. 2015;13(1):42–51.

448. Mellado E, Garcia-Effron G, Alcazar-Fuoli L, Cuenca-Estrella M, Rodriguez-Tudela JL. Substitutions at methionine 220 in the 14α-sterol demethylase (Cyp51A) of *Aspergillus fumigatus* are responsible for resistance in vitro to azole antifungal drugs. *Antimicrobial Agents and Chemotherapy*. 2004;48(7):2747–50.

449. Diaz-Guerra TM, Mellado E, Cuenca-Estrella M, Rodriguez-Tudela JL. A point mutation in the 14α-sterol demethylase gene cyp51A contributes to itraconazole resistance in *Aspergillus fumigatus*. *Antimicrobial Agents and Chemotherapy*. 2003;47(3):1120–4.

450. Monk BC, Tomasiak TM, Keniya M V, Huschmann FU, Tyndall JDA, O'Connell III JD, et al. Architecture of a single membrane spanning cytochrome P450 suggests constraints that orient the catalytic domain relative to a bilayer. *Proceedings of the National Academy of Sciences*. 2014;111(10):3865–70.

451. Snelders E, Karawajczyk A, Schaftenaar G, Verweij PE, Melchers WJG. Azole resistance profile of amino acid changes in *Aspergillus fumigatus* CYP51A based on protein homology modeling. *Antimicrobial Agents and Chemotherapy*. 2010;54(6):2425–30.

452. Chen L, Krekels EHJ, Verweij PE, Buil JB, Knibbe CAJ, Brüggemann RJM. Pharmacokinetics and pharmacodynamics of posaconazole. *Drugs*. 2020;80(7):671–95.

453. Markussen T, Marvig RL, Gómez-Lozano M, Aanæs K, Burleigh AE, Høiby N, et al. Environmental heterogeneity drives within-host diversification and evolution of *Pseudomonas aeruginosa*. *mBio*. 2014;5(5):10–1128.

454. Prigitano A, Esposto MC, Biffi A, De Lorenzis G, Favuzzi V, Koncan R, et al. Triazole resistance in *Aspergillus fumigatus* isolates from patients with cystic fibrosis in Italy. *Journal of Cystic Fibrosis*. 2017;16(1):64–9.

454. Chowdhary A, Kathuria S, Xu J, Meis JF. Emergence of Azole-Resistant *Aspergillus fumigatus* Strains due to Agricultural Azole Use Creates an Increasing Threat to Human Health. *PLoS Pathogens*. 2013;9(10):e1003633.

456. Verweij PE, Mellado E, Melchers WJG. Multiple-triazole-resistant aspergillosis. *New England Journal of Medicine*. 2007;356(14):1481-3.

457. Ahmad S, Joseph L, Hagen F, Meis JF, Khan Z. Concomitant occurrence of itraconazole-resistant and-susceptible strains of *Aspergillus fumigatus* in routine cultures. *Journal of Antimicrobial Chemotherapy*. 2015;70(2):412–5.

458. Kolwijck E, van der Hoeven H, de Sévaux RGL, ten Oever J, Rijstenberg LL, van der Lee HAL, et al. Voriconazole-susceptible and voriconazole-resistant *Aspergillus fumigatus* coinfection. *American Journal of Respiratory and Critical Care Medicine*. 2016;193(8):927–9.

459. Merseguel KB, Nishikaku AS, Rodrigues AM, Padovan AC, e Ferreira RC, Salles de Azevedo Melo A, et al. Genetic diversity of medically important and emerging Candida species causing invasive infection. *BMC Infectious Diseases*. 2015;15:1–11.

460. Tajima F. Statistical method for testing the neutral mutation hypothesis by DNA polymorphism. *Genetics*. 1989;123(3):585–95.

461. Ghazanfari M, Abastabar M, Haghani I, Kermani F, Keikha N, Kholoujini M, et al. Electronic equipment and appliances in special wards of hospitals as a source of azole-resistant *Aspergillus fumigatus*: a multi-centre study from Iran. *Journal of Hospital Infection*. 2024;145:65–76.

462. Rocchi S, Sewell TR, Valot B, Godeau C, Laboissiere A, Millon L, et al. Molecular epidemiology of azole-resistant *Aspergillus fumigatus* in France shows patient and healthcare links to

environmentally occurring genotypes. *Frontiers in Cellular and Infection Microbiology*. 2021;11:729476.

463. Mortensen KL, Jensen RH, Johansen HK, Skov M, Pressler T, Howard SJ, et al. Aspergillus species and other molds in respiratory samples from patients with cystic fibrosis: a laboratory-based study with focus on *Aspergillus fumigatus* azole resistance. *Journal of Clinical Microbiology*. 2011;49(6):2243–51.

464. Fischer J, van Koningsbruggen-Rietschel S, Rietschel E, Vehreschild M, Wisplinghoff H, Krönke M, et al. Prevalence and molecular characterization of azole resistance in Aspergillus spp. isolates from German cystic fibrosis patients. *Journal of Antimicrobial Chemotherapy*. 2014;69(6):1533–6.

465. Vermeulen E, Maertens J, Schoemans H, Lagrou K. Azole-resistant *Aspergillus fumigatus* due to TR46/Y121F/T289A mutation emerging in Belgium, July 2012. *Eurosurveillance*. 2012;17(48):20326.

466. Wiederhold NP, Gil VG, Gutierrez F, Lindner JR, Albataineh MT, McCarthy DI, et al. First detection of TR34 L98H and TR46 Y121F T289A Cyp51 mutations in *Aspergillus fumigatus* isolates in the United States. *Journal of Clinical Microbiology*. 2016;54(1):168–71.

467. Astvad KMT, Jensen RH, Hassan TM, Mathiasen EG, Thomsen GM, Pedersen UG, et al. First detection of TR46/Y121F/T289A and TR34/L98H alterations in *Aspergillus fumigatus* isolates from azole-naive patients in Denmark despite negative findings in the environment. *Antimicrobial Agents and Chemotherapy*. 2014;58(9):5096–101.

468. Chowdhary A, Sharma C, Kathuria S, Hagen F, Meis JF. Azole-resistant *Aspergillus fumigatus* with the environmental TR46/Y121F/T289A mutation in India. *Journal of Antimicrobial Chemotherapy.* 2014;69(2):555–7.

469. Chen Y, Wang H, Lu Z, Li P, Zhang Q, Jia T, et al. Emergence of TR46/Y121F/T289A in an *Aspergillus fumigatus* isolate from a Chinese patient. *Antimicrobial Agents and Chemotherapy*. 2015;59(11):7148–50.

470. Ren J, Jin X, Zhang Q, Zheng Y, Lin D, Yu Y. Fungicides induced triazole-resistance in *Aspergillus fumigatus* associated with mutations of TR46/Y121F/T289A and its appearance in agricultural fields. *Journal of Hazardous Materials*. 2017;326:54–60.

471. Chowdhary A, Sharma C, van den Boom M, Yntema JB, Hagen F, Verweij PE, et al. Multi-azole-resistant *Aspergillus fumigatus* in the environment in Tanzania. *Journal of Antimicrobial Chemotherapy*. 2014;69(11):2979–83.

472. Moore CB, Novak-Frazer L, Muldoon E, Dunn KW, Masania R, Richardson MD, et al. First isolation of the pan-azole-resistant *Aspergillus fumigatus* cyp51A TR46/Y121F/T289A mutant in a UK patient. *International Journal of Antimicrobial Agents*. 2017;49(4):512–4.

473. Abdolrasouli A, Petrou MA, Park H, Rhodes JL, Rawson TM, Moore LSP, et al. Surveillance for azole-resistant *Aspergillus fumigatus* in a centralized diagnostic mycology service, London, United Kingdom, 1998–2017. *Frontiers in Microbiology*. 2018;9:2234.

474. Sewell TR, Zhang Y, Brackin AP, Shelton JMG, Rhodes J, Fisher MC. Elevated prevalence of azole-resistant aspergillus fumigatus in urban versus rural environments in the United Kingdom. *Antimicrobial Agents and Chemotherapy.* 2019;63(9).

475. Hare RK, Gertsen JB, Astvad KMT, Degn KB, Løkke A, Stegger M, et al. In vivo selection of a unique tandem repeat mediated azole resistance mechanism (TR120) in *Aspergillus fumigatus* cyp51A, Denmark. Emerging Infectious Disease. 2019;25(3):577.

476. Auxier B, Debets AJM, Stanford FA, Rhodes J, Becker FM, Reyes Marquez F, et al. The human fungal pathogen *Aspergillus fumigatus* can produce the highest known number of meiotic crossovers. *PLoS Biology*. 2023;21(9):e3002278.

477. van Leer-Buter C, Takes RP, Hebeda KM, Melchers WJG, Verweij PE. Aspergillosis—and a misleading sensitivity result. *The Lancet*. 2007;370(9581):102.

478. Pontes L, Perini Leme Giordano AL, Reichert-Lima F, Gualtieri Beraquet CA, Leite Pigolli G, Arai T, et al. Insights into *Aspergillus fumigatus* Colonization in Cystic Fibrosis and Cross-Transmission between Patients and Hospital Environments. *Journal of Fungi*. 2024;10(7):461.

479. van der Torre MH, Shen H, Rautemaa-Richardson R, Richardson MD, Novak-Frazer L. Molecular epidemiology of *Aspergillus fumigatus* in chronic pulmonary aspergillosis patients. *Journal of Fungi*. 2021;7(2):152.

480. Hatfield L, Bianco B, Gavillet H, Burns P, Rivett D, Smith M, et al. Effects of postage on recovery of pathogens from cystic fibrosis sputum samples. *Journal of Cystic Fibrosis*. 2023;22(5):816–22.

481. Denning DW, Park S, Lass-Florl C, Fraczek MG, Kirwan M, Gore R, et al. High-frequency triazole resistance found in nonculturable *Aspergillus fumigatus* from lungs of patients with chronic fungal disease. *Clinical infectious diseases*. 2011;52(9):1123–9.

482. Latgé JP, Chamilos G. *Aspergillus fumigatus* and Aspergillosis in 2019. *Clinical Microbiology Reviews*. 2019;33(1):e00140-18.

483. Godeau C, Reboux G, Scherer E, Laboissiere A, Lechenault-Bergerot C, Millon L, et al. Azole-resistant *Aspergillus fumigatus* in the hospital: Surveillance from flower beds to corridors. *American Journal of Infection Control*. 2020;48(6):702–4.

484. Vaghar Z, Khodavaisy S, Badali H, Sabokbar A. Molecular Detection of Azole-Resistant *Aspergillus fumigatus* Isolates Carrying TR34/L98H Mutations in Soil Samples from the Critical Hospitals. *Molecular Genetics, Microbiology and Virology*. 2022;37(1):49–53.

485. Gewecke A, Hare RK, Salgård C, Kyndi L, Høg M, Petersen G, et al. A single-source nosocomial outbreak of *Aspergillus flavus* uncovered by genotyping. *Microbiology Spectrum*. 2024; 6;12(8):e0027324

486. ECDC. Surveillance of healthcare-associated infections and prevention indicators in European intensive care units. ECDC Stockholm; 2017. https://www.ecdc.europa.eu/sites/default/files/documents/HAI-Net-ICU-protocol-v2.2_0.pdf. [Date Accessed: 28th June 2023]

487. CDC. National Healthcare Safety Network (NHSN) Patient Safety Component Manual. 2024. *https://www.cdc.gov/nhsn/pdfs/pscmanual/pcsmanual_current.pdf*. [Date Accessed: 28th June 2023].

488. Allegranzi B, Nejad SB, Combescure C, Graafmans W, Attar H, Donaldson L, et al. Burden of endemic health-care-associated infection in developing countries: systematic review and meta-analysis. *The Lancet*. 2011;377(9761):228–41.

489. Damani N. Surveillance in countries with limited resources. *International Journal of Infection Control*. 2008;4(1).

490. Zuckerman JB, Zuaro DE, Prato BS, Ruoff KL, Sawicki RW, Quinton HB, et al. Bacterial contamination of cystic fibrosis clinics. *Journal of Cystic Fibrosis*. 2009;8(3):186–92.

491. Ferroni A, Werkhauser-Bertrand A, Le Bourgeois M, Beauvais R, Vrielynck S, Durand C, et al. Bacterial contamination in the environment of hospitalised children with cystic fibrosis. *Journal of Cystic Fibrosis*. 2008;7(6):477–82.

492. Tanner WD, Leecaster MK, Zhang Y, Stratford KM, Mayer J, Visnovsky LD, et al. Environmental contamination of contact precaution and non-contact precaution patient rooms in six acute care facilities. *Clinical Infectious Diseases*. 2021;72:S8–16.

493. NHS. Royal Brompton & Harefield NHS Foundation Trust Annual Report and Accounts 2019/20. *https://www.rbht.nhs.uk/about-us/annual-publications*. [Dated Accessed: 16th July 2022]

494. Tsitsopoulou A, Posso R, Vale L, Bebb S, Johnson E, White PL. Determination of the prevalence of triazole resistance in environmental *Aspergillus fumigatus* strains isolated in South Wales, UK. *Frontiers in Microbiology*. 2018;26;9:1395.

495. Tsitsopoulou A, Posso R, Vale L, Bebb S, Johnson E, White PL. Determination of the prevalence of triazole resistance in environmental *Aspergillus fumigatus* strains isolated in South Wales, UK. *Frontiers in Microbiology.* 2018;26;9:1395.

496. Hassan A, Zeeshan M. Microbiological indoor air quality of hospital buildings with different ventilation systems, cleaning frequencies and occupancy levels. *Atmospheric Pollution Research*. 2022;13(4):101382.

497. Chazalet V, Debeaupuis JP, Sarfati J, Lortholary J, Ribaud P, Shah P, et al. Molecular typing of environmental and patient isolates of *Aspergillus fumigatus* from various hospital settings. *Journal of Clinical Microbiology*. 1998;36(6):1494–500.

498. Araujo R, Carneiro A, Costa-Oliveira S, Pina-Vaz C, Rodrigues AG, Guimaraes JE. Fungal infections after haematology unit renovation: evidence of clinical, environmental and economical impact. *European Journal of Haematology*. 2008;80(5):436–43.

499. Cho SY, Myong JP, Kim WB, Park C, Lee SJ, Lee SH, et al. Profiles of environmental mold: indoor and outdoor air sampling in a hematology hospital in Seoul, South Korea. *International Journal of Environmental Research and Public Health*. 2018;15(11):2560.

500. Ghazanfari M, Charati JY, Keikha N, Kholoujini M, Kermani F, Nasirzadeh Y, et al. Indoor environment assessment of special wards of educational hospitals for the detection of fungal contamination sources: A multi-center study (2019-2021). *Current Medical Mycology*. 2022;8(4):1.

501. Bader O, Tünnermann J, Dudakova A, Tangwattanachuleeporn M, Weig M, Groß U. Environmental isolates of azole-resistant *Aspergillus fumigatus* in Germany. *Antimicrobial Agents and Chemotherapy*. 2015;59(7):4356–9.

502. Prigitano A, Esposto MC, Romanò L, Auxilia F, Tortorano AM. Azole-resistant *Aspergillus fumigatus* in the Italian environment. *The Journal of Global Antimicrobial Resistance*. 2019;16:220–4.

503. M. Jimenez Madrid A, Paul RA, Rotondo F, Deblais L, Rajashekara G, Miller SA, et al. Triazole resistance in *Aspergillus fumigatus* isolated from a tomato production environment exposed to propiconazole. *Applied Environmental Microbiology*. 2024;90(4):e00017-24.

504. Dladla M, Gyzenhout M, Marias G, Ghosh S. Azole resistance in *Aspergillus fumigatus*-comprehensive review. Archives og Microbiology. 2024;206(7):305.

505. Buil JB, Hare RK, Zwaan BJ, Arendrup MC, Melchers WJG, Verweij PE. The fading boundaries between patient and environmental routes of triazole resistance selection in *Aspergillus fumigatus*. *PLoS Pathogens*. 2019;15(8):e1007858.

506. Amona FM, Oladele RO, Resendiz-Sharpe A, Denning DW, Kosmidis C, Lagrou K, et al. Triazole resistance in *Aspergillus fumigatus* isolates in Africa: a systematic review. *Medical Mycology*. 2022;60(8):myac059.

507. Snelders E, Celia-Sanchez BN, Nederlof YC, Zhang J, Kortenbosch HH, Zwaan BJ, et al. Widely dispersed clonal expansion of multi-fungicide-resistant *Aspergillus fumigatus* limits genomic epidemiology prospects. *bioRxiv*. 2024;2024–7.

508. Taylor MW. Diphtheria in connection with damp and mould-fungi. *Transactions of the Epidemiological Society of London*. 1888;6:104-123.

509. Fan L, Wang J, Yang Y, Yang W, Zhu Y, Zhang Y, et al. Residential airborne culturable fungi under general living scenario: On-site investigation in 12 typical cities, China. *Environment International*. 2021;155:106669.

510. Idrose NS, Dharmage SC, Lowe AJ, Lambert KA, Lodge CJ, Abramson MJ, et al. A systematic review of the role of grass pollen and fungi in thunderstorm asthma. *Environmental Research*. 2020;181:108911.

511. Welsh KG, Holden KA, Wardlaw AJ, Satchwell J, Monteiro W, Pashley CH, et al. Fungal sensitization and positive fungal culture from sputum in children with asthma are associated with

reduced lung function and acute asthma attacks respectively. *Clinical & Experimental Allergy*. 2021;51(6):790–800.

512. Ramachandran G, Adgate JL, Banerjee S, Church TR, Jones D, Fredrickson A, et al. Indoor air quality in two urban elementary schools—measurements of airborne fungi, carpet allergens, CO2, temperature, and relative humidity. *Journal of Occupational and Environmental Hygiene*. 2005;2(11):553–66.

513. O'Gorman CM, Fuller HT. Prevalence of culturable airborne spores of selected allergenic and pathogenic fungi in outdoor air. *Atmospheric Environment*. 2008;42(18):4355–68.

514. Adams RI, Miletto M, Taylor JW, Bruns TD. Dispersal in microbes: fungi in indoor air are dominated by outdoor air and show dispersal limitation at short distances. *ISME Journal*. 2013;7(7):1262–73.

515. Liu W, Huang C, Hu Y, Zou Z, Shen L, Sundell J. Associations of building characteristics and lifestyle behaviors with home dampness-related exposures in Shanghai dwellings. *Building and Environment*. 2015;88:106–15.

516. Belizario JA, Lopes LG, Pires RH. Fungi in the indoor air of critical hospital areas: a review. *Aerobiologia*. 2021;37(3):379–94.

517. Kwaśna H, Kuberka A. Fungi in public heritage buildings in Poland. *Polish Journal of Environmental Studies*. 2020;29(5):3651–62.

518. Lindemann V, Schleiner T, Maier U, Fels H, Cramer B, Humpf HU. Analysis of mold and mycotoxins in naturally infested indoor building materials. *Mycotoxin Research*. 2022;38(3):205–20.

519. Loukou E, Jensen NF, Rohde L, Andersen B. Damp Buildings: Associated Fungi and How to Find Them. *Journal of Fungi*. 2024;10(2):108.

520. Reddy MK, Falaciński P, Karwowska E. Bioreceptivity of unused building materials: effects on microbial colonisation and diversity—a Polish–Indian study. European Journal of Environmental and Civil Engineering. 2024;28(9):2024–33.

521. Yakovleva G, Sagadeev E, Stroganov V, Kozlova O, Okunev R, Ilinskaya O. Metabolic activity of micromycetes affecting urban concrete constructions. *The Scientific World Journal.* 2018;2:8360287.

522. Levinskaitė L, Paškevičius A. Fungi in water-damaged buildings of Vilnius Old City and their susceptibility towards disinfectants and essential oils. *Indoor and Built Environment*. 2013;22(5):766–75.

523. Paterson RRM, Lima N. Filamentous fungal human pathogens from food emphasising Aspergillus, Fusarium and Mucor. *Microorganisms*. 2017;5(3):44.

524. Paluch M, Lejeune S, Hecquet E, Prévotat A, Deschildre A, Fréalle E. High airborne level of *Aspergillus fumigatus* and presence of azole-resistant TR34/L98H isolates in the home of a cystic fibrosis patient harbouring chronic colonisation with azole-resistant H285Y *A. fumigatus*. *Journal of Cystic Fibrosis*. 2019;18(3):364–7.

525. Lavergne RA, Chouaki T, Hagen F, Toublanc B, Dupont H, Jounieaux V, et al. Home environment as a source of life-threatening azole-resistant *Aspergillus fumigatus* in immunocompromised patients. *Clinical Infectious Diseases*. 2017;64(1):76–8.

526. Madsen AM, Matthiesen CB, Frederiksen MW, Frederiksen M, Frankel M, Spilak M, et al. Sampling, extraction and measurement of bacteria, endotoxin, fungi and inflammatory potential of settling indoor dust. *Journal of Environmental Monitoring*. 2012;14(12):3230–9.

527. Viegas C, Viegas S, Gomes A, Täubel M, Sabino R. Exposure to microbiological agents in indoor and occupational environments. Springer. Springer Cham. 2017;1:415

528. Noss I, Wouters IM, Visser M, Heederik DJJJ, Thorne PS, Brunekreef B, et al. Evaluation of a low-cost electrostatic dust fall collector for indoor air endotoxin exposure assessment. *Applied and Environmental Microbiology.* 2008;74(18):5621-7.

529. Normand AC, Ranque S, Cassagne C, Gaudart J, Sallah K, Charpin DA, et al. Comparison of air impaction and electrostatic dust collector sampling methods to assess airborne fungal contamination in public buildings. *The Annals of Occupational Hygiene*. 2016;60(2):161–75.

530. Zhang J, Lopez Jimenez L, Snelders E, Debets AJM, Rietveld AG, Zwaan BJ, et al. Dynamics of *Aspergillus fumigatus* in azole fungicide-containing plant waste in the Netherlands (2016–2017). *Applied and Environmental Microbiology*. 2021;87(2):e02295-20.

531. Fréalle E, Reboux G, Le Rouzic O, Bautin N, Willemin MC, Pichavant M, et al. Impact of domestic mould exposure on Aspergillus biomarkers and lung function in patients with chronic obstructive pulmonary disease. *Environmental Research*. 2021;195:110850.

532. Reboux G, Rocchi S, Laboissière A, Ammari H, Bochaton M, Gardin G, et al. Survey of 1012 moldy dwellings by culture fungal analysis: Threshold proposal for asthmatic patient management. *Indoor Air*. 2019;29(1):5–16.

533. Reboux G, Bellanger AP, Roussel S, Grenouillet F, Sornin S, Piarroux R, et al. Indoor mold concentration in Eastern France. *Indoor Air*. 2009;19(6):446–53.

534. Vesper S, McKinstry C, Ashley P, Haugland R, Yeatts K, Bradham K, et al. Quantitative PCR analysis of molds in the dust from homes of asthmatic children in North Carolina. *Journal of Environmental Monitoring*. 2007;9(8):826–30.

535. Eduard W. Fungal spores: a critical review of the toxicological and epidemiological evidence as a basis for occupational exposure limit setting. *Critical Reviews in Toxicology*. 2009;39(10):799–864.

536. Bottery MJ, van Rhijn NJ, Chown H, Rhodes JL, Celia-Sanchez BN, Brewer MT, et al. Elevated mutation rates in the multi-azole resistant *Aspergillus fumigatus* clade drives rapid evolution of antifungal resistance. *bioRxiv*. 2023;2012–23.

537. Hagiwara D, Arai T, Takahashi H, Kusuya Y, Watanabe A, Kamei K. Non-cyp51A azole-resistant *Aspergillus fumigatus* isolates with mutation in HMG-CoA reductase. *Emerging Infectious Diseases.* 2018;24(10):1889.

538. Paul S, Diekema D, Moye-Rowley WS. Contributions of *Aspergillus fumigatus* ATP-binding cassette transporter proteins to drug resistance and virulence. *Eukaryotic Cell*. 2013;12(12):1619–28.

539. Meneau I, Coste AT, Sanglard D. Identification of *Aspergillus fumigatus* multidrug transporter genes and their potential involvement in antifungal resistance. *Medical Mycology*. 2016;54(6):616–27.

540. Oliver JD, Sibley GEM, Beckmann N, Dobb KS, Slater MJ, McEntee L, et al. F901318 represents a novel class of antifungal drug that inhibits dihydroorotate dehydrogenase. *Proceedings of the National Academy of Sciences.* 2016;113(45):12809–14.

541. Van Rhijn N, Hemmings S, Storer ISR, Valero C, Bin Shuraym H, Goldman GH, et al. Antagonism of the azoles to olorofim and cross-resistance are governed by linked transcriptional networks in *Aspergillus fumigatus*. *mBio*. 2022;13(6):e02215-22.

542. du Pré S, Birch M, Law D, Beckmann N, Sibley GEM, Bromley MJ, et al. The dynamic influence of olorofim (F901318) on the cell morphology and organization of living cells of *Aspergillus fumigatus*. *Journal of Fungi*. 2020;6(2):47.

543. Du Pré S, Beckmann N, Almeida MC, Sibley GEM, Law D, Brand AC, et al. Effect of the novel antifungal drug F901318 (olorofim) on growth and viability of *Aspergillus fumigatus*. *Antimicrobial Agents Chemotherapy*. 2018;62(8):10–1128.

544. Jørgensen KM, Astvad KMT, Hare RK, Arendrup MC. EUCAST determination of olorofim (F901318) susceptibility of mold species, method validation, and MICs. *Antimicrobial Agents Chemotherapy*. 2018;62(8):10–1128.

545. EPA. U.S. Environmental Protection Agency. www.epa.gov. [Date of Access: 5th July 2024]

546. van Rhijn N, Storer ISR, Birch M, Oliver JD, Bottery MJ, Bromley MJ. *Aspergillus fumigatus* strains that evolve resistance to the agrochemical fungicide ipflufenoquin in vitro are also resistant to olorofim. *Nature Microbiology*. 2024;9(1):29–34.

547. Quick J, Ashton P, Calus S, Chatt C, Gossain S, Hawker J, et al. Rapid draft sequencing and real-time nanopore sequencing in a hospital outbreak of Salmonella. *Genome Biology*. 2015;16(1):1–14.

548. Quick J, Loman NJ, Duraffour S, Simpson JT, Severi E, Cowley L, et al. Real-time, portable genome sequencing for Ebola surveillance. *Nature*. 2016;530(7589):228–32.

549. Quick J, Grubaugh ND, Pullan ST, Claro IM, Smith AD, Gangavarapu K, et al. Multiplex PCR method for MinION and Illumina sequencing of Zika and other virus genomes directly from clinical samples. *Nature Protocols*. 2017;12(6):1261.

550. Dal Molin A, Minio A, Griggio F, Delledonne M, Infantino A, Aragona M. The genome assembly of the fungal pathogen *Pyrenochaeta lycopersici* from Single-Molecule Real-Time sequencing sheds new light on its biological complexity. *PLoS One*. 2018;13(7):e0200217.

551. Zhao C, Fraczek MG, Dineen L, Lebedinec R, Macheleidt J, Heinekamp T, et al. High-throughput gene replacement in *Aspergillus fumigatus*. *Current Protocol Microbiology*. 2019;54(1):e88.

552. Furukawa T, Van Rhijn N, Fraczek M, Gsaller F, Davies E, Carr P, et al. The negative cofactor 2 complex is a key regulator of drug resistance in *Aspergillus fumigatus*. *Nature Communications*. 2020;11(1):427.

553. Hoang TNM, Cseresnyés Z, Hartung S, Blickensdorf M, Saffer C, Rennert K, et al. Invasive aspergillosis-on-chip: A quantitative treatment study of human *Aspergillus fumigatus* infection. *Biomaterials*. 2022;283:121420.

554. Richter F, Bindschedler S, Calonne-Salmon M, Declerck S, Junier P, Stanley CE. Fungi-on-a-Chip: microfluidic platforms for single-cell studies on fungi. FEMS Microbiology Reviews. 2022;46(6):fuac039.

555. Kek HY, Tan H, Othman MHD, Nyakuma BB, Goh PS, Wong SL, et al. Perspectives on human movement considerations in indoor airflow assessment: a comprehensive data-driven systematic review. *Environmental Science and Pollution Research*. 2023;30(58):121253–68.

556. Latgé JP, Chamilos G. Aspergillus fumigatus and aspergillosis in 2019. Clin Microbiol Rev. 2020;33(1).

Appendices

Appendix 1:

Custom Github Scripts downloadable at https://github.com/abrackin/thesis_scripts

Appendix 2:

UK *A. fumigatus* dataset/Hospital surveillance, encompassing 912 clinical and environmental isolates with associated metadata available at:

https://microreact.org/project/ohanRa45Se2kRQQugq6mK9-uk

Chronic Respiratory Disease Cohort, encompassing 300 *A. fumigatus* isolates from 83 individuals with associated metadata. available at:

https://microreact.org/project/jhFrB8bNkyEFKwNFndixaY-chronicrespdiseasecohort

Participants home environment and corresponding clinical isolates, encompassing 221 A. fumigatus isolates with associated metadata available at:

https://microreact.org/project/mPKpbn9kxfGScWoywzzXBr-homeclinical

Appendix 3:

Virulence related genes included in screening TR_{34}/L98H and cyp51a wildtype *A. fumigatus* isolates.

Adapted from Puértolas-Balint *et al*., 2019 (388).

Function	Gene ID	Gene Name	Product Description
Resistance to immune response	Afu1g03200	*mfsC*	Putative major facilitator superfamily (MFS) transporter
	Afu1g10380	*nrps1*	Non-ribosomal peptide synthetase (NRPS)
	Afu1g10390	*abcB*	Putative ABC multidrug transporter
	Afu1g12690	*mdr4*	ABC multidrug transporter
	Afu1g13330	*arp2*	Ortholog(s) have ATP binding, ATPase activity
	Afu1g14330	*abcC*	Putative ABC transporter
	Afu1g14550	*sod3*	Putative manganese superoxide dismutase
	Afu1g15490	*mfsB*	Putative major facilitator superfamily (MFS) transporter
	Afu1g17250	*rodB*	Conidial cell wall hydrophobin involved in conidial cell wall composition
	Afu1g17440	*abcA*	ABC drug exporter
	Afu2g17530	*abr2*	Laccase abr2
	Afu2g17550	*ayg1*	Heptaketide hydrolyase ayg1
	Afu2g17600	*pksP*	Conidial pigment polyketide synthase alb1
	Afu3g02270	*cat1*	Mycelial catalase
	Afu3g03500	*mdr3*	Putative multidrug resistance protein
	Afu3g09690	*catA*	Laminin-binding protein with extracellular thaumatin domain
	Afu3g10830	*gstA*	Putative glutathione transferase
	Afu3g12120	*ppoC*	Putative fatty acid oxygenase
	Afu4g00180	*ppoB*	Fatty acid 8,11-diol synthase
	Afu4g11580	*sod2*	Putative manganese-superoxide dismutase
	Afu4g13390	*arpA*	Ortholog(s) have role in conidiophore development, conidium formation, hyphal growth, nuclear migration along microtubule, regulation of growth rate and cytoplasmic dynein complex, hyphal tip localization
	Afu4g14530	*tpcF*	Putative theta class glutathione s-transferase
	Afu5g06070	*mdr1*	ABC multidrug transporter
	Afu5g09240	*sod1*	Cu/Zn superoxide dismutase
	Afu5g09580	*rodA*	Conidial hydrophobin
	Afu6g03470	*fmpD*	ABC transporter fmpD
	Afu6g03890	*catA*	Spore-specific catalase
	Afu6g04360	*atrF*	Putative ABC transporter
	Afu6g07210	*sod4*	Putative copper-zinc superoxide dismutase
	Afu6g09930	*yap1*	bZIP family transcription factor
	Afu6g12522	*skn7*	Putative transcription factor and response regulator of a two-component signal transduction system
	Afu7g00480	*abcE*	Putative ABC transporter
	Afu7g05500	*gstB*	Putative theta class glutathione transferase
	Afu8g05710	*mfsA*	Putative major facilitator superfamily (MFS) sugar transporter
Cell wall	Afu1g01380	*och4*	Putative alpha-1,6-mannosyltransferase
	Afu1g04260	*ENGL1*	Beta-1,3-endoglucanase, associated with cell wall
	Afu1g07690	*afpmt2*	Protein O-mannosyltransferase
	Afu1g12600	*chsD*	Putative chitin synthase-like gene with a predicted role in chitin biosynthesis
	Afu1g15440	*ags3*	Putative alpha(1-3) glucan synthase
	Afu2g01170	*gel1*	1,3-beta-glucanosyltransferase with a role in elongation of 1,3-beta-glucan chains
	Afu2g01450	*mnn9*	Alpha-1,6 mannosyltransferase subunit with a predicted role in N-linked protein glycosylation

	Afu2g01870	*chsA*	Putative class I chitin synthase
	Afu2g05340	*gel4*	Essential 1,3-beta-glucanosyltransferase, GPI-anchored to the plasma membrane
	Afu2g11270	*ags2*	Putative alpha(1-3) glucan synthase
	Afu2g12850	*gel3*	Putative GPI anchored beta(1-3)glucanosyltransferase, belongs to the 7-member GEL family
	Afu2g13440	*chsE*	Putative class V chitin synthase
	Afu2g15910	*anp1*	Ortholog(s) have alpha-1,6-mannosyltransferase activity, role in protein N-linked glycosylation and alpha-1,6-mannosyltransferase complex, endoplasmic reticulum localization
	Afu2g17580	*arp1*	Scytalone dehydratase arp1
	Afu3g00910	*ags1*	Putative alpha(1-3) glucan synthase
	Afu3g12690	*glfA*	Putative UDP-galactopyranose mutase, enzyme in the first step of galactofuranose biosynthesis
	Afu3g13200	*gel6*	Putative beta(1-3)glucanosyltransferase, belongs to the 7-member GEL family
	Afu3g14420	*chsG*	Putative class III chitin synthase
	Afu4g03240	*mp1*	Putative cell wall galactomannoprotein
	Afu4g04180	*chsB*	Putative class II chitin synthase
	Afu4g06820	*ecm33*	Putative glycophosphatidylinositol (GPI)-anchored cell wall protein with similarity to S. cerevisiae Ecm33p
	Afu5g00760	*chsC*	Putative class III chitin synthase
	Afu5g02740	*afmnt3*	Putative alpha-1,2-mannosyltransferase with a predicted role in N-linked protein glycosylation
	Afu5g08580	*och1*	Putative alpha-1,6-mannosyltransferase that initiates the linkage of the N-glycan outer chain
	Afu5g10760	*mnt1*	Putative alpha-1,2-mannosyltransferase with a predicted role in protein glycosylation
	Afu5g12160	*afmnt2*	Putative alpha-1,2-mannosyltransferase with a predicted role in N-linked protein glycosylation
	Afu5g14060	*rho4*	Putative Rho-type GTPase
	Afu6g06900	*rho1*	Putative Rho-type GTPase
	Afu6g11390	*gel2*	GPI-anchored 1,3-beta-glucanosyltransferase
	Afu6g12400	*fks1*	Putative 1,3-beta-glucan synthase catalytic subunit, major subunit of glucan synthase
	Afu6g12410	*gel7*	GPI-anchored putative beta(1-3)glucanosyltransferase involved in cell wall maintenance
	Afu6g14040	*och2*	Putative alpha-1,6-mannosyltransferase
	Afu8g02040	*och3*	Putative alpha-1,6-mannosyltransferase
	Afu8g02130	*gel5*	Putative beta(1-3)glucanosyltransferase, belongs to the 7-member GEL family
	Afu8g04500	*pmt4*	Putative protein O-mannosyltransferase
	Afu8g05630	*chsF*	putative chitin synthase
Toxins and secondary metabolites	Afu1g14660	*laeA*	Protein with similarity to protein methyltransferases, involved in regulation of secondary metabolism
	Afu2g17540	*abr1*	Multicopper oxidase abr1
	Afu2g17970	*fgaFS*	Festuclavine dehydrogenase easG
	Afu2g17980	*easK*	Cytochrome P450 monooxygenase easK
	Afu2g18000	*fgaDH*	Chanoclavine-I dehydrogenase easD
	Afu2g18010	*easM*	Cytochrome P450 monooxygenase easM
	Afu2g18020	*fgaAT*	Fumigaclavine B O-acetyltransferase easN
	Afu2g18030	*fgaCat*	Catalase easC
	Afu2g18040	*dmaW*	Tryptophan dimethylallyltransferase
	Afu2g18050	*fgaOx1*	FAD-linked oxidoreductase easE
	Afu2g18060	*fgaMT*	4-dimethylallyltryptophan N-methyltransferase easF
	Afu3g12900	*hasB*	Putative transporter
	Afu3g12940	*hasF*	C6 transcription factor hasF

	Afu3g12950	*hasG*	FAD-binding domain protein
	Afu4g10460	*hcsA*	Homocitrate synthase, essential enzyme of the alpha-aminoadipate pathway of lysine biosynthesis
	Afu4g14480	*tpcL*	emodin anthrone oxidase
	Afu4g14490	*tpcJ*	Putative dihydrogeodin oxidase
	Afu4g14500	*tpcI*	Questin oxygenase, putative
	Afu4g14520	*tpcG*	Monoogygenase tpcG
	Afu4g14540	*tpcE*	Trypacidin cluster transcription factor
	Afu4g14570	*tpcB*	Trypacidin synthesis protein B
	Afu4g14580	*tpcA*	O-methyltransferase tpcA
	Afu4g14770	*osc3*	oxidosqualene:protostadienol cyclase
	Afu4g14780	*cyp5081A1*	Putative cytochrome P450 monooxygenase
	Afu4g14790	*cyp5081B1*	Putative cytochrome P450 monooxygenase
	Afu4g14800	*sdr1*	Putative short chain dehydrogenase
	Afu6g09630	*gliZ*	C6 finger domain transcription factor gliZ
	Afu6g09660	*gliP*	Nonribosomal peptide synthetase gliP
	Afu6g09670	*gliC*	Cytochrome P450 monooxygenase gliC
	Afu6g09690	*gliG*	Glutathione S-transferase gliG
	Afu6g09710	*gliA*	MFS gliotoxin efflux transporter gliA
	Afu6g09720	*gliN*	N-methyltransferase gliN
	Afu6g09730	*gliF*	Cytochrome P450 monooxygenase gliF
	Afu6g09740	*gliT*	Thioredoxin reductase gliT
	Afu8g00190	*ftmC*	Putative cytochrome P450
	Afu8g00200	*ftmD*	O-methyltransferase ftmD
	Afu8g00370	*fma-PKS*	Fumagillin biosynthesis polyketide synthase
	Afu8g00380	*fmaC*	Fumagillin biosynthesis acyltransferase
	Afu8g00390	*fmaD*	Fumagillin biosynthesis methyltransferase
	Afu8g00410	*metAP*	Methionine aminopeptidase type II
	Afu8g00420	*fumR*	C6 finger transcription factor fumR
	Afu8g00440	*psoF*	Dual-functional monooxygenase/methyltransferase psoF
	Afu8g00470	*fmaE*	Antibiotic Biosynthesis Monoxygenase superfamily monooxygenase fmaE
	Afu8g00490	*Fma-KR*	Stereoselective keto-reductase
	Afu8g00510	*fmaG*	Fumagillin biosynthesis cluster P450 monooxygenase
	Afu8g00520	*fmaA*	Fumagillin biosynthesis terpene cyclase
	Afu8g00550	*psoC*	Methyltransferase psoC
	Afu8g00580	*psoE*	Glutathione S-transferase psoE
Allergens	Afu1g05770	*exg12*	Secreted beta-glucosidase
	Afu1g09470	*aspfAT*	Putative class V aminotransferase
	Afu1g14560	*msdS*	Putative 1,2-alpha-mannosidase
	Afu1g16190	*aspf9*	Cell wall glucanase
	Afu2g00760	*aspfPL*	Putative secreted pectate lyase
	Afu2g03720	*aspf11*	Putative cyclophilin
	Afu2g03830	*aspf4*	Allergen Asp f 4
	Afu2g10100	*aspf8*	Allergen Asp f 8
	Afu2g11260	*luA*	Putative 3-isopropylmalate dehydratase with a predicted role in nitrogen metabolism
	Afu2g11850	*aspf23*	Allergenic ribosomal L3 protein
	Afu2g12630	*aspf13*	Allergen Asp f 13
	Afu2g15430	*AspfSXR*	Sorbitol/xylulose reductase
	Afu3g00590	*aspHS*	Asp-hemolysin
	Afu3g07430	*aspf27*	Putative peptidyl-prolyl cis-trans isomerase
	Afu3g14680	*aspfLPL3*	Putative secreted lysophospholipase B
	Afu4g01290	*csn*	Glycosyl hydrolase family 75 chitosanase
	Afu4g06670	*aspf7*	Allergen Asp f 7
	Afu4g09580	*aspf2*	Allergen Asp f 2
	Afu5g02330	*aspf1*	Allergen Asp f 1
	Afu5g03520	*aspfPUP*	Immunoreactive secreted protein
	Afu5g11320	*aspf29*	Allergen Asp f 29
	Afu6g02280	*aspf3*	Allergen Asp f 3

	Afu6g03620	*mreA*	FAD/FMN-containing isoamyl alcohol oxidase
	Afu6g04920	*fdh*	Putative NAD-dependent formate dehydrogenase
	Afu6g06770	*aspf22*	Putative enolase
	Afu6g10300	*aspf28*	Allergen Asp f 28
Nutrient uptake	Afu1g01550	*zrfA*	Putative plasma membrane zinc transporter
	Afu1g09280	*ptcB*	Putative type 2C protein phosphatase (PP2C) involved in dephosphorylation of SakA MAP kinase in response to osmotic stress
	Afu1g10080	*zafA*	Putative C2H2 zinc-responsive transcriptional activator
	Afu1g16950	*pig-a*	Protein required for the initiation of involved in glycosylphosphatidylinositol (GPI)-anchor biosynthesis
	Afu1g17200	*sidC*	Fusarinine C non-ribosomal peptide synthetase (NRPS), putative
	Afu2g03860	*zrfB*	Low affinity plasma membrane zinc transporter
	Afu2g04010	*tpsB*	Putative trehalose-6-phosphate synthase
	Afu2g05730	*mirC*	Putative siderophore transporter
	Afu2g07680	*sidA*	L-ornithine N5-oxygenase
	Afu2g08360	*pyrG*	Orotidine 5'-monophosphate decarboxylase
	Afu2g09030	*dppV*	Secreted dipeptidyl-peptidase
	Afu3g03400	*sidF*	Siderophore biosynthesis acetylase AceI, putative
	Afu3g03420	*sidD*	Nonribosomal peptide synthetase 4
	Afu3g03640	*mirB*	Putative siderophore iron transporter
	Afu3g03650	*sidG*	Putative acetyltransferase with a predicted role in iron metabolism
	Afu3g05650	*orlA*	Trehalose 6-phosphate phosphatase (T6PP)
	Afu3g11400	*pep2*	Aspartic acid endopeptidase
	Afu3g11970	*pacC*	C2H2 finger domain transcription factor
	Afu4g07040	*ctsD*	Putative secreted aspartic-type endopeptidase
	Afu4g08720	*plb1*	Putative secreted phospholipase B
	Afu4g09320	*dppIV*	Putative extracellular dipeptidyl-peptidase
	Afu4g09560	*zrfC*	Zinc transporter that functions in neutral or alkaline environments
	Afu4g11800	*alp1*	Putative secreted alkaline serine protease
	Afu4g12470	*cpcA*	Transcriptional activator of the cross-pathway control system of amino acid biosynthesis
	Afu4g13750	*mep20*	Putative penicillolysin/deuterolysin metalloprotease
	Afu5g03790	*fetC*	Putative ferroxidase
	Afu5g03800	*ftrA*	Putative high-affinity iron permease
	Afu5g08570	*pkaC2*	Class II protein kinase A (PKA)
	Afu5g09210	*alp2*	Autophagic (vacuolar) serine protease
	Afu5g11260	*sreA*	GATA transcription factor that regulates iron uptake
	Afu5g13300	*pep1*	Putative extracellular aspartic endopeptidase
	Afu6g01970	*areA*	Putative GATA-like transcription factor
	Afu6g03590	*mcsA*	Methylcitrate synthase
	Afu6g04820	*pabA*	Para-aminobenzoic acid synthetase, an enzyme catalyzing a late step in the biosynthesis of folate
	Afu6g12950	*tpsA*	Trehalose-6-phosphate synthase
	Afu7g04930	*pr1*	Putative alkaline serine protease
	Afu7g05930	*mepB*	Putative metallopeptidase with similarity to mammalian thimet oligopeptidases
	Afu8g02760	*amcA*	Putative mitochondrial ornithine carrier protein
	Afu8g07080	*mep*	Putative secreted metalloprotease
Signaling and regulation	Afu1g05800	*mkk2*	Putative mitogen-activated protein kinase kinase (MAPKK)
	Afu1g06900	*crzA*	C2H2-type zinc finger transcription factor involved in calcium ion homeostasis

Afu1g12930	*gpaB*	G protein alpha subunit
Afu1g15950	*pbs2*	Putative mitogen-activated protein kinase kinase (MAPKK)
Afu2g00660	*tcsB*	Putative sensor histidine kinase/response regulator with homology to S. cerevisiae Sln1p
Afu2g01260	*srbA*	Sterol regulatory element binding protein (SREBP)
Afu2g12200	*pkaC*	cAMP-dependent protein kinase catalytic subunit
Afu2g12640	*gprD*	Putative G-protein coupled receptor (GPCR)-like protein
Afu2g13260	*medA*	Putative regulator of adherence, host cell interactions and virulence
Afu3g05900	*ste7*	MAP kinase kinase (MAPKK)
Afu3g10000	*pkaR*	cAMP-dependent protein kinase regulatory subunit
Afu3g11080	*bck1*	Putative mitogen-activated protein kinase kinase kinase (MAPKKK)
Afu3g11250	*ace2*	C2H2 transcription factor with a role in conidiophore development, pigment production, germination and virulence
Afu4g13720	*mpkA*	mitogen-activated protein kinase
Afu5g06420	*steC/ste11*	Ortholog(s) have MAP kinase kinase kinase activity, MAP kinase kinase kinase kinase activity, SAM domain binding activity
Afu5g08420	*sho1*	Putative transmembrane osmosensor with homology to S. cerevisiae Sho1p
Afu5g09100	*mpkC*	Putative mitogen activated protein kinase (MAPK)
Afu5g09360	*calA*	calcineurin a catalytic subunit
Afu5g11230	*rasA*	Ras family GTPase protein
Afu5g12210	*sfaD*	G protein-coupled receptor beta subunit
Afu6g08520	*acyA*	Adenylate cyclase of the cAMP-dependent signaling pathway, involved in regulation of proliferation and conidiophore development
Afu6g10240	*fos-1*	Putative histidine kinase, two-component signal transduction protein
Afu6g12820	*mpkB*	Putative mitogen-activated protein kinase (MAPK)
Afu7g04800	*gprC*	Rhodopsin-like G-protein coupled receptor

Appendix 4:

Preparation of PM additives for OmniLog™ PM arrays

Preparation of glucose stock solution:

Ingredient	Concentration (mM)	g/100ml	Concentration factor
D-glucose	3200	57.644	32x

Preparation of PM3 additive solution:

Ingredient	Concentration (mM)	g/100ml	Concentration factor
potassium phosphate monobasic anhydrous (pH6)	60	0.8166	12 x
sodium sulphate	24	0.341	12 x

Preparation of PM9 and PM10 additive solution:

Ingredient	Concentration (mM)	g/100ml	Concentration factor
yeast nitrogen base	-	8.04	12 x

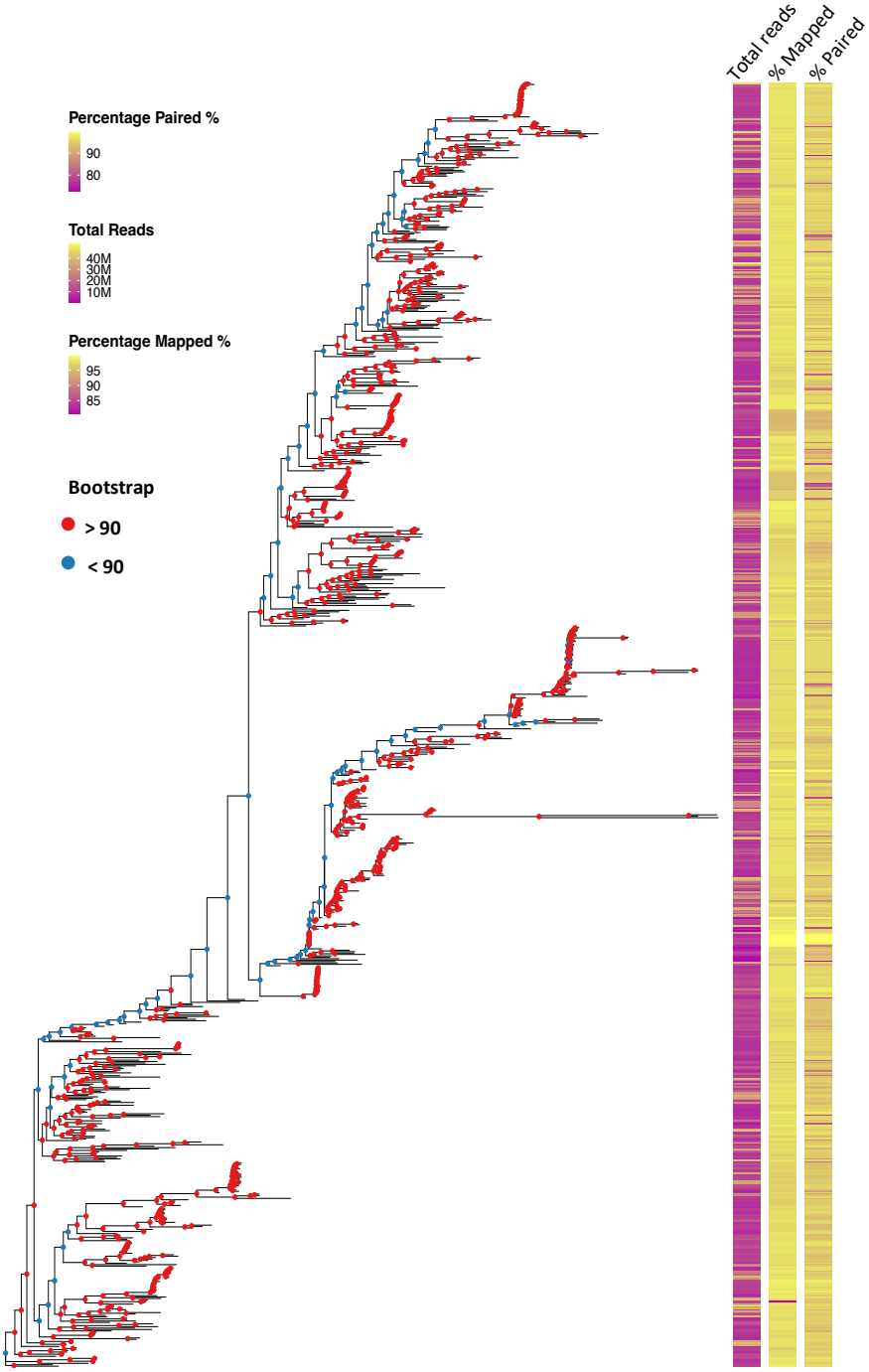
Recipe for PM inoculating fluids from stock solutions:

PM Stock Solution	PM1 (ml)	PM3 (ml)	PM9 & PM10 (ml)
FF-IF	20	12.5	15
D-glucose (32x)	-	0.469	1.25
PM additive (x12) cells	-	1.25	3
cells	0.05	0.03	0.075
sterile water	3.95	0.75	16.8
Total	24	15	36

Appendix 5:

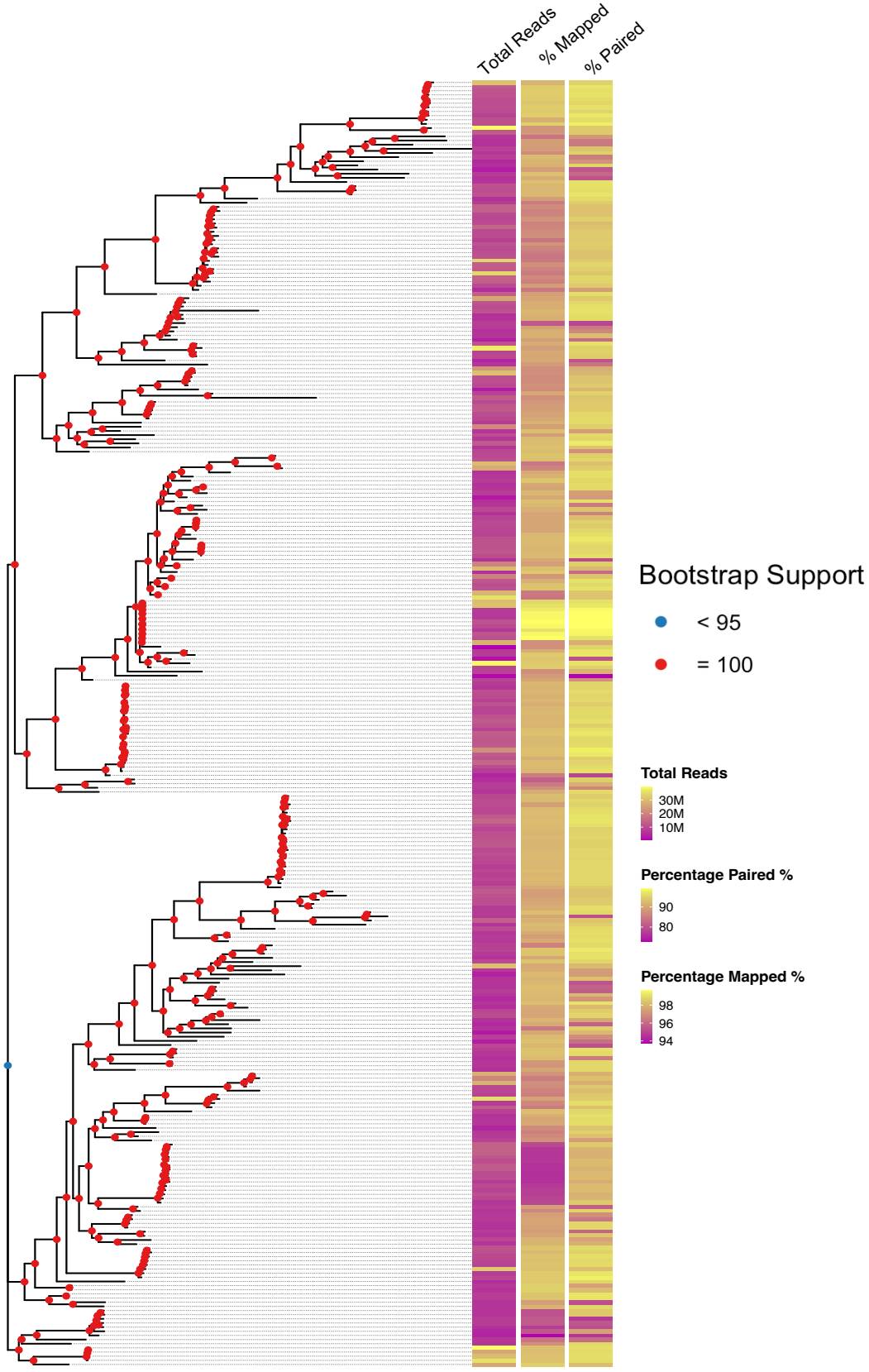
Phylogenetic analyses with bootstrap support and QC metadata

UK: Phylogeny with median bootstrap support of 78%



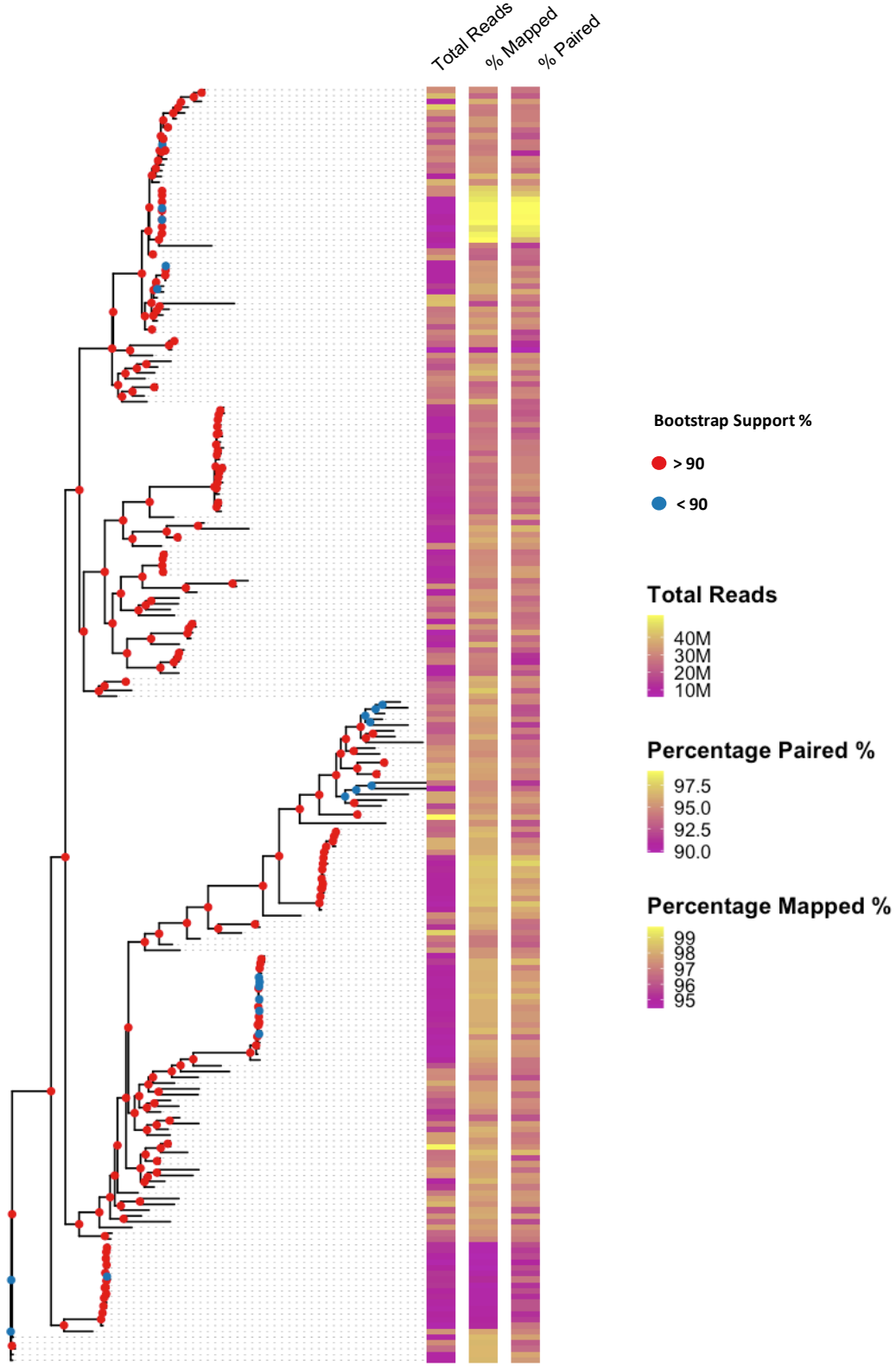
Phylogenetic tree and sequencing metrics *of* UK *A. fumigatus* dataset. Nodes are marked with bootstrap support, with blue representing <90% and red representing >90% support. The accompanying heatmaps provide sequencing metrics for each isolate.

RBH respiratory disease cohort: Phylogeny with median bootstrap support of 92%



Phylogenetic tree and sequencing metrics of RBH respiratory disease cohort. Nodes are marked with bootstrap support, with blue representing <90% and red representing 100% support. The accompanying heatmaps provide sequencing metrics for each isolate.

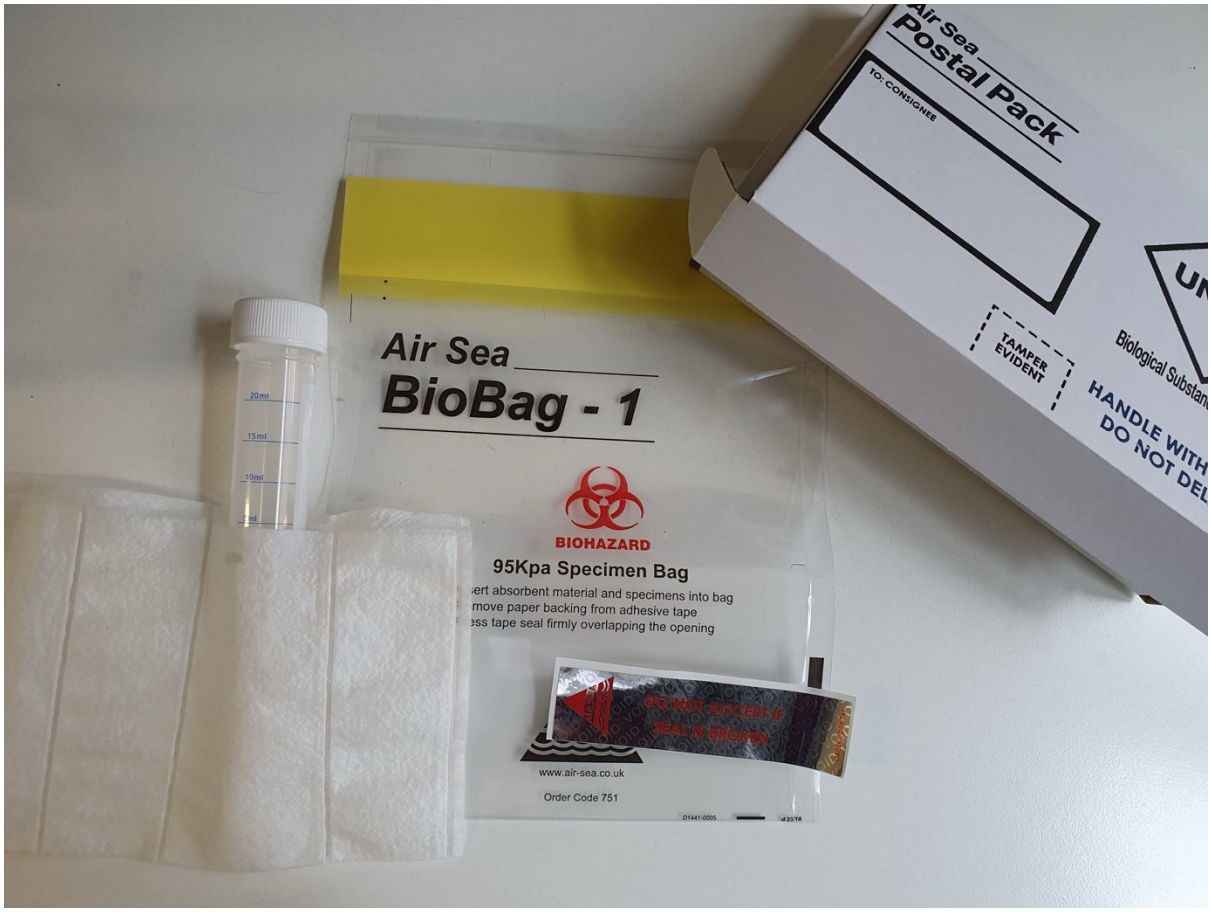
Isolates from participants home environments and corresponding clinical isolates: Phylogeny with median bootstrap support of 98%



Phylogenetic tree and sequencing metrics of *A. fumigatus* isolates from participants home environments and corresponding clinical isolates. Nodes are marked with bootstrap support, with blue representing <90% and red representing 100% support. The accompanying heatmaps provide sequencing metrics for each isolate.

Appendix 6:

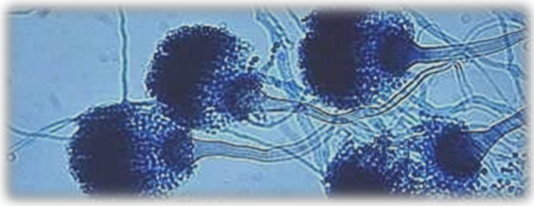
Prospective surveillance remote sputum sampling contents



Appendix 7:

Prospective surveillance remote sputum sampling instructions

Imperial College London

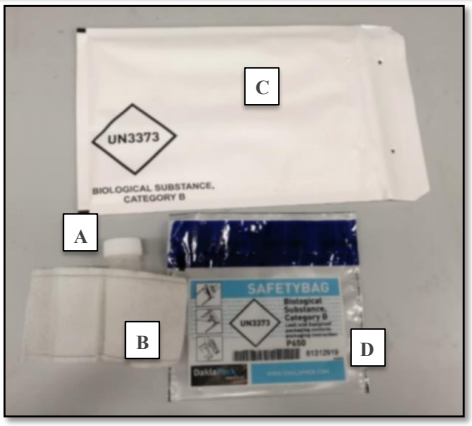


Thank you for taking part in our research project. Your contribution to this study will allow us to further understand and monitor respiratory fungal diseases.

If you would like more information on how to provide a sputum sample, please contact:

Amelie Brackin
a.brackin@Rbht.nhs.uk

Please read the instructions carefully



In this sampling kit you will find:

A. Sample pot
B. Absorbent material
C. Secure BioBag
D. Postal Pack

Step 1.



> Provide a sample that is from deep within your lungs - not just salivary spit from the mouth

> Rinse your mouth out with some tap water to remove any food debris etc.

> Breathe deeply and cough and spit what is coughed up into the pot, alternatively keep the pot at your side for when you have a bout of coughing.

> You should aim to cover the bottom of sample pot

> Secure the top of the sample pot tightly and wash your hands.

Appendix 7 continued:

Step 2.



> Place the sample pot in the absorbent pocket

Step 3.

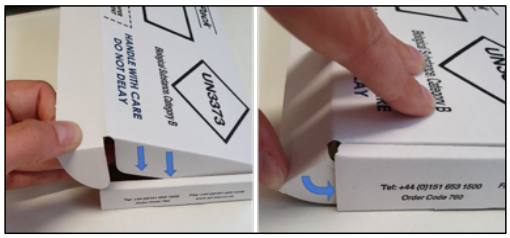


> Place the sample pot and absorbent material into the BioBag provided

> Remove the paper backing from the adhesive tape

> Press the tape seal firmly overlapping the opening

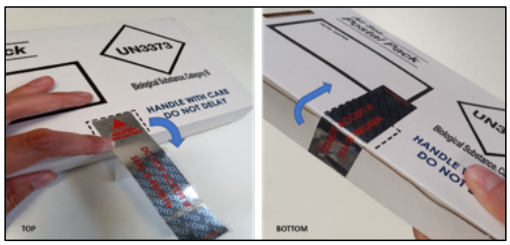
Step 4.



> Please make sure the date the sample was taken is completed at the bottom of this page

> Place the BioBag and this leaflet into the Postal Pack. Close the lid ensuring all tabs are fitted correctly

Step 5.



> Remove the paper backing from the secure seal tag and affix the secure seal over the 'tamper evident' areas, securing the Postal Pack lid firmly in place

> Please post the sealed pack as soon as possible

Appendix 8:

Summary of prospective surveillance participants . Table includes Case ID and associated clinical diagnosis and antifungal treatment history

Case ID	Diagnosis	m/f	Antifungal treatment history
Case 30	CF / CPA	f	Voriconazole, Posaconazole, Isavuconazole and Caspofungin
Case 31	CPA	f	Isavuconazole, Micafungin
Case 32	CPA	f	Caspofungin
Case 33	CPA	f	Itraconazole, Posaconazole, Caspofungin
Case 34	CPA	f	Itraconazole, Voriconazole, Posaconazole, Isavuconazole, caspofungin
Case 35	CPA	f	Itraconazole, Posaconazole, Isavuconazole, Caspofungin
Case 36	ABPA	m	Voriconazole
Case 37	CF	f	Posaconazole
Case 38	CPA	m	Itraconazole
Case 39	CF	m	Itraconazole, Voriconazole, Posaconazole, Isavuconazole, Caspofungin
Case 40	CF	m	Itraconazole
Case 41	ABPA	f	Itraconazole, Posaconazole, Caspofungin
Case 42	ABPA	f	Itraconazole, Posaconazole
Case 43	ABPA	m	Itraconazole, Voriconazole, Posaconazole
Case 44	Af Colonisation	f	nil
Case 60	CPA	m	Itraconazole, Posaconazole
Case 61	ABPA	m	Itraconazole
Case 45	CPA	m	Itraconazole, Voriconazole
Case 46	CPA	f	Itraconazole, Posaconazole
Case 47	ABPA	f	nil
Case 48	CPA	f	Itraconazole
Case 49	ABPA	m	Itraconazole
Case 50	ABPA	f	nil
Case 51	COPD	m	nil
Case 52	ABPA	f	Itraconazole, Voriconazole
Case 53	ABPA	m	nil
Case 54	CPA	m	Itraconazole, Posaconazole
Case 55	CF	f	Posaconazole
Case 56	ABPA	f	nil
Case 57	CF	m	nil
Case 58	CF	f	nil
Case 59	CPA	f	Posaconazole
Case 60	ABPA	m	Itraconazole
Case 61	CPA	f	Posaconazole, Caspofungin
Case 62	CPA	m	Voriconazole, Posaconazole, Isavuconazole and Caspofungin
Case 63	ABPA	f	nil
Case 64	CF	f	Itraconazole
Case 65	CPA	f	Itraconazole, Posaconazole, Caspofungin
Case 66	CF	f	Itraconazole, amphotericin nebulised therapy
Case 67	CPA	f	Itraconazole, Posaconazole, Caspofungin
Case 68	CPA	m	Itraconazole, Voriconazole
Case 69	ABPA	f	Itraconazole, Posaconazole

Case 70	CPA	f	nil
Case 71	ABPA	f	Itraconazole, Voriconazole, Posaconazole
Case 72	ABPA	f	nil
Case 73	ABPA	f	Itraconazole, Posaconazole
Case 74	CPA	m	Itraconazole, Voriconazole, Posaconazole, Caspofungin
Case 75	CPA	m	Voriconazole
Case 76	CPA	m	Itraconazole, Posaconazole, Isavuconazole, Caspofungin
Case 77	ABPA	f	nil
Case 78	ABPA	m	Itraconazole
Case 79	ABPA	f	Itraconazole, Posaconazole
Case 80	ABPA	m	Itraconazole
Case 81	ABPA	m	Itraconazole
Case 82	ABPA	f	Itraconazole

Appendix 9:

Univariate analysis on the associations between azole resistance and clinical demographics

Chi-square (χ^2) test results examining the overall association between azole resistance and clinical demographics. The χ^2 values and corresponding p-values are reported for each variable, indicating the statistical significance of their association with azole resistance.

Variable	x^2	p-value
Diagnosis	61.2	< 0.0001
Gender	10.003	< 0.05
Age	9.83	< 0.05

Chi-square (χ^2) test results examining the association between azole resistance and further categorised diagnosis, gender and age. The χ^2 values and corresponding p-values are reported for each variable, indicating the statistical significance of their association with azole resistance.

Diagnosis	Number of resistant isolates	Number of susceptible isolates	x^2	p-value
ABPA	6	54	38.4	<0.0001
CPA	80	30	22.7	<0.0001
CF	51	49	0	1
Gender	**Number of resistant isolates**	**Number of susceptible isolates**	x^2	**p-value**
Female	100	73	4.2	<0.05
Male	36	61	6.4	<0.05
Age	**Number of resistant isolates**	**Number of susceptible isolates**	x^2	**p-value**
20-39	27	47	5.4	< 0.05
40-59	69	46	4.6	< 0.05
60-89	40	41	0.01	0.9

Appendix 10:

Summary of *A. fumigatus* isolates selected for WGS for prospective surveillance. Table includes *cyp51a* genotype and azole susceptibility profiles for itraconazole (itra.) (4mg/L), voriconazole (vori.) (2mg/L) and posaconazole (posa.)(0.5mg/L) using VIPCheck™ plates. Isolates were screened for tebuconazole susceptibility at 3 concentrations (6mg/L, 8mg/L and 16mg/L). "wildtype" represents isolates without known resistance mechanisms in *cyp51a*. Susceptibility is indicated by "-" and resistance is indicated by "+".

Isolate ID	Sample no.	Case ID	CYP51a genotype	Clinical Azoles			Tebuconazole		
				Itra.	Vori.	Posa.	6mg/L	8mg/L	16mg/L
FP164	retrospective isolate	Case 6	TR_{34}/L98H	n/a	n/a	n/a	n/a	n/a	n/a
FP158	retrospective isolate	Case 12	wildtype	-	-	-	-	-	-
FP169	retrospective isolate	Case 15	wildtype	n/a	n/a	n/a	n/a	n/a	n/a
FP001	2	Case 30	TR_{120}/P216T/M172V/F46Y	+	-	+	-	-	-
FP002	2	Case 30	M172V/F46Y	+	+	+	+	+	-
FP003	2	Case 30	wildtype	+	+	+	+	+	+
FP004	2	Case 30	M172V/F46Y	+	+	+	+	+	-
FP045	2	Case 30	TR_{120}/P216T/M172V/F46Y	+	-	+	-	-	-
FP046	2	Case 30	TR_{120}/P216T/M172V/F46Y	+	-	+	-	-	-
FP047	2	Case 30	TR_{120}/P216T/M172V/F46Y	+	-	+	-	-	-
FP048	2	Case 30	TR_{120}/P216T/M172V/F46Y	+	-	+	-	-	-
FP005	3	Case 30	TR_{120}/M220K/M172V/F46Y	+	-	+	-	-	-
FP006	3	Case 30	TR_{120}/P216T/M172V/F46Y	+	-	+	+	+	-
FP007	3	Case 30	TR_{120}/M172V/F46Y	+	+	+	+	+	-
FP008	3	Case 30	M172V/F46Y	+	+	+	+	+	-
FP009	3	Case 30	M172V/F46Y	+	+	+	+	+	+
FP010	3	Case 30	M172V/F46Y	+	-	+	+	+	+
FP011	3	Case 30	M172V/F46Y	+	-	+	+	+	+
FP108	4	Case 30	M172V/F46Y	+	-	+	+	-	-
FP109	4	Case 30	M172V/F46Y	+	-	+	+	+	-
FP012	6	Case 30	TR_{120}/M220K/M172V/F46Y	+	-	+	+	-	-
FP110	6	Case 30	M220K	+	+	+	+	-	-
FP049	7	Case 30	TR_{120}/M172V/F46Y	+	+	+	+	+	+
FP050	7	Case 30	M172V/F46Y	+	+	+	+	+	+
FP051	8	Case 30	TR_{120}/M172V/F46Y	+	-	+	+	+	+
FP052	8	Case 30	wildtype	-	-	+	-	-	-
FP053	8	Case 30	TR_{120}/M172V/F46Y	+	-	+	+	+	+
FP054	8	Case 30	TR_{120}/M172V/F46Y	+	+	+	+	+	+
FP111	8	Case 30	M172V/F46Y	+	I	+	+	+	+

FP013	1	Case 31	TR_{34}/L98H	+	+	-	+	+	+
FP014	1	Case 31	TR_{34}/L98H	+	+	+	+	+	+
FP015	1	Case 31	TR_{34}/L98H	+	+	+	+	+	+
FP055	1	Case 31	TR_{34}/L98H	+	+	+	+	+	+
FP112	1	Case 31	TR_{34}/L98H	+	+	+	+	+	+
FP125	1	Case 31	TR_{34}/L98H	+	+	+	+	+	-
FP056	2	Case 31	TR_{34}/L98H	-	-	+	+	+	-
FP057	2	Case 31	TR_{34}/L98H	-	-	+	+	+	-
FP113	2	Case 31	TR_{34}/L98H	+	I	+	-	-	-
FP114	2	Case 31	TR_{34}/L98H	-	-	+	-	-	-
FP115	2	Case 31	TR_{34}/L98H	-	-	+	+	+	-
FP058	3	Case 31	TR34/L98H	-	-	+	-	-	-
FP059	3	Case 31	TR34/L98H	-	-	-	-	-	-
FP116	3	Case 31	TR34/L98H	-	-	+	-	-	-
FP117	3	Case 31	TR_{34}	-	-	+	-	-	-
FP060	4	Case 31	TR_{34}/L98H	+	+	-	+	+	+
FP061	4	Case 31	TR_{34}/L98H	+	+	+	+	+	+
FP062	4	Case 31	TR_{34}/L98H	+	+	+	+	+	+
FP063	4	Case 31	TR_{34}/L98H	+	+	+	+	+	-
FP068	5	Case 31	wildtype	-	-	+	+	+	-
FP069	5	Case 31	wildtype	-	-	+	+	+	-
FP070	5	Case 31	wildtype	-	-	-	-	-	-
FP071	5	Case 31	wildtype	-	-	-	-	-	-
FP072	5	Case 31	wildtype	+	-	-	+	-	-
FP162	retrospective isolate	Case 32	wildtype	-	-	-	-	-	-
FP064	1	Case 32	wildtype	-	-	-	-	-	-
FP016	3	Case 32	wildtype	-	-	-	-	-	-
FP017	3	Case 32	wildtype	-	-	-	-	-	-
FP018	3	Case 32	wildtype	-	-	-	+	-	-
FP065	4	Case 32	wildtype	-	-	-	-	-	-
FP066	4	Case 32	wildtype	-	-	-	-	-	-
FP067	5	Case 32	wildtype	-	-	-	-	-	-
FP073	7	Case 32	TR_{46}/Y121F/T289A	-	+	-	+	+	+
FP019	2	Case 33	G448S	+	+	+	+	+	+
FP020	2	Case 33	G448S	+	+	+	-	-	-
FP074	2	Case 33	G448S	+	+	+	+	+	+
FP021	4	Case 33	G448S	+	+	+	I	I	-
FP022	4	Case 33	G448S	+	+	+	-	-	-
FP042	4	Case 33	G448S	+	+	+	+	+	+
FP023	6	Case 33	G448S	-	+	-	+	+	+
FP024	6	Case 33	G448S	-	-	-	-	-	-
FP025	6	Case 33	G448S	-	+	-	-	-	-
FP026	6	Case 33	G448S	-	+	-	-	-	-
FP075	6	Case 33	wildtype	-	+	-	+	+	+
FP076	6	Case 33	G448S	+	+	+	+	+	+
FP118	6	Case 33	M129T	+	+	+	-	-	-
FP077	7	Case 33	G448S	+	+	+	+	+	+
FP078	7	Case 33	G448S	+	+	+	+	+	+
FP079	7	Case 33	G448S	+	+	+	+	+	+
FP080	8	Case 33	G448S	+	+	+	+	+	+
FP081	8	Case 33	G448S	+	+	+	+	+	+
FP082	8	Case 33	G448S	+	+	+	+	+	+
FP119	8	Case 33	G488S	+	+	+	-	-	-
FP027	1	Case 34	TR_{34}/L98H	+	-	+	+	+	+
FP083	1	Case 34	TR_{34}/L98H	+	+	+	+	+	-
FP084	1	Case 34	wildtype	-	-	-	-	-	-
FP085	1	Case 34	TR_{34}/L98H	+	+	+	+	+	-
FP086	1	Case 34	TR_{34}	+	+	+	+	+	-
FP087	2	Case 34	wildtype	-	-	-	-	-	-
FP088	2	Case 34	wildtype	-	-	-	-	-	-
FP153	2	Case 34	I242V	-	-	+	-	-	-
FP089	3	Case 34	wildtype	-	-	-	-	-	-

FP090	3	Case 34	wildtype	-	-	+	-	-	-
FP091	3	Case 34	wildtype	-	-	-	-	-	-
FP092	3	Case 34	wildtype	-	-	-	-	-	-
FP093	2	Case 35	G54R	+	-	+	-	-	-
FP094	2	Case 35	G54E	+	-	+	-	-	-
FP095	2	Case 35	P216L	+	-	+	-	-	-
FP096	2	Case 35	G54R	+	-	+	-	-	-
FP097	2	Case 35	G54E	+	-	+	-	-	-
FP098	3	Case 35	G54E	+	-	+	-	-	-
FP099	3	Case 35	G54E	+	-	+	-	-	-
FP100	3	Case 35	G54E	+	-	+	-	-	-
FP101	3	Case 35	G54E	+	-	+	-	-	-
FP102	3	Case 35	G54E	-	-	+	-	-	-
FP103	4	Case 35	G54E	+	-	+	-	-	-
FP104	4	Case 35	G54E	+	-	+	-	-	-
FP105	4	Case 35	G54E	+	-	+	-	-	-
FP120	4	Case 35	G54E	+	-	+	-	-	-
FP121	4	Case 35	G54E	+	-	+	-	-	-
FP127	4	Case 35	G488S	-	-	-	-	-	-
FP028	1	Case 36	wildtype	-	-	-	-	-	-
FP040	1	Case 36	wildtype	-	-	-	+	-	-
FP029	2	Case 36	wildtype	-	-	-	-	-	-
FP137	2	Case 36	wildtype	-	-	-	-	-	-
FP152	3	Case 36	wildtype	-	-	-	-	-	-
FP138	7	Case 36	wildtype	-	-	-	-	-	-
FP139	7	Case 36	wildtype	-	-	-	-	-	-
FP140	7	Case 36	wildtype	-	-	-	-	-	-
FP141	7	Case 36	wildtype	-	-	-	-	-	-
FP030	1	Case 37	wildtype	+	-	+	+	-	-
FP166	1	Case 37	wildtype	-	-	-	-	-	-
FP031	2	Case 37	wildtype	-	-	+	+	-	-
FP143	2	Case 37	wildtype	-	-	-	+	-	-
FP144	3	Case 37	wildtype	-	-	-	-	-	-
FP171	3	Case 37	wildtype	-	-	-	-	-	-
FP173	3	Case 37	wildtype	-	-	-	-	-	-
FP163	4	Case 37	wildtype	-	-	-	-	-	-
FP126	1	Case 38	G488S	-	+	-	-	-	-
FP128	1	Case 38	G488S	-	-	I	-	-	-
FP106	2	Case 38	G448S	-	+	+	-	-	-
FP122	2	Case 38	G488S	-	-	-	-	-	-
FP123	2	Case 38	G488S	-	I	-	-	-	-
FP124	2	Case 38	G488S	+	+	+	-	-	-
FP107	3	Case 38	G448S	-	+	-	-	-	-
FP129	3	Case 38	G488S		-	-	-	-	-
FP130	3	Case 38	G488S	-	+	I	-	-	-
FP168	3	Case 38	G448S	-	-	I	-	-	-
FP131	1	Case 39	TR_{34}/L98H	-	-	+	+	-	-
FP132	2	Case 39	TR_{34}/L98H	-	-	-	+	-	-
FP133	2	Case 39	TR_{34}/L98H	-	-	+	+	-	-
FP167	2	Case 39	TR_{34}/L98H	+	+	+	-	-	-
FP154	5	Case 40	wildtype	-	-	-	-	-	-
FP155	5	Case 40	wildtype	-	-	-	-	-	-
FP156	5	Case 40	wildtype	-	-	-	-	-	-
FP157	5	Case 40	wildtype	-	-	-	-	-	-
FP142	2	Case 41	D262Y	-	-	-	-	-	-
FP145	2	Case 41	wildtype	-	-	-	-	-	-
FP146	3	Case 41	wildtype	-	-	-	-	-	-
FP151	2	Case 42	M172V/F46Y	-	-	-	-	-	-
FP159	2	Case 42	wildtype	-	-	-	-	-	-
FP032	4	Case 42	wildtype	-	-	-	+	-	-
FP033	4	Case 42	wildtype	-	-	-	+	-	-
FP149	4	Case 42	wildtype	-	-	-	-	-	-

FP150	4	Case 42	wildtype	-	-	-	-	-	-
FP160	4	Case 42	wildtype	-	-	-	-	-	-
FP134	2	Case 43	TR_{34}/L98H	+	+	+	+	+	+
FP135	2	Case 43	TR_{34}/L98H	+	+	+	+	+	+
FP136	2	Case 43	TR_{34}/L98H	+	+	+	+	+	+
FP161	2	Case 43	wildtype	-	-	-	-	-	-
FP170	2	Case 43	wildtype	-	-	-	-	-	-
FP038	1	Case 44	wildtype	-	-	-	-	-	-
FP044	1	Case 44	D262Y	-	-	-	-	-	-
FP165	1	Case 44	wildtype	-	-	-	-	-	-
FP036	2	Case 44	D262Y	-	-	-	-	-	-
FP039	2	Case 44	D262Y	-	-	-	-	-	-
FP041	2	Case 44	wildtype	-	-	-	-	-	-
FP148	2	Case 44	wildtype	-	-	-	-	-	-
FP037	3	Case 44	wildtype	-	-	-	-	-	-
FP147	3	Case 44	wildtype	-	-	-	-	-	-
FP034	4	Case 44	wildtype	-	-	-	-	-	-
FP035	4	Case 44	wildtype	-	-	-	-	-	-
FP043	4	Case 44	D262Y	-	-	-	-	-	-

Appendix 11

Post hoc Dunns test of spatial distribution of CFU counts between Site A, Site B and the external control. The z score and corresponding p-values are reported for each variable, indicating the statistical significance

	Site Comparison (z score, **adj. p value**)	
Site	A	B
B	1.048623, **> 0.05**	
External control	-2.829298, **< 0.05**	-3.403463, **< 0.005**

Post hoc Dunns test of spatial distribution CFU counts between locations and the external control. The z score and corresponding p-values are reported for each variable, indicating the statistical significance

	Comparison of locations. (z score, **adj. p value**)								
Locations	Ambulatory	Basement	CT	External control	ICU	Inpatients ward A	Inpatients ward B	Outpatients	Reception
Basement	-1.740612 **1**								
CT	-1.104619 **1**	0.635992 **1**							
External	-3.316432 **0.0205***	-1.57582 **1**	-2.211813 **0.607**						
ICU	1.158863 **1**	2.643262 **0.1848**	2.100885 **0.8021**	3.987126 **0.0015***					
Inpatients ward A	-0.499524 **1**	1.241087 **1**	0.605094 **1**	2.816907 **0.1091**	-1.584859 **1**				
Inpatients ward B	0.893479 **1**	2.634092 **0.1898**	1.998099 **1**	4.209912 **0.0006***	-0.396901 **1**	1.393004 **1**			
Outpatients	-1.493424 **1**	0.247187 **1**	-0.388805 **1**	1.823007 **1**	-2.43246 **0.3374**	-0.993899 **1**	-2.386904 **0.3823**		
Reception	-3.290683 **0.0225***	-1.550071 **1**	-2.186064 **0.6482**	0.025748 **1**	-3.965167 **0.0017***	-2.791159 **0.1182**	-4.184163 **0.0006***	-1.797259 **1**	
Staff office	-1.165859 **1**	0.423094 **1**	-0.157485 **1**	1.861614 **1**	-2.100433 **0.803**	-0.709858 **1**	-1.981491 **1**	0.197444 **1**	1.838109 **1**

Appendix 12:

Summary of *A. fumigatus* isolates selected for WGS from all hospital locations and sample time points. Table includes *cyp51a* genotype and azole susceptibility profiles for itraconazole (itra.) (4mg/L), voriconazole (vori.) (2mg/L) and posaconazole (posa.)(0.5mg/L) using VIPCheck™ plates. Isolates were screened for tebuconazole susceptibility at 3 concentrations (6mg/L, 8mg/L and 16mg/L). "wildtype" represents isolates without known resistance mechanisms in *cyp51a*. Susceptibility is indicated by "-" and resistance is indicated by "+".

Isolate ID	Sample date	Location	Source	*Cyp51a* allele	Clinical Azoles			Tebuconazole		
					Itra.	Vori.	Posa.	6mg/L	8mg/L	16mg/L
FN014	Nov. 2020	Ambulatory	Air	wildtype	-	-	-	-	-	-
FN060	Dec. 2020	Ambulatory	Air	wildtype	-	-	-	-	-	-
FN099	Mar. 2021	Ambulatory	Air	G448S	-	-	-	-	-	-
FN043	Nov. 2021	Ambulatory	Air	wildtype	-	-	-	-	-	-
FN038	Nov. 2020	Basement	Air	wildtype	-	-	-	-	-	-
FN031	Dec. 2020	Basement	Air	wildtype	-	-	-	+	-	-
FN006	Mar. 2021	Basement	Air	wildtype	-	-	-	-	-	-
FN098	Jun. 2021	Basement	Air	TR_{34}/L98H	+	-	+	+	+	+
FN045	Nov. 2021	Basement	Air	wildtype	-	-	-	-	-	-
FN047	Sept. 2021	Basement	Air	wildtype	-	-	-	-	-	-
FN003	Nov. 2020	CT	Air	D262Y	-	-	-	-	-	-
FN005	Nov. 2020	CT	Air	TR_{120}	-	-	-	+	-	-
FN015	Dec. 2020	CT	Air	wildtype	-	-	-	-	-	-
FN040	Dec. 2020	CT	Air	wildtype	-	-	-	-	-	-
FN044	Nov. 2021	CT	Air	M172/F46Y	-	-	-	-	-	-
FN078	Dec. 2020	Staff office	Air	G448S	-	-	-	-	-	-
FN035	Feb. 2021	Staff office	Air	wildtype	-	-	-	-	-	-
FN064	Mar. 2021	Staff office	Air	wildtype	-	-	-	-	-	-
FN058	Jun. 2021	Staff office	Air	wildtype	-	-	-	-	-	-
FN002	Nov. 2020	Outpatients	Air	TR_{34}/L98H	+	+	+	+	+	+
FN001	Mar. 2021	Outpatients	Air	TR_{34}/L98H	+	+	+	+	+	+
FN075	Jun. 2021	Outpatients	Air	wildtype	-	-	-	+	+	-
FN022	Sept. 2021	Outpatients	Air	TR_{34}/L98H	+	+	+	+	+	+
FN024	Sept. 2021	Outpatients	Air	wildtype	-	-	-	-	-	-
FN042	Nov. 2021	Outpatients	Air	wildtype	-	-	-	+	+	-
FN008	Feb. 2022	Outpatients	Air	M172/F46Y	-	-	-	+	+	-
FN009	Feb. 2022	Outpatients	Air	wildtype	-	-	-	-	-	-
FN010	Feb. 2022	Outpatients	Air	wildtype	-	-	-	-	-	-
FN007	Feb. 2022	Outpatients	Air	TR_{34}/L98H	-	-	+	+	+	+
FN011	Feb. 2022	Outpatients	Air	wildtype	-	-	-	+	+	-
FN012	Feb. 2022	Outpatients	Air	wildtype	-	-	-	-	-	-

FN013	Feb. 2022	Outpatients	Air	A9T	-	-	-	-	-	-
FN033	Nov. 2020	Inpatients Ward A	Air	wildtype	-	-	-	-	-	-
FN093	Dec. 2020	Inpatients Ward A	Air	M172/F46Y	-	-	-	-	-	-
FN065	Mar. 2021	Inpatients Ward A	Air	wildtype	-	-	-	-	-	-
FN084	Sept. 2021	Inpatients Ward A	Air	wildtype	-	-	-	-	-	-
FN030	Dec. 2020	Inpatients Ward B	Air	M172/F46Y	-	-	-	+	-	-
FN048	Mar. 2021	Inpatients Ward B	Air	wildtype	-	-	-	-	-	-
FN094	Jun. 2021	ICU	Air	M172/F46Y	-	-	-	-	-	-
FN055	Nov. 2020	Reception	Air	wildtype	-	-	-	-	-	-
FN079	Dec. 2020	Reception	Air	M172/F46Y	-	-	-	-	-	-
FN069	Mar. 2021	Reception	Air	wildtype	-	-	-	-	-	-
FN102	Feb. 2021	Reception	Air	wildtype	-	-	-	-	-	-
FN017	Jun. 2021	Reception	Air	TR_{34}/L98H	+	+	+	+	+	+
FN023	Nov. 2021	Reception	Air	wildtype	-	-	-	-	-	-
FN076	Nov. 2020	External control	Air	wildtype	-	-	-	-	-	-
FN080	Dec. 2020	External control	Air	wildtype	-	-	-	-	-	-
FN088	Dec. 2020	External control	Air	wildtype	-	-	-	-	-	-
FN092	Feb. 2021	External control	Air	M172/F46Y	-	-	+	+	+	-
FN090	Mar. 2021	External control	Air	wildtype	-	-	-	-	-	-
FN071	Mar. 2021	External control	Air	wildtype	-	-	-	-	-	-
FN059	Jun. 2021	External control	Air	wildtype	-	-	-	-	-	-
FN096	Nov. 2020	Courtyard	Soil	wildtype	-	-	-	-	-	-
FN085	Dec. 2020	Courtyard	Soil	wildtype	-	-	-	-	-	-
FN032	Dec. 2020	Courtyard	Soil	wildtype	-	-	-	-	-	-
FN053	Dec. 2020	Courtyard	Soil	wildtype	-	-	-	-	-	-
FN039	Dec. 2020	Courtyard	Soil	wildtype	-	-	-	-	-	-
FN091	Feb. 2021	Courtyard	Soil	M172/F46Y	-	-	+	+	-	-
FN034	Nov. 2020	Staff entrance	Soil	wildtype	-	-	-	-	-	-
FN062	Dec. 2020	Staff entrance	Soil	M172/F46Y	-	-	-	-	-	-
FN081	Dec. 2020	Staff entrance	Soil	wildtype	-	-	-	-	-	-
FN100	Dec. 2020	Staff entrance	Soil	wildtype	-	-	-	-	-	-
FN016	Feb. 2021	Staff entrance	Soil	wildtype	-	-	-	-	-	-
FN082	Feb. 2021	Staff entrance	Soil	wildtype	-	-	-	-	-	-
FN101	Feb. 2021	Staff entrance	Soil	wildtype	-	-	-	-	-	-

FN018	Jun. 2021	Staff entrance	Soil	M172/F46Y	-	-	-	-	-	-
FN041	Jun. 2021	Staff entrance	Soil	wildtype	-	-	-	-	-	-
FN050	Jun. 2021	Staff entrance	Soil	M172/F46Y	-	-	-	-	-	-
FN086	Jun. 2021	Staff entrance	Soil	wildtype	-	-	-	-	-	-
FN049	Feb. 2021	Outpatients	Soil	I242V	-	-	-	-	-	-
FN004	Feb. 2021	Outpatients	Soil	wildtype	-	-	-	+	+	-
FN103	Feb. 2021	Outpatients	Soil	D262Y	-	-	-	-	-	-
FN051	Jun. 2021	Outpatients	Soil	M172/F46Y	-	-	-	-	-	-
FN054	Nov. 2021	Outpatients	Soil	wildtype	-	-	-	-	-	-
FN046	Nov. 2021	Outpatients	Soil	wildtype	-	-	-	+	-	-
FN087	Nov. 2021	Outpatients	Soil	wildtype	-	-	-	+	-	-
FN089	Nov. 2021	Outpatients	Soil	wildtype	-	-	-	-	-	-
FN057	Nov. 2020	Reception	Soil	wildtype	-	-	-	-	-	-
FN077	Nov. 2020	Reception	Soil	M172/F46Y	-	-	-	-	-	-
FN056	Nov. 2020	Reception	Soil	M172/F46Y	-	-	-	-	-	-
FN070	Nov. 2020	Reception	Soil	wildtype	-	-	-	-	-	-
FN061	Dec. 2020	Reception	Soil	wildtype	-	-	-	-	-	-
FN036	Dec. 2020	Reception	Soil	wildtype	-	-	-	-	-	-
FN066	Dec. 2020	Reception	Soil	wildtype	-	-	-	-	-	-
FN097	Dec. 2020	Reception	Soil	wildtype	-	-	-	-	-	-
FN095	Feb. 2021	Reception	Soil	wildtype	-	-	-	-	-	-
FN019	Jun. 2021	Reception	Soil	TR_{34}/L98H	+	+	+	+	+	+
FN020	Jun. 2021	Reception	Soil	D262Y	-	-	-	-	-	-
FN021	Jun. 2021	Reception	Soil	TR_{34}/L98H	+	+	+	+	+	+
FN072	Jun. 2021	Reception	Soil	M172/F46Y	-	-	-	-	-	-
FN083	Jun. 2021	Reception	Soil	wildtype	-	-	-	-	-	-
FN037	Jun. 2021	Reception	Soil	wildtype	-	-	-	-	-	-
FN067	Jun. 2021	Reception	Soil	wildtype	-	-	-	-	-	-
FN052	Nov. 2021	Reception	Soil	wildtype	-	-	-	-	-	-
FN074	Nov. 2021	Reception	Soil	wildtype	-	-	-	-	-	-
FN063	Nov. 2020	Private Gardens	Soil	wildtype	-	-	-	-	-	-
FN068	Feb. 2021	Private Gardens	Soil	wildtype	-	-	-	-	-	-
FN073	Nov. 2021	Private Gardens	Soil	wildtype	-	-	-	-	-	-
FN026	Feb. 2022	Outpatients	Swab	wildtype	-	-	-	-	-	-
FN028	Feb. 2022	Outpatients	Swab	wildtype	-	-	-	-	-	-
FN029	Feb. 2022	Outpatients	Swab	M172/F46Y	-	-	-	-	-	-
FN025	Feb. 2022	Outpatients	Swab	wildtype	-	-	-	-	-	-

Appendix 13

Imperial College London

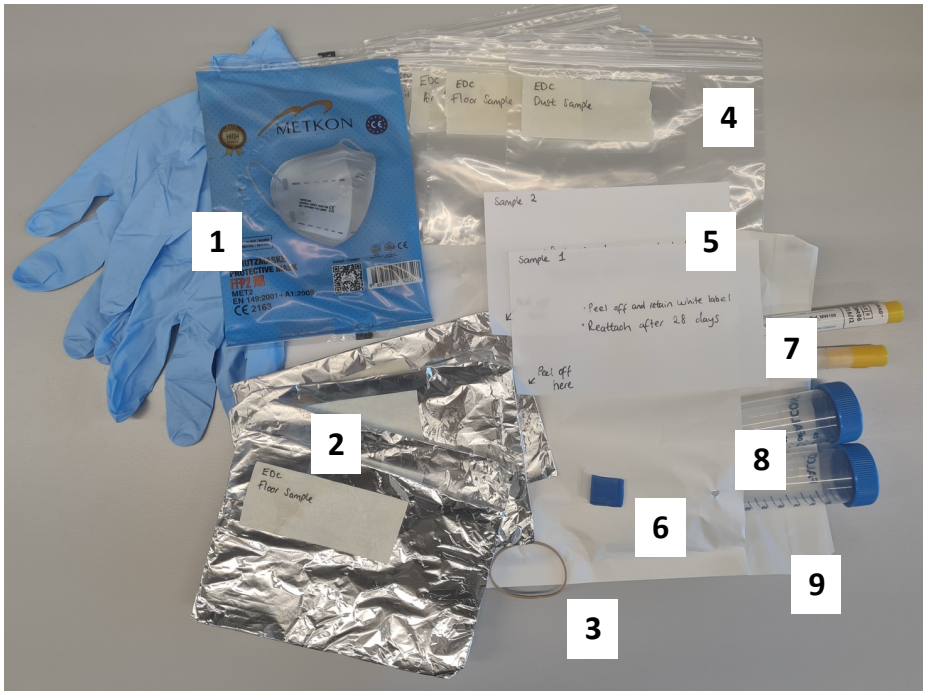
Thank you for taking part in our research project. Your contribution to this study will allow us to further understand and monitor fungal pathogens in the home environment. Please read the sampling instructions carefully prior to sampling

If you would like more information on how to collect your home samples or would like to know more about the study, please contact:

Amelie Brackin, PhD student

a.brackin@imperial.c.uk

Your Environmental Home Sampling Kit



1) Gloves and facemask to use while you carry out your sampling
2) Electrostatic dust cloths
   - 1 x 'floor sample'
   - 1 x 'dust sample
   - 2 x 'air sample'
3) Elastic band to be used with the 'floor sample'
4) Sterile bags for your Electrostatic dust cloth samples
5) 2 x 'Sticky spore traps
6) Blue Tack – to fix your sticky spore traps
7) 2 x Dry swabs
8) 2 x Soil sampling tubes
9) Pre paid envelope to post your samples

Please wear protective gloves and face mask when carrying out the soil and dust sampling around your home



Imperial College London

Sampling the air in your home: Sticky spore traps & Electrostatic Dust Cloths

Thank you for taking part in our research project. Your contribution to this study will allow us to further understand and monitor fungal pathogens in the home environment. Please read the sampling instructions carefully prior to sampling

If you would like more information on how to collect your home samples or would like to know more about the study, please contact:

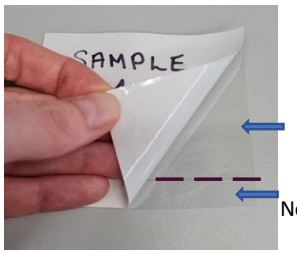
Amelie Brackin, PhD student

a.brackin@imperial.c.uk

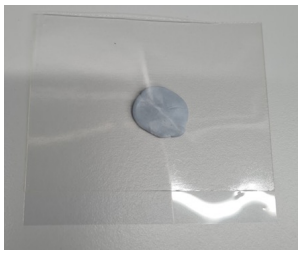
Step 1. Identify 2 different locations in your home that are >1.5m above the floor and out of reach of pets. Place the air samplers labelled 'Sample 1' in one location (e.g living room) and place the air samplers labelled 'Sample 2' in a different location (e.g. bedroom).



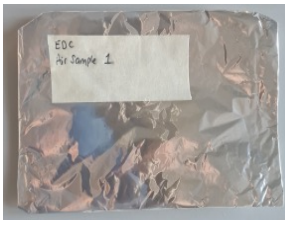
Step 2. Fix the Blu Tack to the clear film/underside of the air samplers

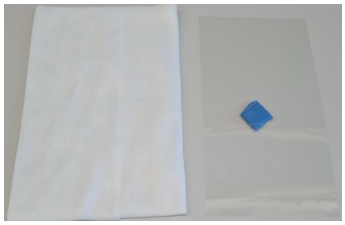


Step 3. Firmly press the air sampler to the surface and carefully peel off (and retain) the white label. Avoid touching the sticky film

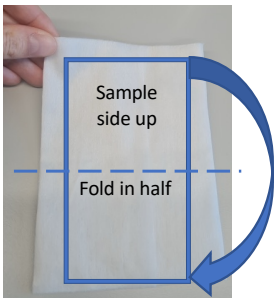


Step 4. After 28 days, reattach the white labels.





Step 5. Carefully remove the sterile dust cloth from the foil wrapper labelled 'EDC Air Sample' and place next to your 'sticky spore trap'. Discard the foil wrapper.





Step 6. After 28 days, carefully fold the cloth in half (sample side up) and place in the sterile bag labelled 'EDC Air Sample'. Secure the sterile zip lock bag and post when possible



Step 7. Record the site locations in the questionnaire provided and post your air

When your sampling is finished, please place all your samples inside the pre-paid return envelope, along with your completed questionnaire, and store in a cool and dark place until you are able to return by post.

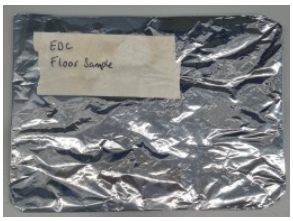


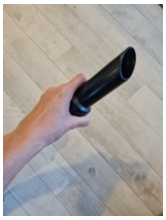
Imperial College London

Sampling the dust around your home: Electrostatic dust cloth

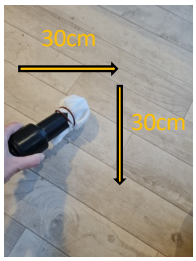
To sample your floor you will need a vacuum cleaner. If you don't use a vacuum in your home you may wipe the floor with the dust cloth labelled 'floor sample' (see surface dust sampling). Please specify your method used in the questionnaire provided.

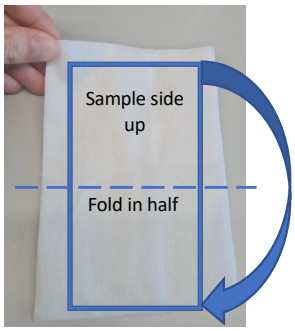
Floor sample





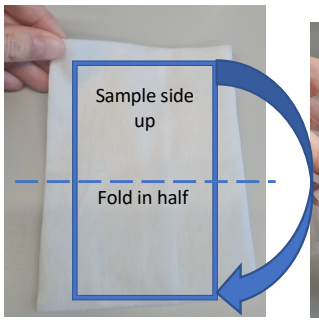

Step 1. Carefully remove the sterile dust cloth from the foil wrapper labelled 'floor sample'.



Step 2. Wrap the cloth around a vacuum nozzle and secure with the elastic band. Vacuum an area of the floor - approximately 30cm x 30cm. Carefully remove the dust cloth, fold in half and place in the sterile bag labelled 'floor sample'

Surface dust sample



Step 3. Carefully remove the sterile dust cloth from the foil wrapper labelled 'dust sample'. Gently wipe the cloth across the surface, fold the cloth in half and place in the sterile bag labelled 'dust sample'.



When your sampling is finished, please place all your samples inside the pre-paid return envelope, along with your completed questionnaire, and store in a cool and dark place until you are able to return by post.

Step 4. Record the site locations in the questionnaire provided.



Imperial College London

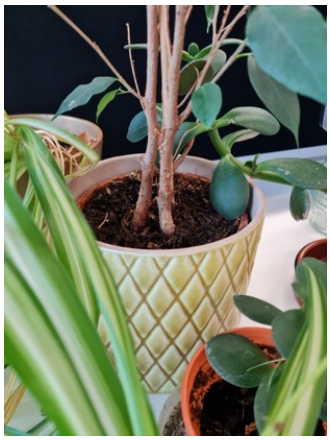
Sampling the soil around your home

Thank you for taking part in our research project. Your contribution to this study will allow us to further understand and monitor fungal pathogens in the home environment. Please read the sampling instructions carefully prior to sampling

If you would like more information on how to collect your home samples or would like to know more about the study, please contact:

Amelie Brackin, PhD student

a.brackin@imperial.c.uk



Step 1. Identify 2 suitable soil sampling sites in your home, such as an indoor plant pot, outdoor flower bed or compost heap.
Please wear a face mask and the gloves provided to carry out your soil sampling



Step 2. Lightly disturb the soil surface and scoop the soil into the sampling tube labelled 'sample 1'. Fill the tube to '20mls', dust off any excess soil and secure the cap.



Step 3. Repeat the process for the second sampling site using the tube labelled 'sample 2'



Step 4. Record the site locations in the questionnaire provided.



When your sampling is finished, please place all your samples inside the pre-paid return envelope, along with your completed questionnaire, and store in a cool and dark place until you are able to return by post.



Appendix 14

Summary of *A. fumigatus* isolates selected for WGS from all homes locations and sample time points. Table includes *cyp51a* genotype and azole susceptibility profiles for itraconazole (itra.) (4mg/L), voriconazole (vori.) (2mg/L) and posaconazole (posa.)(0.5mg/L) using VIPCheck™ plates. Isolates were screened for tebuconazole susceptibility at 3 concentrations (6mg/L, 8mg/L and 16mg/L). "wildtype" represents isolates without known resistance mechanisms in *cyp51a*. Susceptibility is indicated by "-" and resistance is indicated by "+".

Isolate ID	Sample date	Location	Source	CYP51a genotype	Clinical Azoles			Tebuconazole		
					Itra.	Vori.	Posa.	6mg/L	8mg/L	16mg/L
FH012	May-22	Case 31	soil	wildtype	-	-	-	-	-	-
FH014	May-22	Case 32	soil	wildtype	-	-	-	-	-	-
FH015	May-22	Case 32	soil	wildtype	-	-	-	-	-	-
FH016	May-22	Case 32	dust	wildtype	-	-	-	-	-	-
FH018	May-22	Case 32	soil	wildtype	-	-	-	-	-	-
FH019	May-22	Case 32	soil	M172V/F46Y	-	-	-	+	-	-
FH020	May-22	Case 32	dust	wildtype	-	-	-	-	-	-
FH021	May-22	Case 32	soil	wildtype	-	-	-	-	-	-
FH022	May-22	Case 32	soil	M172V/F46Y	-	-	-	-	-	-
FH028	Jan. 2023	Case 32	dust	wildtype	-	-	-	-	-	-
FH029	Jan. 2023	Case 32	dust	wildtype	-	-	-	-	-	-
FH041	Jan. 2023	Case 32	air	wildtype	-	-	-	+	-	-
FH042	Jan. 2023	Case 32	air	M172V/F46Y	-	-	-	-	-	-
FH043	Jan. 2023	Case 32	dust	L98H	+	-	+	+	+	-
FH054	Jan. 2023	Case 32	dust	M172V/F46Y	-	-	-	-	-	-
FH073	Jan. 2023	Case 32	dust	M172V/F46Y	-	-	-	-	-	-
FH030	May-23	Case 33	soil	M172V/F46Y	-	-	-	+	-	-
FH068	May-23	Case 33	soil	wildtype	-	-	-	-	-	-
FH069	May-23	Case 33	soil	M172V/F46Y	-	-	-	-	-	-
FH077	May-23	Case 33	soil	wildtype	-	-	-	-	-	-
FH085	May-23	Case 33	soil	wildtype	-	-	-	-	-	-
FH086	May-23	Case 33	soil	wildtype	-	-	-	-	-	-
FH089	Nov. 2023	Case 33	dust	wildtype	-	-	-	-	-	-
FH094	Nov. 2023	Case 33	dust	wildtype	-	-	-	-	-	-
FH044	Jul. 2023	Case 34	air	L98H	+	-	+	+	+	-
FH045	Jul. 2023	Case 34	air	wildtype	-	-	-	-	-	-
FH049	Jul. 2023	Case 34	soil	wildtype	-	-	-	-	-	-
FH050	Jul. 2023	Case 34	soil	M172V/F46Y	-	-	-	-	-	-
FH059	Jul. 2023	Case 34	air	wildtype	-	-	-	-	-	-
FH064	Jul. 2023	Case 34	air	wildtype	-	-	-	-	-	-
FH080	Jul. 2023	Case 34	air	wildtype	-	-	-	-	-	-

FH081	Jul. 2023	Case 34	air	wildtype	-	-	-	-	-	-
FH083	Jul. 2023	Case 34	air	wildtype	-	-	-	-	-	-
FH090	Jul. 2023	Case 34	air	wildtype	-	-	-	-	-	-
FH091	Jul. 2023	Case 34	air	wildtype	-	-	-	-	-	-
FH092	Jul. 2023	Case 34	soil	wildtype	-	-	-	-	-	-
FH095	Jul. 2023	Case 34	air	wildtype	-	-	-	-	-	-
FH097	Jul. 2023	Case 34	soil	M172V/F46Y	-	-	-	-	-	-
FH103	Nov. 2023	Case 34	soil	wildtype	-	-	-	-	-	-
FH004	Feb. 2023	Case 35	air	wildtype	-	-	-	-	-	-
FH017	Feb. 2023	Case 35	air	wildtype	-	-	-	-	-	-
FH023	Feb. 2023	Case 35	air	TR_{34}/L98H	+	+	+	+	+	+
FH047	Feb. 2023	Case 35	soil	wildtype	-	-	-	-	-	-
FH060	Feb. 2023	Case 35	air	wildtype	-	-	-	-	-	-
FH062	Feb. 2023	Case 35	soil	I242V	-	-	-	-	-	-
FH071	Feb. 2023	Case 35	soil	Y121F/T289A	-	-	-	+	+	+
FH072	Feb. 2023	Case 35	soil	M172V/F46Y	-	-	-	+	-	-
FH099	Jul. 2023	Case 35	soil	L98H	+	-	-	+	-	-
FH101	Nov. 2023	Case 35	dust	wildtype	-	-	-	-	-	-
FH046	May-22	Case 60	soil	M172V/F46Y	-	-	-	-	-	-
FH058	May-22	Case 60	soil	wildtype	-	-	-	-	-	-
FH061	May-22	Case 60	dust	wildtype	-	-	-	-	-	-
FH063	May-22	Case 60	soil	wildtype	-	-	-	-	-	-
FH079	May-22	Case 60	soil	wildtype	-	-	-	-	-	-
FH001	Jan. 2023	Case 37	soil	wildtype	-	-	-	-	-	-
FH003	Jan. 2023	Case 37	soil	wildtype	-	-	-	-	-	-
FH007	Jan. 2023	Case 37	dust	wildtype	-	-	-	-	-	-
FH027	Jul. 2023	Case 37	soil	wildtype	-	-	-	-	-	-
FH033	Jul. 2023	Case 37	soil	wildtype	-	-	-	-	-	-
FH034	Jul. 2023	Case 37	soil	M172V/F46Y	-	-	-	-	-	-
FH038	Jul. 2023	Case 37	soil	wildtype	-	-	-	-	-	-
FH051	Jan. 2023	Case 37	air	wildtype	-	-	-	-	-	-
FH053	Jul. 2023	Case 37	soil	wildtype	-	-	-	-	-	-
FH057	May-22	Case 37	soil	M172V/F46Y	-	-	-	+	-	-
FH066	Jan. 2023	Case 37	dust	M172V/F46Y	-	-	-	-	-	-
FH074	Jan. 2023	Case 37	air	wildtype	-	-	-	-	-	-
FH075	Jan. 2023	Case 37	soil	wildtype	-	-	-	-	-	-
FH076	Jan. 2023	Case 37	dust	wildtype	-	-	-	-	-	-
FH055	May-22	Case 61	air	M172V/F46Y	-	-	-	-	-	-
FH056	May-22	Case 61	soil	M172V/F46Y	-	-	-	-	-	-
FH078	May-22	Case 61	soil	wildtype	-	-	-	-	-	-
FH024	May-22	Case 38	soil	wildtype	-	-	-	-	-	-
FH025	May-22	Case 38	soil	M172V/F46Y	-	-	-	-	-	-
FH026	May-22	Case 38	soil	wildtype	-	-	-	-	-	-
FH031	May-22	Case 38	soil	M172V/F46Y	-	-	-	-	-	-
FH040	May-22	Case 38	soil	wildtype	-	-	-	-	-	-
FH082	May-22	Case 38	soil	I242V	-	-	-	-	-	-

FH084	May-22	Case 38	soil	wildtype	-	-	-	-	-	-
FH088	May-22	Case 38	soil	M172V/F46Y	-	-	-	-	-	-
FH070	Oct. 2023	Case 42	soil	G448S/Y121F/T289A/I364V/S363P	-	-	+	+	+	-
FH002	Jan. 2023	Case 42	dust	wildtype	-	-	-	-	-	-
FH005	Jan. 2023	Case 42	soil	wildtype	-	-	-	-	-	-
FH006	Jan. 2023	Case 42	air	wildtype	-	-	-	-	-	-
FH008	Jan. 2023	Case 42	air	wildtype	-	-	-	-	-	-
FH009	May-22	Case 42	soil	wildtype	-	-	-	-	-	-
FH010	May-22	Case 42	soil	wildtype	-	-	-	-	-	-
FH011	May-22	Case 42	soil	wildtype	-	-	-	-	-	-
FH013	May-22	Case 42	soil	wildtype	-	-	-	-	-	-
FH032	Jan. 2023	Case 42	soil	wildtype	-	-	-	-	-	-
FH035	Jan. 2023	Case 42	soil	wildtype	-	-	-	-	-	-
FH037	Jan. 2023	Case 42	soil	G448S/Y121F/T289A/I364V/S363P	-	-	+	+	+	-
FH039	Jan. 2023	Case 42	soil	wildtype	-	-	-	-	-	-
FH048	May-22	Case 42	air	D262Y	-	-	-	-	-	-
FH052	Jan. 2023	Case 42	soil	M172V/F46Y	-	-	+	+	-	-
FH065	Nov. 2023	Case 42	soil	wildtype	-	-	-	-	-	-
FH067	Jan. 2023	Case 42	soil	G448S/Y121F/T289A/I364V/S363P	-	-	+	+	+	-
FH087	Jan. 2023	Case 42	air	wildtype	-	-	-	-	-	-
FH093	Jan. 2023	Case 42	soil	M172V/F46Y	-	-	-	-	-	-
FH096	Jan. 2023	Case 42	soil	wildtype	-	-	-	-	-	-
FH100	Oct. 2023	Case 42	soil	G448S/Y121F/T289A/I364V/S363P	-	-	+	+	+	-
FH102	Oct. 2023	Case 42	dust	wildtype	-	-	-	-	-	-